



University
of Glasgow

Fallick, Anthony E. (1975) *Some applications of stable isotopes of carbon and oxygen in oceanography*.

PhD thesis

<http://theses.gla.ac.uk/4136/>

Copyright and moral rights for this thesis are retained by the author

A copy can be downloaded for personal non-commercial research or study, without prior permission or charge

This thesis cannot be reproduced or quoted extensively from without first obtaining permission in writing from the Author

The content must not be changed in any way or sold commercially in any format or medium without the formal permission of the Author

When referring to this work, full bibliographic details including the author, title, awarding institution and date of the thesis must be given

SOME APPLICATIONS OF STABLE ISOTOPES
OF CARBON AND OXYGEN IN OCEANOGRAPHY

THESIS

submitted for the degree of

DOCTOR OF PHILOSOPHY

of the

UNIVERSITY OF GLASGOW

by

ANTHONY E. FALLICK

Chemistry Department

August, 1975.

BEST COPY

AVAILABLE

Variable print quality

ACKNOWLEDGEMENTS

I express my gratitude to Dr. M.S. Baxter for his constant advice, criticism and encouragement throughout the course of this work. Drs. J.M. Edmond and W.S. Moore, and Mr. S.S. Jacobs supplied samples and data, to them thanks are extended. Dr. Moore also provided the opportunity for me to participate on the Bartlett cruise.

Much of the equipment used in the project was constructed and maintained by Chemistry Department workshops under the direction of Messrs. A. Anderson, J. Conrolly, J. Hardy and A. Hislop: I am grateful to them for this. Drs. P. Deines and Fiona Williams assisted with the computer program.

My laboratory colleagues Drs. J.G. Farmer, T.D.B. Lyon, M.J. Stenhouse and Messrs. H.M. Blauer, J. Brown, J.A. Campbell, A.B. MacKenzie and D.S. Swan all provided assistance and encouragement, not least through many stimulating discussions, both scientific and social. I. Neale, J. Sercombe, N. Bridger and J. Mitchell gave freely of their advice.

I wish to thank Janet Christie who painstakingly typed this manuscript. The thesis would never have been written without the support of my parents.

Lastly, the financial support of the Natural Environment Research Council is gratefully acknowledged.

TABLE OF CONTENTS

	<u>Page</u>
CHAPTER I INTRODUCTION	
I-1 Prolegomena	1
I-2 Carbon in the oceans	1
I-3 Oxygen in the oceans	11
I-4 Ocean models	21
I-5 Aims of research	27
CHAPTER II EXPERIMENTAL METHODS FOR ECO_2 EXTRACTION, ^{18}O EQUILIBRATION, AND pH AND DISSOLVED OXYGEN DETERMINATIONS	
II-1 Introduction	30
II-2 Stripping of total dissolved inorganic carbon from seawater for ECO_2 and $^{13}\text{C}/^{12}\text{C}$ analyses	30
II-3 ECO_2 extraction efficiency experiments .	37
II-4 Experimental procedures for deter- mination of $\delta^{18}\text{O}$ of water samples	50
II-5 Theory of equilibration technique	53
II-6 Experimental technique for $\delta^{18}\text{O}$ assay ..	57
II-7 Accuracy and precision of $\delta^{18}\text{O}$ analysis.	63
II-8 Determination of pH of seawater	71
II-9 Determination of dissolved oxygen concentration of seawater by modified Winkler titration	75

	<u>Page</u>
CHAPTER III THE MASS SPECTROMETER AND ASSOCIATED EXPERIMENTAL TECHNIQUES	
III-1 Introduction	79
III-2 General description of mass spectro- meter	80
III-3 Mass analyser and vacuum system	82
III-4 Gas handling system	85
III-5 Ratio measurement system	86
III-6 Mass spectrometry errors, correction factors and data reduction	88
III-7 Selection of optimal operating characteristics	108
III-8 Mass spectrometry precision and accuracy	134
CHAPTER IV THE PRESERVATION AND STORAGE OF OCEANOGRAPHIC WATER SAMPLES	
IV-1 Introduction	146
IV-2 Alterations in samples during storage ..	147
IV-3 Closed system biological fractionation experiments	148
IV-4 Effective poisoning and storage of samples	174

	<u>Page</u>
CHAPTER III THE MASS SPECTROMETER AND ASSOCIATED EXPERIMENTAL TECHNIQUES	
III-1 Introduction	79
III-2 General description of mass spectro- meter	80
III-3 Mass analyser and vacuum system	82
III-4 Gas handling system	85
III-5 Ratio measurement system	86
III-6 Mass spectrometry errors, correction factors and data reduction	88
III-7 Selection of optimal operating characteristics	108
III-8 Mass spectrometry precision and accuracy	134
CHAPTER IV THE PRESERVATION AND STORAGE OF OCEANOGRAPHIC WATER SAMPLES	
IV-1 Introduction	146
IV-2 Alterations in samples during storage ..	147
IV-3 Closed system biological fractionation experiments	148
IV-4 Effective poisoning and storage of samples	174

	<u>Page</u>
CHAPTER V MEASUREMENTS IN THE EASTERN TROPICAL PACIFIC OCEAN	
V-1 Introduction	181
V-2 General oceanography	184
V-3 Hydrographic features	189
V-4 Chemical features	223
V-5 Summary	253
 CHAPTER VI RESULTS FROM ANTARCTIC WATERS	
VI-1 Introduction	256
VI-2 General oceanography of the Antarctic region	257
VI-3 Hydrographic features	271
VI-4 Chemical and isotopic results	294
 APPENDIX 1	304
 APPENDIX 2	319
 REFERENCES	324

LIST OF FIGURES

	<u>Page</u>
I-1 Carbon isotope variations in nature	5
II-1 Vacuum line for ΣCO_2 extraction	31
II-2 Sample pipette and transfer system	35
II-3 Variation of sample temperature during ΣCO_2 stripping	47
II-4 Theoretical vs. experimental $\delta^{18}\text{O}(\Sigma\text{CO}_2-25\text{S})$ plot.	51
II-5 Equilibration vessels for $\delta^{18}\text{O}$ determinations ..	58
II-6 Vacuum line for $\delta^{18}\text{O}$ sample pretreatment and drying	59
III-1 Schematic layout of mass spectrometer	81
III-2 Infinite bridge null system	87
III-3 Typical recorder output trace for 45/44 measurement	93
III-4 Scan through CO_2 spectrum	101
III-5 Typical spectrum of instrument background	105
III-6 Schematic diagram of gas handling system	111
III-7 Variation of 45/44 ratio with major beam intensity	113
III-8 Variation of 46/(44+45) ratio with major beam intensity	114
III-9 Variation of 45/44 ratio with major beam intensity at different capillary settings	115
III-10 Variation of major beam intensity with analyser pressure	118

	<u>Page</u>
III-11 Variation of overlap of peak 40 onto 41 with changing peak 40 current for Argon	120
III-12 Variation of I_{41} with I_{40} at constant pressure ..	122
III-13 Variation of overlap current with analyser pressure at constant major beam current	123
III-14 Variation with electron energy voltage of:	
(a) major beam; (b) 46/(44+45)ratio;	
(c) 45/44 ratio	127
III-15 Variation of major beam intensity with half plate voltage	128
III-16 Variation of major beam intensity with ion repeller voltage	130
III-17 Variation of 45/44 ratio with ion repeller voltage	131
III-18 Variation of ion source current with ion repeller voltage	132
III-19 Reduction of pressure effect with amplifier zero .	135
III-20 $\delta^{13}\text{C}$ rel. to PDB of working standard check for analyses 31 to 44	138
III-21 $\delta^{13}\text{C}$ rel. to PDB of working standard check for analyses 81 to 94	139
III-22 $\delta^{18}\text{O}$ rel. to PDB of working standard check for analyses 31 to 44	140
III-23 $\delta^{18}\text{O}$ rel. to PDB of working standard check for analyses 81 to 94.....	141
IV-1 Assimilation and regeneration of phosphate by bacteria	149

IV-2	ΣCO_2 and its $\delta^{13}\text{C}$ and $\delta^{18}\text{O}$ as a function of storage time	151
IV-3	ΣCO_2 and its $\delta^{13}\text{C}$ and $\delta^{18}\text{O}$ as a function of dark storage time for two types of storage vessel	157
IV-4	The variation of $\delta^{18}\text{O}$ with $\delta^{13}\text{C}$ of ΣCO_2 during sample storage	159
IV-5	Variation of dissolved gases with time since collection for Bartlett experiment	165
IV-6	Variation of isotope ratios of ΣCO_2 with time since collection for Bartlett experiment	166
IV-7	All results of Bartlett storage experiment plotted against storage time	170
V-1	Locations of eastern tropical Pacific Stations .	182
V-2	Temperature <u>vs.</u> depth at eastern tropical Pacific Stations	201
V-3	Salinity <u>vs.</u> depth at eastern tropical Pacific Stations	202
V-4	Dissolved oxygen <u>vs.</u> depth at eastern tropical Pacific Stations	203
V-5	Oxygen saturation profile at eastern tropical Pacific Stations	204
V-6	Subsurface temperature profile at eastern tropical Pacific Stations	207
V-7	Subsurface salinity profile at eastern tropical Pacific Stations	208

V-8 Subsurface dissolved oxygen profile at eastern tropical Pacific Stations 209

V-9 Entire profile θ -S plot for eastern tropical Pacific Stations 211

V-10 θ -S plot for eastern tropical Pacific deepwater. 212

V-11 θ -S for Bartlett Station 3 deepwater 213

V-12 θ -S for Bartlett Stations 5 and 7 deepwater 214

V-13 Dissolved oxygen vs. pot. temp. plot for Bartlett deepdata..... 217

V-14 $\delta^{18}\text{O}$ vs. depth for Bartlett samples 220

V-15 $\delta^{18}\text{O}$ - θ plot for Bartlett Stations 221

V-16 $\delta^{18}\text{O}$ -S plot for Bartlett Stations 222

V-17 AOU profile at eastern tropical Pacific Stations 228

V-18 pH at 30°C vs. depth for eastern tropical Pacific Stations 239

V-19 pH in situ vs. depth for Bartlett Stations 241

V-20 ΣCO_2 vs. depth for eastern tropical Pacific Stations 246

V-21 $\delta^{13}\text{C}$ vs. depth for eastern tropical Pacific Stations 251

V-22 Variation of $\delta^{18}\text{O}$ with $\delta^{13}\text{C}$ for Bartlett ΣCO_2 samples 252

VI-1 Antarctic water mass structure - schematic 263

VI-2 Temperature distribution at Cruise 47 Stations . 274

VI-3 Salinity distribution at Cruise 47 Stations 275

VI-4 Dissolved oxygen distribution at Cruise 47 Stations 276

	<u>Page</u>
VI-5 Oxygen saturation at Cruise 47 Stations	277
VI-6 θ -S for complete water column	281
VI-7 Subsurface θ -S plot	283
VI-8 θ -S for deep and bottom waters	284
VI-9 Profile of $\delta^{18}\text{O}$ with depth at Station 1284	288
VI-10 $\delta^{18}\text{O}$ -S plot for Cruise 47 samples	289
VI-11 $\delta^{18}\text{O}$ - θ plot for Cruise 47 samples	290
VI-12 AOU profiles at Cruise 47 Stations	295
VI-13 ΣCO_2 profile at Cruise 47 Stations	301
VI-14 $\delta^{13}\text{C}$ profile for Cruise 47 samples	302

LIST OF TABLES

	<u>Page</u>
I-1 Isotopic composition of precipitation as a function of latitude	20
II-1 Accuracy of ΣCO_2 extraction from sodium carbonate standard solutions	39
II-2 Precision of ΣCO_2 extraction from sets of sea water samples	41
II-3 Reproducibility of $\delta^{13}\text{C}$ of ΣCO_2 extracted from seawater	42
II-4 Precision of $\delta^{18}\text{O}$ analysis of seawaters by Epstein-Mayeda technique	64
II-5 Accuracy of $\delta^{18}\text{O}$ of water by analysis of international standard waters	65
II-6 Isotopic shift in $\delta^{13}\text{C}$ of CO_2 used for equilibration	67,68
II-7 Results of large-scale equilibration experiment.	70
II-8 Reproducibility of pH measurements in successive analyses	76
II-9 Reproducibility of dissolved oxygen determinations using the Manostat Digipet	77
II-10 Reproducibility of dissolved oxygen using the Agla Microburet	78
III-1 Statistical variations within an analysis	98
III-2 Carbon dioxide spectrum	102
III-3 Background conditions	106

	<u>Page</u>
III-4 Comparison of 'pressure effect' characteristics	133
III-5 Short-term reproducibility of measurement	137
III-6 Statistics for working standard check analyses	142
IV-1 Results of Bartlett closed system biological fractionation experiments	164
IV-2 Results for samples poisoned with 4 ml.l. ⁻¹ Hg Cl ₂ solution and stored in glass bottles with ground glass stoppers	175
IV-3 Comparison of different types of storage vessel	177
IV-4 ΣCO ₂ results for samples stored in crown capped bottles with natural cork inserts	179
V-1 Location of oceanographic stations used in discussion of oceanography of eastern tropical Pacific	192
V-2 Re-assigned salinities at Bartlett Station 3 ..	195
V-3 Hydrographic properties at Bartlett Station 3 .	197
V-4 Hydrographic properties at Bartlett Station 5 .	198
V-5 Hydrographic properties at Bartlett Station 7..	199,200
V-6 Bottom water hydrographic characteristics at Bartlett Stations 3, 5 and 7	216
V-7 Results of δ ¹⁸ O of water for Bartlett samples .	219
V-8 Apparent oxygen utilisation at Bartlett Station 3	224
V-9 Apparent oxygen utilisation at Bartlett Station 5	225

	<u>Page</u>
V-10 Apparent oxygen utilisation at Bartlett	
Station 7	226
V-11 Standardising buffers for Bartlett Station 5 ...	232
V-12 Comparison of pH-defining scales for Bartlett	
Station 5	234
V-13 pH measurements at Bartlett Station 3	236
V-14 pH measurements at Bartlett Station 5	237
V-15 pH measurements at Bartlett Station 7	238
V-16 ΣCO_2 and its stable isotope ratios at Bartlett	
Station 3	243
V-17 ΣCO_2 and its stable isotope ratios at Bartlett	
Stations 5	244
V-18 ΣCO_2 and its stable isotope ratios at Bartlett	
Station 7	245
VI-1 Antarctic sampling station locations	272
VI-2 Depths of prominent hydrographic features at	
Cruise 47 Stations	280
VI-3 $\delta^{18}\text{O}$ results at Station 1284	286
VI-4 $\delta^{18}\text{O}$ results at Stations 1270, 1308, 1314	287
VI-5 $\delta^{18}\text{O}$ analyses of surface waters from Cruise 52 .	293
VI-6 ΣCO_2 and $\delta^{13}\text{C}$ at Cruise 50 Station 5.....	296
VI-7 ΣCO_2 results at Station 1270	297
VI-8 ΣCO_2 and its isotope ratios at Station 1284	298
VI-9 ΣCO_2 and its isotope ratios at Station 1308	299
VI-10 ΣCO_2 and its isotope ratios at Station 1314	300

SUMMARY

The fractionation between different stable isotopic species of the elements carbon and oxygen provides a powerful tool for investigation of various physical, chemical and biological processes in nature. Complex systems involving the interaction of several such processes can be studied by combining isotope ratio measurements with other suitable data. The oceans constitute one of the most important of these systems; the distribution of carbon and oxygen in the sea is governed by a balance amongst physical, chemical and biological forces so that information on the isotopic abundances can be profitably used in oceanographic description.

In this work, experimental techniques for determination of $\delta^{18}\text{O}$ of seawater, and extraction and measurement of total dissolved inorganic carbon (ΣCO_2) from seawater and its $\delta^{13}\text{C}$ assay are described. The assumptions involved in these methods are investigated and the associated errors discussed, in particular with regard to the mass spectrometry. The storage of oceanographic water samples between collection and analysis may allow biological activity to alter the dissolved oxygen/carbon system. Inconsistencies in previously published work are pointed out and experiments are detailed which illustrate that temporal ΣCO_2 and $\delta^{13}\text{C}$ variations mirror the changes known to occur in the bacterial population of seawater stored without the addition of poison. Different types of storage vessel are investigated for preserving sample integrity and it is concluded that the importance of immediate poisoning

and proper storage has been seriously underestimated in much previous work.

Water samples have been collected from areas of the Pacific and Antarctic Oceans, and analysed for $\delta^{18}\text{O}$ of the water, ΣCO_2 and its $\delta^{13}\text{C}$ and, in some cases, pH and dissolved oxygen. The $\delta^{18}\text{O}$ results have been taken in conjunction with conventional hydrographic data to provide descriptions of the physical oceanography of the regions; water mass structure and mixing has been elucidated and discussed. In the light of this, the ΣCO_2 , $\delta^{13}\text{C}$, pH and dissolved oxygen measurements have been used to investigate the chemical and biological regimes. Comparison of the results of several different investigators in the Pacific has suggested that systematic errors may exist between directly and indirectly determined ΣCO_2 values. The regional oceanography deduced from this research has been in general accord with commonly accepted views derived from other studies.

CHAPTER I

INTRODUCTION

I-1 Prolegomena

The theoretical foundation on which modern stable isotope geochemistry is built was laid in Urey's seminal paper on the thermodynamic properties of isotopic substances (Urey, 1947). For the light elements H, C, O and S the practical problems of instrumentation were substantially solved by the mass spectrometer designed and built by Nier (1947), and modified and improved by McKinney et al. (1950). In 1957, Craig provided a detailed account of procedures for isotope ratio calculation and standardisation. Major technical difficulties in sample preparation were overcome by McCrea (1950), Epstein and Mayeda (1953), Friedman (1953), Craig (1953) and Deuser and Hunt (1969) amongst many others. The potential of stable isotopes as a tool in oceanographic studies was soon recognised and projects for measurement of $^{13}\text{C}/^{12}\text{C}$, $^{18}\text{O}/^{16}\text{O}$ and D/H ratios in the marine environment were initiated. Progress made in selected areas up to the present will be briefly discussed in later sections of this chapter.

I-2 Carbon in the oceans

Because of the extreme complexity of its chemistry, the behaviour of carbon in the oceans is only inadequately known: because of the importance of carbon in oceanic chemistry,

this ignorance is extended to the more general system. Carbon is reasonably abundant in the ocean (28 mg.l.^{-1}) and is combined in more chemical compounds than any other element (Deuser, 1974, claims that carbon 'forms more chemical compounds than all other elements combined' - a statement of interesting logic). It is fundamental to the life cycle, and the major reservoirs of carbon - atmosphere, biosphere, continent, ocean and sediment - are in constant interaction. Due to the very large number of compounds in which it is involved, particularly organic compounds, carbon is considered to play a major role in the marine chemistry of various other elements, the heavy metals for example. As a result of its ecological significance, there is at the present time considerable interest in the impact on the oceans of man-made carbon compounds, both as organic and inorganic waste products. In particular, there is controversy regarding the ability of the oceanic carbonate system to absorb, without serious consequence, the vast output of CO_2 from the burning of fossil fuels. Unfortunately, there does not seem to be a good, unbiased yet comprehensive review of this topic in the recent literature, (and that would be rather outside the scope of this thesis); the problem has been tackled from a variety of viewpoints, often with conflicting results. Among the more important contributions within the last few years are those of Broecker et al. (1971), Zimen and Altenhein (1973), Fairhall (1973), Whitfield (1974) and Pytkowicz (1973). One major source of

contention is the reaction of the upper layers to an increase in atmospheric partial pressure of CO_2 ; this can be traced directly to the poorly understood chemistry of the oceanic carbonate system. The concentration of carbon dioxide dissolved in seawater may be changed by the following four processes:

- (i) exchange with the atmosphere,
- (ii) biological uptake during photosynthesis and other processes,
- (iii) production during respiration and decay,
- (iv) formation and solution of solid calcium carbonate.

As has been pointed out by Deuser (1974), although not even 1% of the terrestrial living organic matter resides in the ocean, the amount of dead organic matter in the ocean is greater than the combined amounts of living matter both on land and in the sea. The levels of dead organic matter in the sea are quite well known (although there is some discrepancy between Russian data and those of other workers, see Menzel and Ryther, 1968), but its chemical form, participation in biological processes and eventual fate are still problematical. The topic has recently been discussed at some length by Menzel (1974), in what Calvert (1975) has termed a 'timely, if partisan, review'. One potentially powerful way in which deeper insight may be gained into the behaviour of carbon in the sea is through the study of the distribution of the carbon isotopes. Carbon has two stable isotopes with mean per cent abundances of:

$$^{12}\text{C} : ^{13}\text{C} = 98.89 : 1.11$$

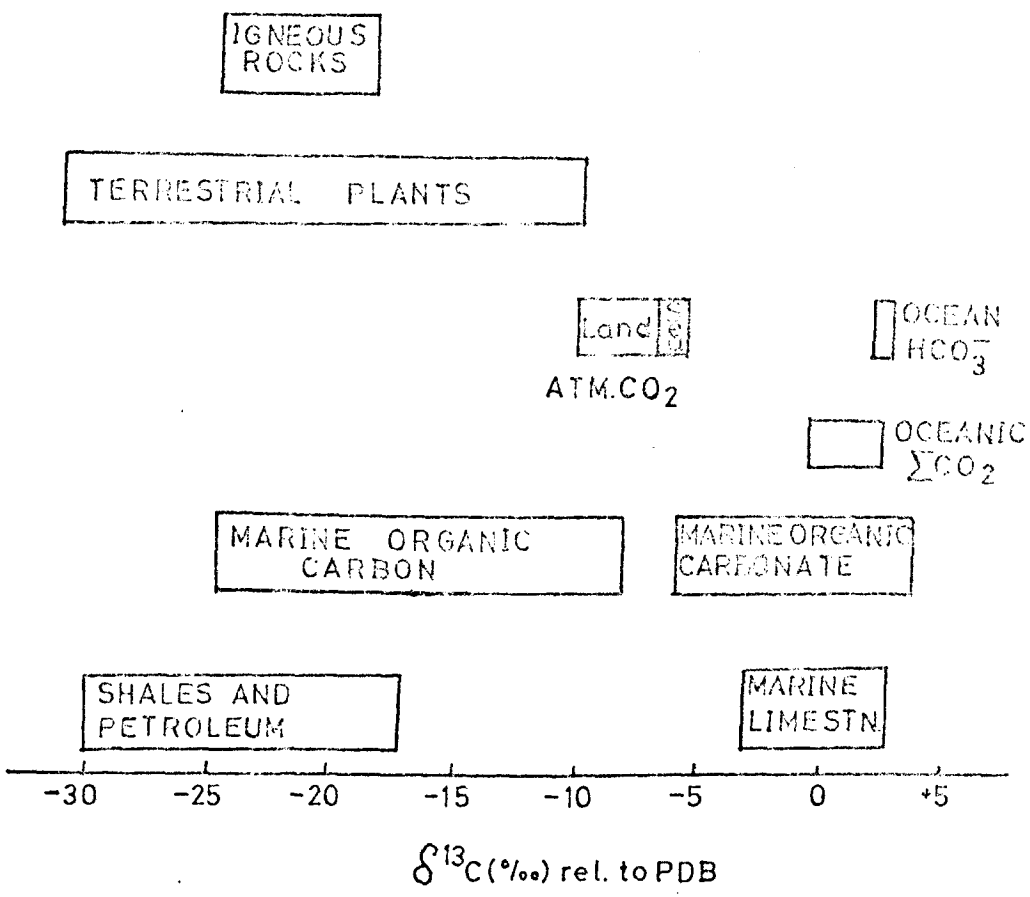
Stable carbon isotope variations in some natural reservoirs are shown in Figure I-1 (the isotope ratios R_S are given as delta values, δ , reported relative to a standard R_R :

$$\delta = \left(\frac{R_S}{R_R} - 1 \right) 10^3$$

and expressed as part per thousand. The standard in Figure I-1 is PDB limestone). $^{13}\text{C}/^{12}\text{C}$ ratios in dissolved and particulate organic matter in the ocean have been studied by Williams and Gordon (1970). Measurements were made down to 4 km. both in the Gulf of Mexico and off the coast of California, but the deep water values found (-21.2 to -24.4‰ relative to the standard PDB) were independent of location and time of year. Furthermore, similar values to those for dissolved material were found for particulates (-22.0 to -24.3‰) and for sediment organic material (-20.8 to -22.3‰), but considerably different values for organic material derived from the Amazon River (-28.5 to -29.5‰). The authors showed that oceanic values were close to those of the cellulose and lignin fractions of phytoplankton, -22.4‰ and -23.1‰ respectively, and concluded that the organic detritus in deep water has marine plankton as its primary source, with the soluble and particulate fractions having similar chemical composition. In previous work, Williams et al. (1969) had measured the ^{14}C age of deep water soluble organic materials as 3,400 years.

FIGURE I-1

CARBON ISOTOPE VARIATIONS IN NATURE (after KROOPNICK, 1970).



The proportions of biologically important elements participating in the biochemical cycle in the sea are governed by the composition of the biomass. Redfield et al. (1963) in a review of this subject presented the atomic ratios:

$$P : C : O : N = 1 : 106 : -276 : 16$$

for the main elements involved in synthesis and degradation. (Since nitrogen and phosphorus are frequently limiting nutrients, there is no a priori reason, of course, why the logic of the above should not be inverted, i.e. the composition of the present biomass is a reflection of the initial concentration of these elements, non-limiting carbon and oxygen then being fixed by stoichiometric considerations. However, it is more orthodox to adopt the former viewpoint.) Thus in the oxidation of phytoplankton, or indeed zooplankton since they have similar elemental compositions (Redfield et al., 1963), 138 moles of oxygen are consumed for every 106 moles of carbon oxidised : $CO_2/O_2 = 106/138 = 0.77$. Most of the biological cycle in the sea is confined to the upper few hundred metres, so that the rain of organic detritus to the deeper layers may not necessarily have the same composition as the bulk of the detritus. Also, other processes such as advection and diffusion alter the deep water concentrations of dissolved nutrients; the former is often catered for by reverting to 'pre-formed' values, the latter - being more difficult to deal with - is frequently neglected, as for example in the model of Postma (1964) which considers the

mass balance of the deep water with particulate, but not diffusive, downward flux. By normalising total CO_2 values (denoted ΣCO_2 and defined by the equation:

$$\Sigma\text{CO}_2 = \text{CO}_2 (\text{diss.}) + \text{H}_2\text{CO}_3 + \text{HCO}_3^- + \text{CO}_3^{2-}$$

to constant chlorinity and allowing for CO_2 produced by solution of carbonate, Postma calculated $\text{CO}_2/\text{O}_2 = 0.82$ in the deep Pacific. Culberson and Pytkowicz (1970) improved Postma's model by taking into account preformed ΣCO_2 and preformed alkalinity; for two east Pacific stations they obtained $\text{CO}_2/\text{O}_2 = 0.75$, in good agreement with the value of Redfield et al. (1963). However, some doubt is attached to the accuracy of the ΣCO_2 data of Culberson and Pytkowicz; this will be discussed in Chapter V. Edmond (1974), in an analysis based, not only on Pacific, but also on Indian - Antarctic profiles, consistently obtained the value 0.865, and even greater ratios have been given : 1.0 by Craig (1969) and approximately 1.2 by Li et al. (1969). These discrepancies have not been resolved at the present time; the situation is not materially improved by appealing to the suggestion of Postma (1964) that, since phosphorus and nitrogen are more rapidly released in descent through the water column, a relatively higher amount of carbon is transported to the deep water - for direct chemical analyses by several workers (Holm-Hansen et al., 1966; Menzel and Ryther, 1968; Holm-Hansen, 1969) indicate that P:C:N ratios of particulate and dissolved organic matter are depth invariant.

Apart from carbon dioxide liberated in respiration and the oxidation of organic material, the deep water also gains carbon dioxide in the solution of the shells of carbonate excreting organisms. This can be considered as an inorganic process: the solubility of calcite in the oceans actually increases with pressure and decreasing temperature -- and so with depth. The inverse process, inorganic precipitation of calcium carbonate is thought to be strongly inhibited by the presence of dissolved organic matter (Suess, 1970) and by the magnesium ion (Pytkowicz, 1965), though neither case is fully understood. The depth at which there is balance between the downward flux of calcareous tests from the upper layers and their dissolution is called the 'compensation depth', and varies with geographical location, current flow and water mass characteristics. Edmond has compiled much of the previous work done on this (Edmond and Gieskes, 1970) and has presented it, together with his own results, in an interesting comparison with the distribution of dissolved silica (Edmond, 1974). In the latter reference, the various explanatory models (equilibrium, steady state and chemical kinetic) used in the study of the calcite compensation depth are critically examined in the light of the most precise data available. The contribution to total dissolved carbon dioxide from the dissolution of carbonate is given by the carbonate alkalinity. Because carbonate and bicarbonate ions are involved in association complexes with various cations, thermodynamic activities are rarely used in marine chemistry,

but rather 'apparent' constants are determined empirically and related to the theoretical thermodynamic activities by activity coefficients. Recent determinations of the dissociation constants of carbonic acid in seawater at atmospheric pressure have been made by Mehrbach et al. (1973) and by Hansson (1972), and have been compared in the former reference. The pressure dependence of the constants has been investigated by Culberson and Pytkowicz (1968).

Apart from temperature and salinity, four parameters are of interest in the study of the carbonate chemistry of seawater. These are:

- (i) pH,
- (ii) the partial pressure of CO_2 , $p\text{CO}_2$,
- (iii) the alkalinity A,
- (iv) the total dissolved carbon, ΣCO_2 .

The total alkalinity and carbonate alkalinity differ by a term due to boric acid; the necessary correction can be made via the chlorinity. Of the four, only two are independent; Park (1969) has discussed the relative merits of the various combinations and has given equations for calculation of ΣCO_2 and its component species in each case. Involved in these equations, of course, are the apparent dissociation constants of carbonic acid referred to above. During the 1969 Geosecs intercalibration cruise, the carbonate chemistry parameters were measured by several workers using a wide variety of techniques (Takahashi et al., 1970); those for ΣCO_2 had previously been successfully compared by analysis of

standard sodium carbonate solutions. However, for seawater, disagreement outside the experimental error was found between directly measured values and those calculated, using Lyman's (1956) dissociation constants, from the measurement of other parameters. It was pointed out (Takahashi et al., 1970) that the discrepancies could be resolved, and the internal consistency restored, by a $(30 \pm 10)\%$ error in Lyman's value for the second apparent dissociation constant of carbonic acid. On the basis of the recent measurements of Hansson (1972) and Mehrbach et al. (1973), such an error is unlikely, yet evidence is presented in Chapter V which confirms the systematic difference in the results of the direct and indirect evaluations of ΣCO_2 . Further discussion is reserved until Chapter V.

From the foregoing, it is apparent that several methods are available for studying the balance of carbon dioxide in the deep ocean. Firstly, the production of CO_2 can be calculated directly by ΣCO_2 measurement and the increase due to carbonate dissolution found from alkalinity measurement. That resulting from organic decomposition may be estimated either by calculating the consumption rate of dissolved oxygen from vertical profiles and using a Redfield-type 'model plankton' multiplying factor such as 0.77, or alternatively, the source of added carbon dioxide can be identified by measurement of stable carbon isotope ratios.

I-3 Oxygen in the oceans

(a) Dissolved oxygen

In the oceans, the distribution of dissolved oxygen is governed by processes of production, consumption and internal mixing. Near the surface, oxygen exchange between the atmosphere and sea maintains a 'mixed' layer in which the oxygen concentration is close to equilibrium, i.e. the partial pressures of oxygen in the water and in the air are almost equal. The direction of the exchange depends to a large extent on the history of the seawater: that upwelled from the deep is usually undersaturated whereas in regions of intense photosynthesis supersaturation may occur, leading to oxygen transfer from ocean to atmosphere. The depth of the near-equilibrium zone is not a fixed feature, but varies both in time and space depending on the local oceanographic and meteorological conditions. Subsurface production of oxygen takes place in the euphotic zone; here photosynthesis dominates over respiration and the increase in dissolved oxygen may lead to concentrations greater than the equilibrium level. Again, the depth is variable - ranging from less than one to over one hundred metres.

There are two major processes of oxygen consumption, viz. respiration, both plant and animal, and oxidation of organic material. Whereas phytoplankton respiration is unlikely to be of importance below about 400 - 500 m., that of zooplankton and larger animals may occur at all depths. Much of the oxygen depletion during decomposition is carried

out by bacteria in the upper few hundred metres of the water column. There is disagreement as to whether or not consumption of oxygen is significant below about 400 m. in the sea. In a series of papers, Menzel and Ryther (Menzel and Ryther, 1968; Menzel, 1970; Menzel and Ryther, 1970) have argued that the decomposition of organic matter is restricted, in general, to shallow depths, any small changes in the deep being masked by circulatory processes. Their conclusions were based on the uniformity of profiles of dissolved organic carbon (DOC) and particulate carbon with regard to both depth and location, and on their demonstration that within the Antarctic Intermediate Water, oxygen changes can be attributed solely to mixing. Mann et al. (1973) have supported the latter on the basis of the silicate distribution in the western basins of the Atlantic Ocean. Ogura (1970) has also presented evidence that the deep DOC is in a highly refractory form not easily decomposed by bacteria. Similar depth distributions of dissolved and particulate organic matter in regions of differing surface productivity imply little relationship between the two. This has been inferred by Menzel (1967) who concluded that the levels of suspended and particulate organic matter in the euphotic zone and in the underlying water were independent. His conclusion has been challenged by Romankevich (1971) on the basis of a synoptic set of data from the eastern Pacific upwelling region which: 'confirm the existence of a genetically conditioned relationship between the amount and distribution

of phytoplankton, its production, suspended matter in the photic zone and in the water itself, heterotrophic microorganisms, organic matter and benthos in bottom deposits.

In situ biological consumption of oxygen in the deep ocean has been a major feature of several important models. Richards (1957) has reviewed early work in this field and in a later paper (Richards, 1965) gives references for some of the more recent contributions. Prominent among the former is Riley's (1951) study of salinity, temperature, oxygen and nutrients in the Atlantic Ocean. By using the general equation for the distribution of variables (see, for example, Sverdrup, Johnson and Fleming, 1942) he calculated the changes attributable to physical processes of advection and diffusion, and considered the balance as his estimate of the rate of biological consumption. Wyrcki (1962), noting that these rates decreased exponentially with depth, represented them by the equation:

$$R = R_0 e^{-\alpha z}$$

where R and R_0 are the consumption rates at depths z and zero, respectively, and α is a constant. The calculated values of R_0 varied from 60 to 140×10^{-10} ml.l.⁻¹ and of α from 3 to 4×10^{-5} cm.⁻¹. In order to explain the depth distribution of dissolved oxygen, Wyrcki (1962) invoked a model in which vertical advection and diffusion dynamically balanced the oxygen consumption. Munk (1966) discussed the scope and physical background of the model and computed a consumption

rate of $4 \times 10^{-3} \text{ ml.l.}^{-1}\text{yr.}^{-1}$ based on it. The vertical-advection, vertical-diffusion approach was extended by Craig (1969) to ΣCO_2 , alkalinity and ^{14}C and then (Craig, 1970) to $^{13}\text{C}/^{12}\text{C}$ of dissolved inorganic carbon. He found that not only were in situ production and consumption necessary, but also that oxidation of local dissolved organic carbon was insufficient to explain the observed profiles, a particulate flux was also required. The model will be further discussed in section 4 of this Chapter.

In a study of calcium carbonate saturation in the oceans, Li et al. (1969) also attributed the deep excess of CO_2 to oxidation of organic matter. Using Riley's (1951) value of $2 \times 10^{-3} \text{ ml.l.}^{-1}\text{yr.}^{-1}$ for the oxygen depletion rate, together with the Stommel-Arons model of abyssal circulation of the world ocean (see section I-4), Kuo and Veronis (1970) solved the two dimensional advection-diffusion-decay equation numerically and obtained good agreement with observational data for the horizontal distribution of dissolved oxygen. They have since brought their estimate up to date (Kuo and Veronis, 1973).

Menzel and Ryther (1968) have claimed that their data 'argue against respiration and the decomposition of organic matter at depth only to the extent that these processes do not appear to have a measurable effect on^a the in situ concentration of oxygen and dissolved organic carbon.' This view has been effectively criticised by Craig (1971) from several angles. Firstly, the Intermediate Waters are a poor

choice on which to base conclusions about long-term consumption processes; in such water masses the ratio of the relative time scales for mixing and for consumption is much greater than unity, so it is not surprising that linear oxygen-salinity relationships are obtained and that mixing effects are dominant. This objection does not apply to the deep waters of the Pacific Ocean and, adopting the requirements of particulate flux and in situ oxygen consumption, Craig (1971) then proceeded to predict the depth dependence of the extrema of both O_2 and ΣCO_2 in the deep Pacific, and to show good agreement with observation. (It is worth noting here that the critical equation (2) of Craig's paper which gives the variation of Z_{XT} , the depth of the oxygen extremum, with latitude is not strictly correct. In Craig's notation, the term multiplying $\frac{dZ_m}{d\phi}$ can easily be shown to be:

$$1 - \frac{Z^* \left(\frac{J/w}{J/w - L'} \right) + \frac{1}{E}}$$

and not:

$$1 - \frac{Z^*}{Z_m} + \frac{1}{E}$$

as in Craig's version. Presumably the calculations performed by Craig used the correct version and (2) merely represents a misprint). A similar program based on the Menzel-Ryther approach would face grave, if not unsurmountable, difficulties. Menzel has recently given an extended account of his views on the subject and deals with some of the points raised against them (Menzel, 1974), but the apt remarks of Calvert (1975)

in his review referred to in section 2 of this chapter should be borne in mind.

(b) Isotopic composition of dissolved oxygen

There are three naturally occurring stable isotopes of oxygen : ^{16}O , ^{17}O and ^{18}O with respective per cent. abundances of 99.76, 0.04 and 0.20. At the present time, technical expertise is not sufficiently developed to permit measurement of variations of ^{17}O , but experimental methods have been developed for assay of ^{18}O changes in a wide variety of environmental fields. In recent years, the study of dissolved oxygen in the oceans has been extended to measurement of its stable isotope ratio $^{18}\text{O}/^{16}\text{O}$, like carbon usually reported as a per mil delta value relative to a standard (Kroopnick, 1971; Horibe and Shigehara, 1972; Kroopnick, Weiss and Craig, 1972). Unfortunately, there seems to have been little work reported in the open literature so far, the first two above references being a doctoral dissertation and the abstract of a conference paper, respectively; consequently only a few brief remarks will be made here.

Since isotope fractionation is involved in the various processes which link the oxygen reservoirs in nature, these reservoirs are typified by different oxygen isotope ratios. In particular, atmospheric oxygen is approximately 23.5‰ (Kroopnick and Craig, 1972) enriched in the heavy isotope relative to SMOW (Standard Mean Ocean Water, which is close to the average expected of seawaters, Craig 1961). Since the bulk of photosynthetic production of oxygen takes place

in the ocean, and in this process the oxygen source has been shown to be water (Ruben et al., 1941), this result is somewhat surprising and cannot be explained by ocean-atmosphere equilibration; it is often referred to as the Dole-Morita effect (e.g. Kamen and Barker, 1945) after the workers who originally observed it. Following earlier suggestions by Barker (quoted in Lane and Dole, 1956) and Rabinowitch (1945), Kroopnick postulated that the effect was due to fractionation during respiration, and presented evidence to support this claim (Kroopnick, 1971). The variation of $\delta^{18}\text{O}$ of dissolved oxygen with depth was also studied by Kroopnick (1971) for several stations in the Pacific Ocean. Comparison of oxygen isotope fractionation in surface and deep waters showed similarities which he interpreted as corroborating the existence of a deep metabolism with consumption of oxygen in the abyss.

(c) Stable isotopes of oxygen in ocean waters

In the oceans H_2^{18}O , like salinity and enthalpy (or temperature), is a 'conservative' property. (There are occasional exceptions to this; for example temperature may have to be excluded sometimes on account of significant heat flux through the sea floor.) By this is meant that the concentration changes caused by biological or geochemical activity are negligible - conservative constituents are those whose distribution is essentially governed by physical oceanographic processes. However, as pointed out by Craig and Gordon (1965), ^{18}O as a tracer has an additional degree

of freedom over salinity, for whereas dissolved salt characterises the complete seawater solution, ^{18}O is specific to the water itself. The initial impetus for the investigation of $\delta^{18}\text{O}$ variations in ocean waters would appear to have come from the field of paleotemperature studies. Because the calculation of a temperature from a carbonate $\delta^{18}\text{O}$ involves knowledge of the $\delta^{18}\text{O}$ of the water in which the carbonate was secreted, it was natural that variations in $\delta^{18}\text{O}$ of natural waters should be of interest. The first systematic project for measurement of $\delta^{18}\text{O}$ in such waters was reported by Epstein and Mayeda (1953). The importance of this study was that it demonstrated that changes in the isotopic system were not always identical to those in the salt system, so that in certain cases ^{18}O may be considered as a quasi-independent tracer. The most striking example of this was that seawater diluted by melting ice could easily be isotopically distinguished from that in mid-ocean of the same salinity but influenced by local precipitation. In addition, Epstein and Mayeda (1953) concluded that not only the salinity, but also the isotopic composition of shallow ocean waters were dependent for their present value on the existence of large polar masses of ice and snow. This, of course, would be of importance in paleotemperature work. This conclusion has, however, been strongly challenged by Craig and Gordon (1965); their paper probably represents the most comprehensive application yet undertaken of the stable molecular isotopic species of water to the study of the oceans and the marine

atmosphere. Samples were collected from most areas of the world's oceans and the results combined in a coherent model of the interaction of the atmosphere - surface ocean system. Attention was also paid to problems of deep water genesis; in particular, Craig and Gordon suggested, on isotopic evidence that the 'third component' of Pacific Deep Water (in addition to deep water from the Atlantic and Antarctic) was likely to be Atlantic Intermediate Water, in opposition to the view of Bolin and Stommel (1961) who considered it to be Pacific Intermediate Water. However, the main effort as regards the deep waters was to broadly characterise the various masses; the topic of intermediate water formation was not dealt with.

The different relationships between salinity and isotope ratio in different oceanic regions is intimately connected to variations in the composition of precipitation which, in Table I-1, is shown as a function of latitude (data from Craig and Gordon, 1965). Ratio differences arise from the fact that whereas the effects of evaporation and precipitation on salinity depend solely on the total water lost, those on oxygen isotopes are also influenced by the ratio of evaporation to precipitation. Thus information can be gained from isotopic data which is not given by salinity alone.

Craig and Gordon (1965) also introduced some useful concepts with regard to δ -S diagrams in stable isotope oceanography (here S represents salinity). These are similar to conventional T-S diagrams except that surface and upper

TABLE I-1

Isotopic composition of precipitation as a function of latitude (Craig and Gordon, 1965).

LATITUDE	FRACTION OF TOTAL PRECIPITATION	$\delta^{18}\text{O}$ OF MEAN (RELATIVE TO SMOW)
0°-20°	0.5	-2‰
20°-40°	0.4	-5‰
40°-90°	0.1	-15‰

waters can be more easily accommodated; this is because the large temperature variations seen at these depths have no isotopic counterpart. δ -S diagrams are thus likely to be particularly useful in upper mixing studies in intermediate and high latitudes. In a T-S diagram, two curves representing separate water masses intersect at a point of common density; in general, however, two water types known as 'pycnotypes' must be ascribed to this point, for they may differ in isotopic composition. Analogously, in the δ -S diagram the intersection of two water mass curves specifies two water types of equal isotopic composition but possibly differing in density; these have been termed 'isotypes' by Craig and Gordon (1965). In conclusion, the distribution of ^{18}O in subsurface ocean waters is governed by the physical processes of advection and mixing of water which has obtained its ^{18}O content at the sea surface as a result of fractionation by evaporation or freezing and by dilution with meltwater, continental runoff or precipitation. The heavy isotopic species of water H_2^{18}O imparts a conservative property to seawater which is used in Chapters V and VI in conjunction with temperature and salinity to characterise water types and to examine the processes by which they mix to form different water masses.

I-4 Ocean models

Many of the problems encountered in attempting to solve the general hydrothermodynamic equations are usually attributed to non-linear characteristics. However, von

Neumann (as reported by Kirwan, 1965) has conjectured that the difficulty lies rather in the lack of a variational principle. The most common approach is to derive specific results from simplified fluid models by solving an abbreviated set of equations. An interesting - and frequently forgotten - feature is that only the density distribution is determined by equations of motion, the other terms in the equation of state (in practice, these reduce to temperature T and salinity S at the appropriate pressure) then being arranged to give the required density at each point. The mass field established, the circulation pattern imposed by geostrophic, thermohaline and wind stress forces places constraints on the distribution of chemical properties.

Stommel (1957) has reviewed early work on theories of ocean currents; his paper is remarkable in that it succeeds in presenting a rigorous exegesis of the various models without resorting to abstruse mathematical manipulation. The assumptions involved, their elaboration and consequences are all treated descriptively and the interconnections between different approaches are exposed in a coherent fashion. Together with several co-workers, Stommel then proceeded to develop a theory of abyssal circulation of the world ocean (Stommel and Arons, 1960(a) and (b); Bolin and Stommel, 1961; Arons and Stommel, 1967; Stommel and Arons, 1972). The dynamical content was derived from the theory of the oceanic thermocline presented by Robinson and Stommel (1958) and from experimental determinations of stationary

planetary flow patterns in bounded basins (Stommel, Arons and Faller, 1958). The model postulated two intense sources of abyssal waters, one being in the Weddell Sea, the other in the North Atlantic. Over the region of the ocean characterised by the existence of the main thermocline, there was a uniformly distributed upwelling of water from the deep to shallower layers in compensation. The magnitudes of the fluxes involved were estimated from classical oceanographic data.

In the model, frictional and eddy effects did not enter into the dynamics: interior flow was balanced geostrophically and only at the basin sides, defined by continental masses, was the geostrophic restraint relaxed in the boundary currents found there. On the other hand, it was well known that eddy diffusivity, both in the horizontal and vertical planes, could not be neglected in many instances of the distribution of tracer properties of water masses (e.g. dissolved oxygen, salinity, etc.). However, Stommel and Arons (1960(b)), by comparing the leading terms in the dynamical equations and the equation describing the flux divergence of a tracer, succeeded in showing that Austausch coefficients sufficiently large to play an important role in defining tracer distributions were nevertheless negligible in considering the dynamics of the basic flow. At the same time, they advised caution in inferring basic flow patterns from observed tracer distributions, because of the significance for the latter of small-scale diffusion effects. In parts IV (Bolin and Stommel,

1961) and III (Arons and Stommel, 1967) of the sequence of papers, the implications of the general circulation for tracer distributions were considered. In the former reference, a 'box model' approach was used, but in the latter this was abandoned in favour of a more sophisticated advection - lateral mixing model; the tracers investigated were temperature, salinity, dissolved oxygen and radiocarbon. Part V (Stommel and Arons, 1972) dealt with some consequences of bottom topography on the inertial boundary currents.

The use of box models in oceanographic studies has been quite common, particularly among radiochemists (Craig, 1958; Broecker, 1963; Wright, 1969; among many others). The general theory of such reservoir models has been discussed by Keeling and Bolin (1967, 1968) and applied by them to a suite of eight chemical tracers in the Pacific Ocean. In essence, dividing the ocean into a number of compartments corresponds to a finite difference approximation of the governing equations; transfer coefficients are related to the more physically meaningful advective and diffusive coefficients of the appropriate space-averaged transport equation. (This must not be interpreted as implying that the latter concepts are free from difficulties).

An alternative approach is to treat the processes of advection and diffusion more directly - in the differential equations, where relevant including source/sink functions and mechanisms for decay. Such a model has been used by Koczy (1958) for radium, by Wyrтки (1962) for oxygen and 'in various

forms goes back to oceanographic antiquity' (Munk, 1966). The inclusion of vertical small scale mixing processes via a parametric 'eddy conductivity' in the theoretical model of Robinson and Stommel (1958) was explicitly stated to be a last resort. Although the order of magnitude of the mixing could be estimated with reasonable confidence (being approximately five hundred times the molecular diffusion coefficient), the physics of the mixing process remained obscure. The situation is probably best summarised by a (rather lengthy) quotation from Stommel (1957):

'... the parametric treatment of the eddy coefficients is exceedingly primitive and misleading. Even if oceanic turbulence at mid-depths is not directly related to the mean flow, it is desirable to have some physical understanding as to what causes this turbulence. At present we simply regard these coefficients as given arbitrarily, at best we infer them from water mass analysis. Our models are, so to speak, externally stirred.'

Munk (1966) described the advection-diffusion model as applied to vertical distributions of temperature, salinity, oxygen, radium and radiocarbon in the central Pacific, and further discussed how to interpret meaningfully the rates of upwelling and diffusion he inferred. The former he related to the volume of bottom water entering the Pacific from the Antarctic each year, and annual budgets of influx and upwelling were found to be in good accord. Various interpretations of the vertical eddy diffusivity or Austausch coefficient were

attempted: boundary mixing, internal tides and thermo-dynamic and biological processes were all investigated, but none found wholly satisfactory. It may be worth remarking, parenthetically, that the problems involved with turbulent processes are notoriously difficult. In 1900, David Hilbert formulated what he considered to be the 23 leading problems in mathematics. In May 1974, a committee of the world's foremost mathematicians drew up a revised version of his list, included in which was 'providing an analytical (rather than statistical) description of turbulence.' (Anon., 1974).

The two dimensional advective-diffusive-decay equation was solved numerically by Kuo and Veronis (1970) for ^{14}C and dissolved oxygen, and a value for the horizontal eddy diffusivity coefficient obtained (around $10^7 \text{ cm.}^2 \text{ sec.}^{-1}$). These authors have recently improved their estimate (Kuo and Veronis, 1973) based on a better method of solution and revised and updated results. Following Munk (1966), the application of the model to explain vertical distributions of tracer properties was pursued by Craig and his colleagues (Craig, 1969; 1970; 1971; Kroopnick, Deuser and Craig, 1972; Kroopnick, 1971; Chung, 1971). They considered a one-dimensional case in which steady state vertical profiles of dissolved components may be taken as independent of interior horizontal flow, so that any tracer with stationary vertical distribution (in the Eulerian sense) can be described by a two point boundary value problem; the profile is solely determined by the upper and lower boundary concentrations, production and decay rates

in the interior and a single mixing parameter with the dimensions of depth. This, the so-called 'scale depth', has a particularly simple physical interpretation. Care must be taken, however, in the physical interpretation of the deduced advection and diffusion parameters, since, for example, horizontal transport processes may be parametrically disguised under vertical eddy diffusion. In dealing with models of this type, the stricture of Munk (1966) should always be borne in mind: 'Until the processes giving rise to diffusion and advection are understood, the resulting differential equations governing the interior distribution, and their solutions, must remain what they have been for so long: a set of recipes.'

I-5 Aims of research

From the discussions in the previous sections of this chapter, it is apparent that the ΣCO_2 /dissolved oxygen system - the major system of non-conservative tracers in the ocean - offers a fruitful field for future long-term study. Not only may much useful immediate information be gleaned from the various parameters of the system, but the mutually exclusive interpretations placed on existing data by different workers may be resolved when a sufficiently world-wide coverage of the oceans has been completed. At the present time, the results are inadequate for firm, definite conclusions to be drawn. There is however, one serious drawback; as Edmond (1974) has commented in connection with the vertical advection-diffusion approach:

'The model makes explicit one of the major obstacles to study in marine chemistry, namely, that a quite complex knowledge of the physical circulation is required before information about specifically chemical processes can be extracted from profiles, sections or maps of species distributions. This problem finds ironic expression in the frequent observation that dissolved species may be a useful tracer of water masses.'

It follows from this that isotope data relating directly to the water, e.g. $^{18}\text{O}/^{16}\text{O}$, D/H can play an important role in the necessary elucidation of the physical oceanography of the appropriate region and hence facilitate the interpretation of observations on the chemical system.

Relatively few oceanographic parameters can be measured in situ; consequently, samples are usually brought to the surface and frequently returned to shore laboratories before the various measurements are performed. These procedures obviously introduce far-reaching assumptions, particularly with regard to the effects of pressure, temperature, illumination and biological activity. It is considered that these assumptions merit further study. The major aims of this research project were therefore:

- (i) development of techniques for extraction of total inorganic carbon from seawater, its volume measurement and stable isotope assay.
- (ii) construction of equilibration systems for determination of $\delta^{18}\text{O}$ of water samples.

(iii) optimisation of mass spectrometer used for isotope analysis and calibration of laboratory working standard gas relative to internationally accepted standards.

(iv) investigation of sources of error, limitations of technique, and validity of assumptions involved in the above methods and appropriate calculations.

(v) study of sampling and storage conditions for oceanographic samples.

(vi) use of $\delta^{18}\text{O}$ of seawater together with conventional hydrographic data to deduce physical structure of selected areas of the ocean.

(vii) application of pH, ΣCO_2 , $\delta^{13}\text{C}$ and dissolved oxygen to study of chemical processes in oceanographic areas described via (vi), so extending and expanding regional coverage.

CHAPTER II

EXPERIMENTAL METHODS FOR ΣCO_2 EXTRACTION, ^{18}O EQUILIBRATION, AND pH AND DISSOLVED OXYGEN DETERMINATIONS.

II-1 Introduction

Description and discussion of the apparatus and experimental techniques used in this work will be divided between two chapters. In this one, attention will be focussed on the procedures for ΣCO_2 extraction from aqueous solutions, and on oxygen isotope equilibration between water and carbon dioxide. The on-board methods used for the determination of dissolved oxygen and pH of seawater will also be mentioned briefly. In the following chapter, the mass spectrometer and associated instrumental techniques will be described.

II-2 Stripping of total dissolved inorganic carbon from seawater for ΣCO_2 and $^{13}\text{C}/^{12}\text{C}$ analyses.

Total dissolved inorganic carbon (ΣCO_2) comprising HCO_3^- , CO_3^{2-} , H_2CO_3 and CO_2 (dissolved) is extracted from seawater by acidification with 100% orthophosphoric acid and subsequent spargefication with pure nitrogen in a pyrex glass vacuum line shown diagrammatically in Figure II-1. The method is a modification of that originally used by Swinnerton and colleagues (Swinnerton et al. 1962(a) and (b)) in chromatographic studies. Similar techniques have been reported by

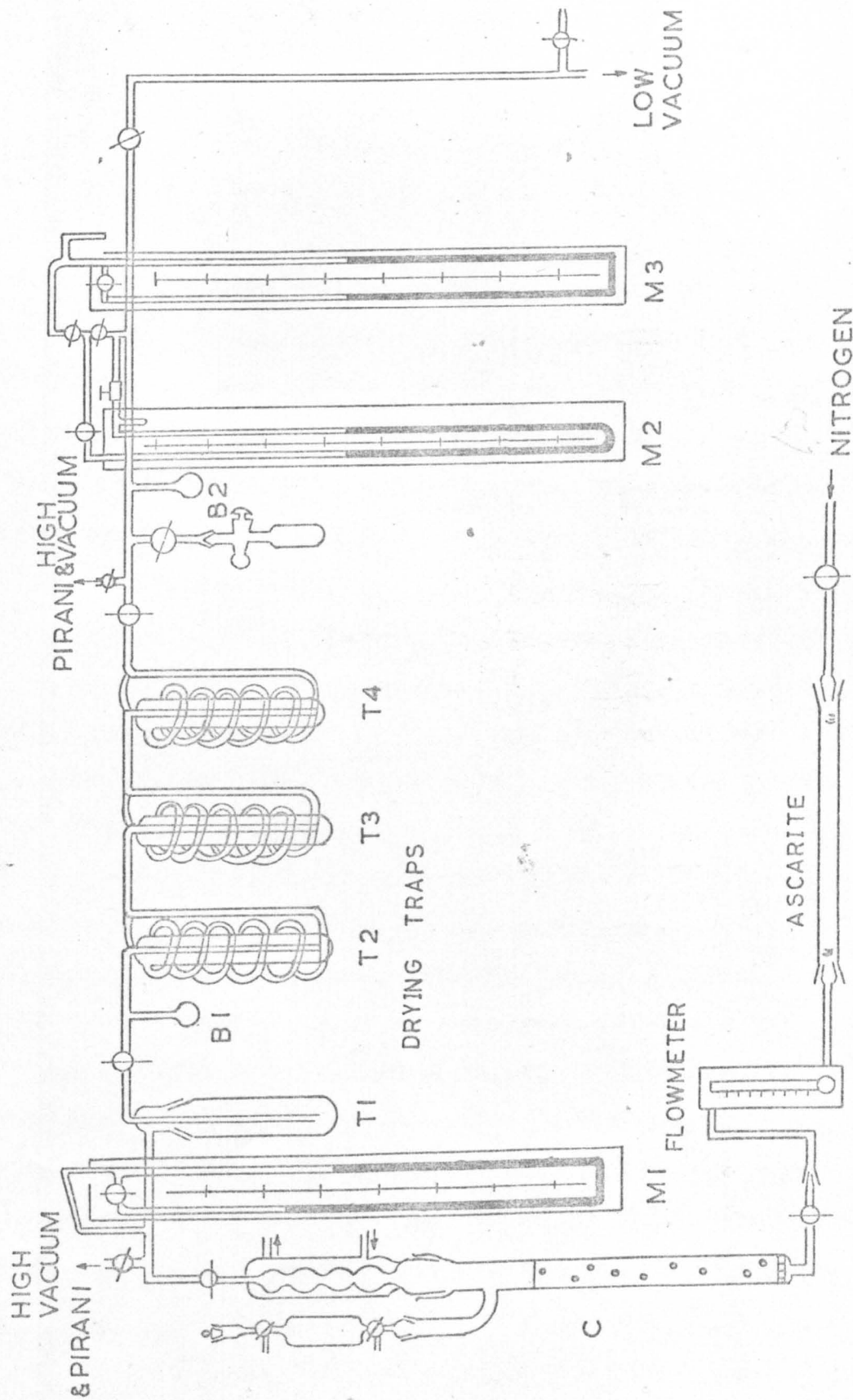


FIGURE II-1 VACUUM LINE FOR CO_2 EXTRACTION.

Deuser and Hunt (1969) and by Kroopnick (1974(a)). The stripping column, 50 cm. long and 2 cm. in diameter, has at the bottom a glass frit which both contains the sample and breaks up the flow of stripping gas into a stream of fine bubbles. A 1 ml. aliquot of 100% H_3PO_4 is injected into the column C, and a previously calibrated constant volume pipette holding the sample is attached. The system is evacuated to the vapour pressure of the acid and the 50 ml. water sample admitted to C. During the evacuation, any CO_2 originally dissolved in the acid is released. Pure CO_2 -free nitrogen, obtained by passing tank N_2 through columns of chromatographic grade 50-100 mesh silica gel and then Ascarite, flows through the glass frit and bubbles through the acidified sample at a rate controlled by the flowmeter. The pipette is flushed with acidified CO_2 -free water and this is added to the column.

The half-time for removal of CO_2 as a function of gas flow rate and stripping period has been studied by Weiss and Craig (1973). They found excellent agreement between measured half-times and those calculated by assuming that the removal follows a Rayleigh 'batch distillation' model with the bubbles of stripping gas in equilibrium with the gas in solution. For a flow rate of 40 ml. min.^{-1} (STP) at room temperature, the extraction half-time is typically of the order of one minute. In practice, flow rates in the range 40 ml. min.^{-1} to 60 ml. min.^{-1} and extraction times from 10 min. to 20 min. are used; during this time the pressure rises by

50-100 torr. The stripping nitrogen and extracted gases are allowed to expand through the water-cooled condenser and dry-ice cooled trap T_1 into the three spiral traps (T_2 , 3 and 4) cooled by liquid nitrogen. The non-condensable gases are then pumped off, the water vapour and carbon dioxide remaining condensed in the system. The pressure in the vacuum line is reduced to 10^{-3} torr. to ensure removal of all of the nitrogen; the dry-ice/acetone trap is isolated, the condensed water warmed to release dissolved CO_2 , refrozen at -78°C and opened to the spiral traps at -196°C . Transfer of CO_2 is assumed complete after 5 minutes and the set of three traps isolated. The liquid nitrogen coolant on T_2 and T_3 is replaced by a slush of dry-ice and acetone at -78°C , and the carbon dioxide thoroughly dried by repeated passes through these two traps. Finally, the stopcock to the manometer section of the line is opened and the CO_2 transferred. The traces of water frozen in T_2 and T_3 are melted and then refrozen, and the CO_2 released added to that already condensed in the manometer section. Any non-condensable gases remaining are removed by opening the line to the high vacuum manifold. The volume of CO_2 gas collected is then measured on the two manometer systems M_2 and M_3 . Removal of all of the CO_2 from the sample during the first stripping can be checked by re-stripping: such blank measurements are carried out frequently and the acceptable maximum is taken as 0.01 ml.STP, the limit of detection.

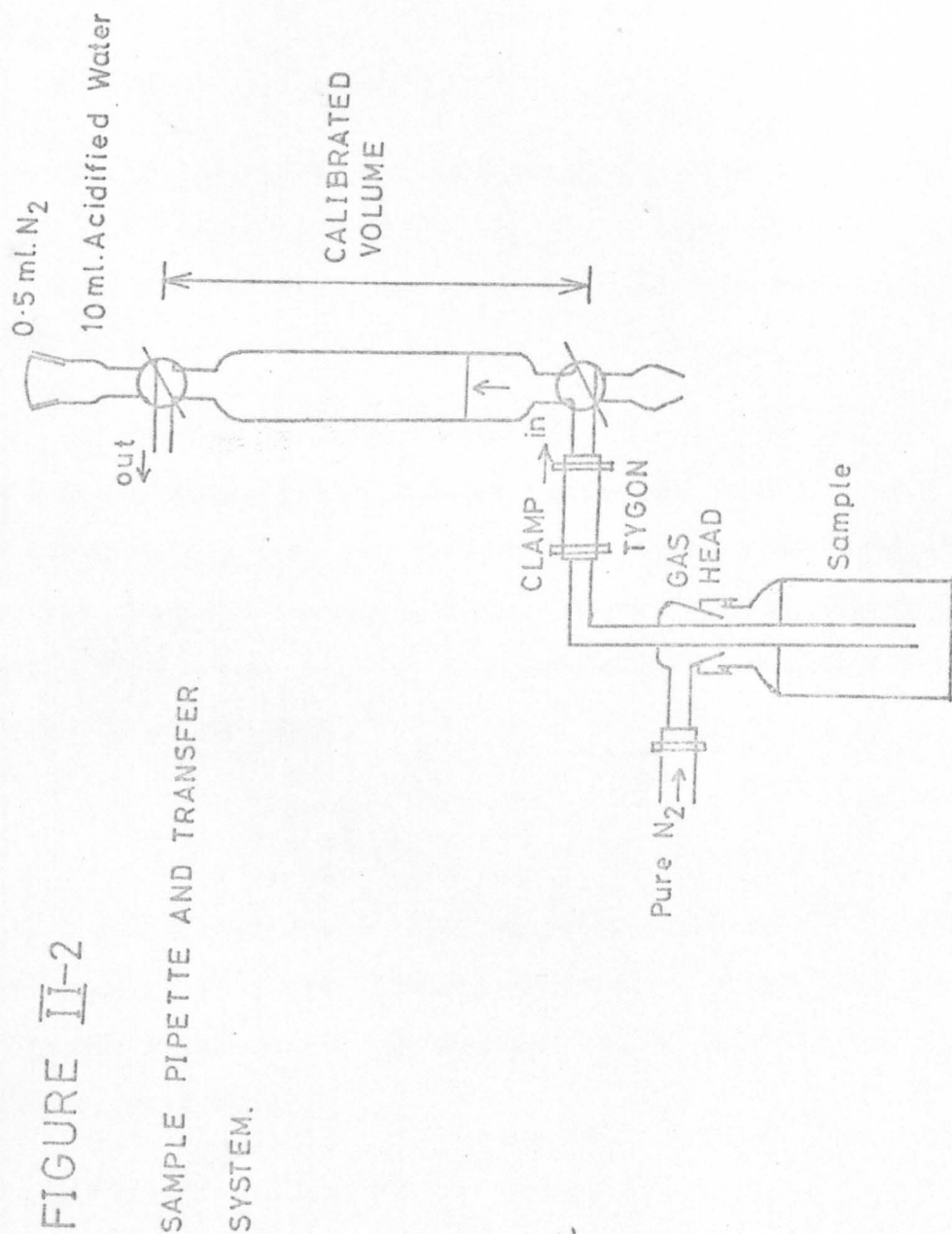
Accurate ΣCO_2 measurements require the following:

(i) no CO_2 exchange between the atmosphere and sample prior to extraction,

(ii) precise calibration of the constant volume pipettes and of the manometer systems.

(Questions of sampling, preservation and storage are, for the time being, ignored). To prevent contact of the seawater sample with the atmosphere, the pipettes are filled with pure nitrogen before introduction of the samples. Gas heads were constructed for each type of storage vessel used; a typical example of a sample transfer is shown in Figure II-2. Using the appropriate gas head, any storage vessel can be directly attached to the pipette and the sample forced in by a constant pressure of pure nitrogen. The pipette is first flushed with its own volume of sample (where possible) and then filled, carefully avoiding the inclusion of bubbles. The pipettes were calibrated by weighing them empty and when filled with distilled water, and using the conversion tables in the "Handbook of Chemistry and Physics" (Weast, 1966).

Three mass spectrometer sample bottles were adopted as standard volumes after gravimetric calibration with mercury; these were then used to calibrate the two manometers by transferring known quantities of pure dry CO_2 to each manometer system and measuring the resultant pressure. The direct readings of pressure were modified according to



formulae given by Kroopnick (1971). Firstly, account is taken of the ambient temperature, the temperature dependence of the density of mercury and the gravitational constant at Glasgow:

$$PA = \frac{P_{raw}}{76} (1 - 0.000181t) 1.001 \frac{273.15}{273.15+t}$$

where P_{raw} is the directly measured pressure in cm.Hg, t is the ambient temperature in °C, and PA is the corrected pressure in atmospheres. Secondly, allowance is made for the non-ideality of carbon dioxide:

$$P = \frac{0.99315 PA}{(1 - PA(0.006611 - 0.00006 t))}$$

A polynomial relationship between corrected pressure and volume for each system was deduced from these data using the Edinburgh Regional Computing Centre curve fitting package program IPAPP which fits the observations to a series of polynomials of the form:

$$Y = X \sum_{i=0}^n A_i X^i$$

(so that $Y = 0$ when $X = 0$ i.e. there is no pressure reading in the absence of gas). The experimental accuracy did not warrant the consideration of $i > 2$ and the 'best fit' equations found were:

$$v = P(13.44 + 4.13P - 0.60P^2) \quad \text{system } M_1;$$

$$v = P(6.818 - 1.457P + 1.951P^2) \quad \text{system } M_2$$

For volumes of carbon dioxide of the order of 2 ml., the standard deviation of fit was less than 1% in each case. The system M_1 can cope with larger volumes than can M_2 , but for either the fractional error on a volume measurement for the reading error on a pressure is less than 0.5%. The accuracy of the manometers was demonstrated during extraction efficiency experiments described below; the intercalibration of the two manometer systems was excellent.

II-3 Σ CO₂ extraction efficiency experiments.

The combined efficiency of pipette calibration, CO₂ extraction and volume measurement was determined in a series of experiments in which standard sodium carbonate solutions and sets of seawater samples were analysed. The carbonate solution measurements also provide an estimate of the accuracy of the technique.

The sodium carbonate was dried after the method of Vogel (1951) and CO₂-free water prepared following Wong's (1970) technique. In summary, analytical reagent grade anhydrous sodium carbonate (manufactured by BDH Chemicals Ltd., specified not less than 99.9% Na₂CO₃ after drying) was heated in a thermostatically controlled electric oven at 260-270°C for approximately 30 minutes until its weight was constant, and then cooled in a vacuum dessicator. Attempts to measure the NaO content by X-ray powder diffraction technique proved inconclusive because of the poor quality of the images obtained. For the water, CO₂-

free nitrogen was bubbled through boiling, freshly distilled water for about 1 hour, and the purged water allowed to cool under the nitrogen stream. Weighed quantities of the carbonate were then dissolved in the water to provide the standard solutions. In the first two cases (standard solutions S1 and S2) the amount of water was determined gravimetrically and in the third case (standard solution S3), volumetrically. Total dissolved inorganic carbon was calculated from knowledge of the volume of extracted gas v (ml.), calculated as described previously, and of the sample pipette V_{pip} (ml.), by substitution in:

$$\Sigma CO_2 = \frac{v}{22.261 V_{pip} \rho_t}$$

In this equation, ΣCO_2 is in $Mkg.^{-1}$ (the unit advocated by Dyrssen and Sillén (1967) as being pressure and temperature independent), and ρ_t is the sample density at the extraction temperature (taken as $1.026 kg.l.^{-1}$ for all seawater samples. That this approximation introduces no appreciable error can be easily seen, for $d\Sigma CO_2 / \Sigma CO_2 \sim d\rho_t / \rho_t$ and, in the ocean, the latter is generally less than 10^{-3}). The results for the three standard solutions are shown in Table II-1; there is good internal agreement within each set (precision at 1σ better than 1%) and also excellent agreement for the mean of each set with the expected yield (accuracy within 1%). The accuracy of the procedure established, the precision for seawater was investigated by analysing in multiple three

TABLE II-1

STANDARD	THEORETICAL ΣCO_2 (mM kg. ⁻¹)	MEASURED ΣCO_2 (mM kg. ⁻¹)	YIELD DEVIATION
S1 FEB. 1972	2.348	2.353	-0.2%
		2.344	+0.2%
	MEAN	2.349±0.006	+0.04%
S2 FEB. 1972	1.629	1.631	
		1.624	
	MEAN	1.628±0.005	-0.06%
S3 SEPT. 1973	1.978	1.999	+1.0%
		1.963	-0.8%
		1.987	+0.5%
		1.986	+0.4%
	MEAN	1.984±0.015	+0.3%

Accuracy of ΣCO_2 extraction from sodium carbonate standard solutions.

different seawater samples of five, six and four aliquots respectively. The results are presented in Table II-2 and indicate that the 1 σ precision for seawater extraction is also 1%. It must be pointed out that the accuracy and precision estimated above refer to the ideal case for a particular bottle of seawater in the laboratory. There are major problems involved in sampling, preservation and storage, and all of these may cause the routinely measured ΣCO_2 to deviate from its initial in situ value. This will be discussed in some detail in a later chapter. As expected for such complete extraction, the $\delta^{13}\text{C}$ error is reduced to the mass spectrometry error; this is illustrated by the results presented in Table II-3.

In the mass spectrometric assay of the extracted gas, the m/e 45 ion beam consists of not only $^{13}\text{C}^{16}\text{O}^{16}\text{O}$, but also $^{12}\text{C}^{16}\text{O}^{17}\text{O}$, so provision for the latter must be made in the $\delta^{13}\text{C}$ calculation. The required correction is most easily applied through the $\delta^{18}\text{O}$ of the gas (as will be explained in Chapter III); for $\delta^{13}\text{C}$ to be accurate to 0.01‰, the appropriate $\delta^{18}\text{O}$ must be known to better than 0.5‰. Kroopnick (1974(a)) has claimed that the $\delta^{18}\text{O}$ of extracted ΣCO_2 is determined by the temperature of the water sample during extraction, at equilibrium being governed by the equation:

$$\delta^{18}\text{O}(\text{CO}_2)\text{‰} = 5.1 - 0.21t \quad (\text{II-3-1})$$

where t is the extraction temperature in $^{\circ}\text{C}$, and $\delta^{18}\text{O}$ is expressed relative to CO_2 which has been equilibrated against

TABLE II-2.

GROUP 1	GROUP 2	GROUP 3
ΣCO_2 mM kg. ⁻¹	ΣCO_2 mM kg. ⁻¹	ΣCO_2 mM kg. ⁻¹
1.944	2.215	2.275
1.928	2.200	2.278
1.959	2.176	2.286
1.983	2.214	2.288
1.940	2.200	Mean:2.282±0.005
Mean:1.951±0.019	2.195	1σ Precision:0.2%
1σ Precision:1%	Mean:2.200±0.014	
	1σ Precision:0.6%	

Precision of ΣCO_2 extraction from sets of seawater samples

TABLE II-3

Reproducibility of $\delta^{13}\text{C}$ of ΣCO_2 extracted from seawater.

GROUP 1	GROUP 2
$\delta^{13}\text{C}_{\text{PDB}}$	$\delta^{13}\text{C}_{\text{PDB}}$
-2.87‰	-3.05‰
-2.77‰	-2.99‰
-2.80‰	-2.90‰
Mean: (-2.81 ± 0.05) ‰	-2.97‰
	Mean: (-2.98 ± 0.05) ‰

SAMPLES: Clyde seawater samples; yields
for each group internally consistent
to 1% at 1σ .

SMOW (the international water standard used for reporting oxygen isotope results) at 25°C. This expression is taken by Kroopnick as giving $\delta^{18}\text{O}$ correctly to within 0.5‰.

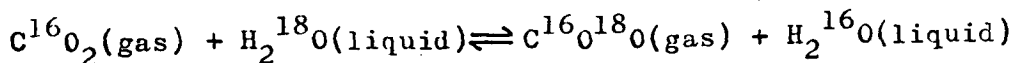
There are two assumptions which are adopted implicitly in using the above procedure to calculate $\delta^{18}\text{O}$. These are:

(i) that the 'extraction temperature' is a well-defined concept, and

(ii) that the extracted CO_2 gas is in isotopic equilibrium with the liquid water sample at the 'extraction temperature'.

If the validity of (i) and (ii) is granted, a further restriction which arises is that the $\delta^{18}\text{O}$ of the water sample relative to SMOW must be less than 0.5‰ in magnitude.

This will be shown later. The right-hand side of equation (II-3-1) is an approximate form of the polynomial in t by which Bottinga and Craig (1969) represented their results for the temperature variation of α , the fractionation factor for the oxygen isotope exchange reaction:



Denoting the $^{18}\text{O}/^{16}\text{O}$ ratio of CO_2 in equilibrium with a water sample at $t^\circ\text{C}$ by $R(\text{CO}_2/\text{SAM})_t$, and of the water itself by $R(\text{SAM})$, then by definition:

$$\alpha_t = R(\text{CO}_2/\text{SAM})_t / R(\text{SAM})$$

and the Bottinga-Craig equation (given as equation (3) in 1969) is:

$$\left(\frac{\alpha_t}{\alpha_{25}} - 1 \right) 10^3 = 5.112 - 0.214t + 0.00041t^2 \quad (\text{II-3-2})$$

Now it follows directly from the definition of α that:

$$\frac{\alpha_t}{\alpha_{25}} = \frac{R(\text{CO}_2/\text{SAM})_t}{R(\text{CO}_2/\text{SAM})_{25}}$$

so the equation:

$$\delta(\text{CO}_2)^\circ/\text{‰} = 5.112 - 0.214t + 0.00041t^2 \quad (\text{II-3-3})$$

is true for CO_2 in equilibrium with the water sample at temperature t relative to CO_2 in equilibrium with the same water at 25°C , and not relative to CO_2 in equilibrium with SMOW at 25°C as claimed by Kroopnick (1974(a)). To investigate when this discrepancy will lead to significant error, the notation $\delta(t\text{S}-25\text{SMOW})$ will be adopted for $\delta^{18}\text{O}$ of CO_2 equilibrated against a water sample S at temperature t relative to that of the same gas equilibrated against SMOW at 25°C . Then, by (II-3-3):

$$\delta(t\text{S}-25\text{S}) = 5.112 - 0.214t + 0.00041t^2$$

According to (II-3-1), (allowing for the legitimate approximation made to the polynomial):

$$\delta(t\text{S}-25\text{SMOW}) = 5.112 - 0.214t + 0.00041t^2$$

However:

$$\delta(t\text{S}-25\text{SMOW}) = \delta(t\text{S}-25\text{S})(1 + 10^{-3}\delta(25\text{S}-25\text{SMOW})) + \delta(25\text{S}-25\text{SMOW})$$

and by definition (Craig, 1961), $\delta(25\text{S}-25\text{SMOW})$ is the $\delta^{18}\text{O}$ of the water sample on the SMOW scale, here denoted $\delta(\text{W}-\text{SMOW})$. Hence, only as long as the absolute value of $\delta(\text{W}-\text{SMOW})$ is less than $0.5^\circ/\text{‰}$, does (II-3-1) hold to within $0.5^\circ/\text{‰}$, as claimed earlier. On the other hand, for waters which differ from SMOW in $\delta^{18}\text{O}$ by more than $0.5^\circ/\text{‰}$, the more correct

expression (II-3-3) should be applied. This is likely to be of importance mainly for near-surface waters affected by processes of evaporation, precipitation and run-off. For example, data from North Pacific surface samples (Expedition Leapfrog, latitudes 44-57°N) given by Craig and Gordon (1965) lie in the range $-0.5\text{‰} > \delta^{18}\text{O} > -1.0\text{‰}$. Even more striking are the figures for surface waters from the North Atlantic in Table 4 of the same paper: of the nine samples listed, only one lies within 0.5‰ of SMOW, and the others deviate by up to 11‰ , although certainly this is an extreme case.

Returning to discussion of the two assumptions involved in deducing the $\delta^{18}\text{O}$ value of ΣCO_2 from the temperature of the water at the time of extraction, differentiation of (II-3-3) with respect to t gives:

$$\frac{d\delta}{dt} = -0.214 + 0.00082t$$

so that at normal room temperatures ($\sim 20^\circ\text{C}$):

$$\frac{d\delta}{dt} = -0.20 \text{ (‰ per deg.)}$$

The required accuracy in δ is 0.5‰ so, if no other errors are present, the maximum temperature error which can be tolerated is 2.5°C . In order to study the variation of the temperature of the water sample during the extraction procedure, a special stripping column was constructed which was dimpled about 7 cm. above the frit. A chromel-alumel thermocouple (when sealed in the dimple almost totally surrounded by the sample) was connected to a Comark electronic

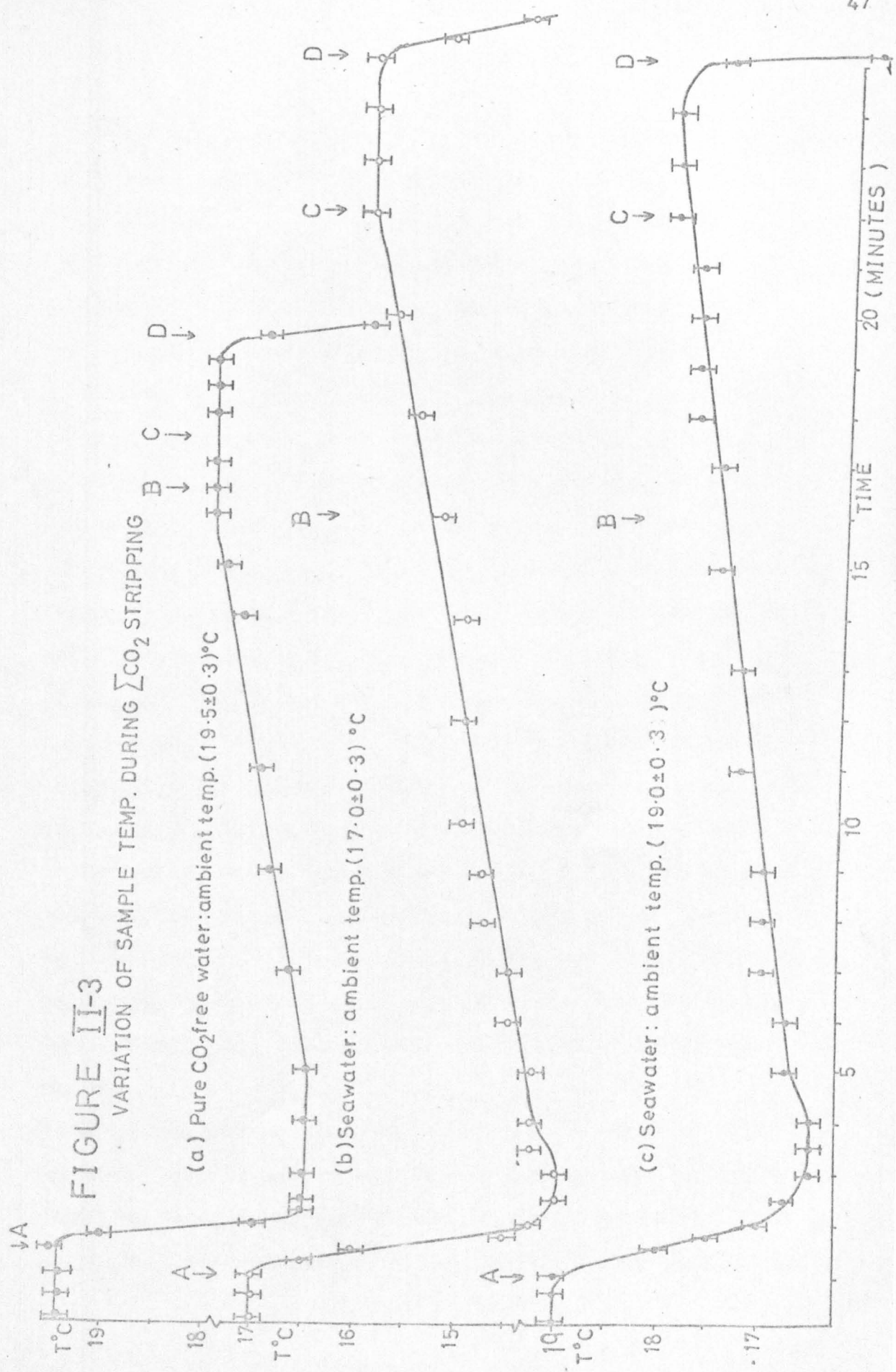
thermometer and the temperature of the sample monitored during three extraction runs, two on seawater samples and the third on one of the numerous reagent blanks run during the course of this work. The results are shown in Figure II-3 and illustrate that there is a common pattern of temperature change - so presumably this applies also to all routine extractions. To aid in the discussion of temperature changes during a typical experiment, define events A,B,C,D as follows:

- A - sample admitted
- B - stripping complete
- C - pumping off of nitrogen commenced
- D - water being pumped off.

Prior to the time of event A, the sample is at the ambient temperature. A temperature minimum is reached in the first few minutes after introduction of the sample into the column, the drop from the initial temperature being 2.5 to 3.0°C. (It is worth recalling here that the half-time for CO₂ extraction is of the order of one minute). Thereafter, the temperature slowly increases, though not in general reaching the temperature of the surroundings. Events B and C occur during this steady warming. After event D, when the pressure has fallen below about 20 torr and the liquid itself is being rapidly vapourised and the vapour pumped off, the temperature again falls rapidly. The explanation for the sudden temperature decrease is presumably the same in both cases - loss of sensible heat from the liquid to latent heat

FIGURE II-3

VARIATION OF SAMPLE TEMP. DURING Σ CO₂ STRIPPING



in the water vapour. The temperature increase between the two then represents the gradual gain of heat from the surroundings. It is thus clear that the sample experiences significant temperature changes during the course of stripping, particularly during the important first few minutes. The validity of an operational definition of 'extraction temperature' is thus dependent on the extent of kinetic isotope effects during the stripping: this leads directly to discussion of the second assumption. This - that the extracted CO_2 gas is in isotopic equilibrium with the liquid water sample at the 'extraction temperature' - is rather more difficult to deal with. Before extraction, the ΣCO_2 will be distributed among the species HCO_3^- , CO_3^{2-} , H_2CO_3 and CO_2 (dissolved), the exact fraction in each being pH dependent (Dyrssen and Sillén, 1967). Under normal circumstances, it is reasonable to assume that all species will be in oxygen isotopic equilibrium with the water at the ambient temperature (see McCrea, 1950). During the stripping process, two factors will affect the $\delta^{18}\text{O}$ of the liquid:

- (i) the addition of oxygen by acidification with H_3PO_4 , and
- (ii) loss of water vapour, and water carried in the nitrogen gas stream, which condenses on other parts of the vacuum system.

Once in the gaseous form, ΣCO_2 can exchange oxygen isotopes with the bulk liquid, water vapour, and any water droplets borne in the gas stream. To examine the consequences of the assumption that the extracted CO_2 is in equilibrium with the

water sample at the 'extraction temperature' (here, for the sake of convenience, defined as the average ambient temperature during the stripping process), the previous notation is again adopted. Thus the $\delta^{18}\text{O}$ value of the extracted ΣCO_2 relative to CO_2 in equilibrium with the water at 25°C is written $\delta(\Sigma\text{CO}_2\text{-}25\text{S})$, and so by (II-3-3):

$$\delta(\Sigma\text{CO}_2\text{-}25\text{S}) = 5.112 - 0.214t + 0.00041t^2$$

Now:

$$\delta(\Sigma\text{CO}_2\text{-}25\text{S}) = \delta(\Sigma\text{CO}_2\text{-PDB}) + \delta(\text{PDB-}25\text{S})(1 + 10^{-3}\delta(\Sigma\text{CO}_2\text{-PDB}))$$

and:

$$\delta(\text{PDB-}25\text{S}) = \frac{-\delta(25\text{S-PDB})}{1 + 10^{-3}\delta(25\text{S-PDB})}$$

so that:

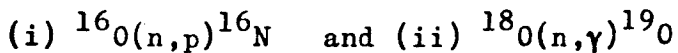
$$\delta(\Sigma\text{CO}_2\text{-}25\text{S}) = \frac{\delta(\Sigma\text{CO}_2\text{-PDB}) - \delta(25\text{S-PDB})}{1 + 10^{-3}\delta(25\text{S-PDB})} \quad (\text{II-3-4})$$

and using (II-3-3), the left-hand side of (II-3-4) may, at equilibrium, be replaced by the Bottinga-Craig polynomial in t . On the right-hand side of (II-3-4), $\delta(\Sigma\text{CO}_2\text{-PDB})$ is the $\delta^{18}\text{O}$ of the extracted ΣCO_2 relative to PDB - which is known since, in this work, it was always determined by mass spectrometric analysis - and $\delta(25\text{S-PDB})$ is the $\delta^{18}\text{O}$ of CO_2 equilibrated against the seawater sample at 25°C relative to PDB. This latter is measured when $\delta^{18}\text{O}$ of seawater is determined by the Epstein-Mayeda technique^a as described in a later section. Both sides of equation (II-3-4) can thus be calculated, and so the procedure for estimation of $\delta^{18}\text{O}$ of the extracted ΣCO_2 tested. The test, of course, is dependent

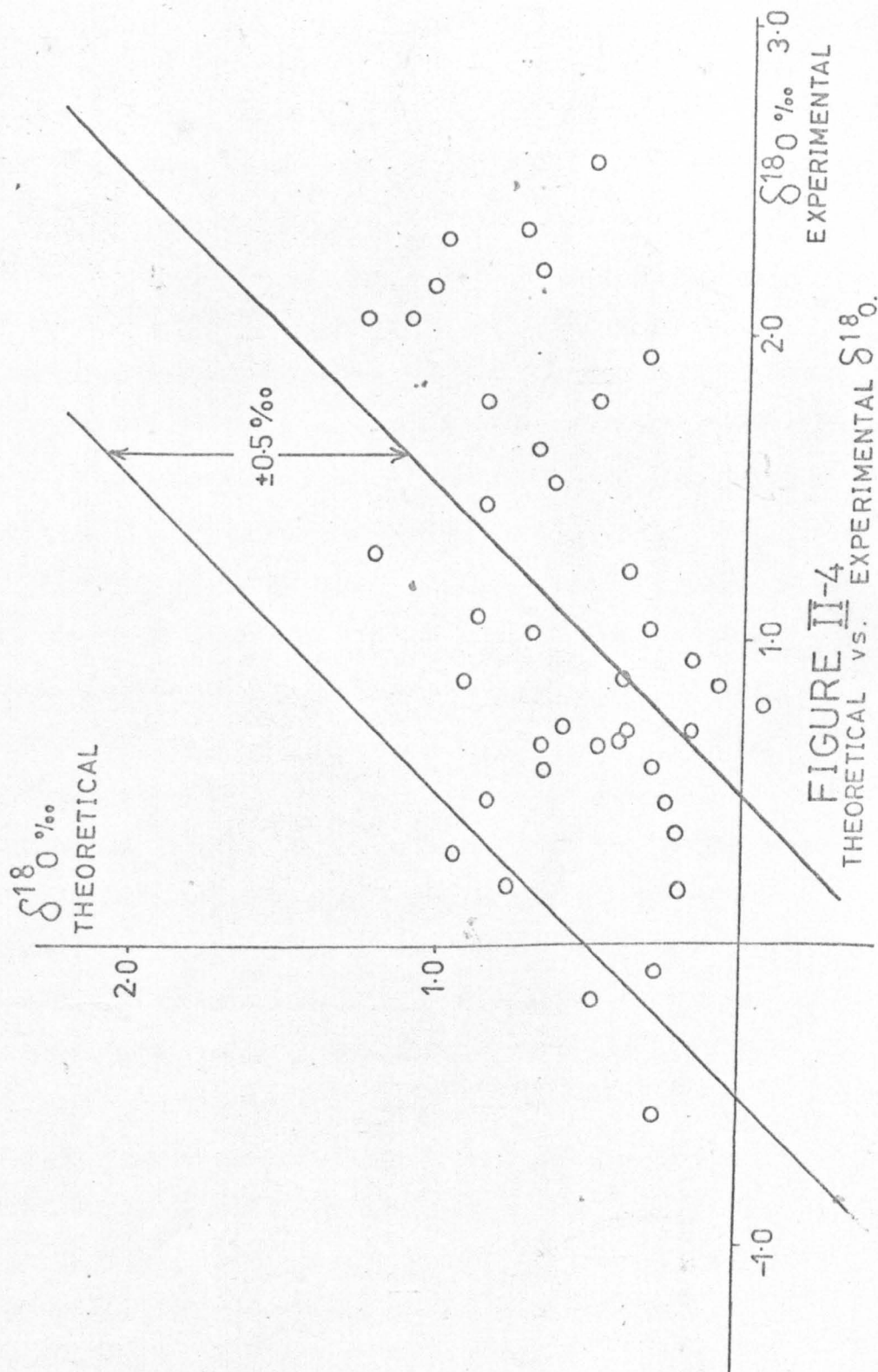
upon the correctness of the identification of the ambient temperature as the 'extraction temperature', but it is difficult to conceive what alternative is open, or how it could be justified. In Figure II-4 are plotted the experimentally determined and theoretically calculated $\delta(\Sigma\text{CO}_2-25\text{S})$ values. It can be seen that many points lie outside the $\pm 0.5\%$ envelope and so, for the stripping technique described earlier, it is considered that the assumptions inherent in the estimation are not justified, for some samples at least. It seems more advisable, where possible, to determine the ^{17}O contribution more directly - that is by $\delta^{18}\text{O}$ assay of the CO_2 on the mass spectrometer. This policy was followed for all samples reported in this work.

II-4 Experimental procedures for determination of $\delta^{18}\text{O}$ of water samples: introduction.

There are at present at least three techniques used for the high precision determination of the $^{18}\text{O}/^{16}\text{O}$ isotope ratio in water samples. In that described by Jackson et. al. (1973), a 5 g. aliquot is irradiated in a fast neutron reactor; the incident neutrons and target oxygen atoms react according to:



and the isotope ratio is measured using subsequent gamma-counting. O'Neil and Epstein (1966) have described a second method, in which milligram quantities of water are decomposed

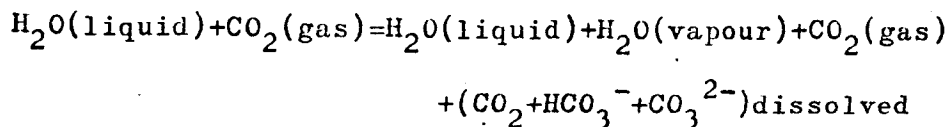


with bromine pentafluoride in a metal vacuum line, and the O_2 converted to CO_2 by reaction with hot carbon. The isotope ratio is then assayed by mass spectrometry. The third method, due to Epstein and Mayeda (1953), is the simplest and most widely used. In it, the water samples are isotopically equilibrated at $25^\circ C$ with carbon dioxide gas of known isotopic composition. The gas is re-analysed on the mass spectrometer after equilibration and from the isotopic shift and knowledge of the original amounts of water and gas present, the oxygen isotope ratio of the water calculated.

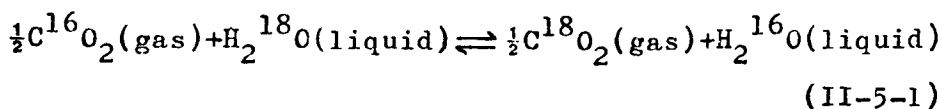
$\delta^{18}O$ measurements on water samples reported in this work used the third of these methods, i.e. the Epstein-Mayeda technique, because of its inherent simplicity yet high precision. As originally described (Epstein and Mayeda, 1953), 25 ml. of water and 175 ml. of carbon dioxide were equilibrated at $25.3^\circ C$. However, in general such large water samples were not available, so a smaller scale system was devised wherein 10 ml. of water and 70 ml. of gas are used. Also, the equilibration temperature chosen was $25.0^\circ C$, as more accurate data exist at this temperature for the oxygen isotope fractionation factor, which is important in the calculations. It is to be realised that the use of a smaller aliquot of sample leads to an increase in the probability of experimental error, particularly because of the much greater effect of evaporation or traces of contaminant water.

II-5. Theory of equilibration technique.

The theory of the equilibration technique has been discussed in some detail by Taylor (1973), so only a condensed account will be presented here. Consider the mass balance before and after equilibration, then (omitting, for clarity, the mass symbol from each side of the equation):



Provided that the volume of the flask is not more than about 50 times the volume of water, it can be shown that, for all natural waters, the contributions to the change in $\delta^{18}\text{O}$ of the water from dissolved carbonate and bicarbonate, and from water vapour, can be neglected. Hence the change in the ^{18}O content can be attributed solely to the exchange of oxygen isotopes between gaseous carbon dioxide and water, i.e. it is sufficient to consider the two-component system:



For a discussion of isotope ratios in a two-component system, consider then a system with two chemical components A and B, say, each containing both isotopes ^{18}O and ^{16}O (the generalisation to other isotopes is obvious) in the respective ratios:

$$(^{18}\text{O}/^{16}\text{O})_A = R_A; \quad (^{18}\text{O}/^{16}\text{O})_B = R_B$$

Further, let the total number of oxygen atoms in each component be denoted:

$$N_A = {}^{18}\text{O}_A + {}^{16}\text{O}_A; \quad N_B = {}^{18}\text{O}_B + {}^{16}\text{O}_B$$

Then the ratio ${}^{18}\text{O}/{}^{16}\text{O}$ in the total system is given by:

$$R_M = ({}^{18}\text{O}_A + {}^{18}\text{O}_B) / ({}^{16}\text{O}_A + {}^{16}\text{O}_B)$$

But ${}^{18}\text{O}_A = N_A \frac{{}^{18}\text{O}_A}{{}^{18}\text{O}_A + {}^{16}\text{O}_A}$ by definition, so:

$$R_M = \frac{N_A \frac{{}^{18}\text{O}_A / {}^{16}\text{O}_A}{{}^{18}\text{O}_A / {}^{16}\text{O}_A + 1} + N_B \frac{{}^{18}\text{O}_B / {}^{16}\text{O}_B}{{}^{18}\text{O}_B / {}^{16}\text{O}_B + 1}}{\frac{N_A}{{}^{18}\text{O}_A / {}^{16}\text{O}_A + 1} + \frac{N_B}{{}^{18}\text{O}_B / {}^{16}\text{O}_B + 1}}$$

$$\therefore R_M = \frac{N_A \left(\frac{R_A}{1+R_A} \right) + N_B \left(\frac{R_B}{1+R_B} \right)}{\left(\frac{N_A}{1+R_A} \right) + \left(\frac{N_B}{1+R_B} \right)} \quad (\text{II-5-2})$$

Let CO_2 and H_2O be respectively represented by A and B before equilibration, and by C and D after equilibration and assume, in accordance with previous discussion, that:

$$(i) \quad N_A = N_C; \quad N_B = N_D$$

(ii) all isotope ratios R are small compared to 1.

Then applying II-5-2 before and after equilibration and using the fact that R_M is, of necessity, constant:

$$\frac{N_A R_A (1+R_B) + N_B R_B (1+R_A)}{N_A (1+R_B) + N_B (1+R_A)} = \frac{N_A R_C (1+R_D) + N_B R_D (1+R_C)}{N_A (1+R_D) + N_B (1+R_C)}$$

Putting $\ell = N_A/N_B$ = ratio of gram atoms of oxygen in the CO_2 to that in the H_2O , and neglecting the product of isotope ratios gives:

$$\ell R_A + R_B = \ell R_C + R_D$$

The reaction (II-5-1) has equilibrium constant α given by:

$$\alpha = \frac{[\text{C}^{18}\text{O}_2]^{1/2} [\text{H}_2^{16}\text{O}]}{[\text{C}^{16}\text{O}_2]^{1/2} [\text{H}_2^{18}\text{O}]} = \frac{R_C}{R_D}$$

so that:

$$\ell R_A + R_B = R_C(\ell + 1/\alpha)$$

or, rearranging to give the isotope ratio of the original water:

$$R_B = R_C(\ell + 1/\alpha) - \ell R_A$$

Converting this to the delta notation:

$$\delta_B = \delta_C(\ell + 1/\alpha) - \ell \delta_A + 10^3(1/\alpha - 1)$$

where all δ values are measured relative to the same standard. To avoid confusion, expand the notation, writing:

$\delta(\text{CO}_2/\text{SAM})$ = per mil enrichment of CO_2 equilibrated with
SAMPLE at 25°C /relative to standard/ δ

$\delta(\text{CO}_2)$ = per mil enrichment of CO_2 relative to standard

$\delta(\text{SAM})$ = per mil enrichment of SAMPLE water relative to
standard

Then the above equation becomes:

$$\delta(\text{SAM}) = (\ell + 1/\alpha)\delta(\text{CO}_2/\text{SAM}) - \ell \delta(\text{CO}_2) + 10^3(1/\alpha - 1)$$

In the limit as $\ell \rightarrow 0$ a system is being considered in which CO_2 is equilibrated with an infinite amount of water, and:

$$\delta(\text{SAM}) = 1/\alpha \delta(\text{CO}_2/\text{SAM})_{\ell=0} + 10^3(1/\alpha - 1)$$

Eliminating $10^3(1/\alpha-1)$:

$$\delta(\text{CO}_2/\text{SAM})_{\ell=0} = (1+\alpha\ell)\delta(\text{CO}_2/\text{SAM}) - \alpha\ell\delta(\text{CO}_2)$$

in agreement with the formula given by Craig (1957). Ocean waters are commonly reported relative to SMOW (Craig, 1961) and it is often convenient when dealing with CO_2 equilibrated against a water, to use as standard CO_2 equilibrated against an infinite amount of SMOW (e.g. Bottinga and Craig, 1969). Now it is obvious that:

$$\delta_{\text{SMOW}}(\text{SAM}) = \delta_{\text{CO}_2/\text{SMOW}}(\text{CO}_2/\text{SAM})_{\ell=0}$$

so that we have that:

$$\delta_{\text{SMOW}}(\text{SAM}) = (1+\alpha\ell)\delta_{\text{CO}_2/\text{SMOW}}(\text{CO}_2/\text{SAM}) - \alpha\ell\delta_{\text{CO}_2/\text{SMOW}}(\text{CO}_2)$$

where the standard is given as the subscript. This is the equation used for calculation of $\delta^{18}\text{O}$ of a water sample relative to SMOW.

The value of α is temperature dependent; Bottinga and Craig (1969) have reviewed this topic and, based on previous measurements and on their own data, quote a best value of (1.04075 ± 0.00016) at 25°C . They also give a polynomial in t , the temperature, which represents the temperature variation of α . The value of ℓ for each sample is calculated from the equation:

$$\ell = \frac{P(V-V_w)273.15 \times 2 \times 18.015}{1.026V_w \times 76 \times 195.15 \times 22.261 \times 10^3}$$

where P is the filling pressure of CO_2 at -78°C in cm.Hg, V is the volume of the equilibration bulb and V_w is the sample

volume. A density of 1.026 kg.l.^{-1} for seawater, and a molar volume for CO_2 of 22.261 litres have been assumed.

II-6 Experimental technique for $\delta^{18}\text{O}$ assay.

The equilibration vessels used in the work reported in this thesis were designed to accommodate 10 ml. of water sample and around 70 - 80 ml. of carbon dioxide gas. Several different types of vessel were constructed and all functioned satisfactorily, though not all were equally simple to use. Examples of the two designs used for the vast majority of the samples are shown diagrammatically in Figure II-5. Type 1 is intended for use on the manifold system shown in the Figure for batch preparations: the other type is for single equilibrations. The batch sample preparation procedure will be described, as the individual case is much simpler though following the same routine.

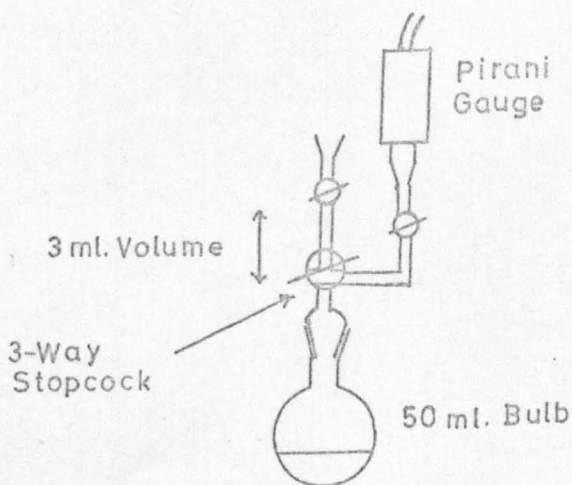
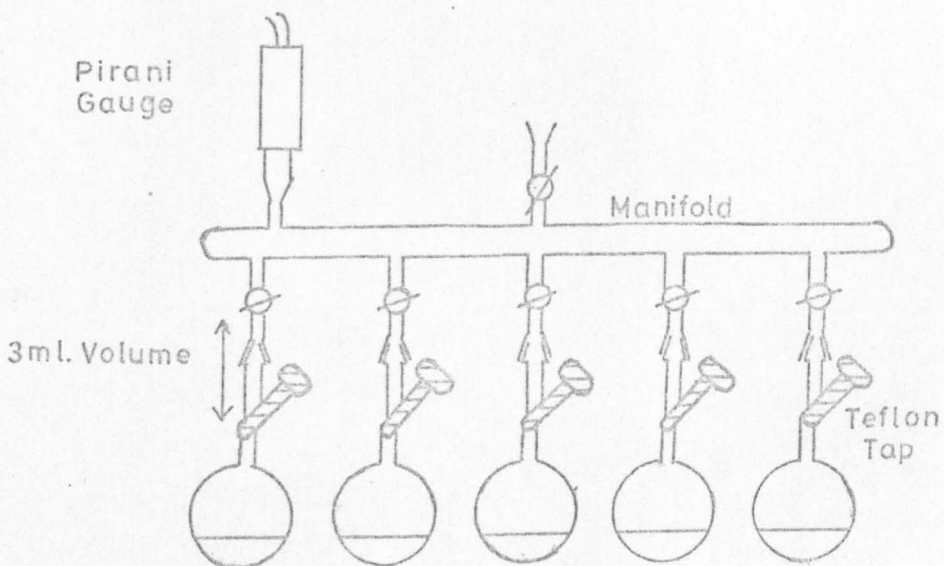
Preparation of samples for equilibration.

Sample pretreatment, and purifying of the equilibrated CO_2 before mass spectrometric analysis, is performed on the vacuum line shown diagrammatically in Figure II-6. Five clean, dry Type 1 equilibration bulbs are fitted onto a manifold and a Pirani gauge attached. The manifold is then connected to the vacuum line shown in Figure II-6 through cone P_1 , the system evacuated to 10^{-3} torr., and isolated from the pumps. Tank nitrogen, dried through a silica gel column and purified of carbon dioxide by passage through two Ascarite columns; is introduced into the vacuum line, through

FIGURE II-5

EQUILIBRATION VESSELS FOR $\delta^{18}\text{O}$ DETERMINATIONS.

(a) TYPE 1 EQUILIBRATION BULBS ON MANIFOLD.



(b) TYPE 2 EQUILIBRATION BULB.

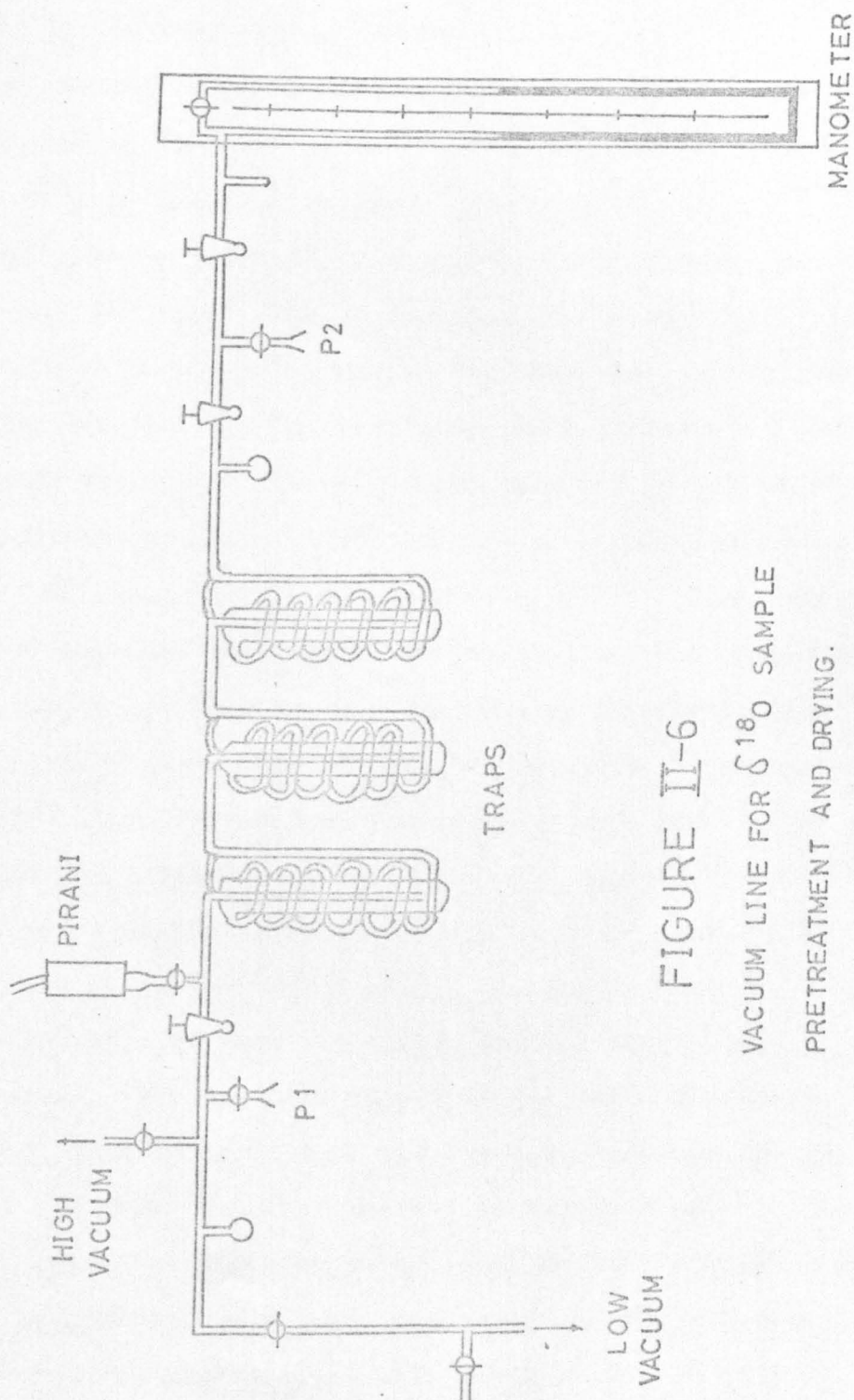


FIGURE II-6
VACUUM LINE FOR $\delta^{18}\text{O}$ SAMPLE
PRETREATMENT AND DRYING.

-cone P_2 , to atmospheric pressure. The teflon taps of all five equilibration bulbs are closed and the nitrogen feed replaced with a five-litre bulb of pure, dry CO_2 , the $\delta^{13}C$ and $\delta^{18}O$ of which are known. Approximately 10 ml. of water sample are transferred from storage to a dry calibrated syringe; the teflon tap of the appropriate equilibration vessel is removed, the sample injected into the bulb of the vessel and the tap replaced and closed. When all five vessels are ready, the bulbs are immersed in a bath of dry-ice/acetone slush at $-78^\circ C$ and the water samples frozen.

The whole manifold is then evacuated to 10^{-3} torr, and the teflon taps are reclosed. The freezing bath is removed and the samples allowed to thaw to release dissolved gases.

The vessels are re-immersed in the freezing mixture, the samples again frozen and evacuated to 10^{-3} torr. When a satisfactory vacuum has been achieved, carbon dioxide is admitted from the large five-litre buffer volume to a pressure of just under 50 cm.Hg, the teflon taps of the equilibration vessels are closed and the excess gas evacuated. The manifold stopcocks are shut, the manifold removed from the cold bath and disconnected from the vacuum line, and placed in the constant temperature water bath.

It is important that the water level be sufficiently high to totally immerse the volume containing the CO_2 and sample, for otherwise condensation will occur at the tops of the vessels.

Stability of the equilibration temperature.

Bottinga and Craig (1969) have expressed the temperature ($t^{\circ}\text{C}$) dependence of the oxygen isotope fractionation factor (α) by the polynomial:

$$\left(\frac{\alpha_t}{\alpha_{25}} - 1\right) 10^3 = 5.112 - 0.214t + 0.00041t^2$$

where subscripts on α denote Centigrade temperature. Differentiating with respect to t and rearranging:

$$\frac{d\alpha}{dt} = 10^{-3} \alpha_{25} (-0.214 + 0.00082t)$$

so that at $t=25$, with $\alpha_{25}=1.0409$:

$$\left(\frac{d\alpha}{dt}\right)_{t=25} = -2.0 \times 10^{-4} \text{ per } ^{\circ}\text{C}.$$

Now putting $dR/R = 10^{-3} d\delta$ and $d\alpha/\alpha = dR_C/R_C$, then the error introduced into δ by a 0.5°C deviation in temperature is 0.1‰ . For this reason, it is desirable to have the water bath temperature accurately at 25.0°C and stabilised to within 0.1°C . The stainless steel water bath used is 225 cm. long, 30 cm. wide and 25 cm. deep; when adequately filled it holds some 135 litres of water. The bath is double walled with glass fibre lagging between the walls to reduce heat loss. The temperature is maintained above ambient by two 150 watt bulbs controlled by independent toluene-mercury regulators. The sensitivity of each such thermostat system is of the order of $\pm 0.01^{\circ}\text{C}$ and one temperature sensor heating unit is maintained at each end of the bath. Uniformity of water temperature throughout the bath is ensured by rapid

circulation, provided by two water pumps of combined throughput 26.5 l.min^{-1} ; the temperature is measured by a high precision thermometer, 70 cm. in length, with a reading error of less than $\pm 0.005^\circ\text{C}$. This thermometer was calibrated absolutely against a standard thermometer with an estimated accuracy of $\pm 0.01^\circ\text{C}$ or better. Fluctuations in water temperature at the thermometer are of the order $\pm 0.02^\circ\text{C}$, so it is considered that negligible error is introduced in the equilibration process by temperature variations. Accepting this, it can be confidently assumed that equilibration at 25.0°C is complete after two days (Mook, 1968; Taylor, 1973), so this is taken as the minimum equilibration period.

Extraction of equilibrated CO_2 and drying procedure.

At the end of the equilibration period, the sample manifold - still in the bath - is connected to the vacuum line of Figure II-6 and evacuated. The stopcocks sealing off the 3 ml. volumes are then closed and each teflon tap opened momentarily to fill the appropriate volume with a sample of equilibrated gas. In turn, the gases are now dried by allowing them to expand into the vacuum line through cone P_2 . The first two spiral traps are immersed in dry-ice/acetone slush and the third in liquid nitrogen; the pressure of non-condensed gases is registered on the Pirani gauge, and pressures greater than 5×10^{-2} torr. are taken to indicate an excessive air leakage, and the sample is discarded. The CO_2 is thoroughly dried by several passes

through the traps at -78°C and finally condensed in a mass spectrometer sample bottle attached to cone P_1 .

II-7 Accuracy and precision of $\delta^{18}\text{O}$ analysis.

The precision of the equilibration technique used for $\delta^{18}\text{O}$ determination was estimated by replicate analyses of seawater samples, the main limitations being ascribed to the mass spectrometer. The accuracy was investigated by measurement of various international standard waters. Several of these are highly depleted in the heavy isotope, so the possibility of error is greatly increased, not only in the mass spectrometry but also in the effect of contaminant water (since this will have a very different isotope composition). The results are given in Table II-4 for the reproducibility and in Table II-5 for the accuracy. Some pertinent data from other laboratories have been included in the latter; those referenced "Brown (1972)" are results reported to the I.A.E.A. From these, it is concluded that $\delta^{18}\text{O}$ measurements on water samples by the equilibration technique are correct to $\pm 0.05\text{‰}$ (1σ) for samples not differing from SMOW by more than about 20‰ . However, outside this range, the accuracy and precision may not be as good. The results of the analyses of the international water standards give weight to the accuracy of the $\delta^{18}\text{O}$ value of the working standard gas, for any discrepancy in the working standard calibration would show up as a systematic error. The accuracy of the working standard calibration will be further discussed in the next chapter.

TABLE II-4

EQUIL. VESSEL	$\delta^{18}\text{O}$	EQUIL. VESSEL	$\delta^{18}\text{O}$	EQUIL. VESSEL	$\delta^{18}\text{O}$
B24/5	0.25‰/‰	B24/1	-0.18‰/‰	TF G	0.28‰/‰
TF A	0.25‰/‰	B24/2	-0.24‰/‰	TF E	0.23‰/‰
TF C	0.16‰/‰	B24/3	-0.22‰/‰	TF D	0.19‰/‰
		B24/4	-0.26‰/‰		
Mean: (0.22±0.05)‰/‰				Mean: (0.23±0.04)‰/‰	

Mean: (-0.23±0.03)‰/‰

Precision of $\delta^{18}\text{O}$ analysis of seawaters by Epstein-Mayeda technique. All $\delta^{18}\text{O}$ values are quoted relative to SMOW.

TABLE II-5

Accuracy of $\delta^{18}\text{O}$ of water by analysis of international standard waters. All $\delta^{18}\text{O}$ values are relative to SMOW.

GROUP 1: N.B.S. and I.A.E.A. Samples

SAMPLE	EQUIL. VESSEL	GLASGOW $\delta^{18}\text{O}$	CRAIG (1961)	TAYLOR AND HULSTON (1972)	RANGE QUOTED BY BROWN (1972)
NBS ₁	TF 11	-7.96	-7.94	-8.03	-7.62 to -8.05
NBS _{1A}	TF 1	-24.37	-24.33	-24.49	-23.45 to -24.94
SLAP	TF H	-55.12	-	-55.96	-54.71 to -56.50

GROUP 2: New Zealand Institute of Nuclear Sciences (INS)

Samples

SAMPLE	EQUIL. VESSEL	$\delta^{18}\text{O}$	TAYLOR AND HULSTON (1972)
INS 3	B24/1	0.54	0.54
INS 4	TF G	-32.24	-32.35
INS 5	B24/5	-49.35	-50.63

Again, it must be pointed out that the accuracy and precision reported above apply to a bottle of water in the laboratory, and not necessarily to the sample as collected on board ship: proper storage is of paramount importance.

It has been consistently noted that there is a change in $\delta^{13}\text{C}$ of CO_2 used for equilibration of seawater in the technique described above. Since the $\delta^{13}\text{C}$ values are corrected for ^{17}O contribution, the shift is to be explained by one or more processes which involve the carbon isotopes themselves. Typical results are given in Table II-6. For the 31 seawater samples listed, the various groups show changes in $\delta^{13}\text{C}$ over the equilibration ranging from 0.39‰ to 0.50‰ and with mean $(0.45 \pm 0.06)\text{‰}$; there is good agreement among the samples of each group. The unequilibrated gases have a range of 0.66‰ and there is no correlation between initial $\delta^{13}\text{C}$ and subsequent change. In contrast to the seawaters, a series of three distilled water samples, included in Group 4 of Table II-6, shows a mean isotopic shift of only 0.04‰ , within the mass spectrometry error.

The simplest explanation for the above observations is that carbon dioxide is taken up by the seawater samples because of its high partial pressure in the equilibration vessel. This CO_2 will be distributed among the various components of the carbonate system (HCO_3^- , CO_3^{2-} , H_2CO_3), isotope fractionation occurring at each stage. Equilibrium fractionation factors for carbon isotopes between gaseous

TABLE II-6

Isotopic shift in $\delta^{13}\text{C}$ of CO_2 used for equilibration.

GROUP 1 All results are relative to PDB.

Unequilibrated gas: $\delta^{13}\text{C} = (-30.35 \pm 0.03) \text{‰}$

Equilibrated gases:

SAMPLE	$\delta^{13}\text{C}$	SAMPLE	$\delta^{13}\text{C}$
JE1 102	-29.92	JE1 233	-29.97
JE1 114	-29.88	JE1 99	-29.98
JE1 224	-29.91	JE1 93	-29.89
JE1 236	-29.92	JE1 102	-29.98
JE1 105	-30.06	JE1 90	-30.00
JE1 111	-29.95	JE1 96	-30.01
JE1 181	-29.89	JE1 230	-29.94

Mean of 14 equilibrated gases: $\delta^{13}\text{C} = (-29.95 \pm 0.05) \text{‰}$

Isotopic shift = 0.40‰

GROUP 2

Unequilibrated gas: $\delta^{13}\text{C} = (-27.79 \pm 0.05) \text{‰}$

Equilibrated gases:

SAMPLE	$\delta^{13}\text{C}$	SAMPLE	$\delta^{13}\text{C}$
JE1 1001	-29.27	JE1 1003	-29.24
JE1 1002	-29.37	JE1 135	-29.32

Mean of 4 equilibrated gases: $\delta^{13}\text{C} = (-29.30 \pm 0.06) \text{‰}$

Isotopic shift = 0.49‰

TABLE II-6 (Continued)

GROUP 3

Unequilibrated gas: $\delta^{13}\text{C} = (-30.05 \pm 0.09) \text{‰}$

Equilibrated gases:

SAMPLE	$\delta^{13}\text{C}$	SAMPLE	$\delta^{13}\text{C}$
JVD 1751	-29.35	JE1 871	-29.53
JVD 1752	-29.68	JE1 872	-29.62
JVD 1753	-29.48	JVD 1771	-29.65
JVD 1754	-29.57	JVD 1772	-29.53

Mean of 8 equilibrated gases: $\delta^{13}\text{C} = (-29.55 \pm 0.10) \text{‰}$

Isotopic shift = 0.50‰

GROUP 4

Unequilibrated gas: $\delta^{13}\text{C} = (-30.45 \pm 0.10) \text{‰}$

Equilibrated gases:

SEAWATER SAMPLE	$\delta^{13}\text{C}$	DISTILLED SAMPLE	$\delta^{13}\text{C}$
B7-1-1	-30.10	INS3	-30.41
B7-1-6	-30.17	INS4	-30.38
B7-3-6	-30.07	INS5	-30.43
B7-3-7	-30.07		
B7-2-E	-29.91		

Mean of 3 equilibrated gases:

$\delta^{13}\text{C} = (-30.41 \pm 0.03) \text{‰}$

Mean of 5 equilibrated gases: Isotopic shift = 0.04‰

$\delta^{13}\text{C} = (-30.06 \pm 0.09) \text{‰}$

Isotopic shift = 0.39‰

and dissolved carbon dioxide and dissolved bicarbonate have been measured and discussed by Mook and co-workers (Vogel, Grootes and Mook, 1970; Mook, Bommerson and Staverman, 1974).

Unlike seawater, the distilled water samples are not highly buffered and so CO_2 uptake, and hence carbon isotope change, is very much less. The fact that similar volumes of seawater and equilibration gas are used and that there is relatively little $\delta^{13}\text{C}$ variation of ΣCO_2 for all seawater samples is reflected in the constancy of the isotopic shift.

If the above explanation is correct, the ΣCO_2 of the equilibrated water should obviously be far greater than the initial pre-equilibration value; moreover, it should be possible to set up balances for both ^{12}C and ^{13}C before and after equilibration. This is difficult to test with the small-scale equilibration system used routinely, so a larger one was constructed in which 150 ml. of seawater and 850 ml. of carbon dioxide were equilibrated. ΣCO_2 was extracted from 50 ml. aliquots of the pre- and post-equilibration waters. The results, together with the mass spectrometric analyses of the gases are given in Table II-7 below. It can be seen that there is indeed a large uptake of CO_2 by the seawater during equilibration. Let Σ denote the total dissolved inorganic carbon in a seawater, C the volume of equilibration carbon dioxide, and subscripts i and f , and e and o the initial and equilibrated samples of these respectively. Then, from mass (i.e. ^{12}C) balance:

$$\Sigma_i + C_o = \Sigma_f + C_e \quad (\text{II-7-1})$$

TABLE II-7

Results of large-scale equilibration experiment.

Before equilibrationDissolved inorganic carbon 0.315mM with $\delta^{13}\text{C} = (-1.10 \pm 0.03) \text{‰}$ (Σ_i, δ_i) Equilibration carbon dioxide 35.45mM with $\delta^{13}\text{C} = (-29.93 \pm 0.06) \text{‰}$ (C_o, δ_o) After equilibrationDissolved inorganic carbon 2.29mM with $\delta^{13}\text{C} = (-29.52 \pm 0.02) \text{‰}$ (Σ_f, δ_f) Equilibrated carbon dioxide 33.48mM with $\delta^{13}\text{C} = (-29.66 \pm 0.04) \text{‰}$

and from isotopic (i.e. ^{13}C) balance:

$$\sum_i \delta_i + C_o \delta_o = \sum_f \delta_f + C_e \delta_e \quad (\text{II-7-2})$$

Combining these gives:

$$\delta_o - \delta_e = \frac{\sum_f (\delta_f - \delta_e)}{C_o} - \frac{\sum_i (\delta_i - \delta_e)}{C_o} \quad (\text{II-7-3})$$

The second term on the right-hand side of (II-7-3) is dominant so the isotopic shift ($\delta_o - \delta_e$) should be approximately constant, as observed. Applying (II-7-2) to the results of the experiment from Table II-7 to test the validity of the proposed explanation:

(i) Before equilibration:

$$0.32(-1.10) + 35.45(-29.93) = -1061.4$$

(ii) After equilibration:

$$2.29(-29.52) + (35.77 - 2.29)(-29.66) = -1060.6$$

The agreement is quite remarkable and lends confidence to acceptance of the proposed explanation. Note that, since after equilibration the ΣCO_2 accounts for over 6% of the total carbon, the agreement is not trivial.

This isotopic shift is of more than passing interest, for it may serve as an indicator - albeit of low sensitivity - of contamination of the equilibrated gas by, say, atmospheric carbon dioxide.

II-8 Determination of the pH of seawater.

Originally, it had been intended to determine the pH, total alkalinity (At), and total carbonate concentration (ΣCO_2) on samples collected on U.S.N.S. Bartlett Cruise T-AGOR 13-73-1 by a shipboard version of the potentiometric

titration method (Dyrssen and Sillén, 1967) using a micro-meter screw burette and a specially fabricated titration cell (Edmond, 1970). However, at sea, the difficulties met with concerning electrical noise, drift and shielding proved insurmountable and the project was curtailed, being restricted to pH measurements on three profiles (Bartlett Stations 3, 5 and 7).

For both theoretical and practical reasons, the determination of the pH of seawater has always presented a considerable problem. In the first place, only in the cases of dilute solutions of simple solutes, in which the pH values correspond closely to those of some reference solution, may the pH be considered to measure the hydrogen ion activity of the solution. Secondly, electrode stability and asymmetry potential, electronic noise and drift in the associated circuitry all impose severe limitations on accuracy and precision; this is particularly true of shipboard measurements at sea.

However, pH values are of more than intrinsic interest, for at pH 7 to 8 seawater is close to a minimum in buffer capacity, so that the effect of processes participating in the carbon dioxide cycle are well illustrated by shifts in pH. Moreover, measurement of both pH and total dissolved carbonate, ΣCO_2 , should indicate the relative importance of various processes (photosynthesis and calcium carbonate skeletal formation) - provided that the seawater cannot adjust its pH by ion exchange, e.g. by interaction with

aluminosilicates of sediments (Dyrssen, 1969). It was therefore thought worthwhile to carry out the limited program.

Many of the theoretical difficulties involving the pH concept in solutions of ionic concentration greater than 0.1M stem from lack of knowledge of the behaviour of liquid junction potentials. Because of this, Dyrssen and Sillén (1967) have advised the use of activities defined on an ionic medium scale, rather than on the more usual infinite dilution scale. It then follows that the ratio of the activity to the concentration of an ionic species tends to unity as the composition of the corresponding solution approaches the pure salt medium. The advantage they claim is that 'the results of measurements are better defined'. Much additional work along the lines suggested by these authors has been pursued by Hansson (1972).

Shipboard technique for pH determination.

Measurements of pH were performed using a Beckman 46850 microblood pH electrode system and a Beckman 101901 Research pH Meter with step-down transformer. This instrument, which is essentially just an electronic potentiometer, has readout graduated in increments of 0.002 pH, corresponding to a reading error of ± 0.0005 pH. The measuring electrode was immersed in a constant temperature water bath at $(30.0 \pm 0.1)^\circ\text{C}$ and the pH samples drawn into 10 ml. plastic syringes and placed in the bath for 10 minutes prior to measurement.

Distilled water was flushed through the electrode system before introduction of the sample. Taking care to avoid the inclusion of air bubbles, the sample was then injected into the measuring electrode and a reading of the electrode potential (in arbitrary units) taken.

The micro pH electrode was calibrated before and after every profile using two N.B.S. precision buffers (pH=7.400 and pH=6.853 at 30.0°C). Let E denote the reading of the pH meter, and subscripts B1, B2 and SW refer to the first and second buffer and seawater respectively, then:

$$\frac{\text{pH}_{\text{SW}} - \text{pH}_{\text{B1}}}{E_{\text{SW}} - E_{\text{B1}}} = \frac{\text{pH}_{\text{B1}} - \text{pH}_{\text{B2}}}{E_{\text{B1}} - E_{\text{B2}}} \quad (\text{II-8-1})$$

and so pH_{SW} can be calculated from:

$$\text{pH}_{\text{SW}} = \text{pH}_{\text{B1}} + \frac{(E_{\text{SW}} - E_{\text{B1}})(\text{pH}_{\text{B1}} - \text{pH}_{\text{B2}})}{E_{\text{B1}} - E_{\text{B2}}} \quad (\text{II-8-2})$$

Applying this procedure to a set of samples collected at an oceanographic station involves two assumptions:

(i) the E-span ($E_{\text{B1}} - E_{\text{B2}}$) remains constant over the profile measuring period,

(ii) E_{B1} remains constant over the measuring period, i.e. there is no drift.

The validity of the former is limited by any span variation observed between the buffer calibrations; that of the latter can be judged by replicate analyses of one solution carried out during the course of the sample measurements. These will be discussed more fully in Chapter V when the results are

presented and discussed, but in general the precision is estimated at ± 0.01 pH. It is to be emphasized that appreciably greater reproducibility is obtained by successive measurement of the replicates within a short period of time. This illustrated in Table II-8 for seawater samples analysed between the stations.

II-9 Determination of dissolved oxygen concentration of seawater by modified Winkler titration.

All oxygen analyses for the samples from Bartlett Cruise T-AGOR 13-73-1 were performed by the modified Winkler oxygen titration method (Carpenter, 1965). For the measurements up to station 2, a Manostat Digipet burette was used, but due to malfunction of this an Agla Syringe Microburet was used after station 2.

For oxygen concentrations above 1.0 ml.l.^{-1} , the precision 'attainable by a good analyst' is generally reckoned to be $\pm 0.05 \text{ ml.l.}^{-1}$ (e.g. Kroopnick, 1971). All measurements were carried out in duplicate, and this reproducibility was achieved using the Digipet (Table II-9); however, with the Syringe Microburet the results were more erratic (Table II-10). This was most probably caused by leakage from the burette tip. Because the volume of the specific Erlenmeyer flask enters the calculation for each titration, and because the order of sample analysis was random, the personal tendency to obtain the same result for the two assays of the same sample was eliminated.

TABLE II-8

Reproducibility of pH measurements in successive analyses.

(a) SAMPLE 1:

7.954

7.949

7.954

Mean: (7.952±0.002)

(b) SAMPLE 2:

7.945

7.946

7.938

Mean: (7.943±0.004)

TABLE II-9

Reproducibility of dissolved oxygen determinations using the Manostat Digipet.

BARTLETT STATION 1 CAST 2.

SAMPLE	DISSOLVED OXYGEN ml.l. ⁻¹	MEAN
1-2-1	0.496	0.504±0.011
	0.512	
1-2-4	-0.026	-0.002±0.034
	0.022	
1-2-5	0.022	0.004±0.025
	-0.014	
1-2-6	-0.022	-0.022±0.000
	-0.022	
1-2-7	-0.022	-0.022±0.000
	-0.022	
1-2-8	-0.026	-0.024±0.003
	-0.022	
1-2-11	-	0.094
	0.094	
1-2-12	0.098	0.071±0.038
	0.044	

TABLE II-10

Reproducibility of dissolved oxygen determinations using the Agla Microburet.

BARTLETT STATION 3 CAST 1

SAMPLE	DISSOLVED OXYGEN ml.l. ⁻¹	MEAN
3-1-1	1.803	1.736±0.095
	1.669	
3-1-12	3.883	33.779±0.148
	3.674	
3-1-11	3.635	3.662±0.038
	3.689	
3-1-10	3.729	3.740±0.016
	3.751	
3-1-8	3.476	3.533±0.080
	3.589	
3-1-7	3.562	3.455±0.152
	3.347	
3-1-6	3.388	3.308±0.114
	3.227	
3-1-5	2.702	2.675±0.027
	2.647	
3-1-4	2.275	2.272±0.004
	2.269	

CHAPTER III

THE MASS SPECTROMETER AND ASSOCIATED EXPERIMENTAL TECHNIQUES.

III-1 Introduction

In this chapter are described the mass spectrometer used in the work of this thesis, the practical techniques of stable isotope ratio measurements, and experiments aimed at elucidating both the potential and limitations of instrumental performance.

Dynamic gas flow mass spectrometers employed for the measurement of stable carbon and oxygen isotope ratios conform, to quite general design standards as first described by Nier (1947).

Although measurement of variations of natural isotopes had been achieved as early as 1939 (Nier and Gulbransen, 1939), it was with the work of McKinney et al. in 1950 (McKinney, McCrea, Epstein, Allen and Urey, 1950) that the Nier instrument became capable of sufficiently high precision for its use to spread rapidly in the various fields where knowledge of relative isotopic abundances and their changes is important. The two main innovations described by McKinney et al. were:

- (i) the use of a vibrating reed electrometer in the circuit for detection of the minor ion beam, and
- (ii) the introduction of a twin gas inlet system, the two

viscous leaks feeding into an automatically operated changeover valve.

III-2 General description of mass spectrometer

The measurements reported in this study were performed on a V.G. Micromass Ltd. 602B instrument (see Bridger, Craig and Sercombe, 1974 for a brief discussion of a related instrument). The schematic layout of the mass spectrometer is shown in Figure III-1. The 150 mm. radius of curvature, 90° sector mass spectrometer has a permanent magnet of approximately 3000 gauss field strength and an ion accelerating voltage, for m/e 44 ion beam from CO₂, of approximately 2500 volts. Typical operating statistics for the ion source are 3.65A. filament current, 200 μA. trap current and 71 volts electron accelerating voltage.. The source current at m/e 44 is 0.78 mA. and the ion repeller voltage for well-resolved, flat-topped peaks is around 30 - 40 volts. Under normal analytical conditions, with 50 torr of carbon dioxide at the high pressure side of the gas feed capillaries, an m/e 44 ion beam intensity of 4.0×10^{-9} A. is achieved; the pressure in the system is then approximately 10^{-6} torr and the flow rate is of the order of 5×10^{13} molecules sec.⁻¹. Thus, the overall efficiency is about 5×10^{-4} collected ions per molecule.

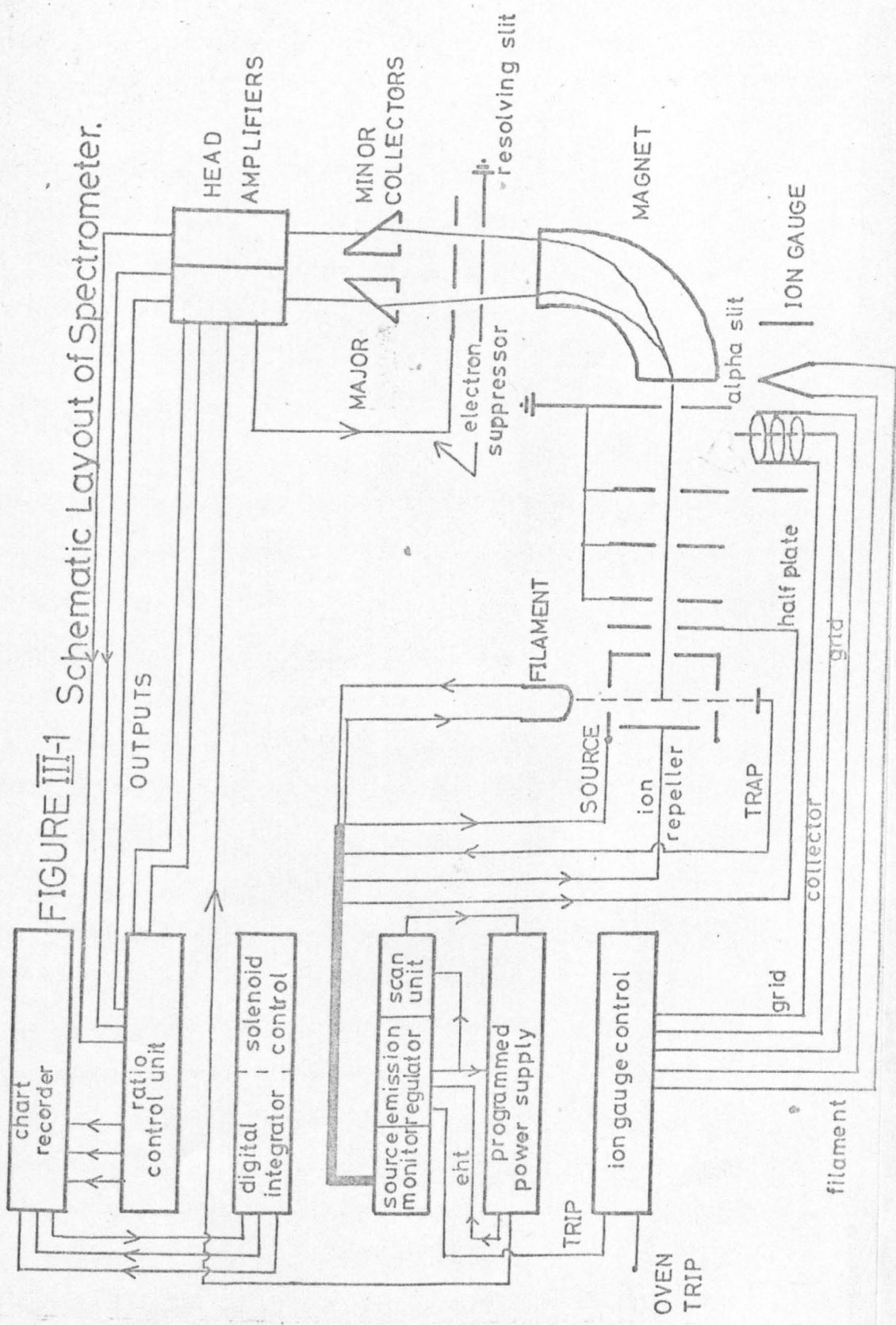


FIGURE III-1 Schematic Layout of Spectrometer.

III-3 Mass analyser and vacuum system.

The ion source, designed for high sensitivity, is such that the analyser tube operates at sufficiently low pressure for minimal scattering of the accelerated ions; the peak tail overlap correction factors are thus kept low - less than 1.001. Three adjustments are made in the ion source region to optimise performance:

(i) The half-plate voltage

Close to the ion source, two electrodes are mounted symmetrically around the beam. The half-plate voltage is applied to one of these in order to align the beam with the apertures along its path.

(ii) The ion repeller voltage

As ions are produced in the source chamber by electron bombardment, they are extracted and focussed by the ion repeller voltage which is applied to an electrode close to the electron beam.

(iii) The magnet compensator

Because different magnets may vary in field strength, the magnet compensator is necessary to adjust the overall voltage gain of the supply, and to match ion acceleration voltage and mass scale alignment.

In order that frequent retuning be unnecessary, it is required that the peaks be 'flat-topped' and well resolved. The resolving section comprises two slits arranged on a single electrode. The smaller slit receives the minor ion beam; there is good rejection of stray ions and, in the

single beam mode, high resolving power. The other slit, some ten times wider, passes the ion beam of the major isotope and in this case the contribution from stray ions is negligible. In addition, variations in ion beam position due, for example, to different magnet positions, can be tolerated. To ensure that the scanned peak shape is flat-topped, the smaller slit width is twice that of the minor isotope beam.

Several other electrodes are incorporated into the collector section to improve the performance. Those mounted between the resolving slits and the Faraday plate collector buckets reduce ion drift between major and minor collectors and deflect secondary electrons produced by ion bombardment. The electron suppressor electrodes are maintained at a stabilised voltage of -45 volts and small magnets, mounted on the assembly, further restrict secondary electron drift.

The two Faraday buckets are deep along the axes of the incoming ion beams and are gold plated, thus providing adequate ion entrapment while minimising charging effects. The ion current resulting from the major and minor beams are fed to two matched chopper amplifiers and thence to the ratio control unit. The head amplifiers are directly attached to the collector flange; leakage currents and transient potentials from cables are thus avoided. To eliminate leakage currents across the ceramic insulators separating the collector buckets and suppressor plates, a guard ring is maintained at earth potential between the two. As a final

deterrent to stray charged particles, the entire assembly is surrounded by a cylindrical stainless steel shield mounted on the collector feedthrough flange.

The vacuum system for the analyser comprises a water cooled 150 l.sec.⁻¹ polyphenyl ether oil diffusion pump with baffle, a room temperature molecular sieve foreline trap and a two-stage rotary pump. There is a foreline valve between diffusion pump and trap and an automatic magnetic isolation valve on the rotary pump. The diffusion pump is fitted with a thermostat so that, in the event of partial or total failure of the water supply, the pump will heat up until the thermostat cuts out. Also, a Pirani trip unit, actuated from a Pirani gauge in the foreline conduit, switches off the diffusion pump if the backing pressure rises above 0.01 torr. This provides protection against rotary pump failure, which might otherwise result in the distillation of diffusion pump oil into the analyser section. This protection device is not a regular feature of the 602B instrument, but was fitted during the course of the work, after an electrical short circuit had caused the analyser rotary pump to breakdown. The subsequent increase of the backing pressure at the analyser and bleed diffusion pumps forced the distilling oil fractions into the analyser chamber and bleed lines, and the instrument was unable to be used for analytical work for a four month period while repairs, cleaning and oven baking were carried out. In view of the catastrophic results of such failure, a Pirani trip unit such as that described above is

highly recommended for rotary-backed diffusion pumps in similar systems.

With the above arrangement, the background pressure is typically in the 10^{-9} torr range and the residual spectrum shows that background correction factors are negligible. In the event of mild contamination, the mass analyser and other parts of the system can be oven baked to 250°C . After bakeout, the background pressure falls to below 5×10^{-9} torr.

III-4 Gas handling system.

A dual inlet system is used, one side being for the reference gas and the other for the sample gas. Variable volume gas reservoirs are employed to facilitate adjustment of operating pressures. The capillary viscous leaks, 800 mm. long and 0.15 mm. bore, are of stainless steel and are fitted with adjustable crimps at the ends nearer the mass spectrometer. The capillaries are connected to the inlet system by means of modified 'Hoke' type couplings and indium wire seals, and to the changeover valve by clamped flanges with gold ring seals. The main body of the McKinney changeover valve is stainless steel and the spherical sealing balls are of highly polished tungsten carbide to reduce the cross-mixing correction term to the order of 1.001. The valve is solenoid controlled and may be manually or automatically switched, the period of changeover in the automatic cycle mode being variable from 45 sec. to 110 sec.

A second diffusion pump, also protected against overheating and failure of backing line pump, is connected to the

bottom of the valve to remove that gas which is not flowing into the instrument. The system is designed so that, on changeover, minimal delay is experienced before the gas pressure reaches its former value, thus ensuring stable flow conditions.

III-4 Ratio measurement system.

The ratio measurement is by an infinite bridge null system (Figure III-2) so that the enrichment readings are independent of the absolute signal level. The measuring slidewire on the chart recorder is incorporated into the bridge measuring circuit and is an integral part of the resistor divider network. Both the output signal from this network and that from the minor amplifier are together fed into the recorder comparator amplifier and, since the bridge null point is within the recorder servo loop, balance is always attained (provided, of course, the signals are within the range of the recorder chart). The divider network thus controls the chart calibration, and this calibration in no way depends on the signal levels. There is no null point to be determined since there is always automatic balance, and hence the system is free of the corrections inherent in the chart calibration necessary for bridge/amplifier balance systems (see, for example, Mook and Grooteq, 1973, and Gonfiantini, 1970).

The recorder also performs useful functions in providing a more sensitive display than the meters for adjusting signal height and ensuring that amplifiers are zeroed and, in the

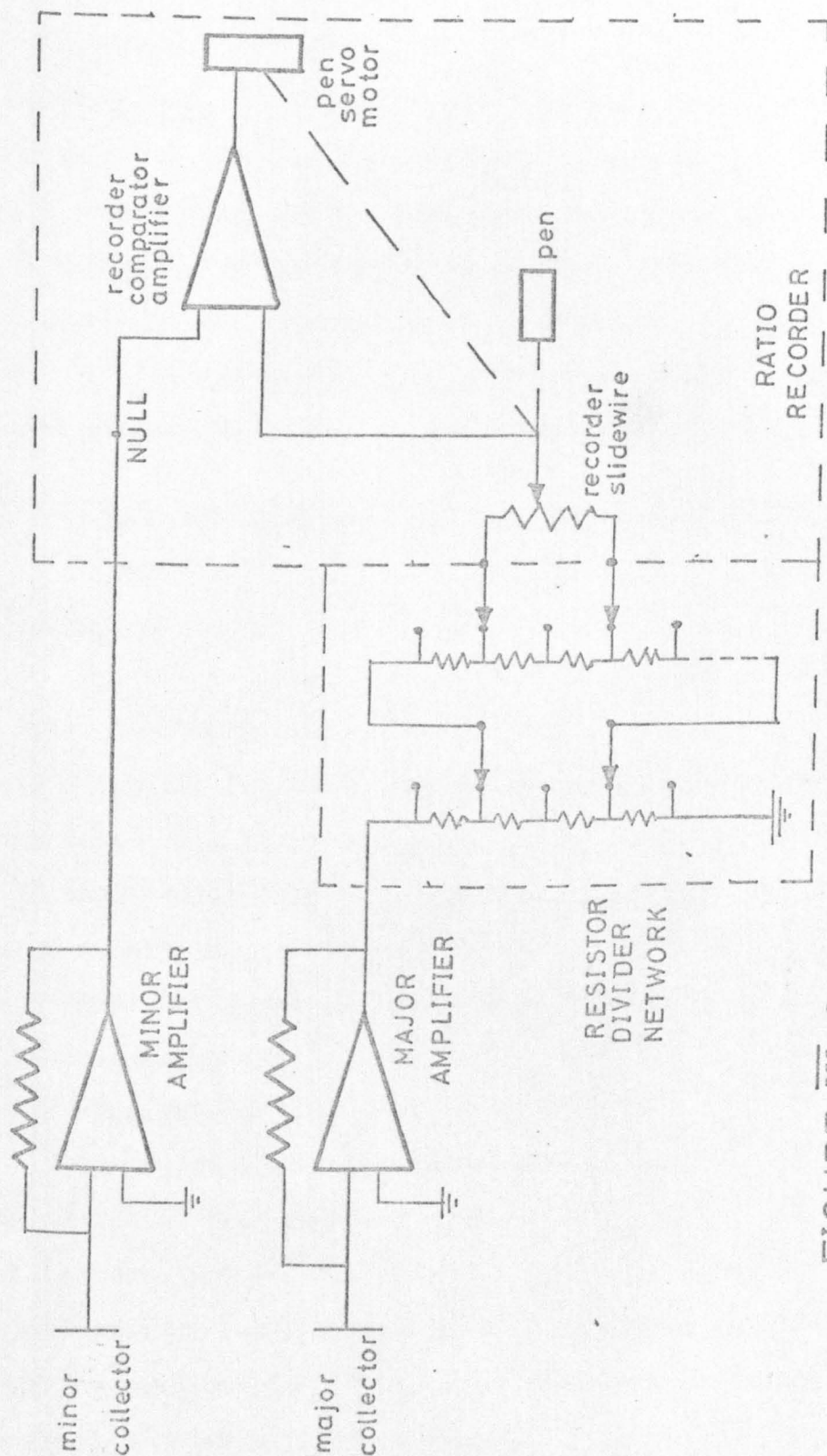


FIGURE III-2

Infinite Bridge Null System.

single beam scanning mode, for checking resolution, peak shapes, peak overlap tails and sample and background spectra. In order to objectively average and present the output ratio, the signal from the recorder re-transmitting slidewire is fed to a digital integrator which provides significance to six figure readout. The signal is integrated over the final 30 sec. of the automatic switching period and is displayed, from changeover, over the whole of the next measuring cycle.

III-6 Mass spectrometry errors, correction factors and data reduction.

(a) Errors

For convenience, instrumental errors may be divided into three broad categories:

- (1) those determined by the inherent statistical nature of the quantities being measured,
- (2) those determined by non-reproducibility of the measurement conditions,
- (3) those, of a systematic nature, determined by instrumental and analytical techniques.

Each type will be discussed in turn.

The first group includes errors introduced internally by deviation from stable gas flow conditions, by instabilities of ionising and accelerating voltages, and by amplifier fluctuations. Some errors of this type can be minimised by instrumental design: others by sufficiently careful attention to details of technique. 'Noise', however, must always be expected as a permanent feature of the system.

The second group refers to the effects of such external parameters as temperature, humidity, stray field etc., and to such internal factors as changing background conditions and transient memory effects. The overall result of these is that, in cases of extreme variation, measurements will be both time-dependent and condition-dependent. Reduction of these errors can be achieved by carefully controlling the ambient temperature and humidity, avoiding too highly enriched samples, and by shielding. In addition, the time interval between changeover valve switching should be optimal. If this period is too short, stable measurement conditions will not have been attained before the second gas is introduced into the system. On the other hand, too long an interval will lead to errors originating from time-dependent instrument characteristics. In practice, it is found that transient lifetimes are short, seldom lasting more than a few seconds. The integrating period is arranged to exclude these transient signals.

The third group of instrumental errors is the most important. Incomplete resolution of ion beams at the collectors ('peak tail overlap'), leakage across the changeover valve seatings, isotopic fractionation in the gas flow, and permanent contributions from residual vacuum peaks may all seriously impair machine performance. In the cases in which the above cannot be reduced to insignificance, the appropriate correction factors must be measured, and applied in the data analysis. Since these errors are of a systematic nature, they

should not affect reproducibility, once they have been properly accounted for.

In addition to the instrumental errors discussed above, there may also exist errors which arise from impurities in the sample gas. (It is assumed that the standard gas is clean: this was frequently checked by observation of its spectrum). There are several sources of contamination which are likely to be especially troublesome:

(i) traces of organic solvents used for cleaning purposes; for example, acetone gives a peak at mass 43 (CH_3CO^+), alcohol at 45 ($\text{C}_2\text{H}_5\text{O}^+$), and petroleum ether peaks in the range 40 to 44.

(ii) the samples themselves may contain hydrocarbons or inorganic contaminants (e.g. N_2O) which would require special procedures for their removal.

(iii) samples may become impure by leakage of air into the sample bottle prior to analysis. This can usually be detected and remedied easily.

One contaminant which is relatively common, yet should be avoided if possible, is water vapour. Wet samples do not give stable ratio traces and even minute quantities of water vapour are particularly difficult to remove from the gas handling system. Over and above this, exchange of oxygen isotopes between the carbon dioxide and the water may, in cases of gross contamination, lead to modification of the isotope ratio of the gas.

(b) Correction factors and data reduction.

The analytical results of carbon and oxygen isotope measurements are commonly reported in the 'delta' (δ) notation. In this, the deviation of the sample isotopic abundance ratio from that of a standard, or reference, is represented. Thus, delta values are defined as:

$$\delta^{13}\text{C} = \frac{(^{13}\text{C}/^{12}\text{C})_{\text{sample}}}{(^{13}\text{C}/^{12}\text{C})_{\text{reference}}} - 1$$

$$\delta^{18}\text{O} = \frac{(^{18}\text{O}/^{16}\text{O})_{\text{sample}}}{(^{18}\text{O}/^{16}\text{O})_{\text{reference}}} - 1$$

Delta values are usually (but not always) given as 'per mil', or part per thousand, written ‰; thus:

$$\delta^{13}\text{C} \text{‰} = \left(\frac{(^{13}\text{C}/^{12}\text{C})_{\text{sample}}}{(^{13}\text{C}/^{12}\text{C})_{\text{reference}}} - 1 \right) \times 10^3$$

In practice, on the '602B instrument, $^{13}\text{C}/^{12}\text{C}$ and $^{18}\text{O}/^{16}\text{O}$ ratios are not measured directly. Rather, mass 45/44 and mass 46/(44+45) ratios are measured; these are then related to the required quantities.

Four steps will be distinguished in the data reduction:

- (i) measurement of average 45/44 and 46/(44+45) ratio differences between sample and standard,
- (ii) correction of the above differences for various instrumental characteristics,

(iii) calculation of delta values with respect to the working standard in terms of $^{13}\text{C}/^{12}\text{C}$ and $^{18}\text{O}/^{16}\text{O}$ ratios determined from the corrected differences,

(iv) conversion of the above delta values to those with respect to some conventional reporting standard(s).

A typical recorder output trace obtained from the mass spectrometer is shown in Figure III-3. The last four figures of each ratio are obtained from the digital integrator; the first of these is added onto the third figure of the decade potentiometer setting. The 'ratio factor' is that fraction of the major ion beam signal used for comparison with the minor ion beam signal in the ratio measurement system. To allow for linear drift in the ratio reading during a run (due to sample depletion, for example), each successive pair of reference readings is averaged.

Defining δR as a raw, uncorrected delta value, put:

$$\delta R = \frac{\bar{X}}{\bar{Y}} \cdot 10^3 \text{‰}$$

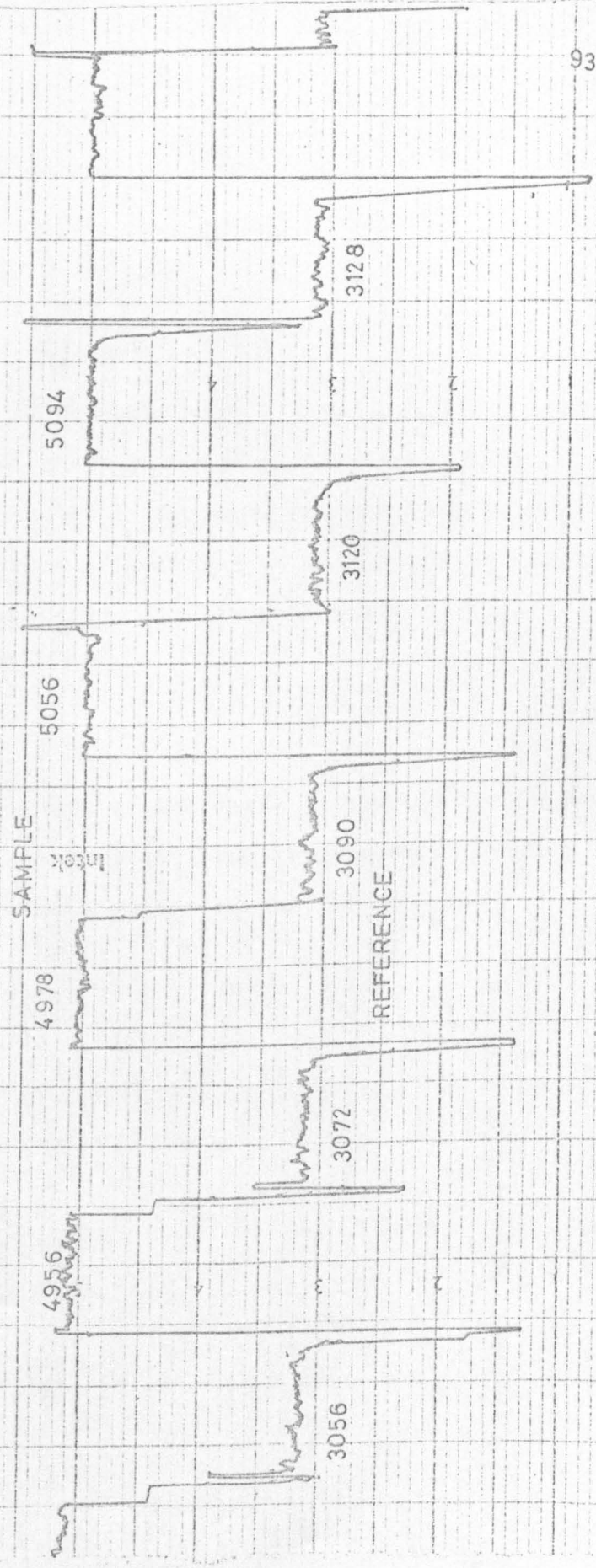
where \bar{X} is the mean difference between sample and standard output signals, allowing for linear drift; and \bar{Y} is the mean standard signal.

The random errors originating in statistics, discussed under group one (1) above, are manifested in two ways. Firstly, by the crenulate nature of the ratio traces, and secondly by scatter of the individual X_i and Y_i values about their respective means. A measure of the scatter in the X_i

FIGURE III-3

Typical Recorder Output Trace
for 45/44 Measurement

RATIO FACTOR = 0.02
RATIO DECADE SETTING = 0.610
 $\delta^{13}\text{C} = 3.14\text{‰}$
 $\sigma_{\text{C}} = 0.04$ $2\sigma_{\text{C}} = 0.08$



is given by the standard deviation σ_x :

$$\sigma_x = \sqrt{\frac{\sum_{i=1}^n (X_i - \bar{X})^2}{n-1}}$$

The mean value of \bar{X} obtained over a finite number, n , of comparisons is not identical with the mathematically expected value, denoted X (Galimov, Grinenko and Ustinov, 1965). The deviation of \bar{X} from X is random and is known as the representative error; its absolute value Δ_x is of interest:

$$\Delta_x = |\bar{X} - X|$$

since this is a measure of the error introduced into \bar{X} by the statistics of comparison. The representative error follows Student's distribution (Meyer, 1965). Let:

$$t = \frac{\Delta_x \sqrt{n}}{\sigma_x}$$

then Student's t -distribution with $(n-1)$ degrees of freedom is given by (Meyer, 1965 p.258):

$$h_{n-1}(t) = \frac{\Gamma(n/2)}{\Gamma(\frac{n+1}{2}) \sqrt{2\pi(n-1)}} \left(\frac{1+t^2}{n-1} \right)^{-n/2}, \quad -\infty < t < \infty$$

where:

$$\Gamma(m) = \int_0^{\infty} x^{m-1} e^{-x} dx \quad \text{is the Gamma Function.}$$

For a given confidence coefficient α , $0.5 < \alpha < 1$, the values of $t_{n-1, \alpha}$ satisfying the condition:

$$\int_{-\infty}^{t_{n-1, \alpha}} h_{n-1}(t) dt = \alpha$$

are tabulated (Meyer, 1965, Appendix Table 4). It is to be noted here that $t_{n-1, \alpha}$ may be of either sign; so, given $\Delta_x \sqrt{n} / \sigma_x$ and confidence coefficient α , the aforementioned table gives the values of $t_{n-1, \alpha}$ such that the probability of $\left| \frac{\Delta_x \sqrt{n}}{\sigma_x} \right| \leq t_{n-1, \alpha}$ is α . This is written:

$$P\left(\left| \frac{\Delta_x \sqrt{n}}{\sigma_x} \right| \leq t_{n-1, \alpha} \right) = \alpha$$

i.e.

$$P(-t_{n-1, \alpha} \leq \frac{\Delta_x \sqrt{n}}{\sigma_x} \leq t_{n-1, \alpha}) = \alpha$$

using the fact that $t_{n-1, \alpha}$ may be of either sign. In fact, what is of interest, is:

$$P\left(\frac{\Delta_x \sqrt{n}}{\sigma_x} \leq t_{n-1, \alpha} \right)$$

Now:

$$\begin{aligned} \alpha &= P(-t_{n-1, \alpha} \leq \frac{\Delta_x \sqrt{n}}{\sigma_x} \leq t_{n-1, \alpha}) \\ &= P\left(\frac{\Delta_x \sqrt{n}}{\sigma_x} \leq t_{n-1, \alpha} \right) - P\left(\frac{\Delta_x \sqrt{n}}{\sigma_x} \geq t_{n-1, \alpha} \right) \end{aligned}$$

$$= P\left(\frac{\Delta_x \sqrt{n}}{\sigma_x} \leq t_{n-1, \alpha}\right) - \left[1 - P\left(\frac{\Delta_x \sqrt{n}}{\sigma_x} \leq t_{n-1, \alpha}\right)\right]$$

$$\text{i.e. } P\left(\frac{\Delta_x \sqrt{n}}{\sigma_x} \leq t_{n-1, \alpha}\right) = \frac{1+\alpha}{2}$$

The choice of α is dependent on the confidence to be placed on the reliability of the results. Taking $\alpha=0.05$ (two sigma law), so that only in 5 cases out of 100 does the statistical error exceed the calculated Δ_x :

$$P\left(\frac{\Delta_x \sqrt{n}}{\sigma_x} \leq t_{n-1, \alpha}\right) = \frac{1+\alpha}{2} = 0.975$$

Taking this value, 0.975, and the number of degrees of freedom, $(n-1)$, the corresponding value of $t_{n-1, \alpha}$ can be found from the tables. Now:

$$t = \frac{\Delta_x \sqrt{n}}{\sigma_x}$$

so the representative error can be calculated from:

$$\Delta_x = \frac{t \sigma_x}{\sqrt{n}}$$

Note that Δ_x increases with σ_x but decreases with n . Hence, when there is a lot of scatter among the X_i leading to high σ_x , the number of comparisons, n , should be increased in compensation.

In a similar manner:

$$\Delta_y = \frac{\sigma_y t}{\sqrt{n}}$$

Let representative errors Δ_x and Δ_y introduce into δ errors Q_x and Q_y respectively. Now:

$$d\delta = d\left(\frac{\bar{X}}{\bar{Y}} 10^3\right) = \frac{10^3}{\bar{Y}} \Delta_x + 10^3 \frac{\bar{X}}{\bar{Y}^2} \Delta_y$$

so that:
$$Q_x = \frac{10^3}{\bar{Y}} \Delta_x \text{ } \text{‰}$$

$$Q_y = \frac{10^3 \bar{X}}{\bar{Y}^2} \Delta_y \text{ } \text{‰}$$

Normally, in practice, $Y \gg X$ so that Q_y is negligible. In Table III-1 below is shown, for $\alpha=0.95$, an example of the variation of Δ_x and Q_x with increasing n , for one run. Bearing in mind that the $Q_x \text{ } \text{‰}$ column is applicable at the two sigma level, it is considered that, for reasonable σ_x , a value of n between 5 and 10 is adequate. As emphasised earlier, however, n should be increased if the measurement conditions deteriorate, for the error discussed is essentially of a random nature and cannot be corrected for. The last row of Table III-1 shows the standard deviation of the various individual deltas for the different values of n . It will be noted that, unlike Q_x , this error does not decrease with increasing n . This may indicate that the ion statistics are the ultimately limiting factor.

The various correction factors for instrumental characteristics which must be applied will now be discussed, and their measurement and importance for the Micromass 602

TABLE III-1

n	5	10	15	20
$\delta^{\circ}/\text{‰}$	-3.325	-3.359	-3.345	-3.349
\bar{X}	-2041	-2061	-2053	-2056
\bar{Y}	613922	613728	613904	614070
σ_x	23	27	27	24
Δ_x	28.6	19.3	14.9	11.2
$Q_x^{\circ}/\text{‰}$	0.047	0.031	0.024	0.018
$\sigma_{\delta}^{\circ}/\text{‰}$	0.036	0.046	0.045	0.040

Statistical variations within an analysis.

described. There exist in the literature several reports of this type of work (among others, Craig 1957; Deines 1970; Mook and Grootes 1973). However, different models of instrument have quite different characteristics and the credibility placed on results is limited by machine performance, so a brief account of the details for the Micromass 602 B will be given. In presentation and notation, the approach of Deines (1970) is followed as perhaps the most lucid of the above cited papers.

Leak correction (LC)

It is well known that isotope fractionation effects are inherent in the capillary system by which CO_2 is introduced into the ion source of the mass spectrometer (Halstead and Nier, 1950; and Kistemaker, 1953). Furthermore, from time to time small differences may occur in the isotope ratio of the working standard gas. To take into account these two possible sources of error, a system of six one-litre aliquots of working standard gas is used. All analyses are carried out with one of these aliquots as reference gas. The other five are compared against this, one per day, through the sample side of the inlet system, and the mean of these measurements is used as the standard relative to which all sample measurements are calculated.

All the following correction factors^a originate from extraneous contributions to the ion currents.

Abundance sensitivity correction (AC)

Two factors are claimed by Mook and Grootes (1973) to cause spreading of the major ion beam and subsequent detection of its ions at the minor collector.

These are:

- (i) collisions between the ions and molecules of the residual gas, and
- (ii) coulombic repulsion of similarly charged ions.

The definition of abundance sensitivities is given by Deines (1970) as the inverse fraction of the number of ions of mass M which are collected at the position of mass $M+1$, $M+2$ etc. To estimate these, the ion beam currents corresponding to m/e 44, 45 and 46 are measured under normal operating conditions. The instrument is then switched to a high sensitivity mode and a scan through the spectrum taken, (see Figure III-4). By extrapolation of the 44 peak tail, the overlap ion currents at masses 45 and 46 can then be calculated. It will be noted from Figure III-4 that peaks at 47 and 48 are also recorded. It is suggested that these arise from CO_2 also. In Table III-2 are compared the observed ion currents and the theoretical relative probabilities of occurrence of the various mass species of CO_2 . The current expected at peak 49 on the basis of the calculated theoretical probability of occurrence would be of the order of 8×10^{-15} A, well below the limit of detection at the sensitivity used. The agreement for the other peaks is considered sufficiently good to accept the hypothesis

FIGURE III-4
Scan through
CO₂ Spectrum.

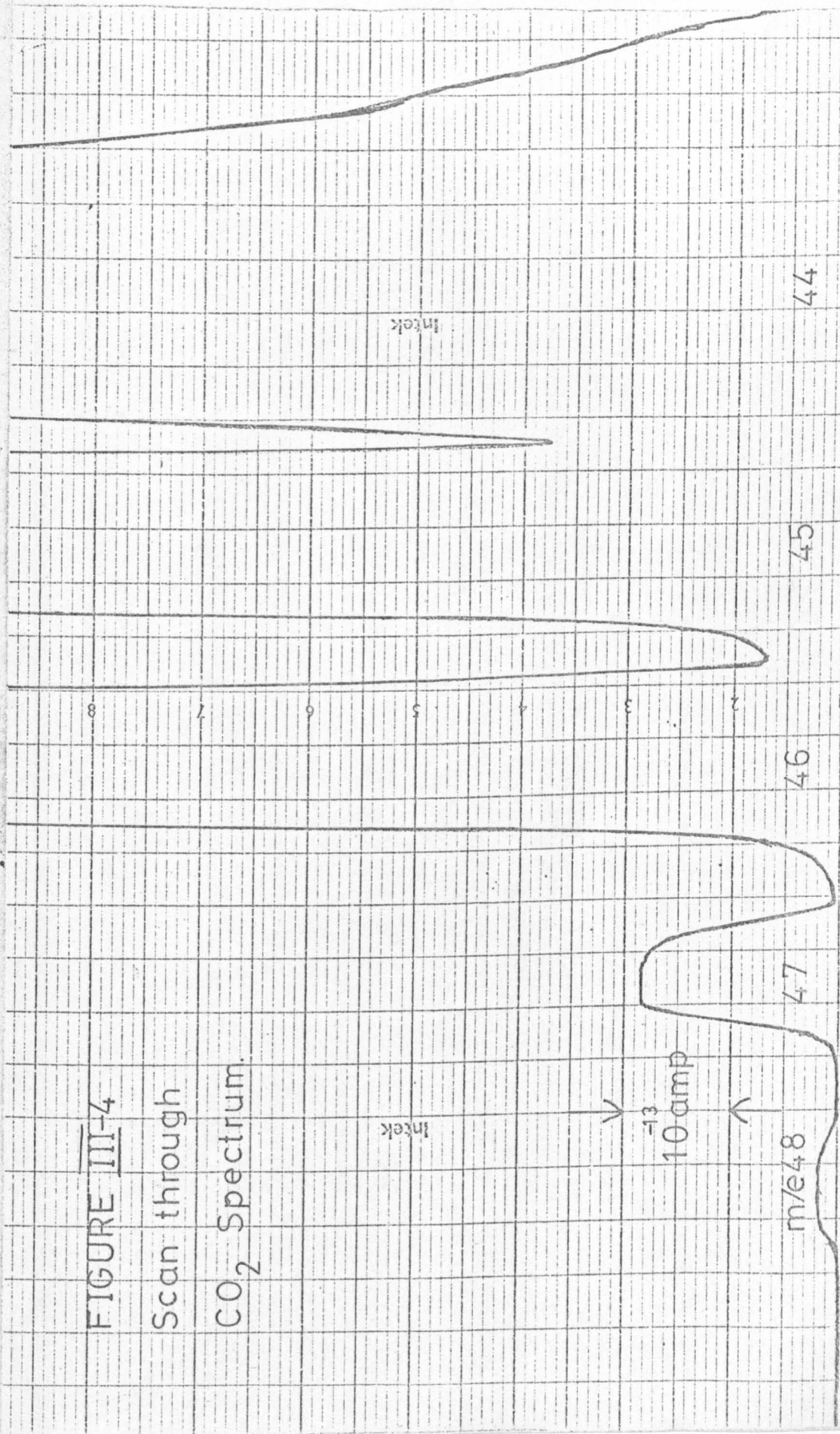


TABLE III-2

m/e	$I^{m/e}$ A.	$I^{m/e} / I^{44}$	COMPONENTS	CALCULATED RELATIVE PROB.
44	4×10^{-9}	1	$^{12}\text{C } ^{16}\text{O } ^{16}\text{O}$	1
45	5×10^{-11}	0.0125	$^{13}\text{C } ^{16}\text{O } ^{16}\text{O} + ^{12}\text{C } ^{16}\text{O } ^{17}\text{O}$	0.0120
46	1.8×10^{-11}	0.0045	$^{13}\text{C } ^{16}\text{O } ^{17}\text{O} + ^{12}\text{C } ^{16}\text{O } ^{18}\text{O} + ^{12}\text{C } ^{17}\text{O } ^{17}\text{O}$	0.0041
47	1.8×10^{-13}	0.000045	$^{13}\text{C } ^{16}\text{O } ^{18}\text{O} + ^{13}\text{C } ^{17}\text{O } ^{17}\text{O} + ^{12}\text{C } ^{18}\text{O } ^{17}\text{O}$	0.000049
48	$\sim 0.2 \times 10^{-13}$	0.000005	$^{13}\text{C } ^{18}\text{O } ^{17}\text{O} + ^{12}\text{C } ^{18}\text{O } ^{18}\text{O}$	0.000017
49			$^{13}\text{C } ^{18}\text{O } ^{18}\text{O}$	0.00000019

Carbon dioxide spectrum.

meantime. The estimated overlap currents in Figure III-4 are 0.04×10^{-12} A. at peak 45 and 0.007×10^{-12} A. at 46. With 4×10^{-9} A. major beam current, these correspond to abundance sensitivities of 1×10^5 and 5.7×10^5 respectively. The multiplicative correction factors for delta values (Deines 1970) are then:

$$ACC = 1.0008 \text{ for } 45/44$$

$$ACO = 1.0004 \text{ for } 46/(44+45)$$

The percentage of the total ion currents which the 44 tail currents contribute are 0.08% at 45 and 0.04% at 46; for the former, Bridger *et al.* (1973) quote 0.07%.

Background correction (BC)

The background discussed under this heading is that of the residual gas in the mass spectrometer when evacuated. There are two methods of monitoring this background:

- (i) measurement of total pressure by the ion gauge, and
- (ii) measurement of individual mass peaks by background scanning at high sensitivity.

Under normal conditions after bakeout, the pressure in the mass spectrometer analyser region falls to less than 5×10^{-9} torr. Only four peaks are then observed with currents greater than 5×10^{-15} A. These occur at m/e 28, 32, 36 and 44. However, after introduction of CO_2 , the background increases, typically to a pressure of around 7×10^{-9} torr, due mainly to increases in 28 and 44 peak heights. Except when hydrocarbon contamination is present, all ion currents except for

peaks 28, 32, 36 and 44 are again less than 5×10^{-15} A. A typical background spectrum is shown in Figure III-5, and Table III-3 summarises data for examples of the two cases discussed above.

During operation, the mass 44 ion current is of the order of 4×10^{-9} A, so that the background represents a sufficiently small fraction of the total ion beam intensity for it to be ignored.

Valve mixing correction (VMC)

When sample CO_2 is being analysed, a small proportion of the gas reaching the ion source comes, in fact, from the reference side of the inlet system, and vice versa. This is caused by imperfect mating of the changeover valve seal components. The valve mixing correction is a multiplicative factor which allows for this effect.

With one side of the inlet system being pumped, CO_2 is admitted to the other to give a major ion beam current of 10^{-8} A. The above-background signal for the evacuated side is then measured at the highest possible sensitivity. The inlet roles are reversed and the measurement repeated; typical values are of the order of 5.0×10^{-12} A, i.e. 0.05% which, when added, give a valve mixing correction factor of around 1.001. The procedure is carried out periodically, but little variation has been observed. This is the largest of the measured correction factors.

The formulae for the conversion of 45/44 and 46/(44+45) ratios to delta values in terms of $^{13}\text{C}/^{12}\text{C}$ and $^{18}\text{O}/^{16}\text{O}$ ratios

FIGURE III-5

TYPICAL SPECTRUM OF INSTRUMENT BACKGROUND

Pressure = 8×10^{-9} torr

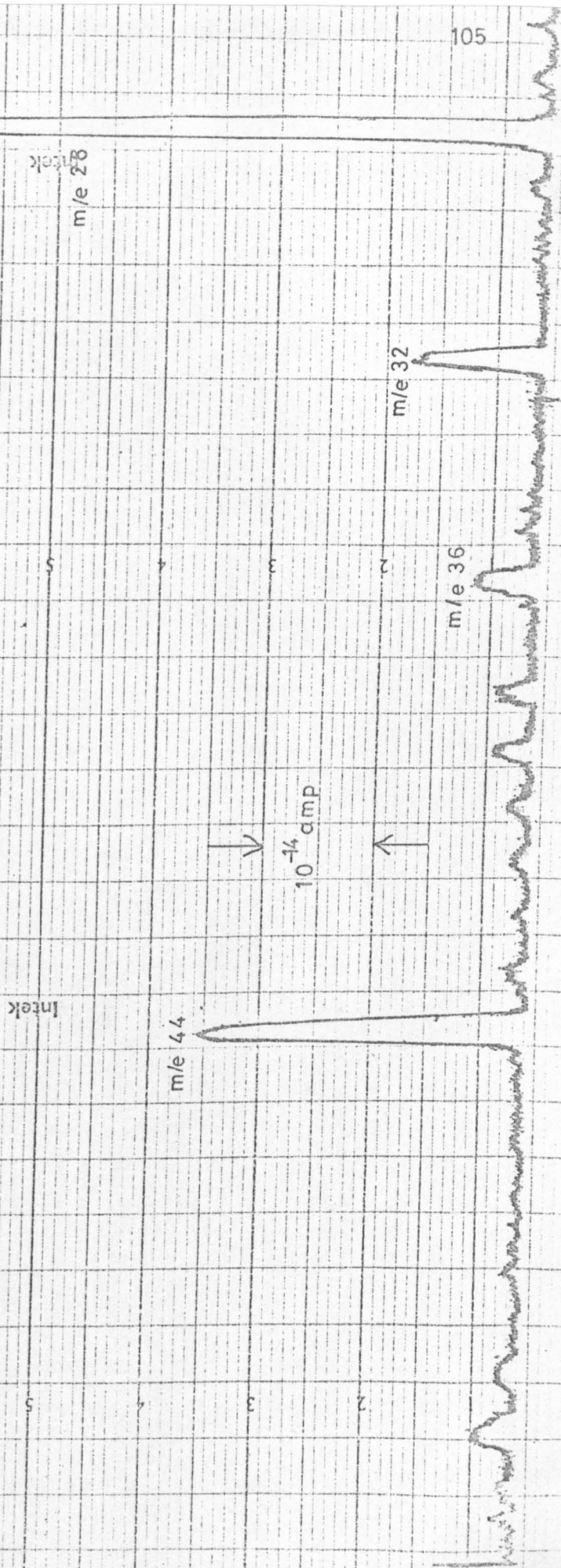


TABLE III-3

m/e	ORIGIN	13.11.73 (10^{-14} A.)	2.9.74. (10^{-14} A.)
28	N_2^+ , CO^+	3.8	7.8
32	O_2^+	0.5	1.2
36	HCl^+ FROM CLEANING COMPOUND	0.4	0.6
44	CO_2^+	2.8	3.0

Background Conditions:

After bakeout 13.11.73: ion gauge pressure
> 2×10^{-9} torr.

Normal 2.9.74: ion gauge pressure $\sim 8 \times 10^{-9}$ torr.

have been given by Craig (1957). Their deduction is straightforward, though tedious, and will not be elaborated here. Adopting Craig's notation:

δ_m = the measured enrichment corrected for the previously discussed instrumental characteristics;

δ_c = the true enrichment;

and Solenhofen Limestone as the standard, gives:

$$\delta_c^{13}\text{C} = 1.0677\delta_m^{13}\text{C} - 0.0338\delta_c^{18}\text{O}$$

$$\delta_c^{18}\text{O} = 1.0014\delta_m^{18}\text{O} + 0.0091\delta_c^{13}\text{C}$$

The δ_c values are then found to the required accuracy by iteration. The formulae for standards other than Solenhofen are readily calculated from knowledge of their delta values relative to Solenhofen.

It is conventional to report $\delta^{13}\text{C}$ results relative to PDB and $\delta^{18}\text{O}$ results for water relative to SMOW. The PDB standard is CO_2 produced from the Cretaceous belemnite Belemnitella americana by reaction with 100% H_3PO_4 at 25.2°C (Urey et al., 1951). The SMOW standard (Craig, 1961) is very close to the mean $\delta^{18}\text{O}$ concentration of seawater.

To change from one standard (A, say) to another (B) is a simple matter, the relevant formula being (Craig, 1957):

$$\delta_{(\text{SAM}-\text{B})} = \delta_{(\text{SAM}-\text{A})} + \delta_{(\text{A}-\text{B})} + 10^{-3}\delta_{(\text{SAM}-\text{A})}\delta_{(\text{A}-\text{B})}$$

Note that this implies:

$$\delta_{(B-A)} = \frac{-\delta_{(A-B)}}{(1+10^{-3}\delta_{(A-B)})}$$

A FORTRAN computer program which takes the raw data, corrects for instrumental characteristics and calculates the results relative to any selected standard is given as Appendix 1. Various relevant statistical data are included in the print-out.

III-7 Selection of optimal operating characteristics.

In previous sections have been described many of the fine adjustments which can be made in order to improve the performance and reliability of the mass spectrometer. In this section are briefly outlined experiments undertaken to find the optimal working characteristics.

There are, in general, three main criteria which are applied in the selection of operating characteristics:

- (i) maximisation of ion beam intensities;
- (ii) minimisation of variation of beam intensity with particular parameter;
- (iii) minimisation of variation of ratio with particular parameter.

These three are not mutually exclusive and, in fact, frequently coincide.

Craig (1957) has termed the variation of the recorded ratio with ion beam intensity the 'pressure effect'; he suggested that it was caused by the tail of the m/e 44 peak

overlapping onto the 45 and 46 ion beams. It is trivial to show that an overlap current (I_t) which is proportional to the major ion beam current (I_{44}) does not lead to a pressure effect, so a linear functional dependence is ruled out.

Craig therefore proposed that the tail contributions varied as the square of the major beam intensity:

$$I_t = k_1 I_{44}^2 + k_2 I_{44}$$

and considered a coulombic effect the most likely physical explanation. It had been discovered empirically in Urey's Chicago laboratory that the pressure effect could be eliminated by the application of a small potential bias on the vibrating reed amplifier. Putting I_{46} and I_r as, respectively, the minor ion beam currents derived from the mass 46 ions and the reed bias potential, the total measured minor beam current is given by ($I_{46} + I_r + I_t$). The measured ratio is thus:

$$R_m = (R + k_2) + I_r/I_{44} + k_1 I_{44}$$

where $R = I_{46}/I_{44}$ is the true ratio. It is then clear that changes in I_{44} and $1/I_{44}$ can be arranged to cancel, thus eliminating the pressure effect. On the basis of the above equation Craig predicted, and subsequently verified, the functional dependence of R_m on I_{44} . Thus for small I_{44} , R_m decreased with increasing I_{44} , with gradient $- I_r/I_{44}^2$. After passing through a minimum, R_m subsequently increased linearly with slope k_1 . As pointed out by Craig (1957), a reed bias of opposite polarity leads to R_m increasing

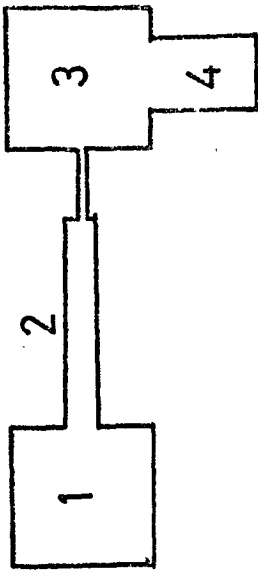
monotonically with I_{44} , finally reaching linear dependence with gradient k_1 .

Mook and Grootes (1973) also found that the recorded ratio decreased, went through a minimum and then increased linearly with I_{44} (in fact, in their case, the voltage V_{44} rather than the current was measured). The two causes they discussed were negative voltage gradients of the high input resistances in the collector circuits, and peak broadening. For the latter, they claimed to show that the overlap was dependent on ion scattering by gas molecules only: coulombic effects were negligible. For natural carbon samples, the correction necessary to compensate for a 1% pressure differential was 0.07%/o.

An as yet unmentioned way in which changes in inlet pressure could induce ratio changes arises from the gas flow through the capillary constriction. Figure III-6, taken from Kistemaker (1953), shows diagrammatically the components of the gas-handling system. The flow of the i^{th} component of a gas mixture along the constriction is given by a modified form of the Knudsen equation (Kistemaker, 1953):

$$Q_{i23} = \frac{k_{23}}{M_i^{\frac{1}{2}}} (P_{i2} - P_{i3}) + \frac{\nu P_{i2}}{P_2} \frac{P_2 + P_3}{2} (P_2 - P_3)$$

where P refers to pressure; ν is the coefficient of viscous flow; k_{23} is a constant for a given temperature and geometry; M is molecular mass and the numerical subscripts refer to regions identified in Figure III-6.



Regions 1 and 2 are duplicated for sample and standard gases.

- Region 1 Gas Reservoir
- Region 2 Long Capillary (viscous flow) and Short Constriction (molecular flow)
- Region 3 Ion Source
- Region 4 Diffusion Pump

Figure III-6
Schematic Diagram of Gas Handling System

Although the second term is not mass-dependent (viscous flow), the first term is (molecular flow); hence, isotope fractionation occurs and is a function of the partial pressure gradient ($P_{i2} - P_{i3}$).

The variation of recorded ratio with major ion beam intensity for the Glasgow Micromass 602B is shown in Figure III-7 for 45/44 and in Figure III-8 for 46/(44+45). In stark contrast to the observations of Craig (1957) and Mook and Grootes (1973), the ratio is always seen to decrease with increasing major ion current. Over the ranges studied, no local minima are seen.

To estimate the effect of capillary fractionation, measurements were made at two different capillary settings. (Thus the inlet pressures - and so pressure gradients - necessary to attain the various major ion beam intensities were different). The results are plotted in Figure III-9 and indicate that such capillary effects are negligible. Since different aliquots of gas were used in the two experiments, the agreement of the absolute ratios is surprising and perhaps fortuitous.

The argument against a significant capillary effect can be considerably strengthened by the following analysis. Let i refer to the major isotopic species and j the minor, then the ratio of flows is Q_{j23}/Q_{i23} and this is taken as directly proportional to the ratio of collected ion beams, R_m . (This assumes no mass discrimination effect during ionization - a

Figure III-7
Variation of 45/44 Ratio with Major Beam Intensity.

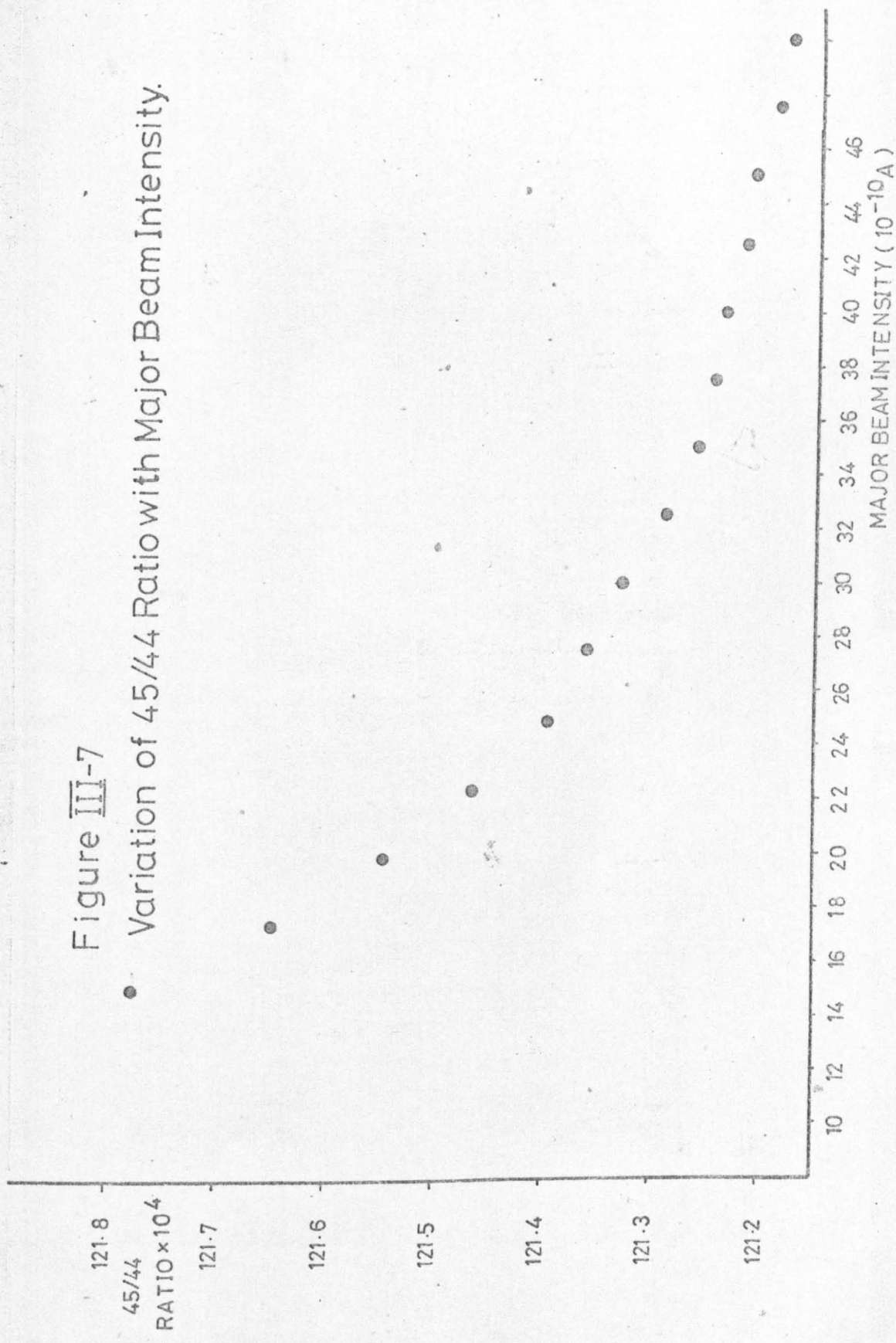
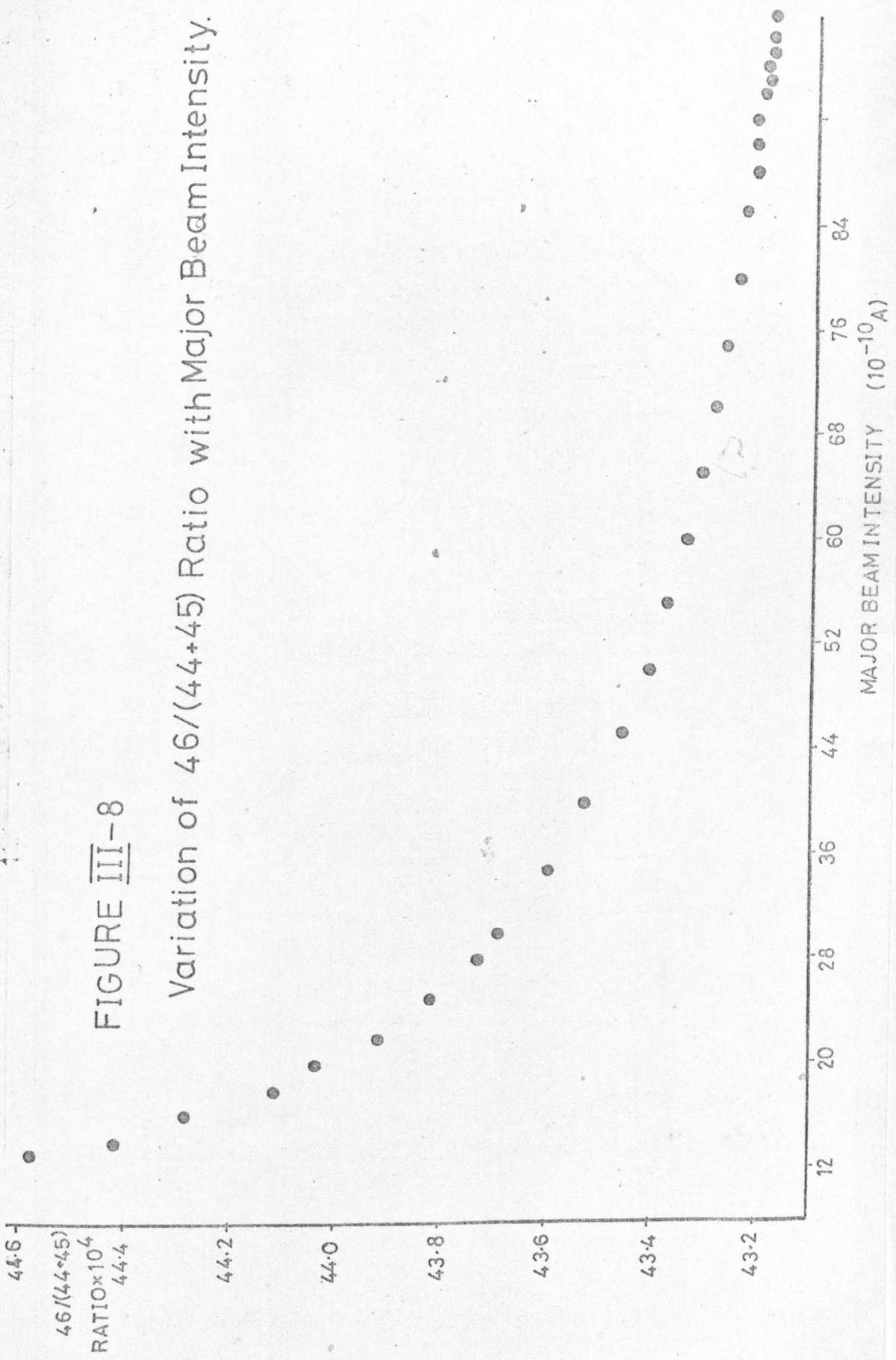
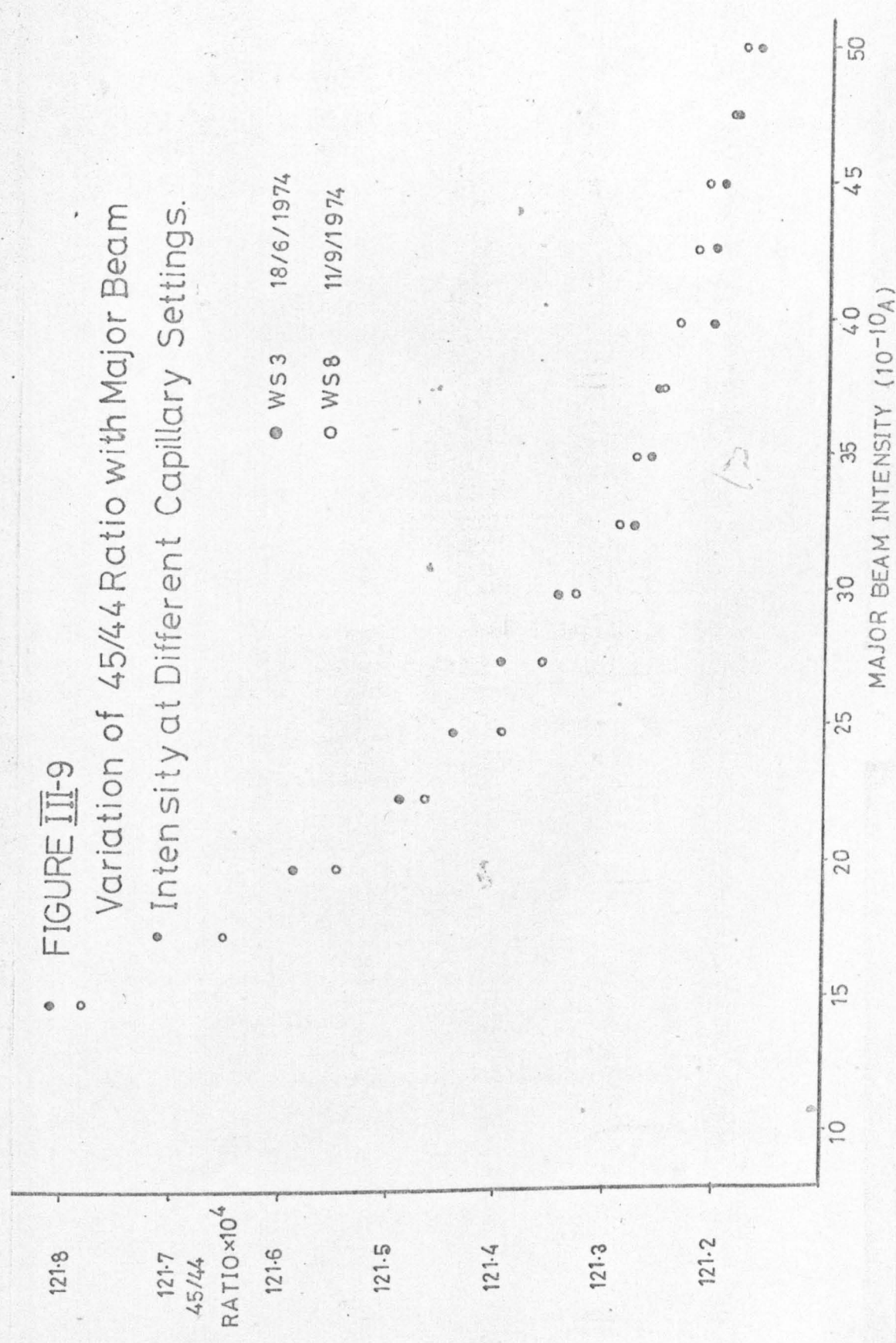


FIGURE III-8

Variation of $46/(44+45)$ Ratio with Major Beam Intensity.



• FIGURE III-9
 • Variation of 45/44 Ratio with Major Beam Intensity at Different Capillary Settings.



not unreasonable hypothesis in view of experiments described later).

$$\therefore R_m = \frac{Q_{j23}}{Q_{i23}} = \frac{\frac{k_{23}}{M_j^{\frac{1}{2}}}(P_{j2}-P_{j3})+(P_2-P_3)\frac{\nu P_{i2}}{P_2}\left(\frac{P_2+P_3}{2}\right)}{\frac{k_{23}}{M_i^{\frac{1}{2}}}(P_{i2}-P_{i3})+(P_2-P_3)\frac{\nu P_{i2}}{P_2}\left(\frac{P_2+P_3}{2}\right)}$$

Now there are at least two orders of magnitude more i than j molecules, so to good approximation:

$$P_{i2} = P_2 ; \quad P_{i3} = P_3$$

and in a typical case for 45/44:

$$(P_{j2}-P_{j3}) \simeq 10^{-2}(P_2-P_3); \quad P_{j2} \simeq 10^{-2}P_2,$$

so that:

$$R_m = \frac{\frac{k_{23}}{M_j^{\frac{1}{2}}} + \frac{\nu}{2}(P_2 + P_3)}{\frac{k_{23}}{M_i^{\frac{1}{2}}} + \frac{\nu}{2}(P_2 + P_3)} \quad (\times 10^{-2})$$

$$\therefore \frac{dR_m}{d(P_2+P_3)} = \frac{\frac{\nu}{2}\left\{\frac{k_{23}}{M_i^{\frac{1}{2}}} + \frac{\nu}{2}(P_2+P_3)\right\} - \frac{\nu}{2}\left\{\frac{k_{23}}{M_j^{\frac{1}{2}}} + \frac{\nu}{2}(P_2+P_3)\right\}}{\left\{\frac{k_{23}}{M_i^{\frac{1}{2}}} + \frac{\nu}{2}(P_2+P_3)\right\}^2} \quad (\times 10^{-2})$$

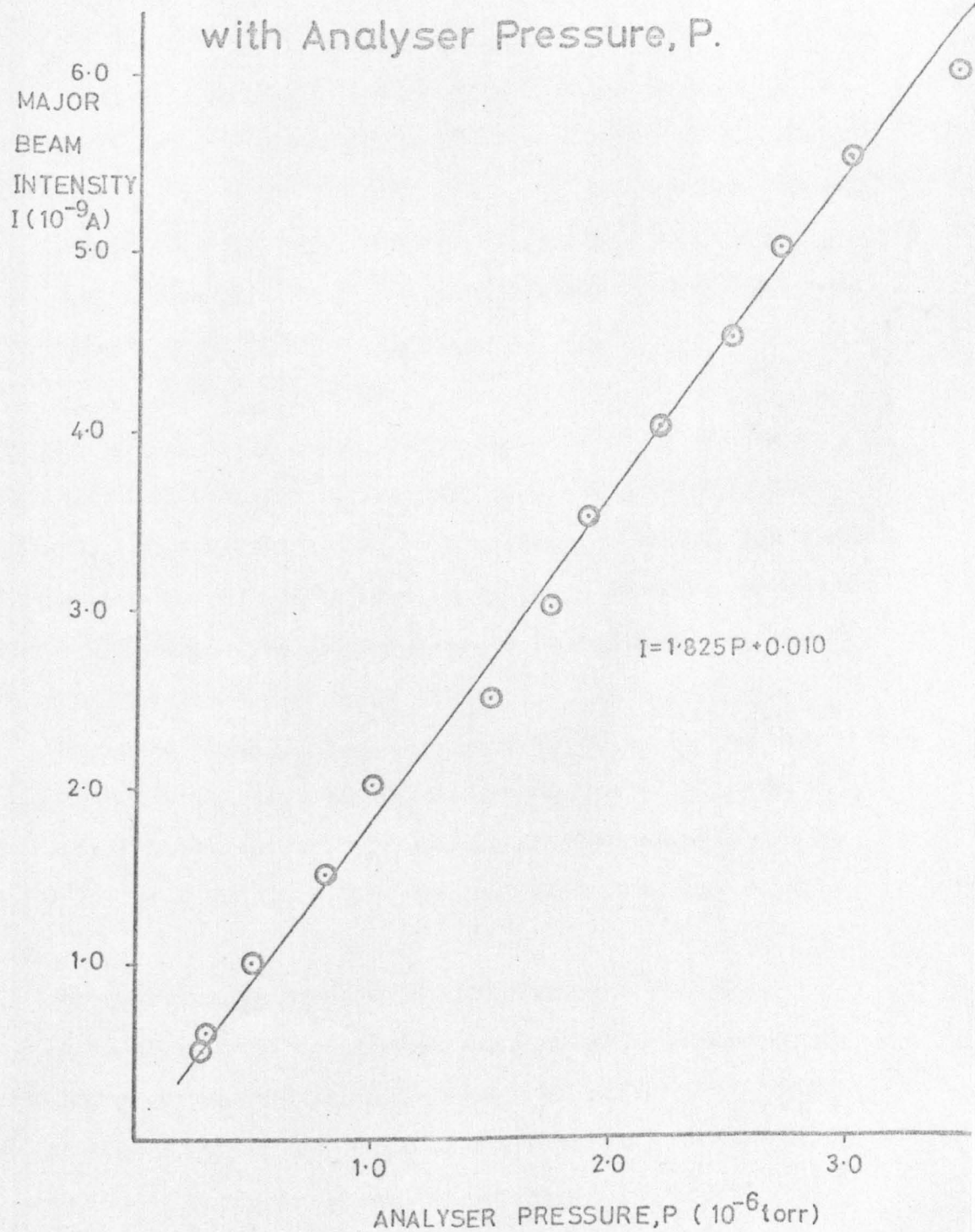
$$\therefore \frac{dR_m}{d(P_2+P_3)} = \frac{\frac{\nu}{2} k_{23} 10^{-2} \left(\frac{1}{M_i^{1/2}} - \frac{1}{M_j^{1/2}} \right)}{\left(\frac{k_{23}}{M_i^{1/2}} + \frac{\nu(P_2+P_3)}{2} \right)^2}$$

Now ν and k_{23} are both obviously positive, the denominator is a squared term, and $M_i < M_j$ so that $(1/M_i^{1/2} - 1/M_j^{1/2})$ is also positive, i.e. $dR_m/d(P_2+P_3) > 0$. But the major ion beam intensity is positively linearly correlated to pressure (as shown in Figure III-10), so $dR_m/dI_{\text{major}} > 0$ for changes induced by gas flow variation. Hence the observed dependence of measured ratio on ion beam intensity cannot be explained by changing flow conditions caused by pressure variations. It is clear that this argument is not invalidated by errors in any of the numerical values assumed - only the signs are of importance.

No high resistors are used in the 602B collector circuits, so resistor voltage gradient effects can be ignored. Because of the naturally occurring 45 peak, it is very difficult to measure changes in the peak overlap with differing major beam intensities, using carbon dioxide. For this reason, a series of experiments was conducted using argon, having natural isotopes with mass numbers 36, 38 and 40 and respective per cent. abundances of 0.337, 0.063 and 99.600. The 40 contribution to 41 could then be accurately observed as a function of various parameters. (Note that, in these experiments, the relative tail contribution as defined by Mook and Grootes (1973) ceases to have significance). In

Figure III-10

Variation of Major Beam Intensity, I
with Analyser Pressure, P.



order to eliminate currents at the minor collector due, for example, to background, and chart recorder and amplifier null levels, the overlap current above baseline was measured each time. In practice, gas was admitted to one side of the inlet system only, and the instrument tuned to give m/e 40 on the major collector. Thus the minor collector monitored m/e 41 and, for the evacuated side, the 41 baseline signal.

Figure III-11 shows a plot of I_{41} ($10^{-13}A$) versus I_{40} ($10^{-9}A$); a computer least squares analysis of the data gave the best fitting straight line as:

$$I_{41} = 0.061I_{40} - 0.015$$

The root-mean-square error was 0.003, the error on the gradient ± 0.001 (1.6%) and on the intercept ± 0.002 (13.3%).

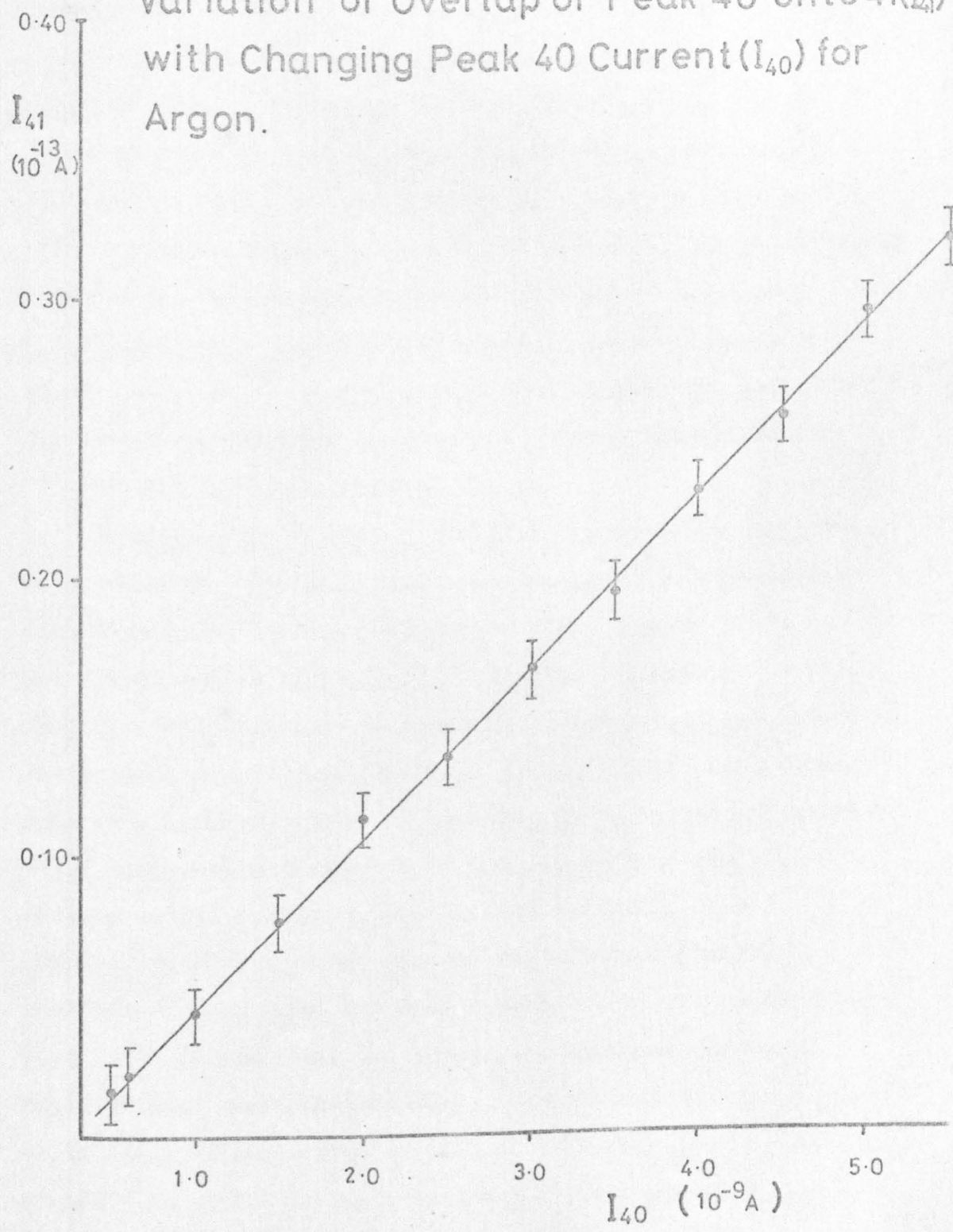
While I_{41} should represent a true overlap current, there may be a small constant contribution to I_{40} caused by maladjustment of the major amplifier zero, which would account for the negative intercept term.

The most striking fact is, however, that I_{41} varies linearly with I_{40} over an I_{40} range from $5 \times 10^{-10}A$ to $6 \times 10^{-9}A$. This would indicate that the origin of the pressure effect is not to be found in a tail contribution from the major ion beam.

As pointed out previously, the two usually quoted explanations of peak broadening are coulombic repulsion and scattering of ions by gas molecules. In order to separate the effects of these two causes, the overlap current was measured as a function of major beam intensity at constant

Figure III-11

Variation of Overlap of Peak 40 onto 41(I_{41}) with Changing Peak 40 Current (I_{40}) for Argon.

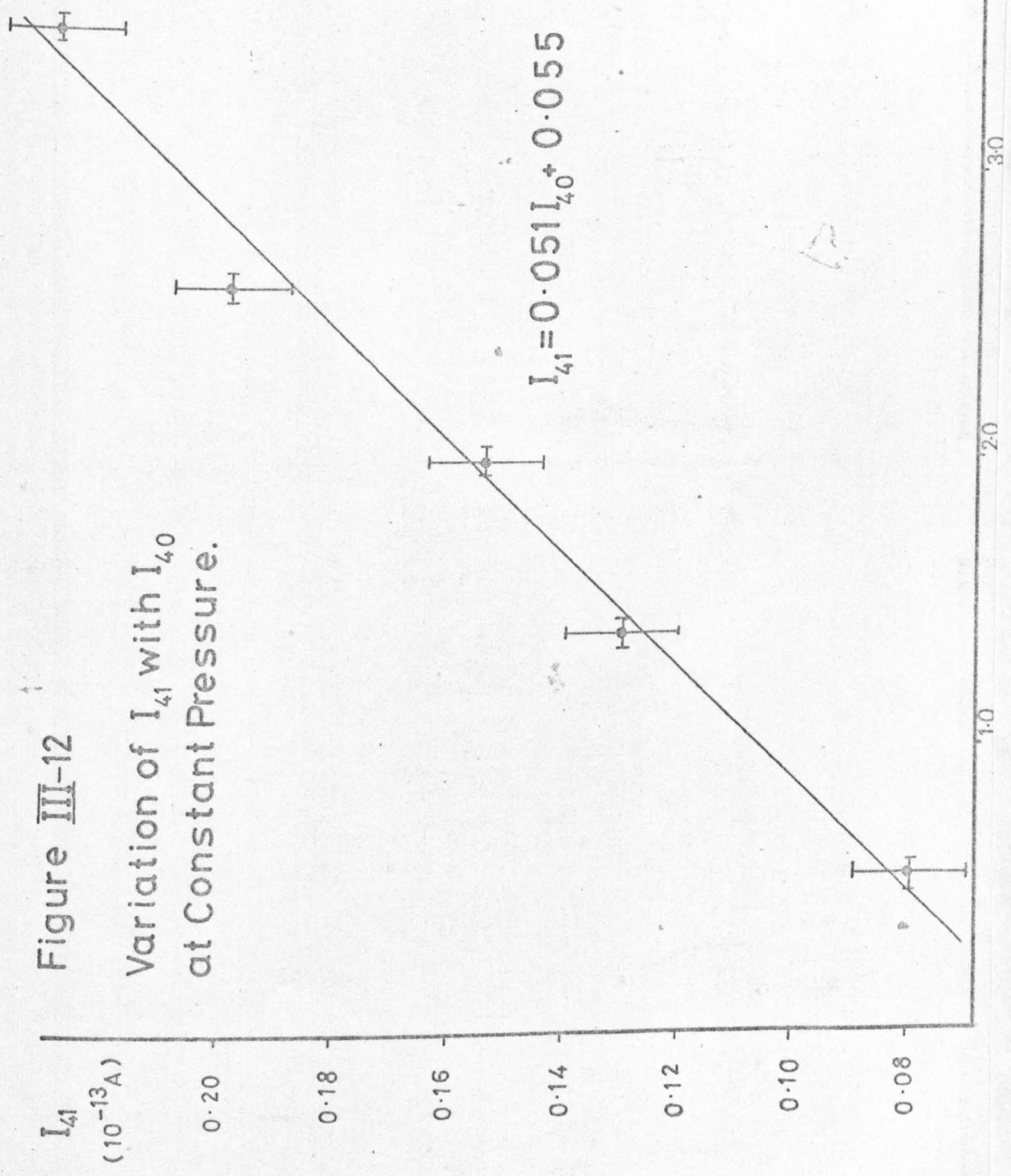


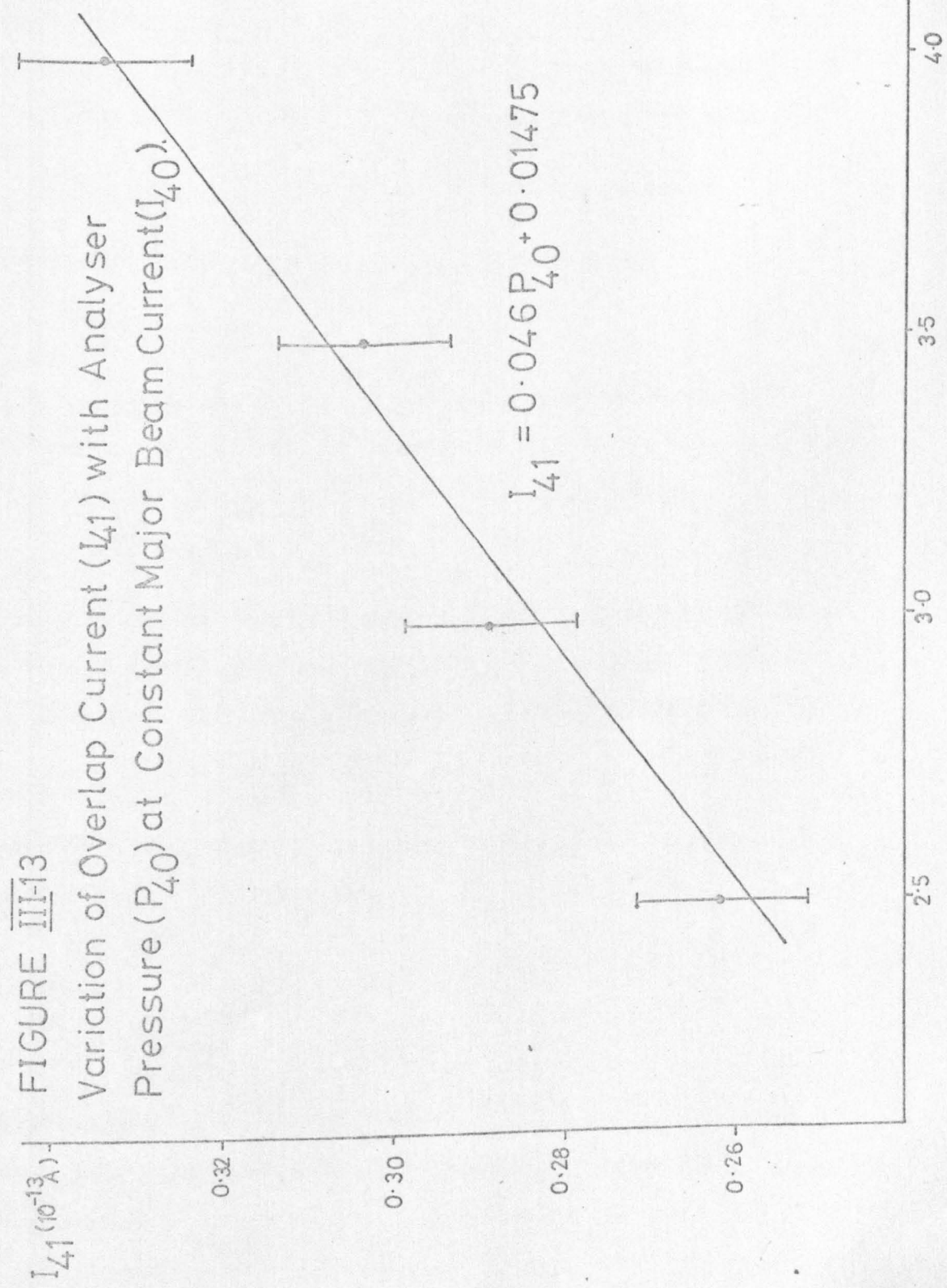
gas pressure, and then as a function of gas pressure at constant major beam intensity. The respective graphs are plotted as Figures III-12 and III-13. At constant gas pressure, the intensity of the major beam was altered by changing the electron emission energy. It is to be noted that the precision of the pressure measurements is poor, and their range limited; this was inevitable under the experimental conditions. As expected, though, both sets of data are reasonably well represented by straight lines of positive gradient: it would be rather coincidental were the individual functional dependences non-linear yet the combined one (as illustrated in Figure III-11) linear.

From Figures III-12 and III-13 it can be seen that, for this instrument at least, Craig's assumption of a quadratic tail dependence due to a coulombic effect (Craig, 1957) is not valid, nor is the conclusion of Mook and Grootes (1973) that peak broadening is independent of major ion beam intensity. The assumption of Craig, although ad hoc, seems to have been generally accepted (Mook and Grootes, 1973; Taylor and Hulston, 1972), presumably on account of its intuitive plausibility. Although ionic coulomb repulsion will certainly exist, whether its effect on the overlap contribution will be quadratic in the major ion beam intensity, or of a sufficiently high order of magnitude to explain the observed abundance sensitivity, remain problematical. Unfortunately, the physical situation is complicated, so in the following treatment several simplifying conditions will be assumed - the accelerations

Figure III-12

Variation of I_{41} with I_{40}
at Constant Pressure.





P_{40} (10^{-6} torr)

I_{41} (10^{-13} A)

caused by the external electric and magnetic fields are ignored and the ion beam is considered as an axially symmetric cylindrical distribution of charge of radius R and charge density ρ (M.K.S. units are used throughout).

The electric field at a distance r from the axis is:

$$E = \frac{\rho r}{2\epsilon_0}, \quad \epsilon_0 = \text{permittivity constant}$$

Hence the force exerted on a test charge e is:

$$F = eE = \frac{e\rho r}{2\epsilon_0},$$

and the force is radially outward for similarly charged particles. By Newton's Second Law, this force will give the test charge, of mass m , an acceleration a , where:

$$a = \frac{F}{m} = \frac{e\rho r}{2m\epsilon_0}$$

If it is assumed that the acceleration is constant and that the test charge has zero initial velocity, after a time t it will have travelled a distance x radially outward, where:

$$x = \frac{1}{2} at^2 = \frac{e\rho r t^2}{4m\epsilon_0}$$

Now the charge density, ion beam velocity (v), and ion beam current (I) are related by:

$$I = \rho\pi R^2 v$$

so that:

$$x = \frac{eIrt^2}{4\pi\epsilon_0 m R^2 v}$$

This expression is intended for use in an order-of-magnitude calculation only; that it is dimensionally correct can readily be checked.

The separation of the two collectors, d , is fixed and is much greater than the ion beam radius R , so it is possible to calculate the distance r' from the axis a test charge would have to be before it would be sufficiently displaced by coulomb repulsion to arrive at the minor collector, i.e. for x to equal $(d-r')$:

$$x = d-r' = \frac{eIr't^2}{4\pi\epsilon_0 mR^2 v}$$

$$\therefore r' = d \left(1 + \frac{eIt^2}{4\pi\epsilon_0 mR^2 v} \right)^{-1}$$

Now it can easily be shown that $eIt^2/4\pi\epsilon_0 mR^2 v \ll 1$, so $r' \approx d$ and, since $d \gg R$, it follows that $r' \gg R$ i.e. there is little probability of coulomb repulsion leading to a significant peak overlap under the conditions assumed. Were the analyser-collector geometry such that r' and R were comparable, the functional dependence of the tail contribution can be found, for the overlap current I_0 would be given by:

$$I_0 = pI(1 - r'^2/R^2)$$

where p is a very small positive constant reflecting geometrical considerations. It can be seen that this does not lead to a squared dependence on I .

The increase of I_{41} with I_{40} in Figure III-12 must then be explained by some other physical process which, moreover, predicts a linear response. The most obvious cause fulfilling this condition is that an increase in the number of ions leads directly to more collisions, and so to

a linear rise in tail contribution. Similarly, Figure III-13 is explained by the same mechanism - more collisions - this time caused by a higher density of gas molecules.

It is to be noted that the experiments with argon described above do not rule out a tail contribution resulting from interaction of the two ion beams. There will be mutual attraction of the major and minor ion beams, the force of attraction being proportional to the product of the two currents. However, this attraction cannot account for an increase in the measured ratio of minor to major current with decreasing major ion beam intensity.

To find the optimal energy for the electron beam which produces ionization of the gas, the m/e 44 ion beam intensity, 45/44 ratio and 46/(44+45) ratio were measured, for CO_2 , with varying electron accelerating voltage. The results are plotted in Figure III-14; it is clear from this figure that ionization can cause isotope fractionation, but the magnitude of the effect is extremely small. A voltage of 71 volts was chosen as the most appropriate, since the beam current is a maximum yet any drift will have the minimum consequences.

Figure III-15 shows how the m/e 44 ion beam intensity depends on half-plate voltage; since it is desirable to have as high an ion current as possible (everything else being equal), the half-plate voltage used during normal operation was 55 volts, corresponding to maximum signal. As in the last example, this is also the most stable position.

FIGURE III-14

VARIATION WITH ELECTRON ENERGY VOLTAGE OF:

(A) MAJOR BEAM, (B) 46/(44+45), (C) 45/44 RATIO.

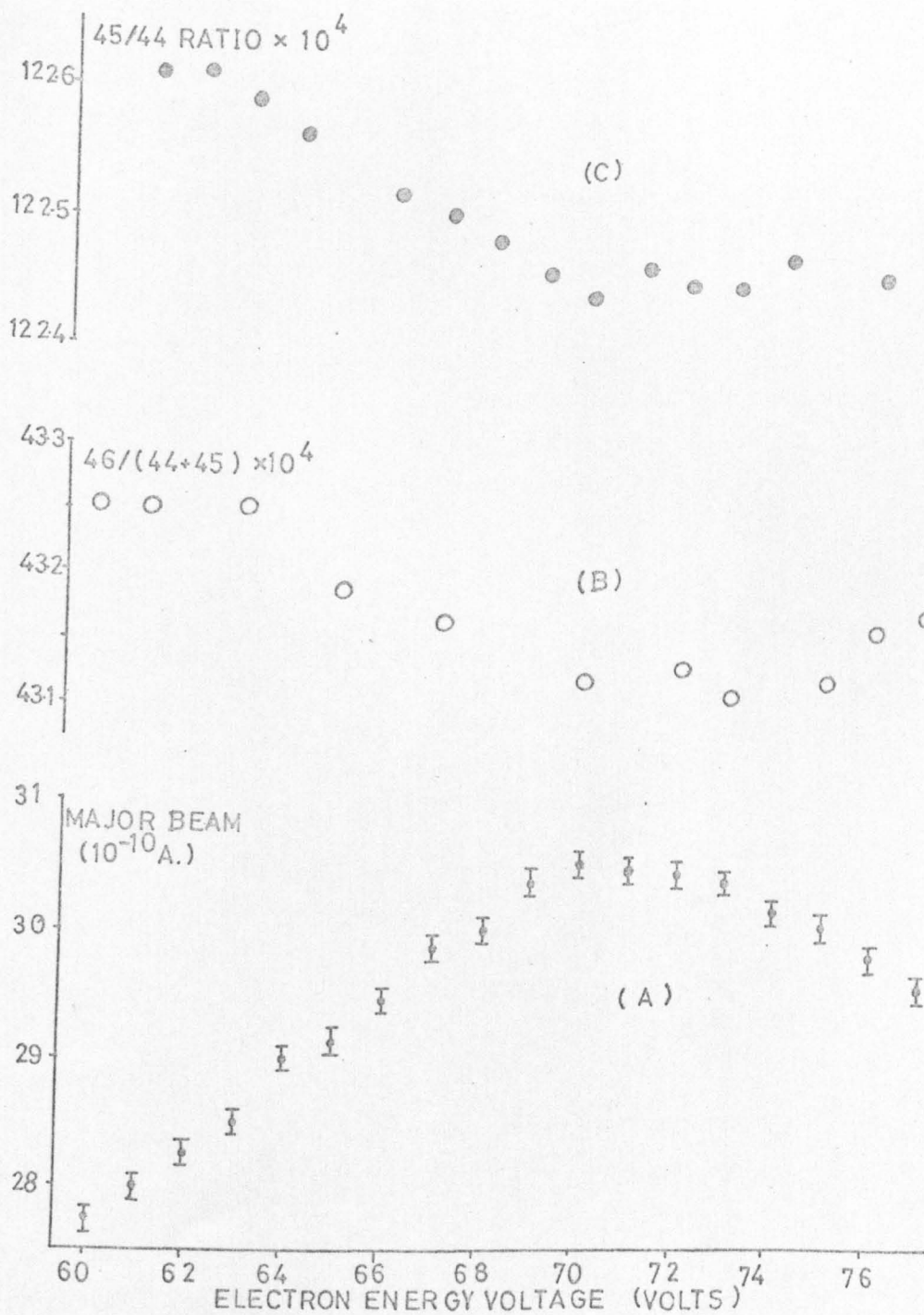
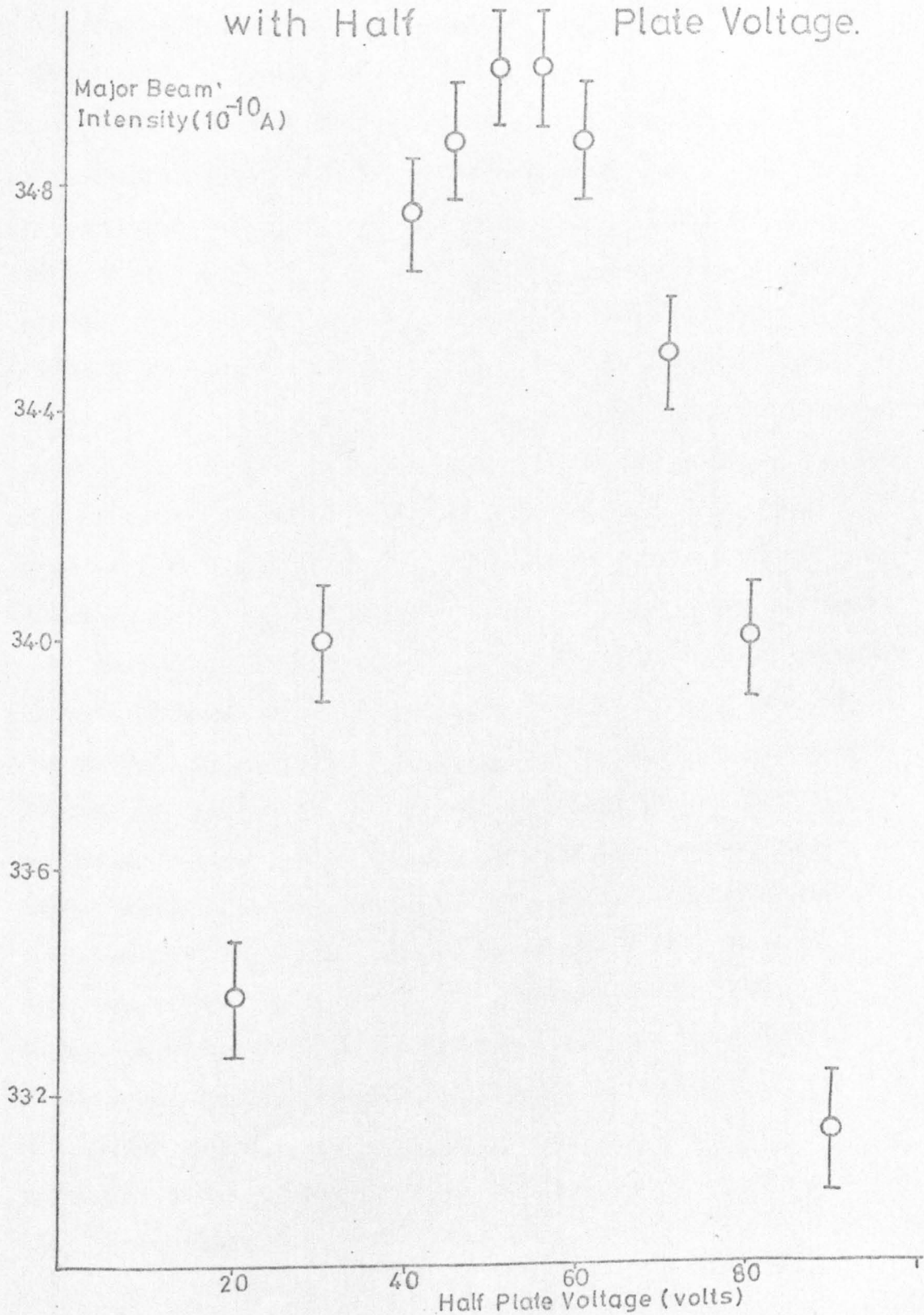


FIGURE III-15

Variation of Major Beam Intensity

with Half

Plate Voltage.



Adjustment of the ion repeller voltage has a much larger effect on the major ion current than had the previous two parameters: ion beam position is critically dependent on the repeller voltage. Figure III-16 illustrates the variation of m/e 44 ion beam intensity, and Figure III-17 that of the 45/44 ratio, with ion repeller voltage. Based on the selection criteria given above, an ion repeller voltage of 20 volts was selected as most suitable. That a stable ratio could not be measured below 10 volts is somewhat surprising in the light of Figure III-18, which shows a plot of ion source current versus repeller voltage (the trap current remaining constant). The linear curve is quite typical, no irregularities are seen at low repeller voltages.

On returning to the problem of the origin of the pressure effect, it must first be pointed out that the magnitude of the effect measured for the Glasgow 602B compares well with similar parameters quoted by other workers (Table III-4). Secondly, evidence has been gained that little or no mass discrimination occurs during gas flow and ionization, and the peak tail overlap contribution to the minor ion beam appears, on the basis of the argon experiments, to be incapable of explaining the effect. The same experiments would seem to eliminate also such possible causes as variations in collector sensitivity and response. The arguments based on this evidence are convincing though by no means irrefragable.

FIGURE III-16
 Variation of Major Beam
 Intensity with Ion Repeller
 Voltage.

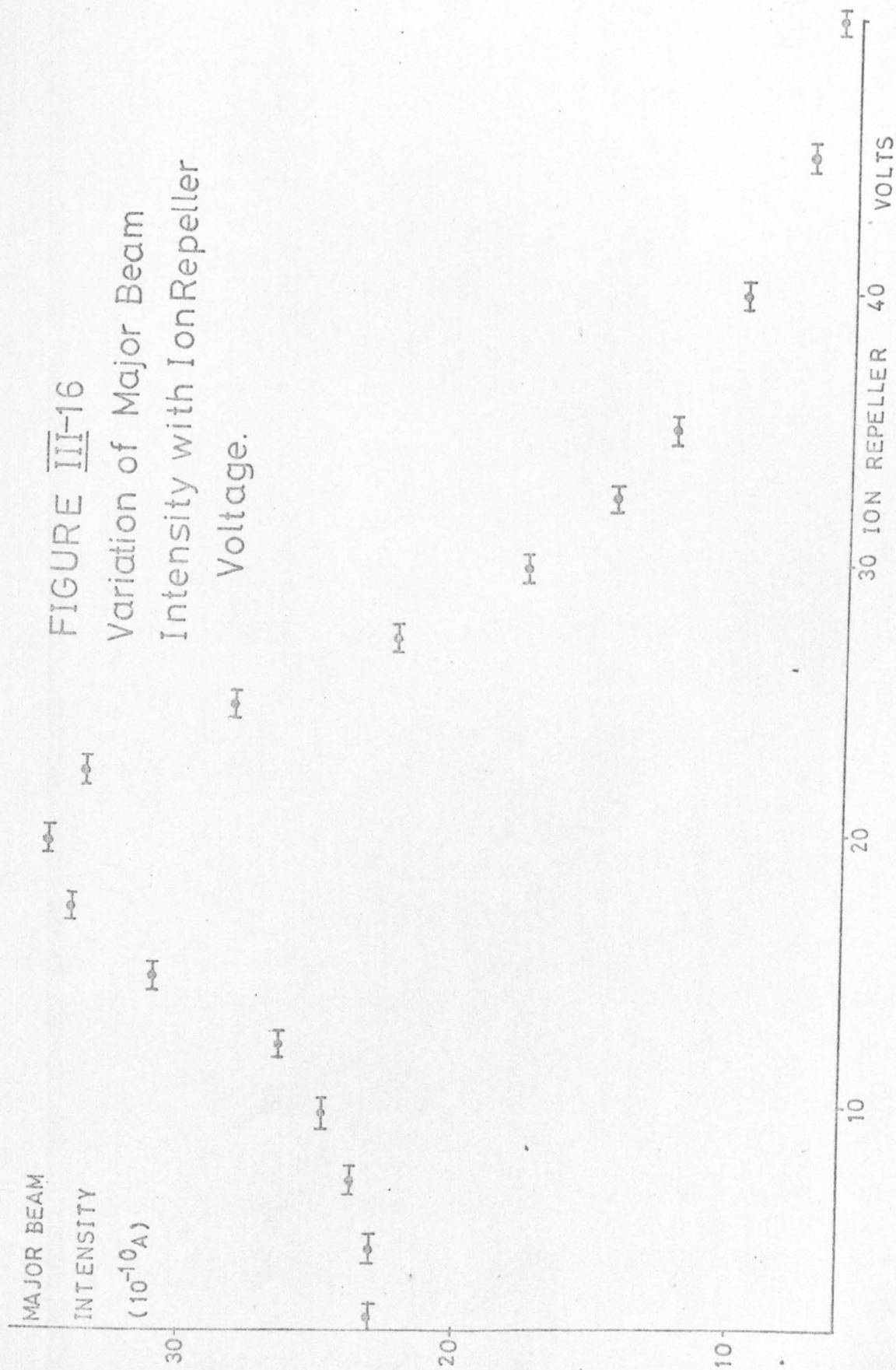
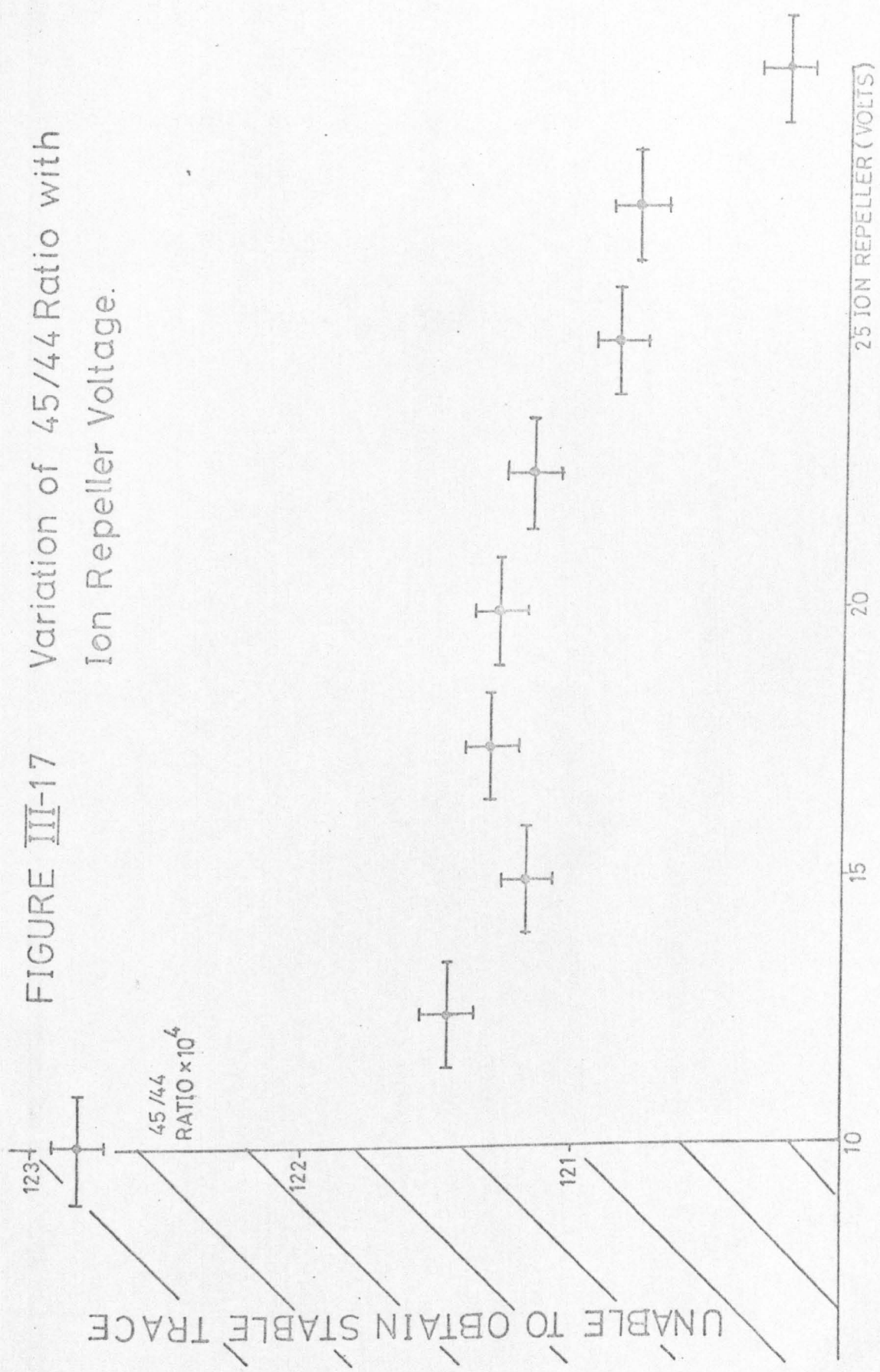


FIGURE III-17 Variation of 45/44 Ratio with Ion Repeller Voltage.



UNABLE TO OBTAIN STABLE TRACE

45/44
RATIO x 10⁴

25 ION REPELLER (VOLTS)

123

122

121

10

15

20

FIGURE III-18

Variation of Ion Source Current
with Ion Repeller Voltage.

TRAP CURRENT CONSTANT AT $190 \mu\text{A}$.

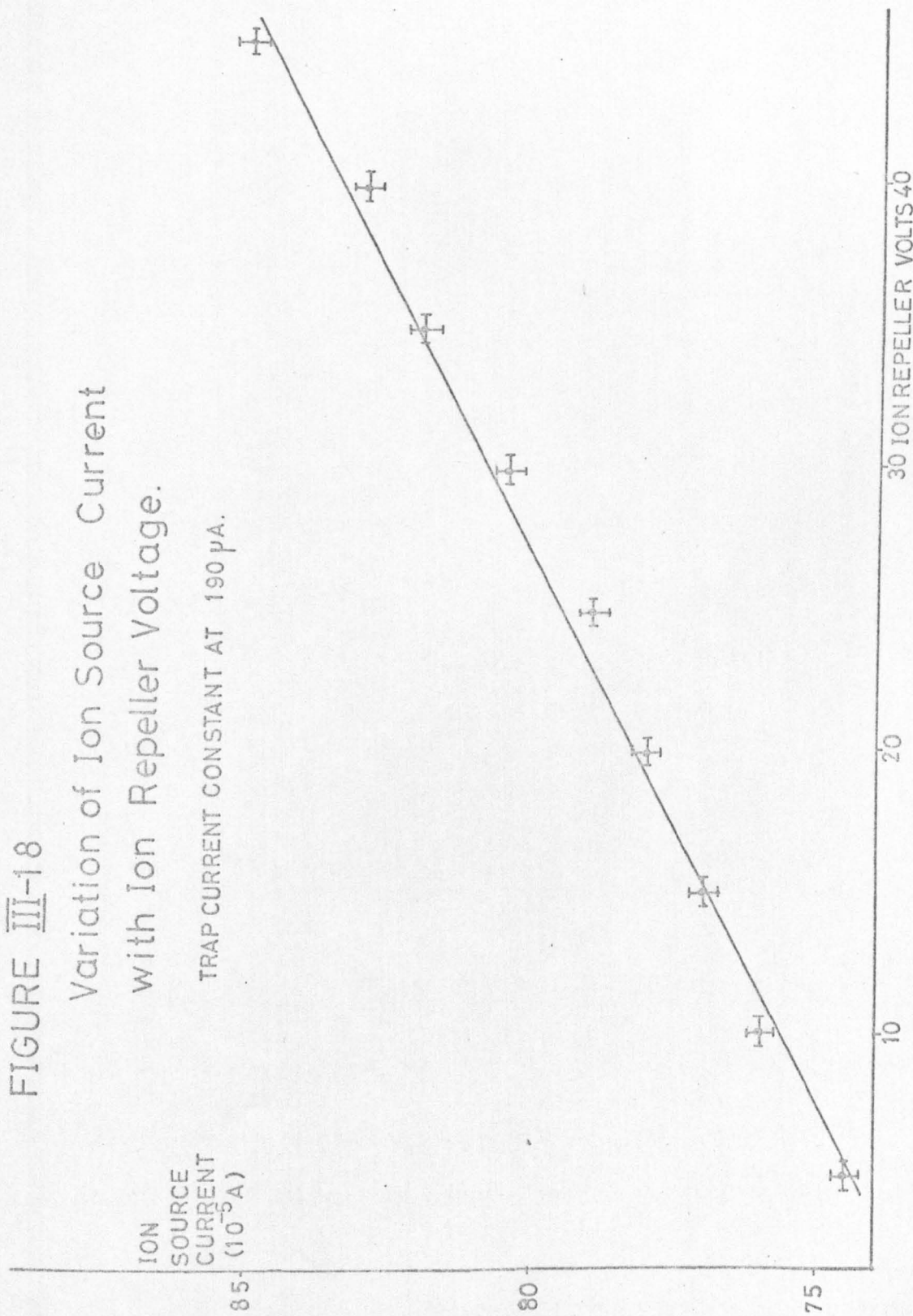


TABLE III-4

AUTHOR(S)	PARAMETER	AUTHOR'S MAGNITUDE	GLASGOW MAGNITUDE
CRAIG (1957)	$\frac{dR_m}{dI}$ FOR $\frac{m}{e}$ 46	25,000 A ⁻¹	1,400 A ⁻¹
TAYLOR AND HULSTON (1972)	ESTIMATE OF ERROR IN δ FOR 0.1 VOLT PRESSURE VARIATION	0.03%/oo	<0.01%/oo
MOOK AND GROOTES (1973)	CORRECTION FOR 1% PRESSURE MALADJUSTMENT FOR NATURAL CARBON	0.07%/oo	0.03%/oo
BECKINSALE et al. (1973)	INLET GAS PRESSURE COEFFICIENT OF 46/(44+45) RATIO	0.3%/oo per 10 ⁻⁹ A	0.35%/oo per 10 ⁻⁹ A
V.G. MICROMASS 602C TEST SCHEDULE	RATIO CHANGE FOR 10% CHANGE IN m/e 44 PEAK HEIGHT	≤0.5%/oo	0.5%/oo

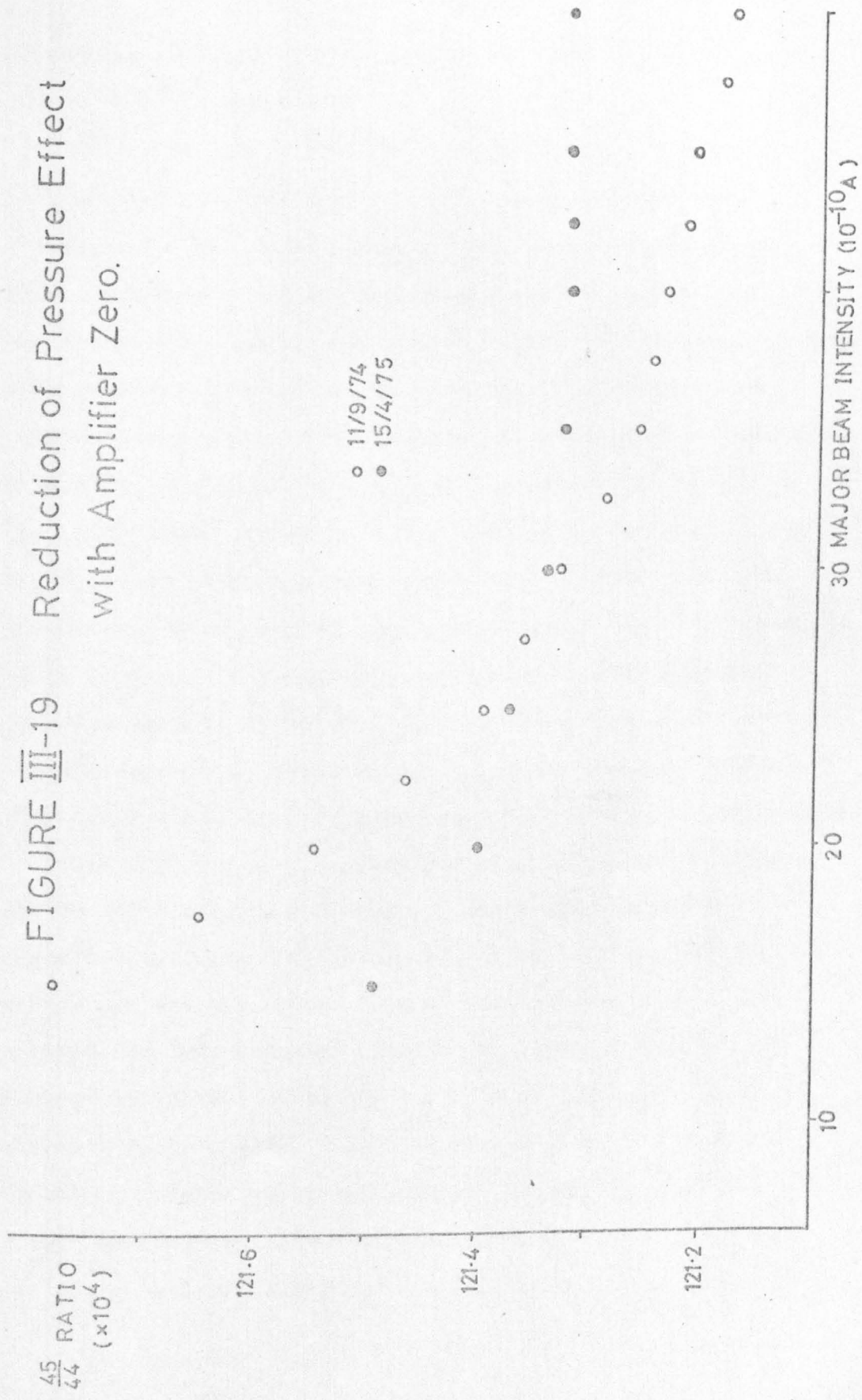
Comparison of 'pressure effect' characteristics.

It has been mentioned earlier that, in connection with Figure III-11, there could exist a small major current signal in the absence of gas flow, and hence ion beam, even after normal amplifier zero adjustment. The required current is very small, being the upper limit of major amplifier null setting. The presence of such a limit for the minor amplifier is thus to be expected, and it is clear that this contribution can easily explain the tendency for rapidly increasing ratio with decreasing major ion beam at low values of major ion beam, as observed in Figures III-7 and III-8. Following a suggestion by N.I. Bridger (personal communication to the author, 1975) for virtually complete elimination of null signal from the head-amplifiers/recorder system, it was later found possible to considerably reduce the effect. This is illustrated in Figure III-19.

III-8 Mass spectrometry precision and accuracy.

The precision of mass spectrometric measurements is limited, in the final analysis, by ion statistics. In practice, the instrumental stability is critically important: this will be discussed by referring to the reproducibility of results, both in the short-term (over a period of a day) and in the longer term (of the order of months). Obviously the former should not be significantly greater than the latter. To gauge the reproducibility attainable within a single set of analyses, two gases were compared seven times over the course of a day. The results

• FIGURE III-19 Reduction of Pressure Effect
with Amplifier Zero.



are shown in Table III-5; the mean was -4.54‰ and the 1σ standard deviation $\pm 0.03\text{‰}$.

The reproducibility over longer periods of time can be estimated by consideration of the results of the working standard checks. Within the scatter of the daily analyses, good long-term stability has been observed for periods of up to at least one year. Of course, since the inception of this work some improvement has been achieved in measurement technique, mainly as a consequence of realisation of possible sources of error and of increase in instrument stability. To best illustrate and discuss the machine performance in terms of the daily check standards, two sets of data have been chosen at random from the instrument log. They are separated by an interval of 14 months, during which time the mass spectrometer was disabled on several occasions with faults of varying degrees of severity (one of them being the diffusion pump oil distillation into the analyser mentioned previously).

These data are presented in graphical form in Figures III-20 and III-21 for analysis numbers 31 to 44, and in Figures III-22 and III-23 for numbers 81 to 94. The delta values are for the various check working standards (quoted relative to PDB) measured against the primary aliquot of working standard; the error bar on each point is the 1σ standard deviation for that particular assay. The check working standards were used in rotation and no systematic trends were noted. The relevant statistics for each period are given in Table III-6 for both $\delta^{13}\text{C}$ and $\delta^{18}\text{O}$. The only

TABLE III-5

ANALYSIS NUMBER	$\delta^{13}\text{C}\text{‰}$
1	-4.54 ± 0.04
2	-4.58 ± 0.02
3	-4.51 ± 0.04
4	-4.50 ± 0.03
5	-4.56 ± 0.01
6	-4.55 ± 0.05
7	-4.53 ± 0.05

Short-term reproducibility of measurement.

FIGURE III-20

$\delta^{13}\text{C}$ REL. TO PDB OF WORKING STANDARD CHECK,
FOR ANALYSES 31 TO 44.

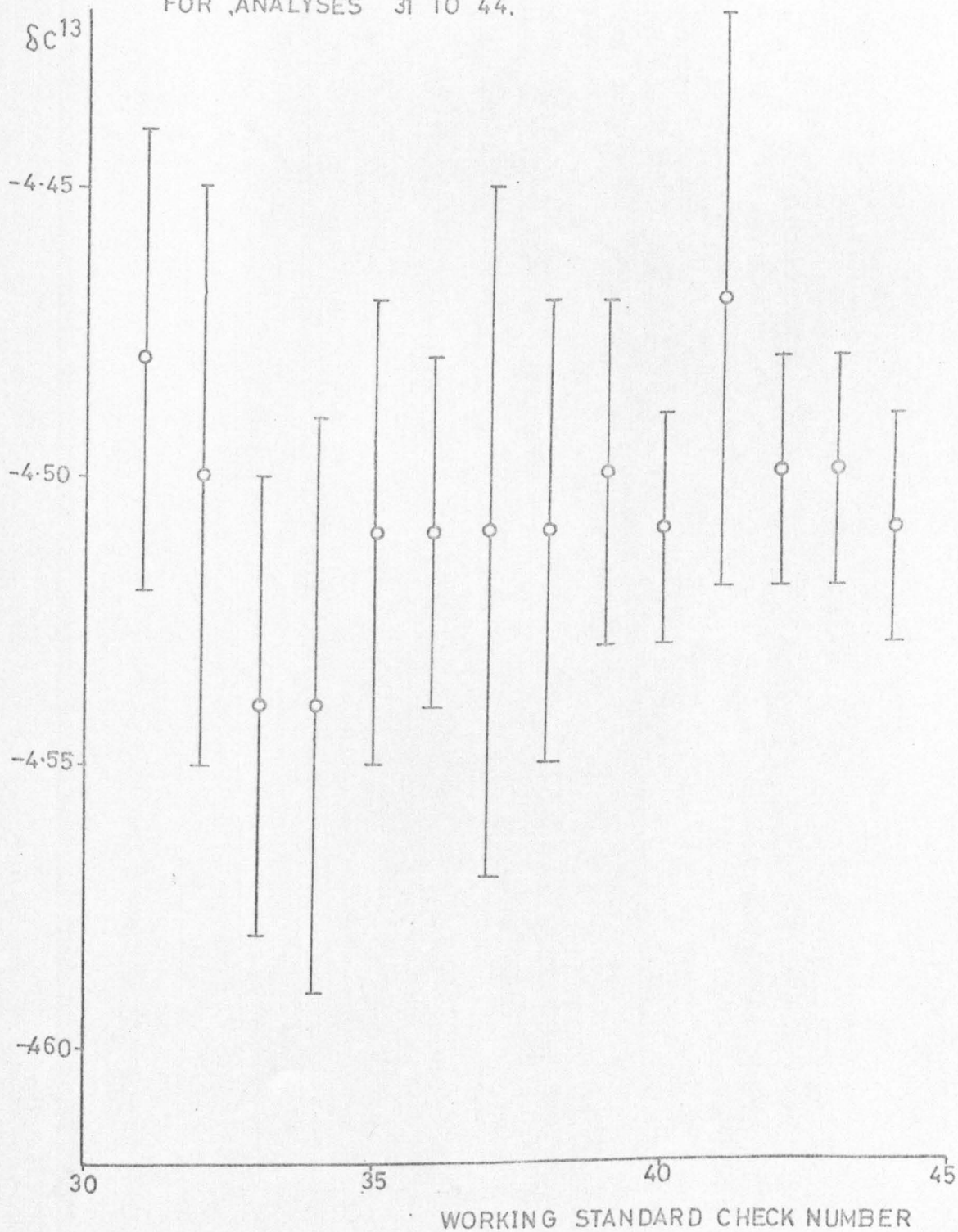


FIGURE III-21

$\delta^{13}\text{C}$ REL. TO PDB OF WORKING STANDARD CHECK
FOR ANALYSES 81 TO 94.

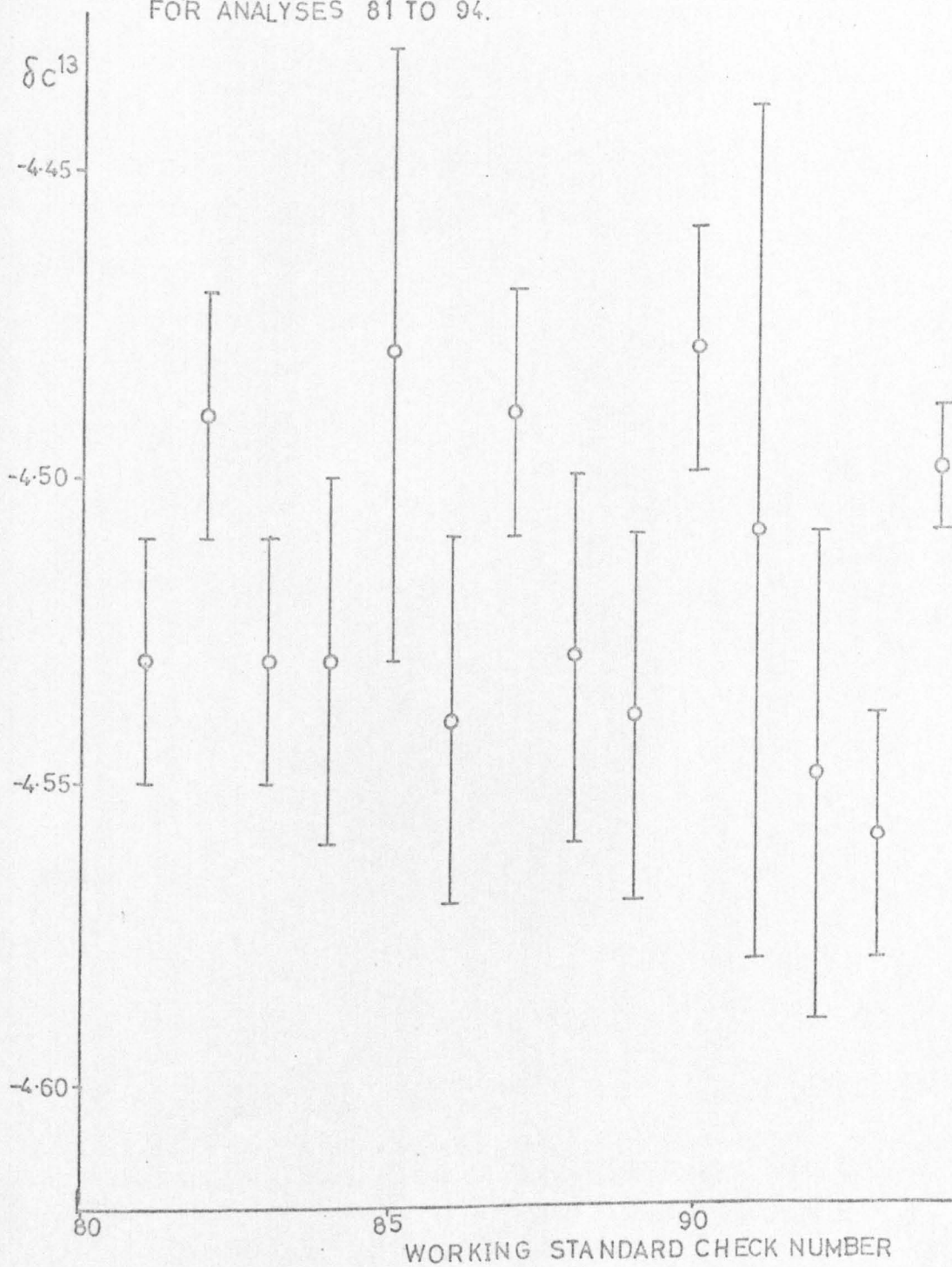


FIGURE III-22
 $\delta^{18}\text{O}$ REL. TO PDB OF WORKING STANDARD CHECK
FOR ANALYSES 31 TO 44.

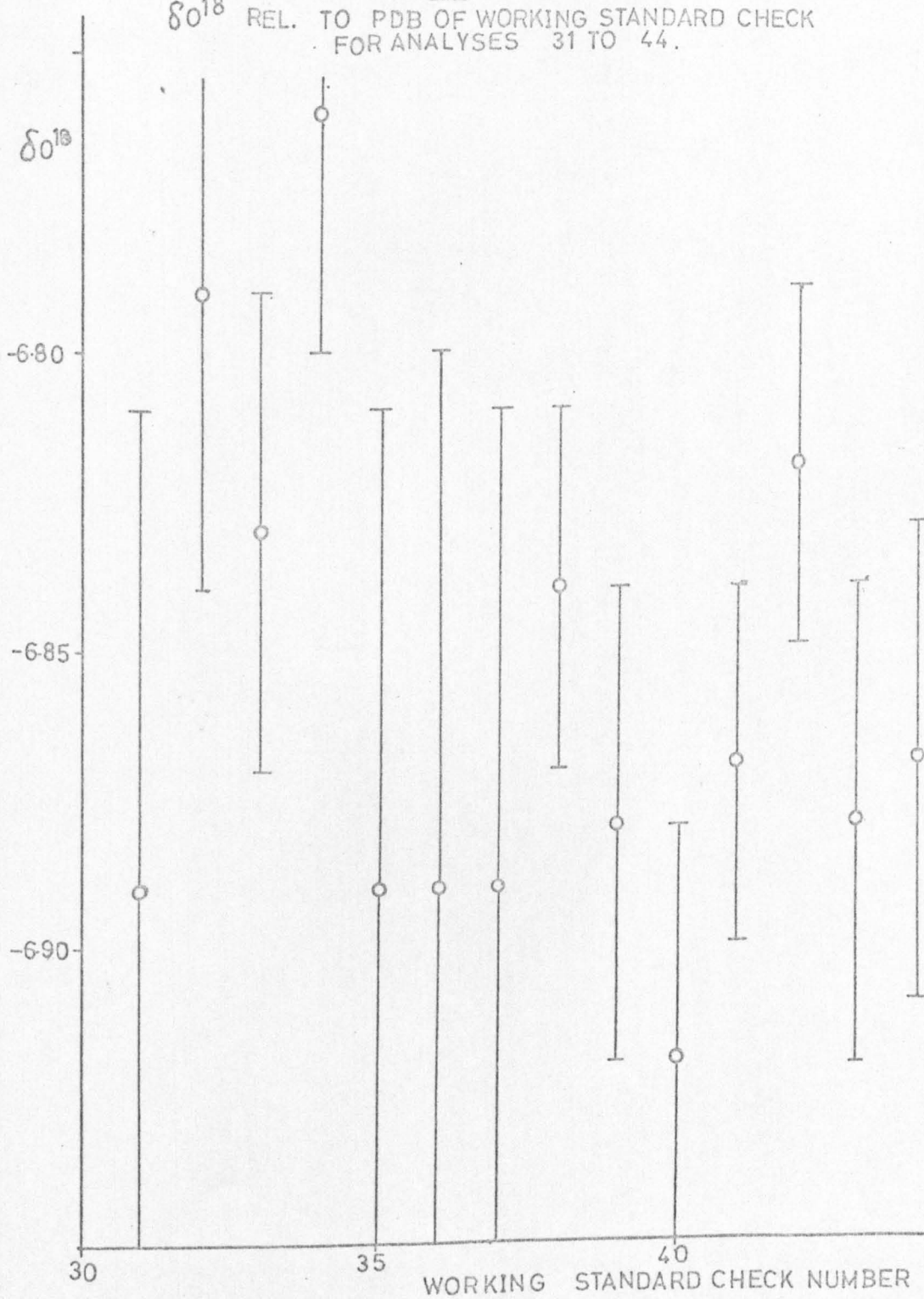


FIGURE III-23

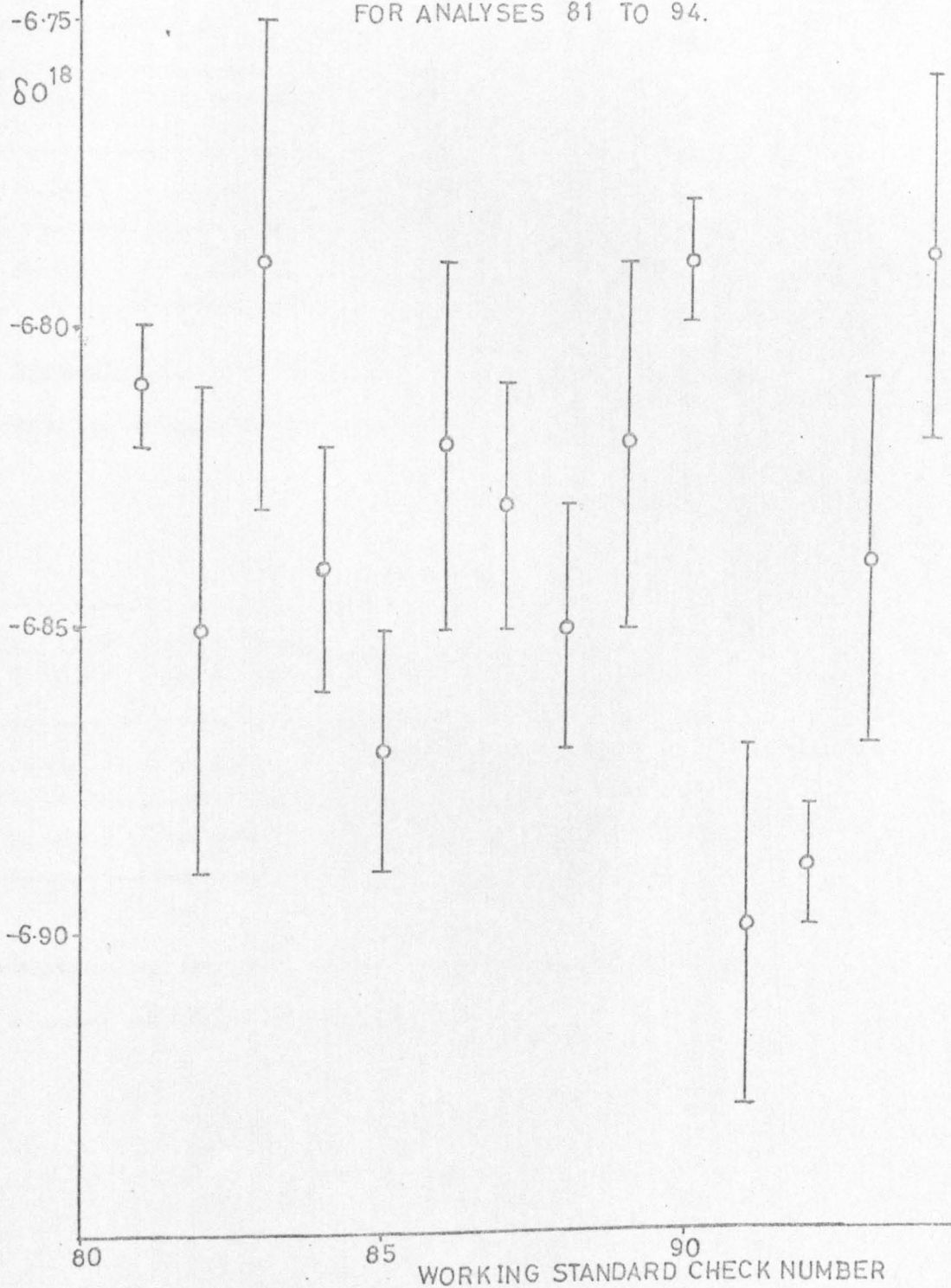
 $\delta^{18}\text{O}$ REL. TO .PDB OF WORKING STANDARD CHECK
FOR ANALYSES 81 TO 94.

TABLE III-6

ANALYSIS NUMBERS	MEAN ERROR ON AN ASSAY	MEAN $\delta^{13}\text{C}$	ERROR ON MEAN $\delta^{13}\text{C}$
31-44	0.04‰	-4.51‰	0.02‰
81-94	0.03‰	-4.52‰	0.03‰

(a) Statistics for $\delta^{13}\text{C}$ (rel. to PDB) for two sets of working standard check analyses.

ANALYSIS NUMBERS	MEAN ERROR ON AN ASSAY	MEAN $\delta^{18}\text{O}$	ERROR ON MEAN $\delta^{18}\text{O}$
31-44	0.05‰	-6.86‰	0.05‰
81-94	0.03‰	-6.84‰	0.04‰

(b) Statistics for $\delta^{18}\text{O}$ (rel. to PDB) for two sets of working standard check analyses.

significant difference is considered to be the reduction, for both $\delta^{13}\text{C}$ and $\delta^{18}\text{O}$, in the mean of the standard deviations within the individual runs (i.e. the error bars, in Figures III 20-23). This is attributed to an increase in the short-term instrument stability by optimisation of the operating characteristics. The complete list of results is given in Appendix 2.

Since the above results are quite typical, they will be used as indicative of the mass spectrometry errors in analysis of samples of pure CO_2 which do not differ isotopically to a great extent, (a few per cent), as compared to the standard. Obviously, additional error is introduced in assay of abnormally enriched or depleted gases. Thus, for both $\delta^{13}\text{C}$ and $\delta^{18}\text{O}$, the precision at 1 σ in the mass spectrometric measurement is considered to be within $\pm 0.05\%$.

Delta values are measured by comparison against a laboratory working standard, but are reported relative to some international standard (e.g. PDB, SMOW). The accuracy of the delta value for any sample is thus dependent on the calibration of the working standard relative to the international standard.

Several generally accepted standards have been prepared and compared against each other and against the working standards. They consisted of two limestones, one graphite and three water samples. Discussion of the water samples has already been given in Chapter II.

Following McCrea (1950), carbon dioxide was liberated from carbonates by hydrolysis with 100% orthophosphoric acid at 25°C. Several batches of NBS20 (Solenhofen Limestone) and of TSS Marble (the I.A.E.A. standard) have been prepared in this way. Quoted precisions for this procedure are generally in the range 0.05 to 0.10‰; Mook (1968) has pointed out that a 95% H₃PO₄ solution may be more reliable. Good agreement has been found among the δ¹³C results, but greater scatter for δ¹⁸O. Taking Solenhofen relative to PDB as reported by Craig (1957):

$$\delta^{13}\text{C} = -1.03\text{‰} ; \quad \delta^{18}\text{O} = -4.14\text{‰}$$

then six intercalibrations with TSS Marble gave TSS relative to PDB as:

$$\delta^{13}\text{C} = (2.04 \pm 0.05)\text{‰} ; \quad \delta^{18}\text{O} = (-2.29 \pm 0.07)\text{‰}$$

Values reported to I.A.E.A. by other laboratories range from 1.64 to 2.05 for δ¹³C, and from -1.90 to -2.56 for δ¹⁸O (R.M. Brown, personal communication).

NBS21 graphite, converted to CO₂ by combustion in a stream of oxygen, was compared to NBS20; it was found to have δ¹³C = (-27.84 ± 0.05)‰.

The laboratory working standards have been calibrated for δ¹³C against the various carbonates twenty times during the progress of the work. Relative to PDB the mean is:

$$\delta^{13}\text{C}(\text{WS}) = (-4.54 \pm 0.04)\text{‰}$$

The precision of the δ¹⁸O calibration is not so good, as might have been expected. Eleven comparisons give (relative to PDB):

$$\delta^{18}\text{O}(\text{WS}) = (-6.86 \pm 0.09) \text{‰}$$

However, in this case, the analyses of the water standards described earlier lend confidence to the accuracy of the calibration results.

CHAPTER IV

THE PRESERVATION AND STORAGE OF OCEANOGRAPHIC WATER SAMPLES.

IV-1 Introduction

Of the major shortcomings of the work reported in this thesis, it is believed that many may be traced to difficulties related to collection, preservation and storage of oceanographic water samples. Some of the grounds for justification of this belief will be given in the present chapter; further elucidation will, hopefully, follow from the analysis of the results presented in later chapters. The problems inherent in the reliable collection and storage of oceanographic samples are known to all who are actively engaged in the field. However, there is no general agreement regarding the various practical procedures of preservation, nor over the effects of storage. A familiar feature of technical reports on oceanographic cruises is a statement reminding the reader of 'the large and random errors greater than the quoted precision' (Kroopnick, 1971) which often occur. Such effects have diverse causes, ranging from malfunction of hydrographic sampling bottles to incorrect labelling of the samples when on deck.

IV-2 Alterations in samples during storage.

Since this study is concerned mainly with the interaction of the chemical and biological systems in seawater, and with the consequences for the stable isotope distribution, attention will be focussed initially on previous work in these areas. Early experiments on seawater stored without the addition of poison were aimed at investigating the nature of the relationships between the bacteria and the organic matter in the water (Waksman and Carey, 1935; Waksman and Renn, 1936; Waksman and Vartiovaara, 1938). In these experiments, the bacterial population, oxygen consumption and organic matter were measured as a function of time since collection, collection location and storage conditions. Except in extreme cases, it was found that the number of bacteria increased, the organic matter was decomposed and oxygen was consumed as time progressed. More precisely, under normal conditions the bacterial population was observed to rise rapidly (the phase of logarithmic increase), reach a peak in two to three days (the maximum stationary phase), thereafter falling to a persistent low count (the re-adjustment phase). The oxygen consumption increased rapidly for the first three days and then levelled off. Later experiments (Zobell and Anderson, 1936), showed that the amplitude and time of occurrence of the maximum stationary phase were dependent on the ratio of volume to surface area of the storage vessel. Further, the number of species of bacteria was drastically reduced.

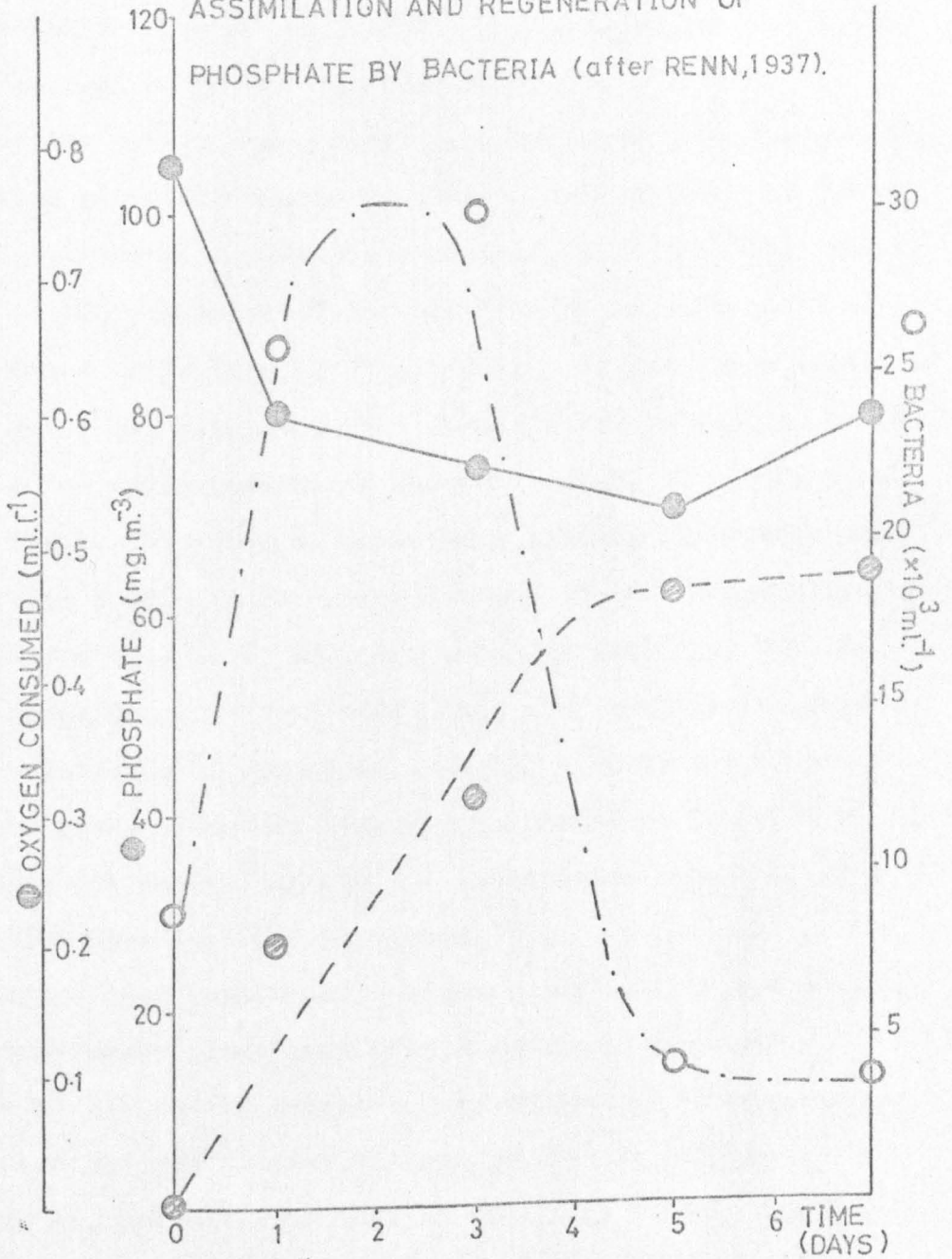
One might expect in the decomposition of organic matter by bacterial activity, the release of nutrient constituents (e.g. NH_3 , PO_4) suitable for diatom and algal nutrition. On the other hand, an alternative process would be direct assimilation of the dissolved organic substances into bacterial cells, thus entering the food web by a different route. Knowing that bacterial cell substance is rich in phosphorus, Renn then studied the relationship between bacterial multiplication and phosphate assimilation (Renn, 1937). In Figure IV-1, which is taken from the above cited paper by Renn, are shown the bacteria count, oxygen consumed and phosphate level as a function of storage time for seawater enriched with K_2HPO_4 . Renn concluded that the development of the bacteria indeed withdrew significant quantities of phosphate from solution; only when the population had fallen to a constant low level and the oxygen consumption steadied, did phosphate regeneration commence.

IV-3 Closed system biological fractionation experiments.

The proffered explanation for the above experiments has important consequences for the ΣCO_2 level and for the stable isotope ratios of both ΣCO_2 and dissolved oxygen in stored seawater. If oxidation of organic matter dominates over fixation of inorganic carbon, ΣCO_2 should increase and its $\delta^{13}\text{C}$ decrease, reflecting the lower content of the heavy isotope in the organic material. Furthermore, $\delta^{18}\text{O}$ of the dissolved oxygen should increase as the lighter isotope is

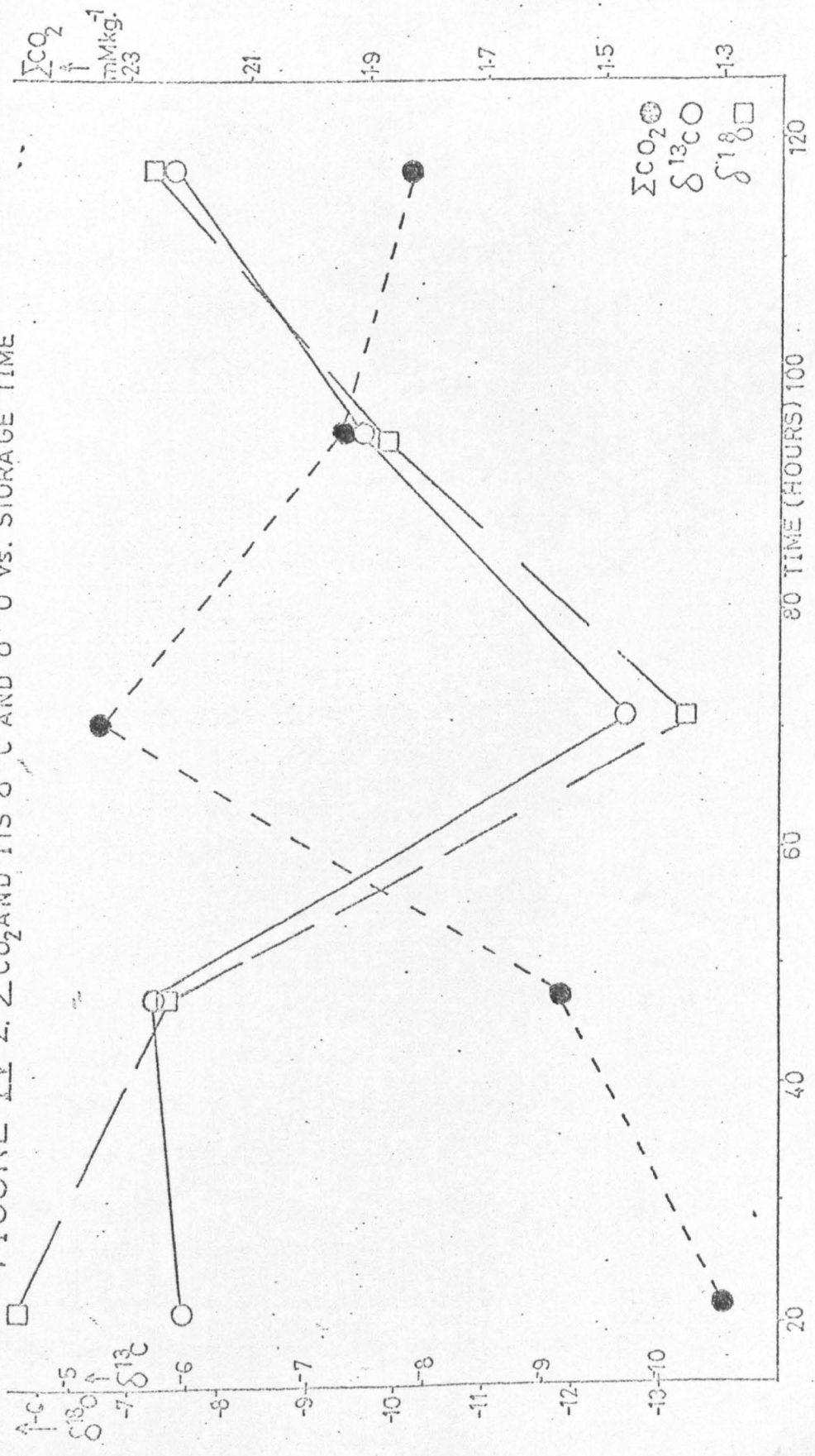
FIGURE IV-1

ASSIMILATION AND REGENERATION OF
PHOSPHATE BY BACTERIA (after RENN, 1937).



taken up preferentially. This latter has been observed by Kroopnick (1971). To test the other hypotheses, ΣCO_2 and $\delta^{13}\text{C}$ were measured, over a five day period, on seawater stored without prior poisoning. The samples were collected off the end of the pier at Loch Aline, were filtered to remove the considerable amount of suspended detritus present, and were stored in the dark, at room temperature, in 100 ml. glass bottles with bakelite screw-on caps. The ΣCO_2 and $\delta^{13}\text{C}$ of the inorganic carbon are plotted as a function of time since collection in Figure IV-2. As has been mentioned in Chapter II, extracted ΣCO_2 does not always seem to be in oxygen isotopic equilibrium with the water; it can be seen from Figure II-4 that in many cases the gas is lighter than the value predicted for equilibration at the 'temperature of extraction'. $\delta^{18}\text{O}$ of ΣCO_2 was measured routinely for the mass spectral cross correction and, when the results were being analysed, it was noted that the $\delta^{18}\text{O}$ values of the various gases also followed the same trend as the $\delta^{13}\text{C}$ values so, with due recognition of the limitations involved, they have also been included in Figure IV-2. It is to be emphasised that considerable scatter may be expected due to non-homogeneity since each bottle analysed contained a different aliquot of seawater. In accordance with previously described biological observations of Waksman and his colleagues, and with the work of Kroopnick (1971) who showed that ^{16}O is consumed in preference to ^{18}O , the following sequence of events is postulated to explain the results:

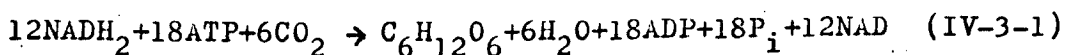
FIGURE IV-2. ΣCO_2 AND ITS $\delta^{13}C$ AND $\delta^{18}O$ vs. STORAGE TIME



(i) 0-3 days: bacteria multiplied rapidly accompanied by decomposition of organic material; phosphate was assimilated, oxygen rapidly consumed and CO_2 released into the inorganic carbonate system. Since the organic material was depleted in ^{13}C relative to the inorganic pool, and the consumed oxygen was lighter than that remaining, the $\delta^{13}\text{C}$ and $\delta^{18}\text{O}$ of the ΣCO_2 decreased. During this period the net result was that ΣCO_2 was increased by 1.00 mM kg.^{-1} with CO_2 of $\delta^{13}\text{C} \sim -14\text{‰}$ relative to PDB. Typical values for organic matter in seawater are of the order of -23‰ but, as emphasised, the values given are net values reflecting both respiration and oxidation. Not all of the carbon will have been released in inorganic forms - bacteria also play an important role as synthesisers of new complexes in the sea. Indeed Waksman and Renn (1936) estimated that in their laboratory studies approximately 50% of the organic matter was readily attacked by bacteria; about 60% of this was oxidised and the remaining 40% converted into bacterial cell substance, and it is well known that isotope fractionation occurs during degradation and synthesis (Degens et. al., 1968(a) and (b)).

(ii) 3-5 days: the available organic material exhausted, the bacterial population rapidly diminished and oxygen consumption steadied; the production of inorganic carbonate species fell and loss of ΣCO_2 by carbon fixation became dominant. There are several possible mechanisms for this CO_2 uptake - both algae and some bacteria are capable of synthesising high -

energy organic compounds from low-energy inorganic compounds such as carbon dioxide and water. The inorganic carbon source can be free carbon dioxide, bicarbonate or carbonate. Methane bacteria, which reduce carbon dioxide to methane, are well known and Rabinowitch (1945) cites the example of the chemautotrophic bacteria, colourless marine organisms which reduce carbon dioxide to organic matter in the dark by coupling this reaction with different energy releasing chemical processes. The fixation of carbon dioxide in chemosynthesis can be represented by the equation (Parsons and Takahashi, 1973):



in which:

NADH_2 = reduced nicotinamide adenine dinucleotide

ATP = adenosine triphosphate

ADP = adenosine diphosphate

NAD = nicotinamide adenine dinucleotide

P_i = inorganic phosphate

It is worth noting, in view of Renn's (1937) observations on phosphate regeneration after 5 days, that one result of the above process is the release of inorganic phosphate. Dark CO_2 uptake is not restricted to chemosynthesis; heterotrophic processes - both bacterial and algal - can also result in the uptake of CO_2 in the absence of light. Numerous other examples of biological CO_2 removal by bacteria are known, many of them probably involving carboxylations.

Isotope fractionation occurs in the process of CO_2 removal, lighter molecules being preferred: hence the $\delta^{13}\text{C}$ of the total dissolved inorganic carbon increases. $\delta^{18}\text{O}$ of the CO_2 should also, initially, be higher than the original value. However, isotope exchange with oxygen of the water molecules will act to bring the water and ΣCO_2 to isotopic equilibrium. The remarkable parallelism of the two isotope ratio versus time curves may demonstrate that the approach to equilibrium was not sufficiently rapid to disguise the effects of biological fractionation. Over the 3-5 day period, the net change was a decrease of ΣCO_2 by 0.5 mM kg.^{-1} , the fixed CO_2 having $\delta^{13}\text{C} \sim -21\text{‰}$. This is in good agreement with typical values of -20 to -25‰ found by Williams and Gordon (1970) for marine organic matter.

The problems of respiration in the dark are notoriously difficult. As Abelson and Hoering (1961) have commented in discussion of their work on photosynthetic organisms:

"Isotope fractionation by living matter is not an easy subject of study."

As another example, Degens and co-workers (Degens et al., 1968(a)) studied dark storage of two populations: in one, Dunaliella - a green flagellate - the cell $\delta^{13}\text{C}$ decreased by 5‰ in 5 days, thereafter remaining approximately constant whereas in the other, Skeletonema - a neritic diatom - much smaller changes were seen and no systematic $\delta^{13}\text{C}$ trend was evident.

(iii) >5 days: ΣCO_2 and isotope measurements did not extend into this period, but Renn (1937) noted rapid phosphate regeneration levelling at fourteen days toward completion. He concluded that bacterial cells do not bind phosphorus for more than a few days under storage conditions.

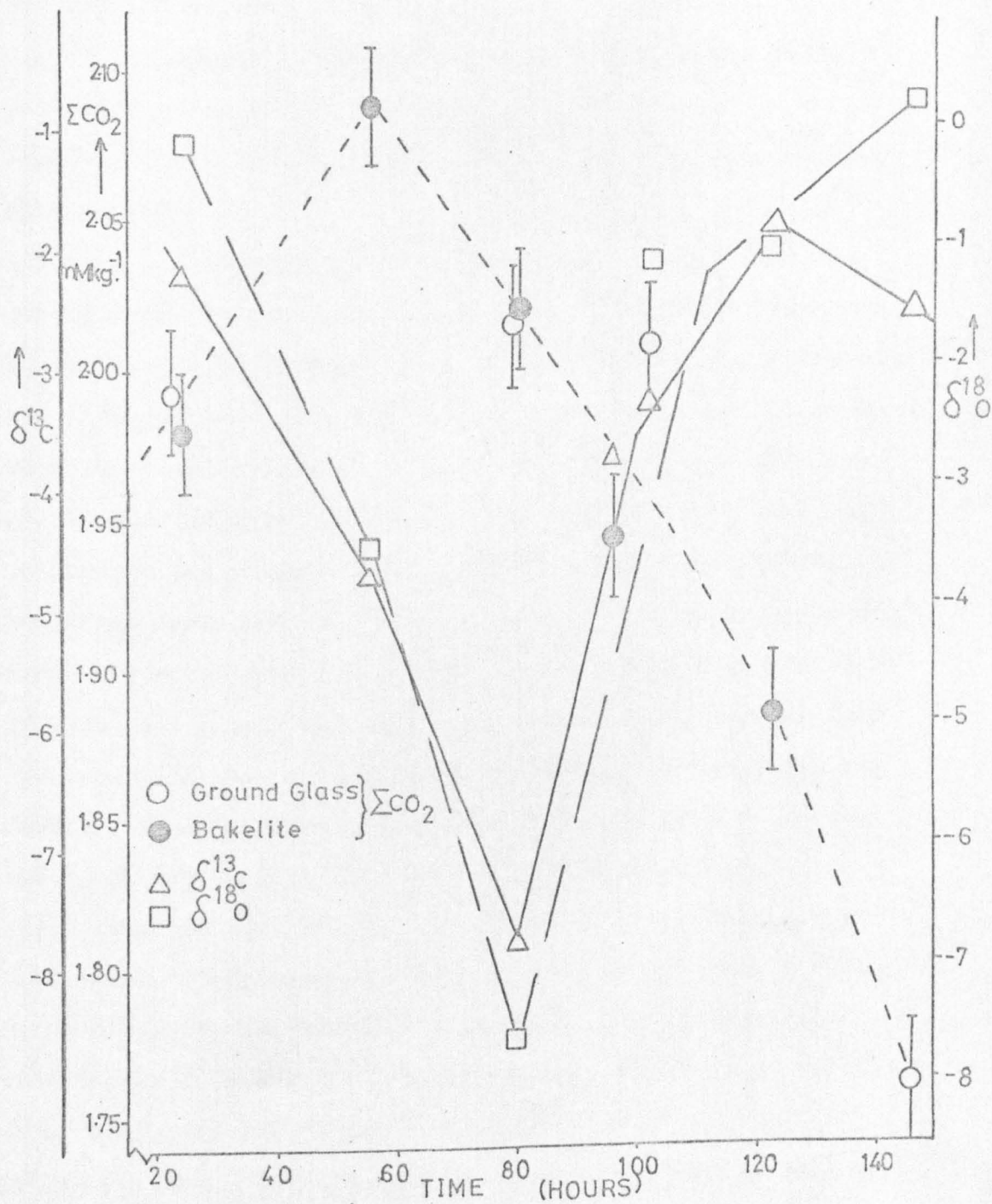
A second, completely independent explanation for the changes in ΣCO_2 and isotope ratios must be mentioned. It is that CO_2 may have been transferred between seawater and the insert of the bottle cap. This disc, of vinyl-covered composition cork, ensured a tight seal between bottle and cap, thus preventing CO_2 exchange with the atmosphere. Alteration of ΣCO_2 and $\delta^{13}\text{C}$ of stored seawater sealed with natural cork inserts has been observed in an investigation of the storage capabilities of crown-capped bottles (described later in this chapter). The possibility that such interaction was responsible for the variations shown in Figure IV-2 was eliminated in a second experiment which involved also the use of bottles with ground glass necks and mated stoppers.

Surface water was collected from the Clyde just North of Rhu Narrows, Gareloch. On returning to the laboratory, the two litre glass container was thoroughly shaken to minimise inhomogeneity and the water distributed to nominally 100 ml. storage vessels. Two types of vessel were used: those with screw-on bakelite caps mentioned previously, and 100 ml. glass flasks with ground glass necks. The ground glass stoppers were lightly and evenly coated with Edwards Silicone

High Vacuum Grease. As stated above, Zobell and Anderson (1936) have shown that the rate of bacterial population increase is a function of the ratio of volume to surface area of the container; for this reason, the two types of storage vessel were carefully chosen to avoid such effects. The samples were stored in the dark, at room temperature, and were analysed over a 6 day period. The ΣCO_2 and its $\delta^{18}\text{O}$ values are plotted in Figure IV-3 as a function of storage time. Again, the measured properties go through extrema after about three days of storage, and it is obvious from the figure that the effect is independent of the storage vessel used. Hence, large scale uptake or release of CO_2 , or alteration of the isotope ratios, by the composition cork of the bottle cap inserts in the first experiment is ruled out. The alternative explanation - that the variations are due to biological activity - seems more plausible, and the isotope ratio measurements on the inorganic carbon system thus confirm and extend the theories of marine biologists concerning the development of the bacterial population.

Further comparison between the two experiments must be undertaken with care; the fact that different samples of seawater have different isotopic, chemical and biological compositions renders duplication of results impossible - at least in the generally accepted sense of the term. The elucidation of microbiological experiments is difficult for a number of reasons. In general, several steps are involved

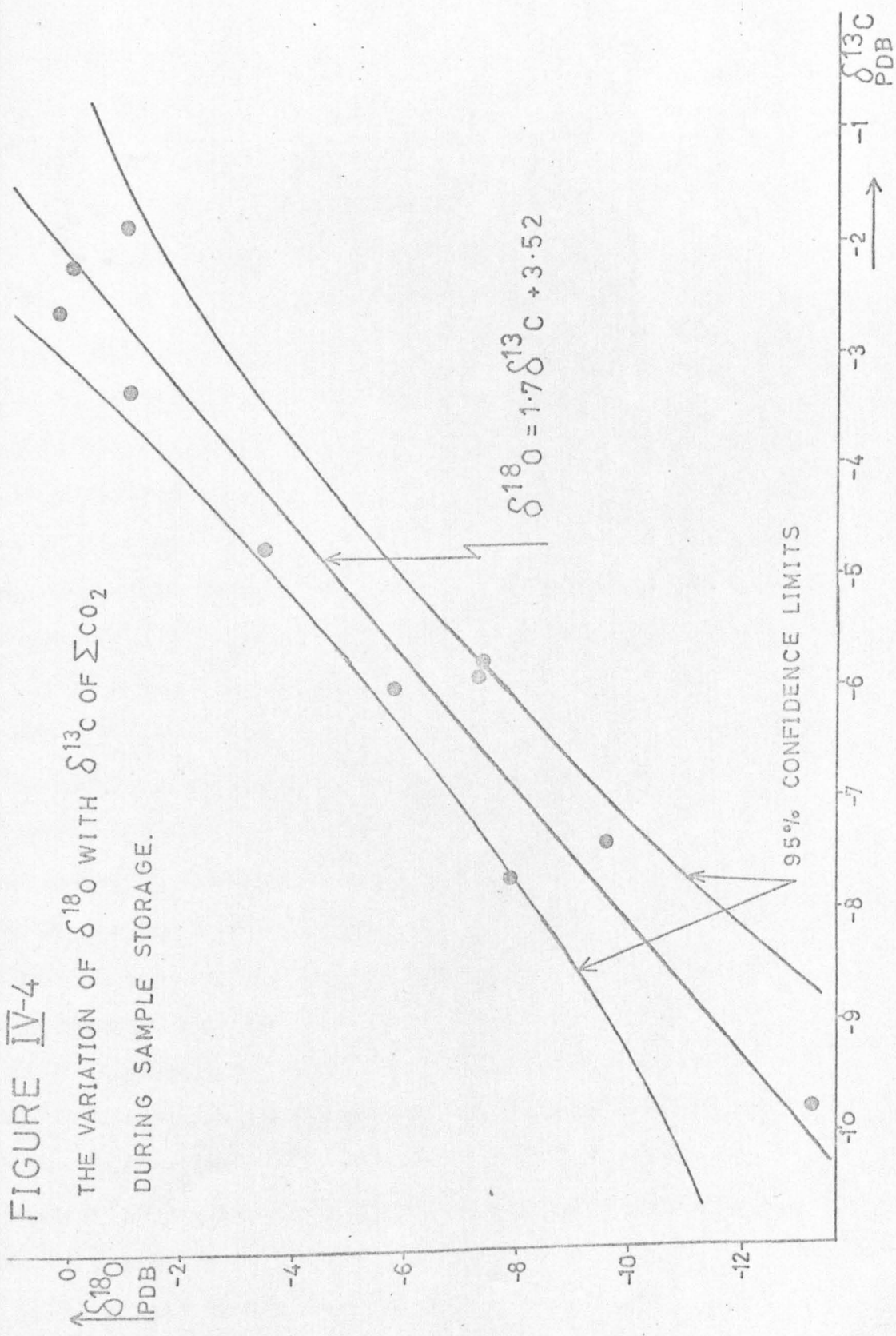
FIGURE IV-3 ΣCO_2 AND ITS $\delta^{13}\text{C}$ AND $\delta^{18}\text{O}$
 VS. DARK STORAGE TIME FOR TWO STORAGE VESSELS.



and the net isotope fractionation is a function of the isotope effects involved in each step. As Cook *et al.* (Cook, Wellman and Krouse, 1973) have pointed out:

"... experience shows that factors such as temperature, medium, ... organism etc. significantly alter the relative rates of the individual steps and hence the overall isotope behaviour."

However, a few points are worthy of note. Taking the net change after 60 hours (the approximate position of the peak) in the second experiment, 0.29 mM kg.^{-1} of CO_2 were removed; the $\delta^{13}\text{C}$ value of this was $\sim -23\text{‰}$, in reasonable agreement with the first experiment and figures obtained by Williams and Gordon (1970). The increase in ΣCO_2 from the start of storage to the maximum was almost a factor of ten greater in the first experiment than in the second; the explanation for this is most probably to be found in the fact that the scale of bacterial population increase is critically dependent on the level and form of the dissolved organic material in the sample. This is clearly illustrated in the work of Waksman and Carey (1935, Fig. 1). Again, it is conspicuous that, apart from the last sample, the isotope curves follow the same trend. This suggests that changes in $\delta^{18}\text{O}$ and $\delta^{13}\text{C}$ may be related; the correlation coefficient for the combined results for $\delta^{18}\text{O}$ and $\delta^{13}\text{C}$ from both experiments was calculated to be +0.97 and the linear relationship is clearly demonstrated in Figure IV-4. The straight line best fitting the data was found by least squares analysis to be:



$$\delta^{18}\text{O} = 1.7\delta^{13}\text{C} + 3.52$$

and is included in the Figure together with the 95% confidence band for the line as a whole.

It is highly unlikely that the correct explanation of the $\delta^{18}\text{O}$ results lies in a kinetic isotope effect during stripping: it is more plausible to assume that they reflect consequences of biological fractionation similar to those which have influenced $\delta^{13}\text{C}$. If it is assumed that the $\delta^{18}\text{O}$ results for extracted gases do give a measure of the oxygen isotope distribution in the dissolved carbonate system, and that all samples have been modified by isotope exchange with water molecules in a uniform manner, then the linear relationship:

$$\delta^{18}\text{O} = 1.7\delta^{13}\text{C} + 3.52$$

between $\delta^{18}\text{O}$ and $\delta^{13}\text{C}$ can be explained by a rather simplistic model which considers that similar chemical and biochemical reactions occurred in both experiments and that the isotope fractionation, per unit mass difference, was the same for both oxygen and carbon so that the $\delta^{18}\text{O}$ changes were (to within the accuracy of the experiments) twice those of $\delta^{13}\text{C}$, the corresponding mass difference (18-16) being twice that of (13-12). Being so naive, this explanation is open to much criticism, but it would appear from the results of the two experiments that $\delta^{18}\text{O}$ of extracted ΣCO_2 has been influenced in a consistent manner by biological activity prior to stripping.

In contrast to the work described above, there are

several reports in the literature of experiments with anomalous results; these serve to highlight the conflicting views of different investigators. Rakestraw (1947), in a study of oxygen consumption in seawater which extended over two years, noted that surface samples incubated at 25°C showed erratic behaviour. No explanation was suggested, but the effect was obviously dependent on the storage temperature. On the other hand, Kroopnick (1971) claimed to combine measurements on dissolved oxygen and its $\delta^{18}\text{O}$, for surface samples stored at 18°C in the dark, in a consistent Rayleigh batch distillation model with a single stage enrichment factor $(20.8 \pm 3)\text{‰}$. Broecker and Takahashi (1966, and also as quoted in Takahashi et al., 1970) reported that unpoisoned water samples from the Bahama Banks, stored in salinity bottles, gave the same ΣCO_2 values as those poisoned with C_6H_6 , HgCl_2 or CCl_4 , even after several months had elapsed. This point of view was still maintained three years later (Li, Takahashi and Broecker, 1969):

"There is no measurable change, however, in ΣCO_2 of water samples kept in salinity bottles even after one month storage."

On the Geosecs intercalibration cruise, however, biological activity in unpoisoned samples resulted in ΣCO_2 being altered by as much as 5% compared with samples poisoned with HgCl_2 ; the storage time was 10 weeks, for 7 of which the samples were refrigerated at around 4°C. The use of chloroform as a poisoning agent on the same cruise was found to be unsatis-

factory in that it caused greater scatter in the data. Subsequent work in the laboratory confirmed the effect without indicating any systematic trend (Takahashi *et. al.*, 1970). Moreover, the manner of introducing the poison is vitally important. Kroopnick (1971) showed that solid HgCl_2 does not immediately inhibit biological activity: a 4% decrease in dissolved oxygen was noted in 8 days. HgCl_2 in solution, though, appeared to be completely effective. Yet the samples analysed by W. Deuser at WHOI in the successful Geosecs $\delta^{13}\text{C}$ intercalibration had been poisoned with solid mercuric chloride and had spent 13 days in unrefrigerated transport whereas, for those analysed by P. Kroopnick at SIO, the poison had been added as a saturated solution and the samples kept cold until the time of extraction (Kroopnick, Deuser and Craig, 1970). The mean deviation between the two sets of data was -0.02‰ .

Simpson and Broecker (1973) attributed the unusual nature of the inorganic carbon system in a 45 litre sample of Pacific deep water to oxidation of organic material from the polyethylene storage bottles, and suggested heterotrophic microbes as the likely agents.

On cruise T-AGOR 13-73-1 of U.S.N.S. Bartlett in the eastern tropical and equatorial Pacific, a set of surface samples was taken to investigate interactions among the systems of nutrients, dissolved oxygen, ΣCO_2 and its stable isotope ratios. The oxygen samples were analysed on board at specified intervals; the other samples were poisoned with

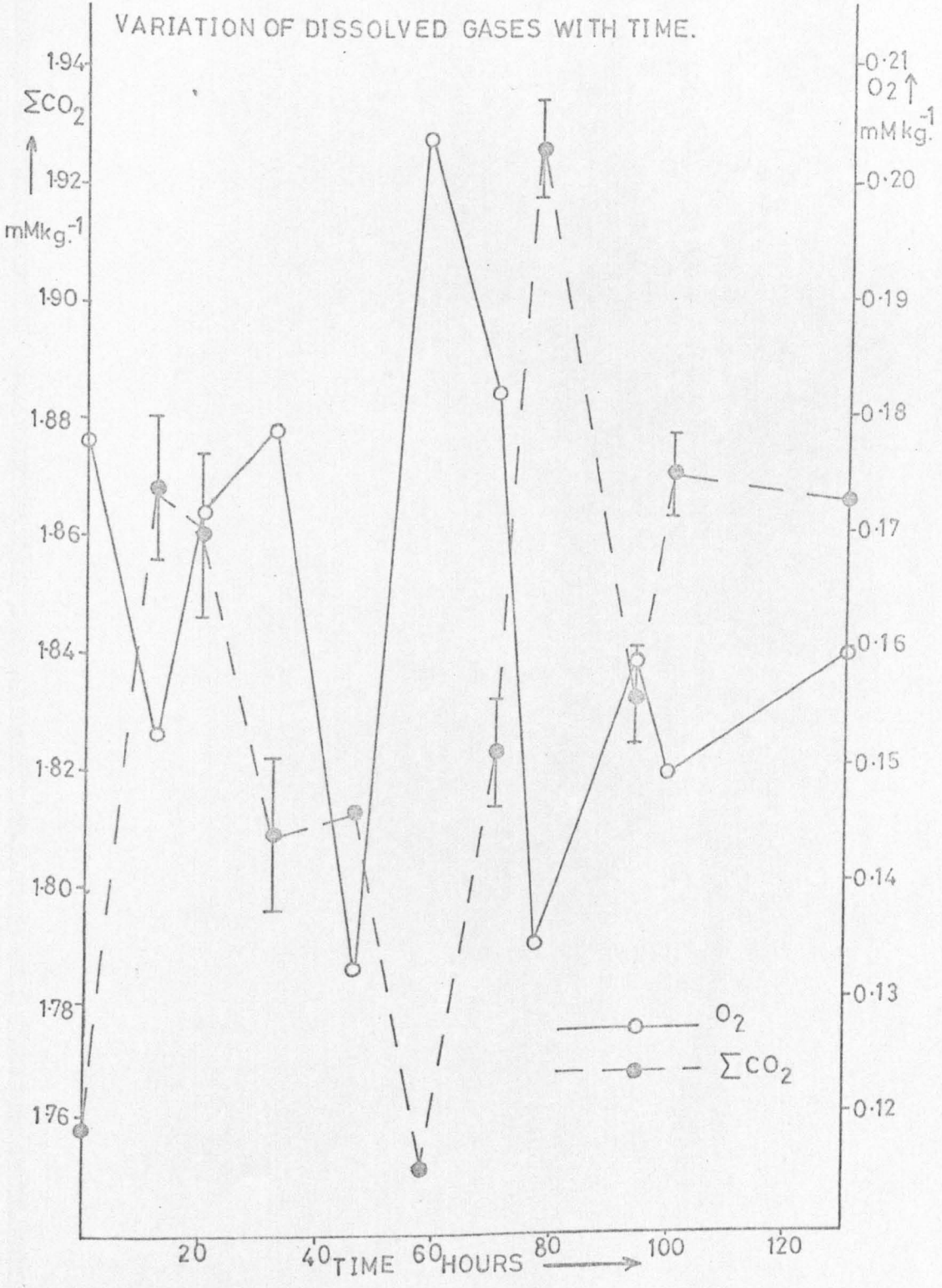
4 ml.l.⁻¹ of saturated mercuric chloride solution at the appropriate time and stored at room temperature until returned to shore laboratories where the various other measurements were to be carried out. Unfortunately, all nutrient samples from this cruise were found to have been contaminated before analysis, so no data are available (W.S. Moore, personal communication). The other results are not consistent with those of the two previous experiments and indicate that additional processes, not earlier considered, were taking place. It is considered likely that some of the discrepancies found by other workers and described above are also due to these as yet unconsidered sources. That the seemingly erratic nature of the results is not an artifact of the particular storage bottles or conditions is demonstrated by the fact that dissolved oxygen and ΣCO_2 measurements were made on independent samples, stored in separate ground glass stoppered bottles in different locations. Most of the ΣCO_2 extractions were performed in duplicate. The reasons for this were twofold: firstly, to increase the precision of the results, and secondly to prove that the large scatter among some of the other oceanographic samples described in later chapters was not caused by stripping technique in the laboratory. The results are given in Table IV-1, and are plotted in Figures IV-5 and 6 against the storage time without poison. The maximum percentage error in ΣCO_2 was 1% and the mean was $(0.6 \pm 0.2)\%$; the results are therefore in excellent agreement

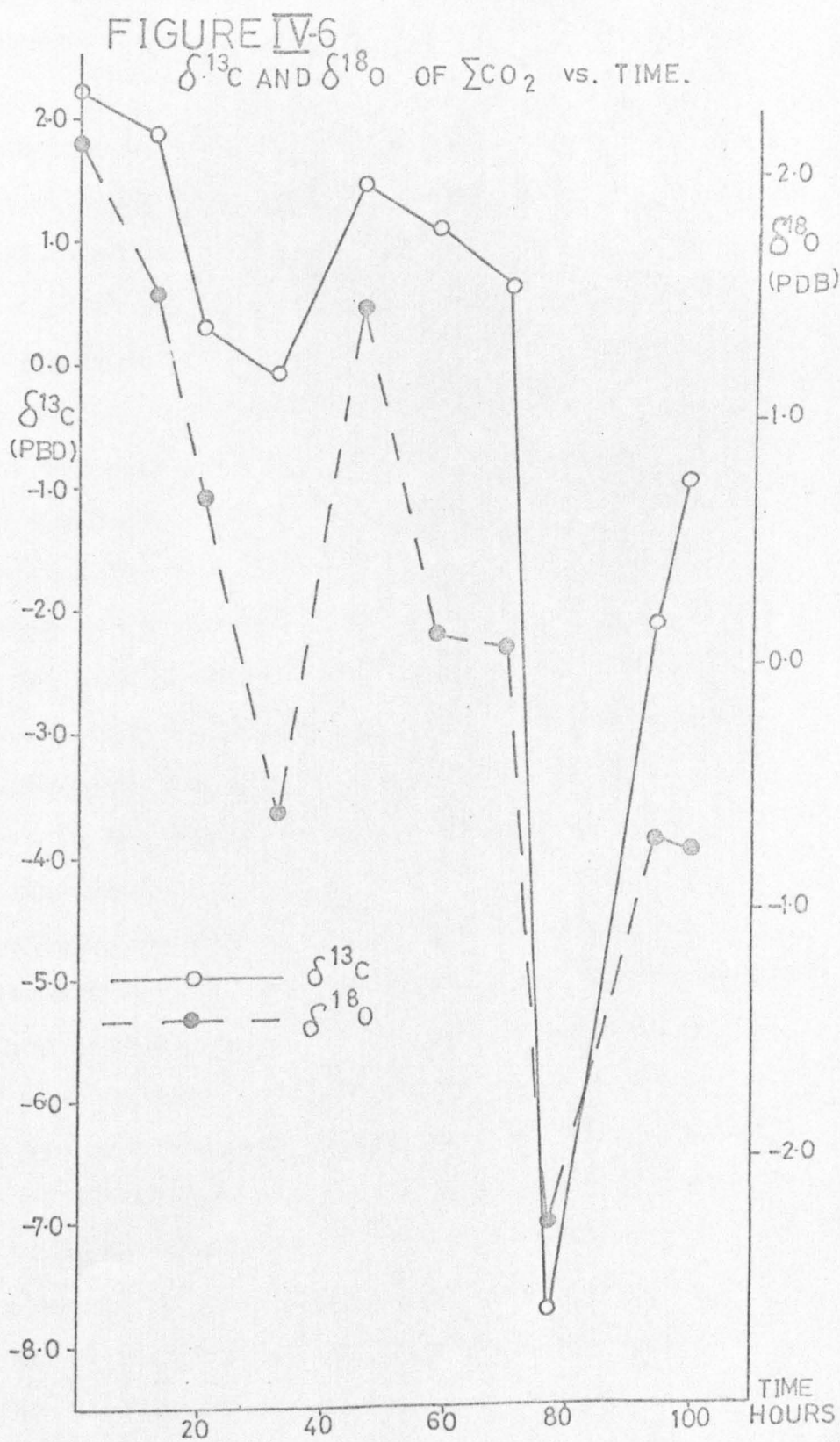
TABLE IV-1

Results of Bartlett closed system biological fractionation experiments.

TIME SINCE COLLECTION (HOURS)	ΣCO_2 (mM kg. ⁻¹)	$\delta^{13}\text{C}$ PDB	$\delta^{18}\text{O}$ PDB	O_2 (mM kg. ⁻¹)
0	1.771) 1.745) 1.758(18)	2.21	2.14	0.178
12	1.859) 1.876) 1.868(12)	1.87	1.52	0.153
20	1.849) 1.872) 1.860(14)	0.30	0.69	0.172
32	1.818) 1.800) 1.809(13)	-0.09	-0.61	0.179
46	1.813	1.46	1.47	0.133
58	1.751	1.10	0.14	0.204
70	1.829) 1.816) 1.823(9)	0.63	0.09	0.182
77	1.931) 1.920) 1.926(8)	-7.74	-2.27	0.135
94	1.826) 1.837) 1.832(8)	-2.16	-0.70	0.159
99	1.875) 1.865) 1.870(7)	-1.00	-0.75	0.149
129.5	1.865	-	-	0.159

FIGURE IV-5

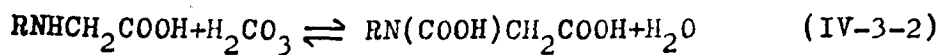




with the precision claimed in Chapter II and the variations in ECO_2 among samples can be considered as real. That the isotope ratios presented adequately describe the inorganic carbon dioxide system is, however, open to question. When the mass spectrometric assays were being performed, it was noted that many of the gases, - particularly those which had been left longest without poison - gave ratio traces which were either slightly convergent or divergent. These symptoms are normally associated with 'dirty' gases, i.e. sample contamination. The mass spectra of several of the gases, up to m/e 60, were obtained using the instrument in the single beam scanning mode. Samples poisoned soon after collection had small contaminant peaks at m/e 43, 47 and 58; those poisoned later showed greater contamination with the same peaks plus additional ones at m/e 35, 37 and 39. Contributions to the 44, 45 and 46 ion beams cannot, of course, be recognised.

In an attempt to further clarify the situation, a sample of the extracted gas was analysed by gas chromatography. A 180 cm. long, 60-85 mesh silica gel column was used with a 50 - 300°C at 10° min.⁻¹ temperature program. A sample of town gas was used for peak standardisation. The major contaminant of the CO_2 was registered by a single peak in the region of C_6 hydrocarbons. To extend mass spectral information, an AEI MS 12 instrument was used; above m/e 60, four peaks were observed. The biggest of these was at m/e 77, with a smaller one at 69, the other two being much

smaller and of much higher mass to charge ratio. A definite ratio could not be assigned to either, but it was tentatively estimated that they were around (130 ± 5) and (190 ± 10) . No corresponding peaks were visible in the instrument background. Several interesting points immediately arise: Swinnerton and Linnenbom (1967) in a gas chromatographic analysis of Bahamas seawater from 50 m. depth also observed a significant peak in the region following the pentanes. Their calibration only extended to C_4 hydrocarbons, however, and they were unable to further identify the compound - labelling the peak 'unknown'. Of the CO_2 photosynthetically fixed by the phytoplankton, it is reported by Parsons and Takahashi (1973) that up to 50% may be released as soluble organic carbon; the major products of this exudation include short chain amino acids, glycerol, carbohydrates and polysaccharides. As Riley and Chester (1971) have pointed out, in organic rich waters carbon dioxide and amino acids may react to form carbamino-carboxylic acids:



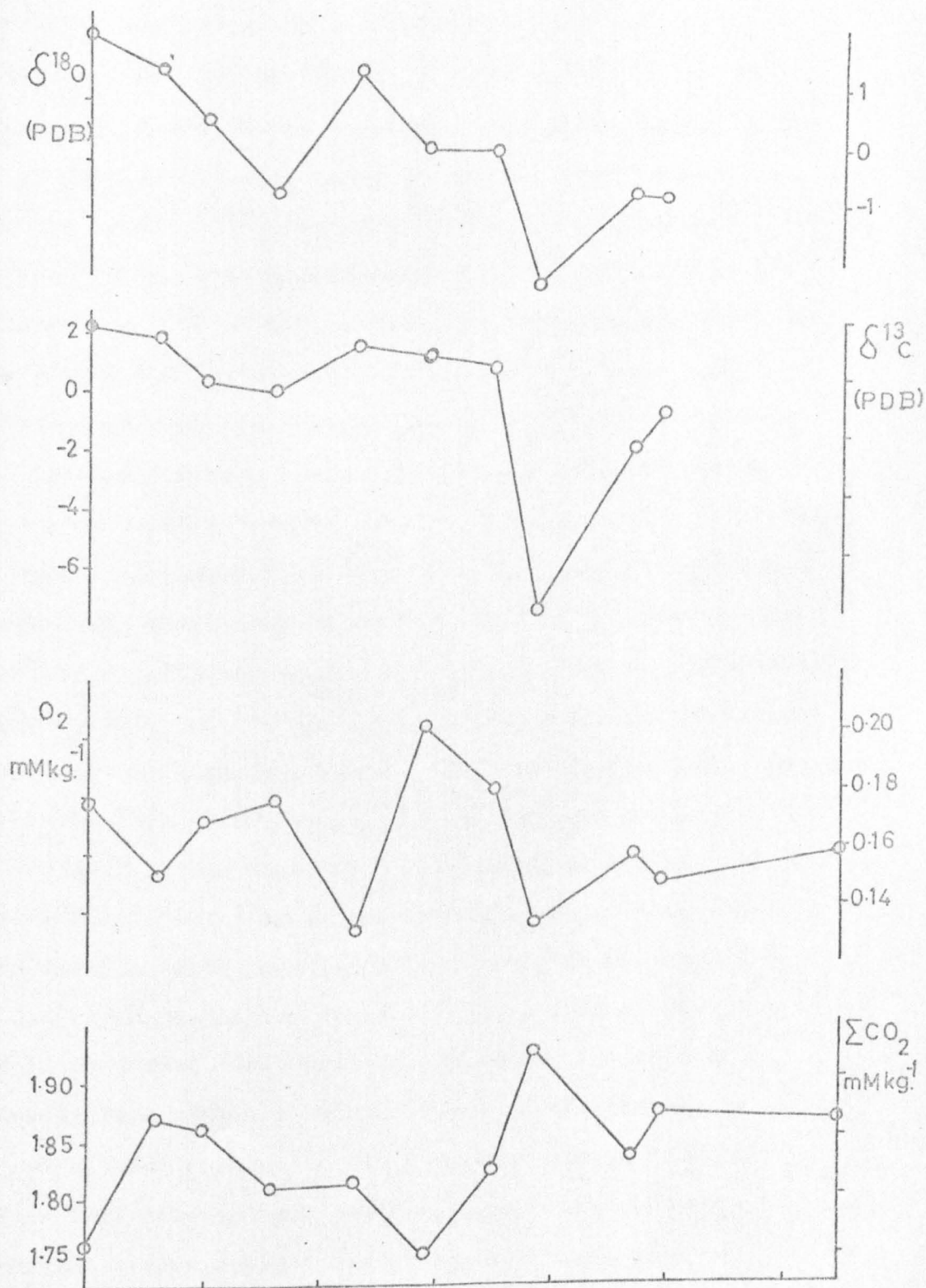
Also, it can be seen from equation (IV-3-1) that $C_6H_{12}O_6$ is a product of chemosynthetic fixation of CO_2 . Sutcliffe et al. (1963) claimed to show that when air is bubbled through seawater (cf. stripping procedure), organic particles are formed. Furthermore, Baylor and Sutcliffe (1963) considered that these particles could support the growth of the brine

shrimp. However, Menzel (1966) and Barber (1966) have effectively criticised some of the experimental evidence for these findings.

To return, then, to the results plotted in Figures IV-5 and 6, it is obvious that the analysis must proceed with care. The most precise data are probably those for ΣCO_2 , but each number may include an unknown contribution from the organic contamination. The fraction this constitutes, though, is unlikely to be much greater than about 1%. The reliability of the oxygen data has already been discussed in Chapter II: the samples for this experiment were analysed using the syringe Microburet. As indicated previously, contributions to the 44, 45 and 46 ion beams from the contaminant cannot be recognised, and so cannot be accounted for. The sample poisoned immediately, however, should be genuine. The $\delta^{13}\text{C}$ value of this sample was 2.2‰ , in excellent agreement with values (2.0 to 2.2‰) reported by Kroopnick (1974(b)) for ΣCO_2 extracted from Pacific surface samples from equatorial and mid-latitudes. Also, the errors introduced into δ by extraneous major and minor ion currents are of opposite sign and so, to a certain extent, cancel; the true isotope ratio of the CO_2 is measured when the fractional contribution from the contaminant is the same in both cases.

In order to permit easy comparison of the four sets of results, they have all been plotted on a single graph in Figure IV-7. It is immediately apparent that, as expected,

FIGURE IV-7
ALL BARTLETT STORAGE RESULTS vs. STORAGE TIME.



there is an inverse correlation between dissolved oxygen and ΣCO_2 , the correlation coefficient being -0.71 . This would suggest that the HgCl_2 solution was an effective inhibitor of biological activity. In concurrence with the other experiments, CO_2 added to the dissolved carbonate pool is light in ^{13}C , and in the fixation of inorganic carbon ^{12}C is used in preference to ^{13}C , resulting in an increase in $\delta^{13}\text{C}$ of ΣCO_2 . The correlation coefficient for the ΣCO_2 and $\delta^{13}\text{C}$ data was -0.70 . It might have been anticipated that the samples returned to Glasgow for ΣCO_2 and isotope analyses would have had a sufficient storage period (8 months) for any initial alteration of $\delta^{18}\text{O}$ of ΣCO_2 to have been masked by isotope exchange with the seawater, so that the correlation of $\delta^{13}\text{C}$ with $\delta^{18}\text{O}$ observed in the previous experiments would have been destroyed. Surprisingly, however, this was not the case - the calculated coefficient was 0.86 . This figure, though, is considerably lower than the value (viz. 0.97) found earlier, and the gradient $d\delta^{18}\text{O}/d\delta^{13}\text{C}$ of the best fitting straight line decreased from 1.7 to 0.4 . Still, it is somewhat surprising that any relationship at all was preserved: the extent to which this is due to contamination is obviously an unknown factor. In conclusion, then, the Bartlett experiment is taken as demonstrating that the changes which occur in seawater stored without poison are not always as straightforward as the initial descriptions would suggest. The fact that the dissolved oxygen content was in several cases seen to be

higher than the original value (with concomitant decrease in ΣCO_2) is most easily explained by the occurrence of photosynthesis. Light adaption - the adaptive changes in photosynthesis which occur in algae cells in response to surrounding light conditions - can take up to three days, and is a complex process involving several morphological or biochemical changes, including a change in the availability of enzymes for the photosynthetic dark reaction (Parsons and Takahashi, 1973). Temperature is also important; for instance, Ichimura et al. (1962) showed that temperate Pacific phytoplankton had their highest maximum gross photosynthesis at about 20°C, in spite of in situ temperatures which varied between -0.9 and 17.9°C. 'Photorespiration' - the enhancement of respiration in the light - is also known to occur, though the mechanism of it is obscure and not at present understood. The $\delta^{13}\text{C}$ versus $\delta^{18}\text{O}$ correlations observed in all three experiments, when taken in conjunction with the findings of section II-3, cast doubt on the validity of Kroopnick's (1974(a)) procedure for estimation of $\delta^{18}\text{O}$ of ΣCO_2 , particularly in studies of this sort. The unsolved problem of the influence of the contaminant(s) on the results must, however, always be borne in mind. From the results given in Table IV-1, it would seem advisable for samples to be poisoned as soon after collection as possible. Takahasi et al. (1970) claimed 24 hours as an upper limit for the reliable storage of unpoisoned samples, based on results which:

'... showed no significant change in ΣCO_2 after 24 hours. Zobell and Anderson (1936) also found no significant bacterial activity during the first 24 hour period.'

The validity of this claim centres on the word 'significant' to quote Zobell and Anderson (1936) directly:

'Although there is evidence of multiplication within eight hours after the water is bottled, little or no difference is found in the density of the bacterial populations in the different volumes during the first two days.'

This was contrasted with the results after the first two days which showed that the rate of bacterial multiplication varied with the ratio of volume to surface area. Moreover, the work of Zobell and Anderson used:

'... chemically clean, sterilised apparatus and aseptic technique'; these precautions were not taken in the work reported by Takahashi et al. who, in fact, used the contribution of organic carbon from storage bottles to support other arguments they presented. This is of critical importance for, as Waksman and Carey (1935) pointed out:

'The addition of a small amount of organic matter of a type comparable in chemical nature to that which is found in the sea has a decided stimulating effect upon bacterial multiplication.'

IV-4 Effective poisoning and storage of samples.

From previous discussion, it is apparent that a certain amount of controversy exists over the most appropriate manner of sample poisoning. The most unambiguous results reported, however, have been obtained using 4 ml.l^{-1} of saturated mercuric chloride solution (Kroopnick, 1971). To test the efficacy of this method of preventing biological development, a 1 litre seawater sample was so treated and distributed to four 250 ml. storage vessels. The vessels were closed with ground glass stoppers using three different types of seal:

- S : a light, even coating of Edwards Silicone High Vacuum Grease,
- T : a Teflon sleeve,
- A : a light, even coating of Apiezon 'N' Grease.

The samples were stored in the dark at room temperature and analysed over an eight month period. The ΣCO_2 and $\delta^{13}\text{C}$ results are presented in Table IV-2 and demonstrate that this sterilisation procedure is indeed reliable.

Having dealt at some length with the necessity and procedure for poisoning samples which must be stored before analysis, attention will now be directed to the problem of changes in the seawater due to factors other than poisoning. Ideally, the seawater sample should totally fill the storage vessel from the moment of its collection until processing. In certain cases, particularly in inshore and estuarine

TABLE IV-2

Results for samples poisoned with 4 ml.l.⁻¹ HgCl₂ solution and stored in glass bottles with ground glass stoppers.

ANALYSIS DATE	SEAL*	ΣCO_2 (mN kg.l. ⁻¹)	$\delta^{13}\text{C}$ PDB
10.11.72	S	2.275	-3.05
13.11.72	T	2.278	-2.99
15.1.73	T	2.286	-2.90
30.7.73	A	2.288	-2.97
MEAN :		2.282±0.005	-2.98±0.05

* see text for details

areas, this may be achieved, as for example in some of the work of Tan et al. (1973) in which samples are stored at 4°C. However, in general oceanographic samples have much longer storage periods and the problems of transportation to the shore laboratory are much greater, so the ideal is costly and seldom attained. When refrigerated storage is unavailable, it is often false economy to completely fill the sample bottle, for with cold waters the subsequent volume increase on warming may exert sufficient pressure to crack the vessel, resulting in leakage or even total loss of the sample. Usually, a compromise must be reached whereby the samples are stored at room temperature with sufficient free space above to allow for volume changes. This, of course, introduces a possible source of error both through CO₂ exchange and contamination. An investigation into the storage capability of several different types of sample bottle was thus undertaken. Four varieties of vessel were compared:

- (i) glass bottle with ground glass stopper
- (ii) glass bottle with bakelite screw-on cap with vinyl covered composition cork insert
- (iii) glass bottle with metal crown cap with natural cork insert
- (iv) plastic bottle with plastic screw-on cap

The seawater stored in these bottles was poisoned with 4 ml. l.⁻¹ of HgCl₂ solution and the samples analysed at various times. The results are shown in Table IV-3. In

TABLE IV-3

Comparison of different types of storage vessel.

DATE	STORAGE VESSEL	ΣCO_2 (mM kg. ⁻¹)	$\delta^{13}\text{C}$ PDB
3.11.72	NONE	2.215	-2.36
7.11.72	BAKELITE CAP	2.200	-2.31
15.11.72	PLASTIC	2.155	-2.81
15.11.72	CROWN CAP WITH NATURAL CORK INSERT	2.251	CONTAM.
25.5.73	GROUND GLASS	2.200	-2.42
16.8.73	GROUND GLASS	2.195	-

accord with the observations of Simpson and Broecker (1973), the plastic container was found to be unsatisfactory; in addition, an unexpected result was obtained for the crown-capped bottle. Since it was intended to use crown-capped bottles for collection of Antarctic water samples from Cruise 56 of U.S.N.S. Eltanin, a closer look was taken at this type of bottle seal. (The cruise, incidently, was subsequently cancelled). The results of five samples analysed over a 1 month period are given in Table IV-4 and are seen to be very erratic, thus demonstrating the unsuitability of such bottle seals for storage of oceanographic water samples for this type of work. When mass spectrometric assay was attempted, the extracted gases were all found to be highly contaminated. Some workers (e.g. Broecker and Takahashi, 1966) have used salinity bottles, but Craig and Gordon (1965) have commented on the occasional unreliability of the gaskets, complete batches being found to be of poor quality. Glass bottles with ground necks and mated stoppers emerge as the most appropriate choice of storage vessel for work of the type reported here. However, the supply of bottles for collection of samples from oceanographic profiles was - because of logistic difficulties - totally dependent on the organising scientist on the various cruises from which samples have been obtained, and in practice such bottles were not available, and so inferior substitutes had to be used. Similarly, for several of the profiles, the responsibility for ensuring that the samples were poisoned

TABLE IV-4

ΣCO_2 results for samples stored in crown capped bottles with natural cork inserts.

ANALYSIS DATE	ΣCO_2 (mM kg. ⁻¹)
31.10.72	2.030
8.11.72	1.987
10.11.72	1.983
24.11.72	2.153
31.11.72	1.872

adequately was outside the author's control. These deficiencies are reflected in the quality of the data from the oceanographic profiles discussed in the next two chapters.

CHAPTER V

MEASUREMENTS IN THE EASTERN TROPICAL PACIFIC OCEAN.

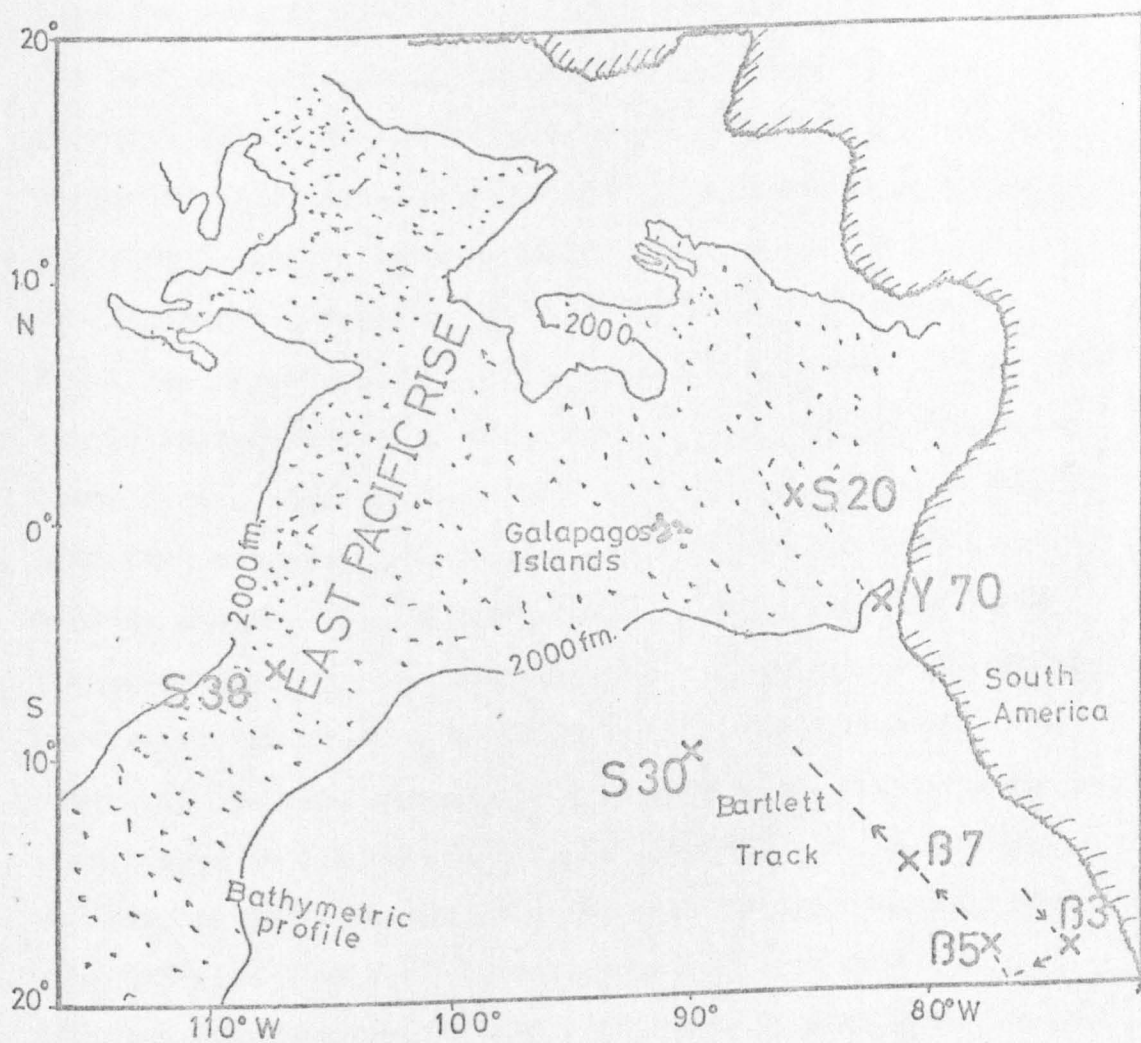
V-1 Introduction

The complex interplay of physical, chemical and biological processes necessitates, in the full description of the oceanography of some region, the consideration of as many, and of as wide a range of tracers as is possible. In general, the overall picture is synthesised from the work of several different groups of workers - falling roughly into the three categories mentioned in the previous sentence. The work reported in this chapter was undertaken as a contribution towards the understanding of the oceanography of the eastern tropical Pacific. Measurements were made on both conservative and non-conservative properties in the hope that the relative importance of various processes could, to some extent at least, be distinguished. Appreciation of the full significance of the results is, however, dependent on them being incorporated into a general scheme emerging both from the assessment of samples taken at the same locations by other scientists (e.g. for ^3H , ^{228}Ra , ^{226}Ra , ^{222}Rn , ^{210}Pb) and from previous work in the same area.

Samples were collected at three stations during cruise T-AGOR 13-73-1 of U.S.N.S. Bartlett in March 1973 from Callao, Peru to Acapulco, Mexico. The relevant portion of the ship's track is shown in Figure V-1. The sampling

FIGURE V-1

LOCATIONS OF EASTERN TROPICAL PACIFIC STATIONS.



B : Bartlett

S : Scan

Y : Yaloc

bottles used were 30 litre Niskin bottles made of PVC, these occasionally being strung along a hydro-wire in the conventional manner, but more often nine of them were arranged around a rosette surface activated multiple sample (SAMS). The SAMS was also fitted with a salinity - temperature - pressure (or depth) (STD) probe and bottom pinger, and was supported by a conducting cable to permit continuous telemetering on deck. Bottles were closed at the desired depths by electronic triggering from the surface. On return to deck, the seawater was drawn from the Niskin into the various sample storage vessels. Dissolved oxygen samples were always drawn first, followed by stable isotope samples, then pH, salinity, nutrients and any other samples. The method of drawing samples was, by means of a catheter attached to the Niskin spigot, to fill the storage vessel from the bottom up, to discard the water as a bottle rinse, and then refill the vessel in the same manner and seal securely. Where appropriate, sterilising or fixing agents were added as soon as possible. The samples for ΣCO_2 and stable carbon isotope analyses were poisoned with 4 ml.l.⁻¹ of saturated mercuric chloride solution (see Chapter IV) and were, for the most part, stored in amber glass bottles with threaded bakelite caps. A seal was formed between the top of the glass bottle and the insert of the cap. It is suspected that prolonged contact with this insert (e.g. when the bottle was upside down during transportation) may in certain cases have altered the carbonate system of the seawater. Finally, the caps were

securely taped to prevent loosening and possible leakage of contents or exchange with the atmosphere.

V-2 General oceanography

A rather brief outline of the general oceanography of the eastern tropical Pacific will now be given so that the specific station analyses following can be placed in a wider context. Unfortunately, remarkably little is known about the general circulation of the Pacific Ocean, although certainly great strides forward have been taken in recent years, particularly with the work of Reid (1965) on the Intermediate Waters, of Tsuchiya (1968) on the Upper Waters and with the recently reported 'Scorpio' Expedition trans-oceanic cruises of U.S.N.S. Eltanin (Warren, 1973; Reid, 1973). Nonetheless, as recently as 1970 Warren in an article entitled 'General Circulation of the South Pacific' pointed out that knowledge of surface currents has not increased greatly over the last 100 years, and restricted himself mainly to specific problems within the general circulation, not attempting 'to present a comprehensive description of the overall circulation in the South Pacific, because we really do not know it very well.' (Warren, 1970).

(a) Upper layers

Here, the upper layers will be considered as the top 1,000m. or so. The surface, of course, is strongly influenced by the action of the wind stress - indeed Warren (1970) considers the South Pacific to be possibly the ocean most aptly described in terms of the general theory of wind-driven

circulation. In high southern latitudes, the waters of the Atlantic, Indian and Pacific Oceans meet around Antarctica. The West Wind Drift (or upper flow of Antarctic Circumpolar Current) flows eastward and part of it branches to the north into the South Pacific; this northward flow is generally restricted to the eastern regions of the ocean until, at about 20°S or so, it veers westward to join the South Equatorial Current. This great cyclonic gyre is completed by an intense narrow western boundary current, the East Australian Current, moving southwards off the coast of Australia.

In the east, the subantarctic tongue at 600 - 1,000 m. depth is distinguished by its low salinity (34.6‰ and less) and is clearly illustrated on Reid's (1965) chart of the distribution of salinity on the 125 cl. ton^{-1} isanostere (surface of constant specific volume anomaly). Off the coast of northern South America, the circulation in the upper layers is dominated by the Peru-Chile current system. This was studied in some detail by Gunther (1936) and has since been subjected to intensive investigation by Peruvian and Chilean scientists because of the economic and environmental problems caused by the phenomenon known as 'El Nino'. However, as pointed out by Wooster (1970), the 'multiplicity of current designations reflects our ignorance of a large and complex system of surface and subsurface circulation. The taxonomy of this system badly needs a careful and systematic revision'. For the present purpose, a simple description will suffice

and that of Idyll (1973) will be adopted. Idyll recognises four components as listed below, the first two being northerly flowing, the other two southerly:

(i) Coastal Current. This flows next to the shore and is seldom more than 200m. in depth.

(ii) Oceanic Current. Further out to sea than (i), this current may be as deep as 700m. or more and contains sub-antarctic water. It has also been called the Humboldt Current, particularly in early work.

(iii) Peru Countercurrent. This is a warm subsurface current which flows between (i) and (ii). Rarely exceeding 300m. in depth, yet only occasionally reaching the surface, it represents the eastern limb of an anti-cyclonic movement. From November to March, it is most pronounced and is situated about 500 km. offshore.

(iv) Peru Undercurrent. Underneath all three flows this deeper southward migrating current characterised by relatively high salinity but low dissolved oxygen. It has been studied by Wooster and Gilmartin (1961).

An interesting feature of the Peru-Chile current system is the disruption of the general stream in the coastal belt resulting in upwelling or the 'inversion' of the surface layer near the mainland coast. Upwelling is usually attributed to the influence of the component of the wind stress, pointing equatorward, parallel to the coastal boundary. In terms of simple Ekman theory, the offshore transport - and therefore the upward flux of water from

below - is directly proportional to the component of the wind stress and inversely proportional to the Coriolis parameter. The processes of upwelling are thus associated with certain definite regions, depending to a large extent on atmospheric circulation, and off the Peruvian coast the low latitude and high trade wind stress combine to produce a zone of intense divergence with consequent strong and prolonged upwelling. These replenishing waters bring with them characteristics of the depth from which they originated, resulting in low salinities and temperatures but high nutrient content. These latter two properties are extremely conducive to production of anchovies and, indeed, support the largest single species fishery in the world (Kasahara, 1970), providing some 22% of the total world catch (Idyll, 1973). According to Gunther (1936), the evidence of isotherms and isohalines suggests that upwelling is generally restricted to the upper 200m. with occasional deeper excursions in certain localities (e.g. off Callao and Caldera). The same author estimates the breadth of the zone of upwelling to vary between 5 and 30 miles, but points out that this is extremely narrow compared with the breadth of the region influenced by upwelled water. Also, perhaps surprisingly, upwelling is not always seen to be in immediate contact with the coast.

Under normal conditions, the southernmost extension of the Peru Countercurrent is within a few degrees of the equator, but given certain meteorological regimes which result in the

relaxation of the trade wind system, the north flowing wind driven currents abate allowing the warm Countercurrent to penetrate further south, with disastrous results for the cold water living organisms. This episodic phenomenon is known as 'El Nino'; the theory of a seven year periodicity has been largely discredited, but does give an indication of the time scale involved. The economic and ecological consequences can be severe.

(b) Lower layers

Much less is known about the deep circulation of the Pacific than about that in the upper layers. In the most successful (if not the only) dynamical theory of deep-water circulation, that of Stommel and co-workers (Stommel, 1958; Stommel and Arons, 1960(b)) a broad cyclonic gyre exists with an upward flux of water into the thermocline balanced by deep input of bottom water from the Antarctic. The deep western boundary current predicted by the model has been observed by Reid *et al.* (1968) and studied in some detail during the 'Scorpio' Expedition (Warren, 1973).

In the eastern Pacific, the cold Antarctic Bottom Water is not observed in the Chile and Peru Basins because the Chile Ridge forms a natural barrier between these more northerly basins and the Bellinghausen Basin in the south. Apart from Antarctic Bottom Water, which^s with its mixtures with Pacific water fills the southern basins below about 3,500m., all other deep waters found in the Pacific are considered to be secondary masses (in the technical sense of

the term). In general, they are distinguished by high uniformity of hydrological features. In the scheme given by Muromtsev (1963), these deep waters are formed by mixing of Pacific water proper and water arriving from the Indian Ocean (via Australia) and the Atlantic Ocean (via the Drake Passage). Two regimes are recognised by Muromtsev (1963) in the South Pacific, identified both by depth and other characteristics. The South Pacific Upper Deep Water is typified by temperatures in the range 2 - 2.5°C, salinities of 34.61 - 34.66‰ and dissolved oxygen concentrations of 2.81 - 3.84 ml.l.⁻¹ corresponding to 42 - 48% saturation. This water is formed in northern tropical latitudes by mixing of equatorial intermediate and underlying waters and spreads southwards to 65.5 at depths of approximately 2,000m. In contrast, the Lower Deep Water with temperatures of 1.7 - 2.0°C, salinities of 34.63 - 34.73‰ and dissolved oxygen concentrations of 3.5 - 4.2 ml.l.⁻¹ (48 - 57% saturation) in the south, is formed in high southern latitudes. The higher oxygen concentrations are a reflection of the Antarctic component of this mass.

V-3 Hydrographic features

In this section the hydrographic features observed at Bartlett Stations 3, 5 and 7 will be described; discussion will be in relation both to the general oceanography given in section V-2, and to the water mass structure revealed by selected data from other investigations in the same region.

Taxonomic problems are not restricted to those, mentioned previously, of current system designation but also extend to water mass nomenclature. However, the necessity for a consistent approach and classification is obvious so that of Muromtsev (1963) will be adopted as a basis, but will be adapted as required in the light of more recently available data. According to classical definition (e.g. Sverdrup, Johnson and Fleming, 1942) a water type is identified by single temperature (T) and salinity (S) values, whereas a water mass is normally characterised by a portion of a T-S curve. For practical reasons, this distinction was largely ignored by Muromtsev who employed temperature, salinity and dissolved oxygen to classify water types, these being 'understood to consist of a given volume of water of commensurable area and depth with the general body of water and displaying a relative uniformity of physicochemical features formed under given physical and geographical conditions.' (Muromtsev, 1963).

For comparison purposes, and to widen the scope of the discussion, data from several other cruises in the same region will be used. From the limited choice of suitable candidates available, SCAN X Stations 30 and 38 and YALOC 69 Station 70 have been selected, using as selection criteria:

- (i) a reasonable geographical proximity so as to approach uniform hydrological structure,
- (ii) relatively recent station occupation in order to minimise time dependent changes,

(iii) sampling of complete water column and high precision assay of relevant parameters.

Station locations are given in Table V-1 and are indicated in Figure V-1. The SCAN Expedition of R.V. Argo (Scripps Institution of Oceanography) was conducted in 1970; station data gathered during leg X have been reported by Weiss and Craig (1973), Chung and Craig (1973) and Kroopnick (1974(a)). The YALOC Expedition aboard R.V. Yaquina (Department of Oceanography, Oregon State University) took place in 1969; the relevant data for Station 70 are to be found in Culbersop and Pytkowicz (1970). Of course, due to local differences, considerable caution must be exercised in such a comparison. For example, YALOC 69-70 lies much nearer to the continental margin than the other stations; SCANX 30 and 38 - particularly the latter - are situated close to the East Pacific Rise, and Bullard (1963) has pointed out that locally high values of heat flow through the sea floor are typical of oceanic ridge systems.

Unfortunately, a final report of the Bartlett cruise containing corrected hydrographic data is not as yet available. The following sources of data have been used:

(i) On-board direct measurements of salinity, temperature and dissolved oxygen. Salinities were measured using a Bisset-Berman Corporation Model 6220 Portable Laboratory Salinometer calibrated with IAP0 Standard Sea Water; the precision of analysis was $\pm 0.005\text{‰}$ (M.S. Baxter, personal communication). Temperatures were measured using conventional reversing thermometers and oxygen determinations carried out

TABLE V-1

Location of oceanographic stations used in discussion of oceanography of eastern tropical Pacific.

CRUISE	STATION NUMBER	LATITUDE	LONGITUDE
BARTLETT T-AGOR 13-73-1	3	18° 57'0S	75° 03'1W
BARTLETT T-AGOR 13-73-1	5	19° 16.7'S	77° 56'.4W
BARTLETT T-AGOR 13-73-1	7	15° 23'6S	80° 42'.3W
YAQUINA YALOC-69	70	4° 00'S	82° 00'W
ARGO SCAN X	30	10°00'S	90° 09'W
ARGO SCAN X	38	6° 30'S	107° 24'W

by the author using the technique described in Chapter II.

(ii) SAMS probe STD data, both uncorrected and corrected for observed temperature, salinity and probe characteristics (W.S. Moore, personal communication). The probe printout gives temperatures to 0.01°C and salinities to 0.01‰ . As was to be expected, consistency was not always achieved; there can be many causes for this, such as instrument malfunction, analyst error, Niskin bottle pretrip etc., but every effort has been taken to present the 'best' values obtainable at the time of writing - 'best' being understood as most likely and most reliable. The possibility of some revision in the light of future data availability (such as, for example, expendable bathythermograph, XBT, profiles) cannot be ruled out, but is unlikely to affect the majority of the results or the conclusions drawn. A brief rationale of the reduction and analysis of the existing data will now be given. Several lines of approach are open, providing independent assessment of the reliability of the results. Firstly, it is to be expected that a general relationship will hold at each station between probe response and directly determined temperature and salinity. Secondly, erroneous measurements should show up as discrepancies in the T-S diagram. The justification for this assumption comes from Defant (1961): 'If the value for a particular depth at an oceanographic station does not fall on the simple, regular and usually smooth [TS]-curve it can be confidently assumed that there is an observational error or a fault in calculation.'

Thirdly, comparison between the Bartlett data and those of SCAN and YALOC permit the consistency of the adopted approach to be tested. Accordingly, graphs of conductivity salinity versus probe salinity, and thermometric temperature versus probe temperature were constructed. Excellent agreement was found between corrected probe and directly measured temperature data, the uncorrected probe results being systematically 1°C too high. The probe salinity response proved to be linear, but surprisingly enough the corrected data were in poorer agreement with conductivity measurements than the uncorrected results. The reason for this is not apparent at the present time. The salinity values for three depths at Station 3 deviated significantly from the general linear relationship. Since the probe values for these depths were consistent with those from neighbouring depths, the conductivity salinities were taken to be in error, and salinity values were re-assigned on the basis of the linear plot; these are given in Table V-2. When T-S diagrams for the various stations were drawn, the three anomalous salinities were observed to lie off the curve through the other Station 3 points; use of the re-assigned salinities restored consistency, so these values were assumed to be correct. With the exception of cast 2 of Station 7 which obviously mistripped, all other measurements were found to be satisfactory. It is to be noted that this method of data analysis allows elimination of both random and systematic errors.

TABLE V-2

Re-assigned salinities at Bartlett Station 3.

DEPTH (m.)	SAMPLE	MEASURED SALINITY	RE-ASSIGNED SALINITY
32	3-2-4	34.540	35.170
1203	3-1-1	34.592	34.529(!)
2949	3-1-7	34.667	34.694

The hydrographic results are given in Tables V-3, 4, 5 for Bartlett Stations 3, 5 and 7 respectively. Potential temperatures* (θ) were calculated from the tables of Wust (1961) and checked against those computed at the U.S. Naval Oceanographic Office (W.S. Moore, personal communication). For arithmetical ease, the more recent polynomials of Bryden (1973) were not used; in any case they would not have significantly affected the results. Oxygen saturation values were calculated from tables given by Green and Carritt (1967). The depth distributions of temperature, salinity, dissolved oxygen concentration and oxygen saturation for the entire water column have been plotted in Figures V-2, 3, 4, 5; in these profiles the SCAN data (Chung and Craig, 1973) and YALOC data (Culberson and Pytkowicz, 1970) have been included. The station key given in Figures V-2 will be used throughout this chapter, except where otherwise stated. The temperature and salinity profiles are seen to be reasonably uniform at the six stations, so that the existence of a common hydrological regime may be broadly assumed; detailed inter-station differences will be discussed later. The oxygen profiles are also similar, with a bare tendency for the more southerly Bartlett stations to have higher concentrations in the deeper waters; again, discussion is reserved until later.

* The 'potential temperature' is the temperature that a water sample attains when lifted adiabatically to the sea surface.

TABLE V-3

Hydrographic properties at Bartlett Station 3.

SAMPLE	DEPTH (m.)	SALINITY ‰	TEMPERATURE °C	POTENTIAL TEMPERATURE	DISSOLVED OXYGEN* μMg. ⁻¹	OXYGEN SATURATION %
3-2-1	7	35.587	24.46	24.46	199	96
3-2-4	32	35.170	20.20	20.19	205	91
3-2-5	62	34.907	17.59	17.58	182	77
3-2-6	91	34.933	14.78	14.77	110	44
3-2-7	120	34.888	14.30	14.28	41	16
3-2-8	195	34.852	12.83	12.80	20	8
3-2-10	476	34.564	8.33	8.29	45	16
3-2-11	705	34.452	5.77	5.68	62	20
3-2-12	936	34.493	4.55	4.49	71	23
3-1-1	1203	34.529	3.66	3.57	76	24
3-1-4	1470	34.582	2.95	2.84	99	30
3-1-5	1981	34.657	2.25	2.11	116	35
3-1-6	2468	34.703	1.91	1.73	144	43
3-1-7	2949	34.694	1.80	1.57	150	45
3-1-8	3445	34.689	1.77	1.50	154	46
3-1-10	3692	34.686	1.74	1.44	163	48
3-1-11	3971	34.684	1.74	1.41	159	47
3-1-12	4031	34.684	1.73	1.40	164	49

* 1 ml.l.⁻¹ = 43.48 μMg.⁻¹

TABLE V-4

Hydrographic properties at Bartlett Station 5.

SAMPLE	DEPTH (m.)	SALINITY ‰	TEMPERATURE °C	POTENTIAL TEMPERATURE	DISSOLVED OXYGEN $\mu\text{Mkg.}^{-1}$	OXYGEN SATURATION
5-3-A	50	35.212	19.31	19.30	-	-
5-1-1	279	34.765	10.85	10.81	19	7
5-1-4	406	34.662	8.90	8.86	11	4
5-1-5	529	34.566	7.36	7.31	45	15
5-1-6	774	34.493	5.52	5.45	42	14
5-1-7	1027	34.518	4.36	4.28	73	23
5-1-8	1348	34.559	3.35	3.25	85	26
5-1-10	1677	34.589	2.75	2.63	103	31
5-1-11	1988	34.624	2.32	2.18	110	33
5-1-12	2315	34.642	2.05	1.86	135	40
5-2-A	1200	34.534	3.49	3.40	76	24
5-2-B	3200	34.686	1.76	1.48	151	45
5-2-C	3600	34.677	1.76	1.47	156	47
5-2-D	3900	34.683	1.70	1.38	160	48
5-2-E	4100	34.681	1.73	1.39	155	46

TABLE V-5

Hydrographic properties at Bartlett Station 7

SAMPLE	DEPTH (m.)	SALINITY ‰	TEMPERATURE °C	POTENTIAL TEMPERATURE	DISSOLVED OXYGEN μMg. -1	OXYGEN SATURATION
7-3-1	52	35.066	17.78	17.78	216	92
7-3-4	151	34.790	12.70	12.68	10	4
7-3-5	297	34.754	10.99	10.95	23	9
7-3-6	496	34.565	8.09	8.03	23	8
7-3-7	895	34.502	4.83	4.74	63	20
7-3-8	1095	34.518	4.02	3.92	84	26
7-3-10	1241	34.542	3.55	3.44	104	32
7-3-11	1491	34.577	2.94	2.82	80	25
7-3-12	1739	34.610	2.51	2.37	104	32
7-1-4	2088	34.641	2.03	1.89	119	36
7-1-5	2692	34.667	1.81	1.61	156	47
7-1-6	2995	34.669	1.80	1.57	148	44
7-1-7	4496	34.682	1.79	1.40	138	41
7-1-8	4594	34.682	1.80	1.39	148	44
7-1-10	4617	34.680	1.80	1.39	148	44
7-1-11	4631	34.679	1.80	1.39	144	43

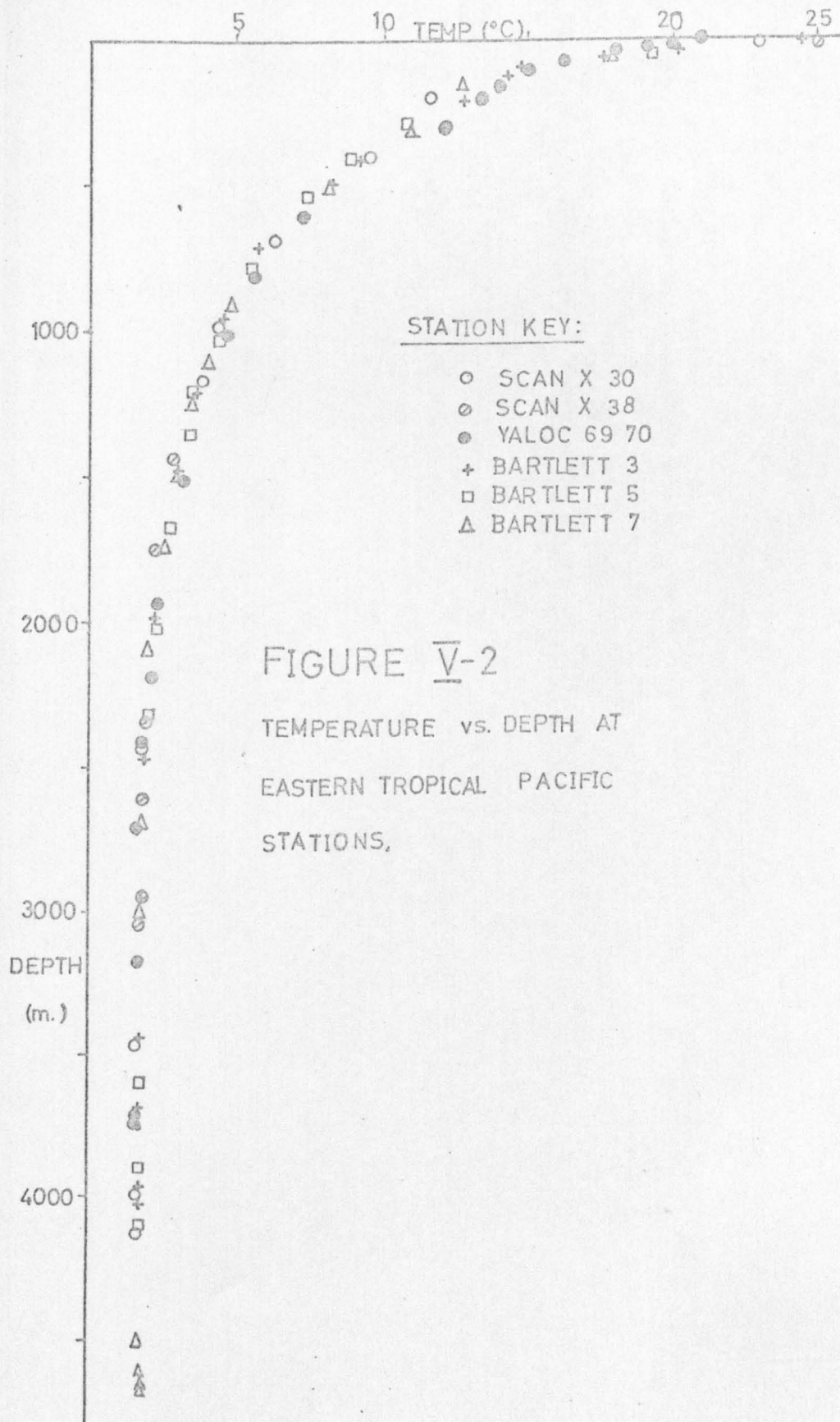
TABLE V-5 (continued)

Hydrographic properties at Bartlett Station 7

SAMPLE	DEPTH (m.)	SALINITY ‰	TEMPERATURE °C	POTENTIAL TEMPERATURE	DISSOLVED OXYGEN $\mu\text{Mkg.}^{-1}$	OXYGEN SATURATION
7-1-12	4561	34.680	1.80	1.39	122	36
7-1-1	4669	34.684	1.80	1.39	145	43
7-2-A**	2800?	34.531	3.96	-	79	-
7-2-B**	3600?	34.518	-	-	40	-
7-2-C**	4000?	34.494	5.24	-	49	-
7-2-D**	4300?	34.515	4.28	-	75	-
7-2-E**	4500?	34.809	-	-	54	-

** Cast 2 mistrrippped

? Indicates originally assigned, but later questioned, depth.



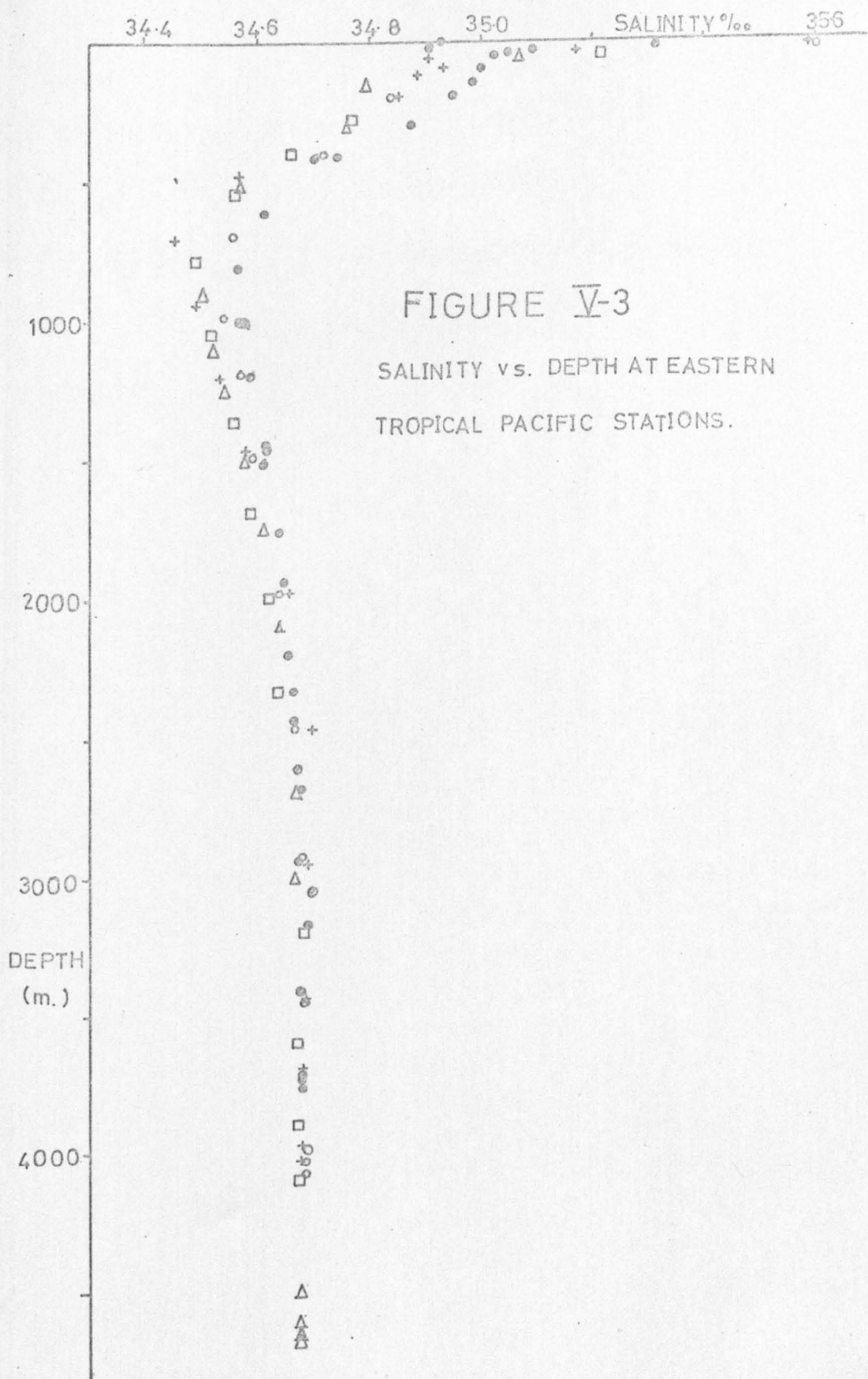
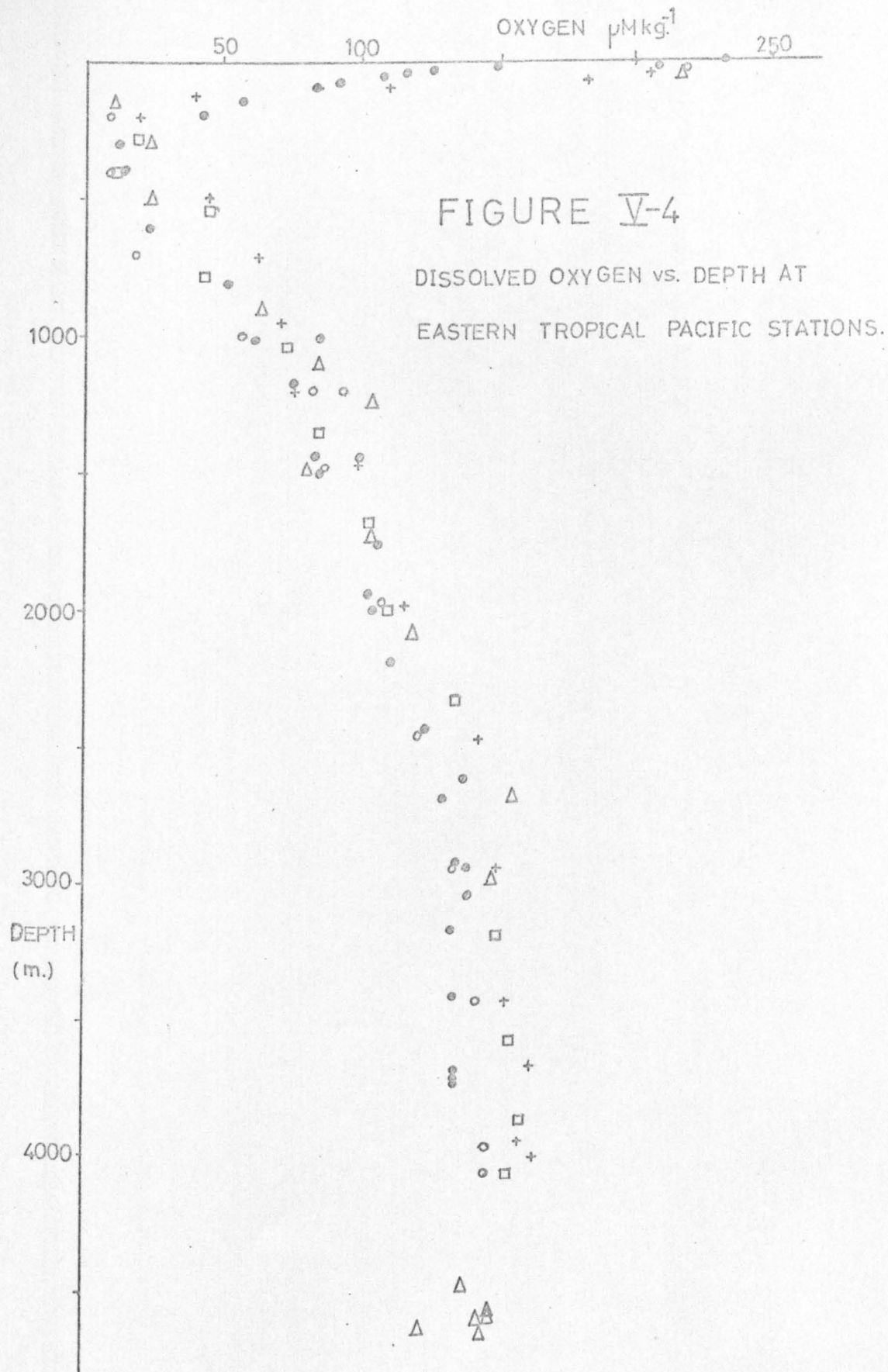
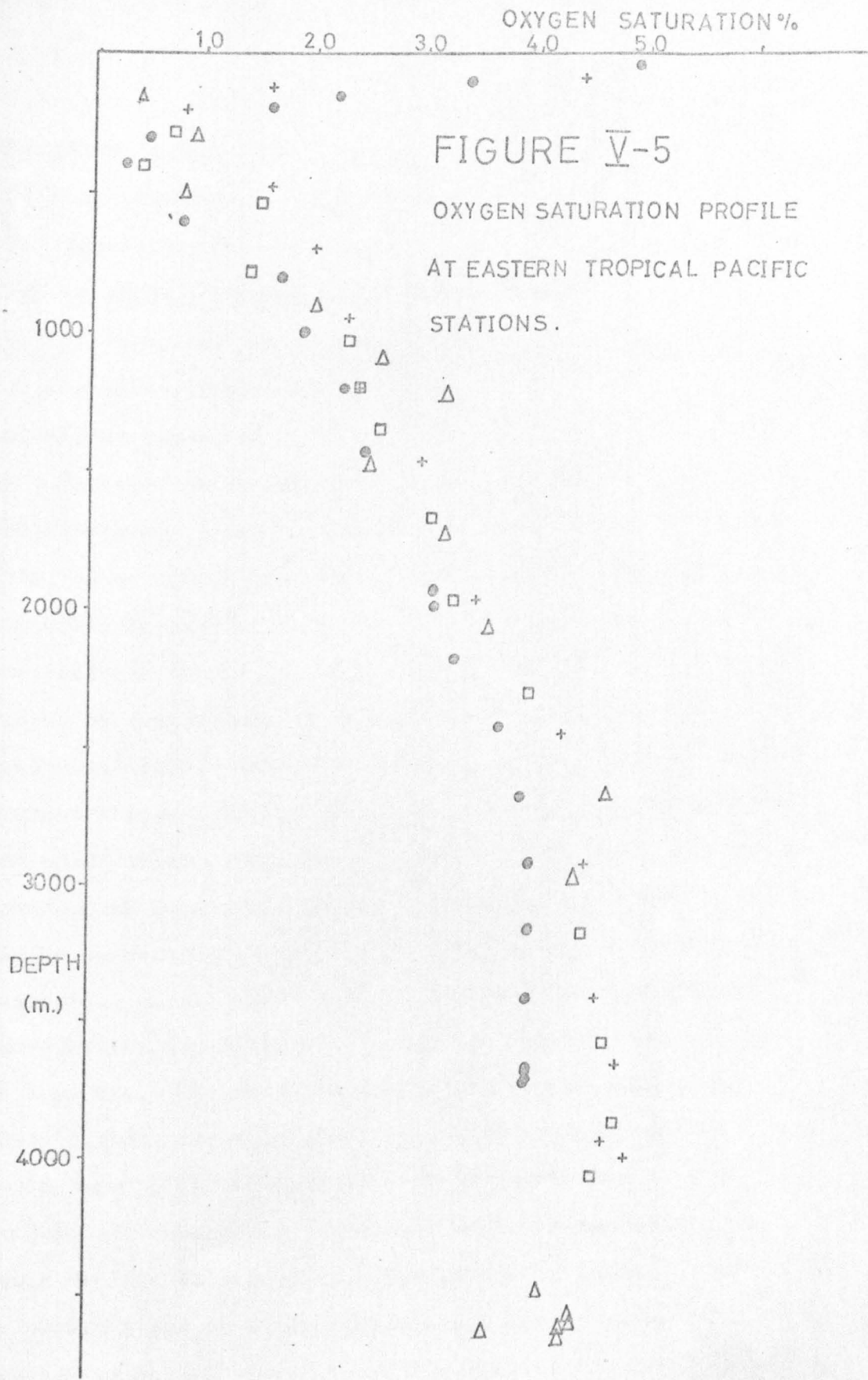


FIGURE V-3
SALINITY vs. DEPTH AT EASTERN
TROPICAL PACIFIC STATIONS.





The gross features of:

- (i) high gradients in upper layers,
- (ii) regularity in the deep,
- (iii) a strongly developed main thermocline,
- (iv) an intermediate salinity minimum,
- (v) a shallow oxygen minimum

are all as expected.

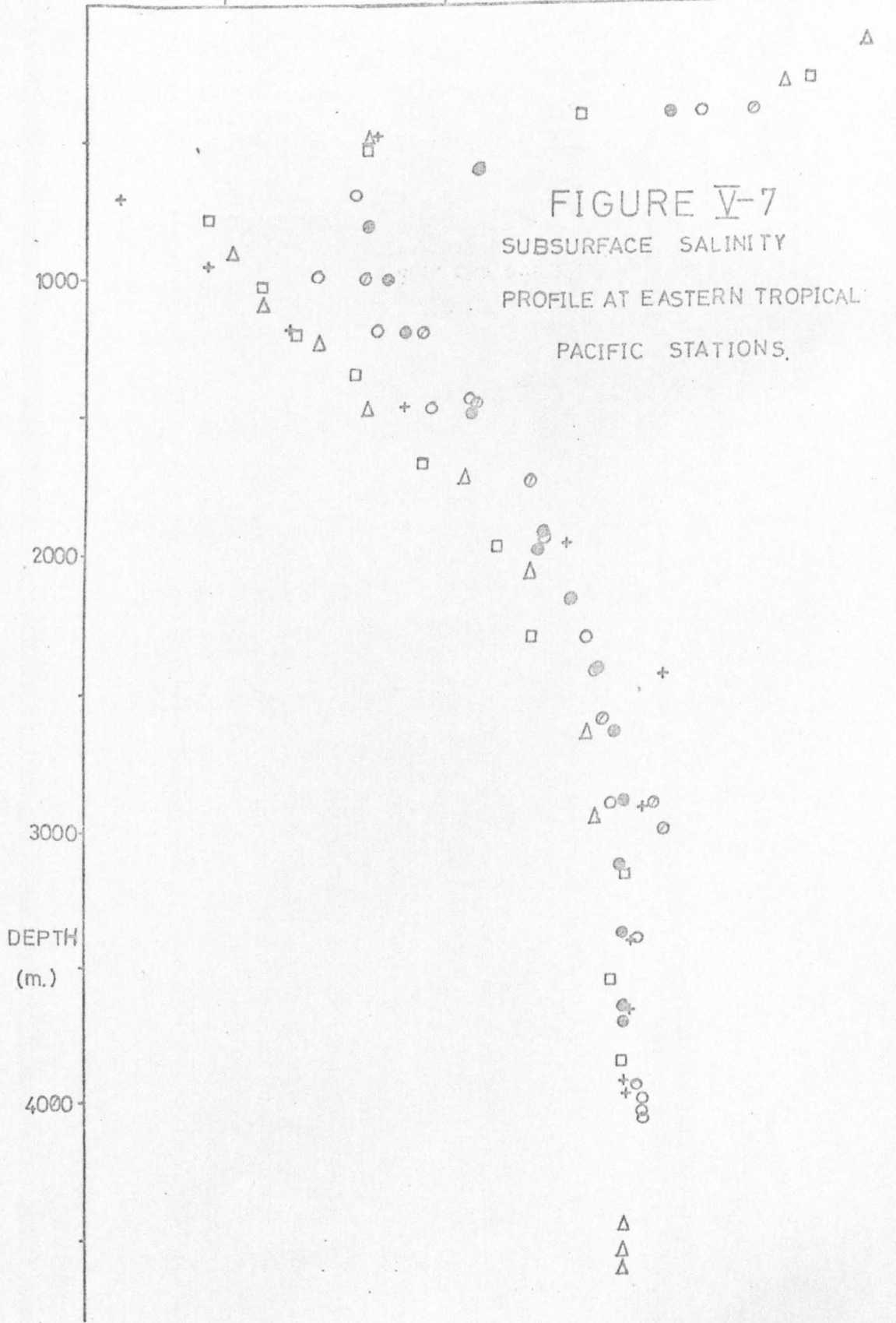
Elucidation of the upper water structure has been facilitated by study of logarithmic depth plots. The top 100m. or so are Peru Surface Water, distinguished from more northerly Equatorial Surface Water by having lower temperatures but higher salinities. This reflects a greater excess of evaporation over precipitation than in the equatorial belt, caused by atmospheric circulation. Oxygen concentrations typically decrease rapidly with depth below the mixed layer. Underneath, down to 400 - 500m. lie South Subtropical Subsurface Waters containing the oxygen minimum. Oxygen concentrations at the minimum are quite uniform with saturation values below 10% - indicative of high biological consumption; no variation of depth of minimum with latitude is apparent. The intermediate waters in the depth range 400 - 1,400m. are characterised by the salinity minimum layer. Formed in the Antarctic convergence zone by mixing of surface and subsurface waters and advected northwards, the South Pacific Intermediate Water gradually loses its identity by vertical mixing with shallower and deeper layers and eventually merges laterally with southward flowing inter-

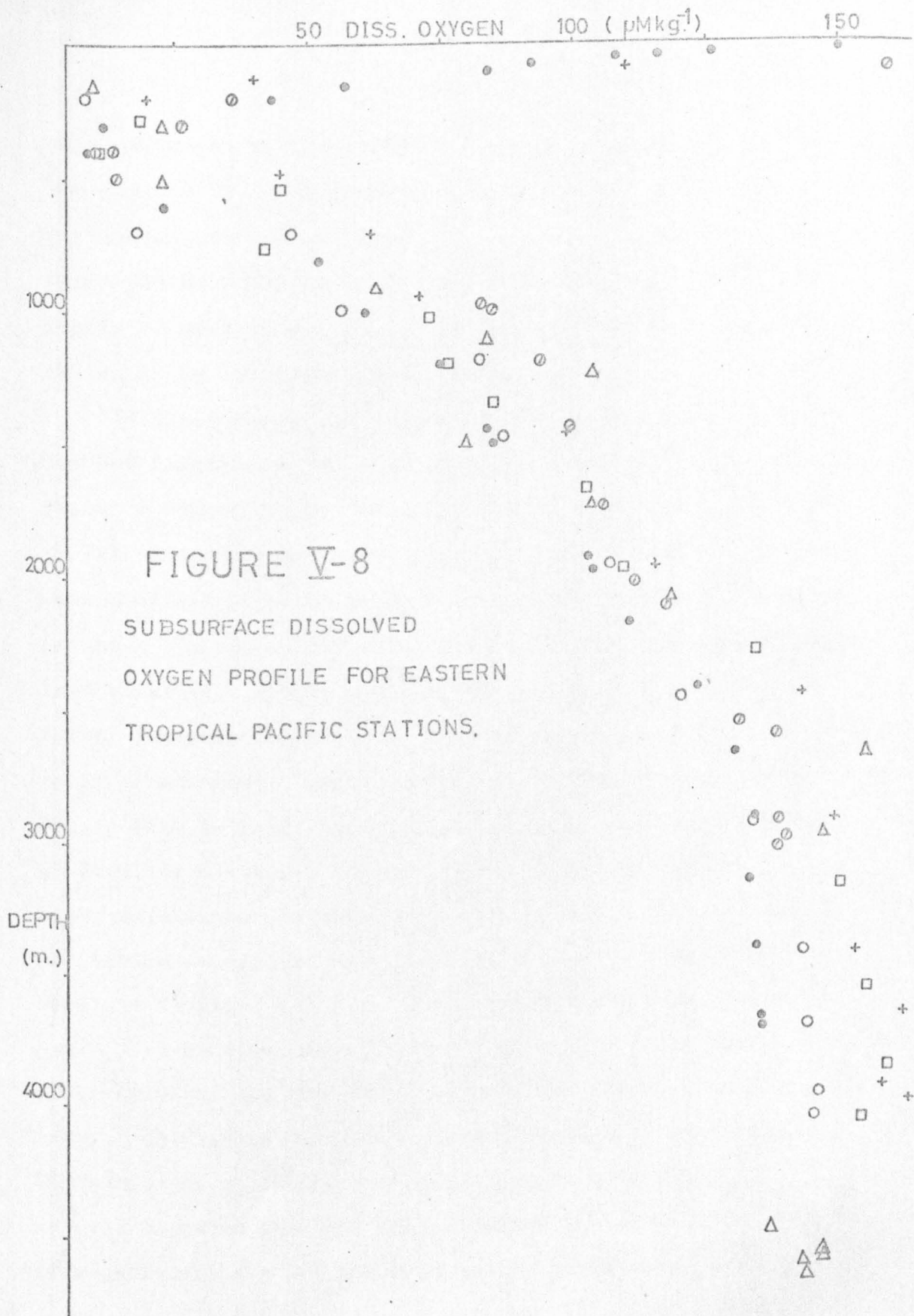
mediate waters in low latitudes. The erosion of the salinity minimum, and so of the intermediate core, as the equator is approached can be clearly seen in the profiles of Figure V-7 in which the salinity scale has been expanded by omission of the surface layers. The depth to which intermixing with Intermediate waters influences the Deep water salinity is at least 2,000m. There is also some indication of a mid-depth salinity maximum at around 2,500m. at Bartlett Station 3. The corresponding temperature plot (Figure V-6) shows relatively uniform thermal structure through the main thermocline, presumably maintained by dynamical considerations. Oxygen concentrations increase more or less linearly with depth, in contrast to the constant values found in the overlying subsurface water (Figure V-8). Muromtsev (1963) uses the 2°C isotherm to divide deep waters in the region of interest into South Pacific Upper Deep Water and underlying Lower Deep Water. The former, originating in northern tropical latitudes, shows low oxygen concentrations, the saturation increasing linearly with depth; the latter is formed in high southern latitudes and has a higher, rather constant oxygen concentration. The lower dissolved oxygen concentrations in the Lower Deep Water at the more northerly YALOC station (a 5% difference in saturation is evident from Figure V-5) is in agreement with Muromtsev's classification scheme. Neither Antarctic Bottom Water ($0.24^{\circ}\text{C} < T < 0.85^{\circ}\text{C}$) nor any of its mixtures with Pacific Bottom Water ($1.0^{\circ}\text{C} < T < 1.6^{\circ}\text{C}$) are seen this far north in the eastern basins. The water

34.5

34.6

34.7 SALINITY ‰





mass structure outlined above is nicely illustrated in a θ -S plot of the entire water column given in Figure V-9. In particular, the three component types beneath the subsurface water can be observed to mix along smooth curves, with the degree of mixing, and direction of intermediate flow, clearly indicated by inter-station differences.

To aid analysis of mixing processes in the abyssal waters, the θ -S diagram for the deep layers below about 1,000 m. is given in Figure V-10. The effect of latitudinal differences in intermediate water salinities is obvious, with the deepest waters at all stations being considerably more uniform; there are thus two linear θ -S loci connecting the intermediate and bottom waters. There is some evidence for a slight (0.1 to 0.2°C) increase in bottom water temperature at the lower latitude stations. One intriguing possibility suggested by Figure V-10 is that the apparent mid-depth salinity maximum at Bartlett Station 3 mentioned previously corresponds to a high salinity core centred at about 2,500 m. The intermediate and bottom waters are similar to those at the other two Bartlett Stations and fall on the general θ -S line, but below 1,470 m. and above about 3,900 m. the higher salinities observed carry the points beyond even the more northerly mixing locus. In Figures V-11 and 12 are plotted the values for Station(s) 3, and 5 and 7, for the depths under discussion. It will be noted that for these Figures the usual station key is superfluous and has not been used. Error bars corresponding to $(\pm 0.005)\text{‰}$ in salinity and $(\pm 0.02)\text{°C}$ in potential

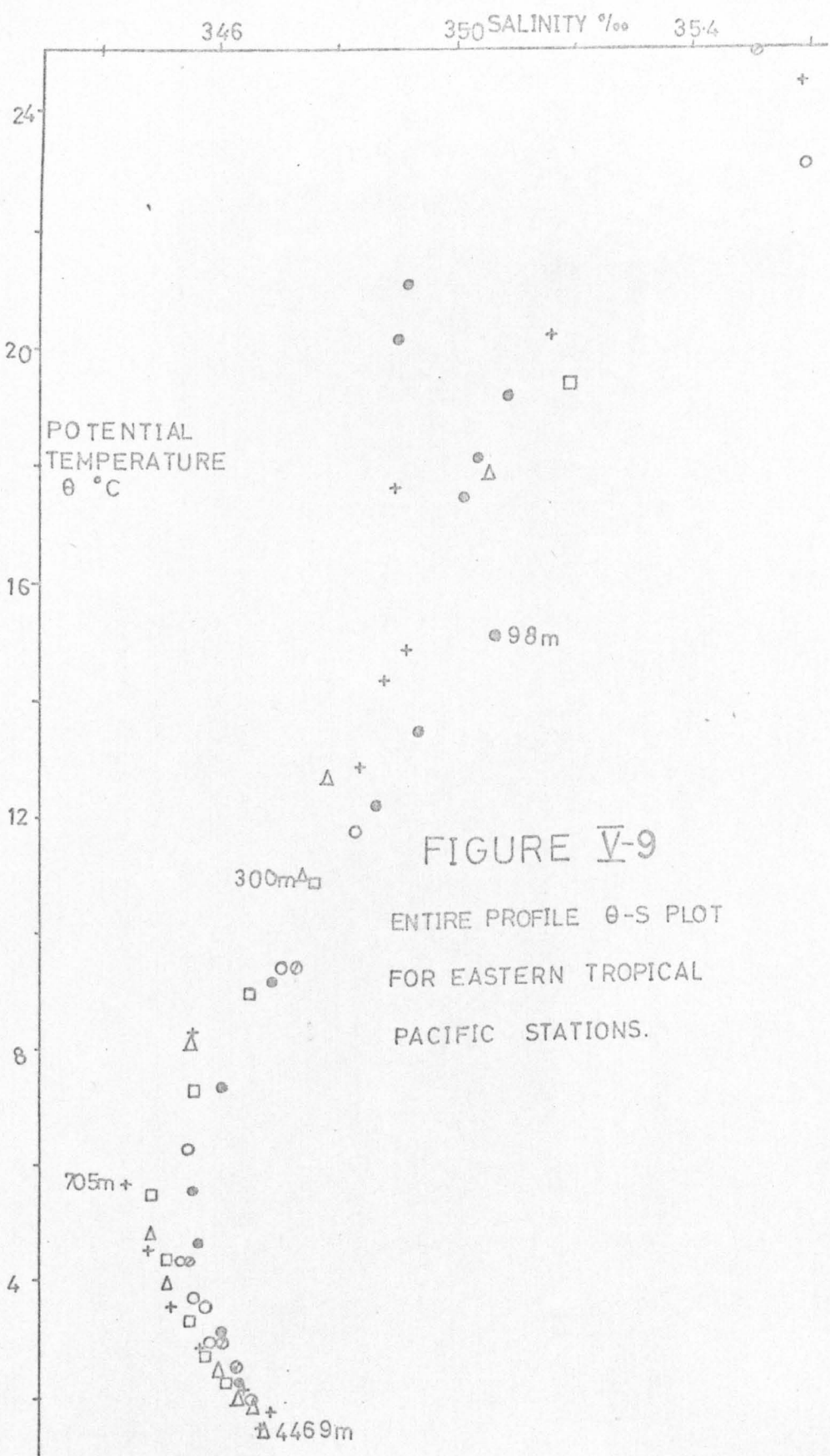
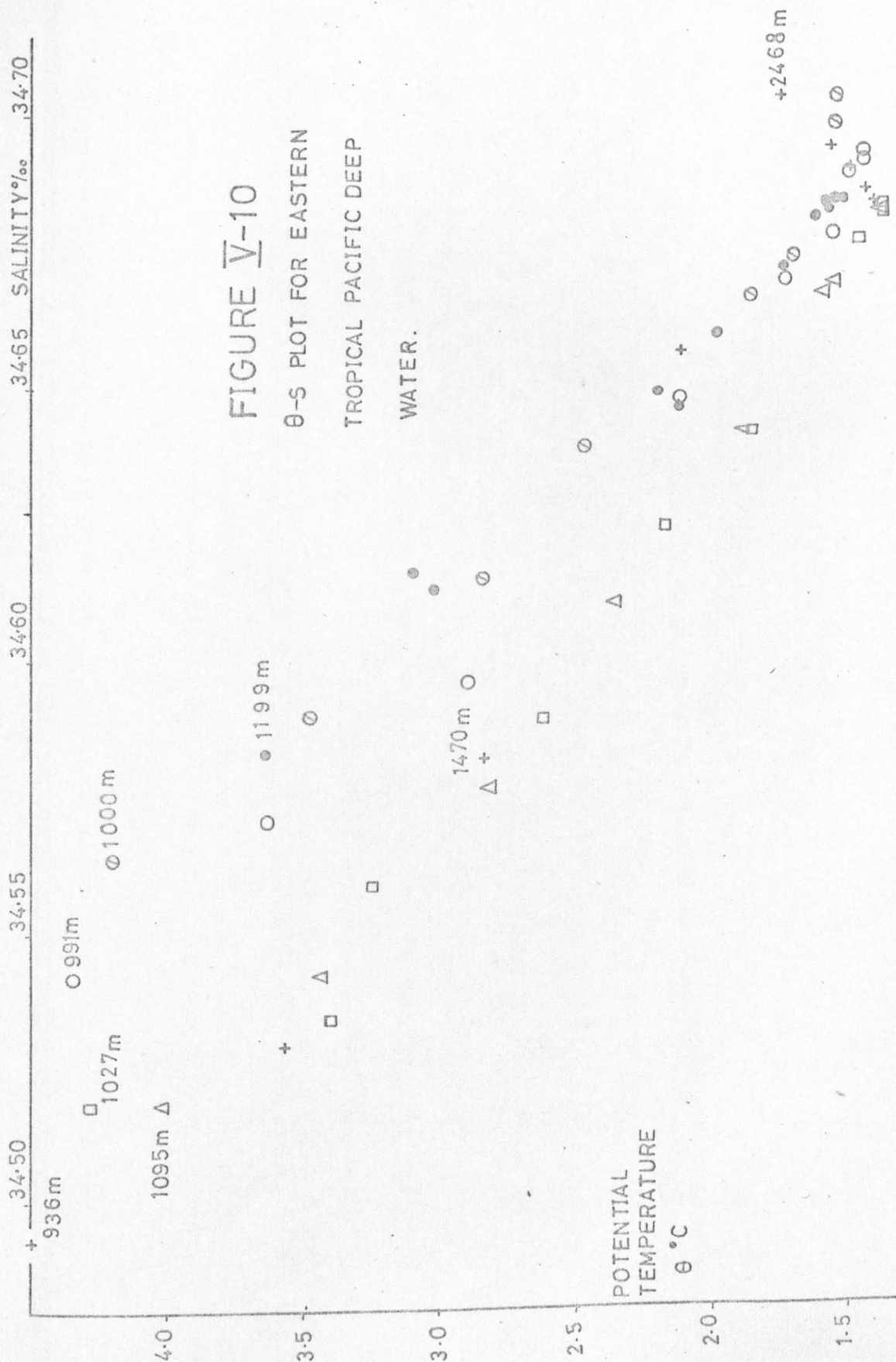
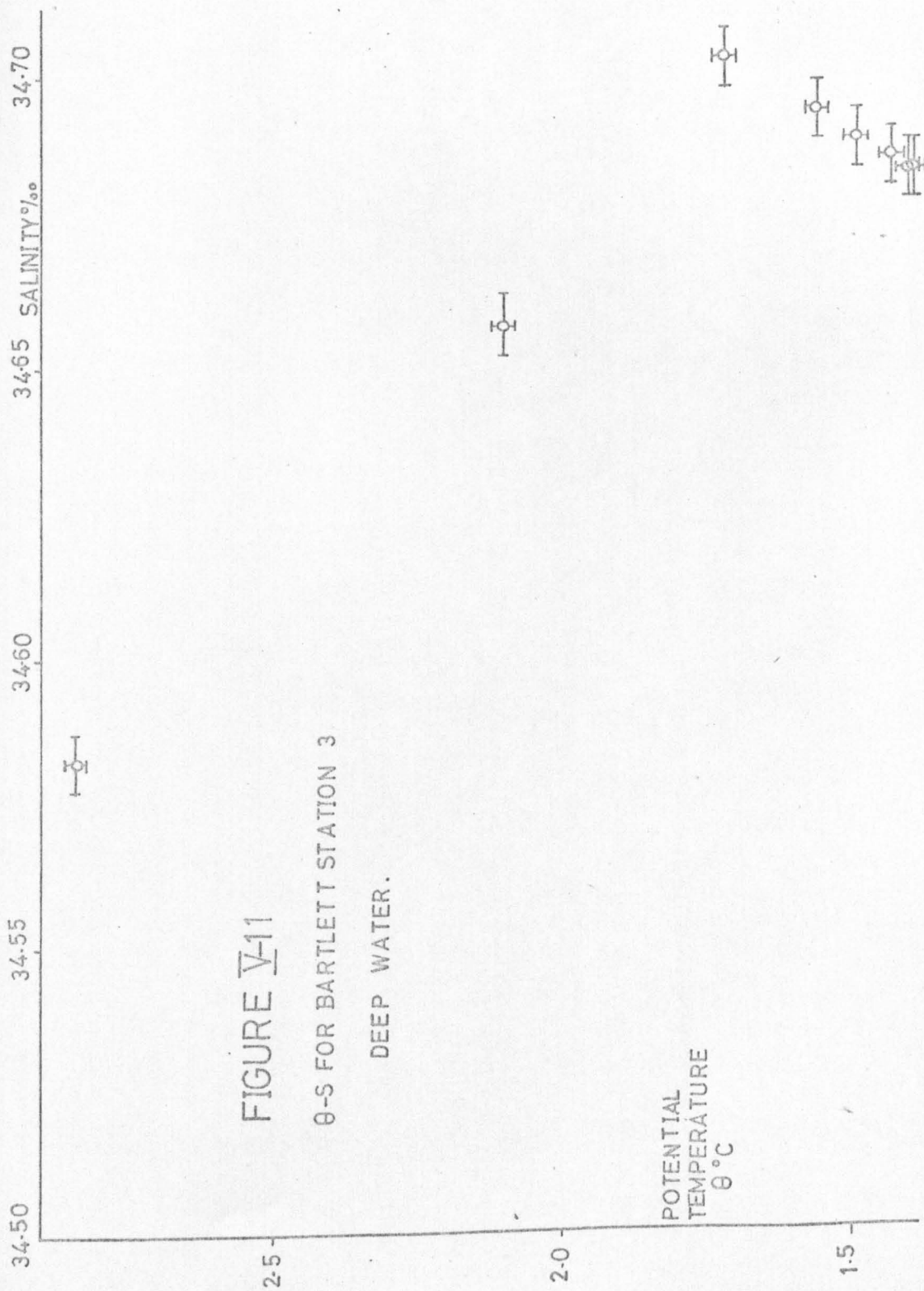
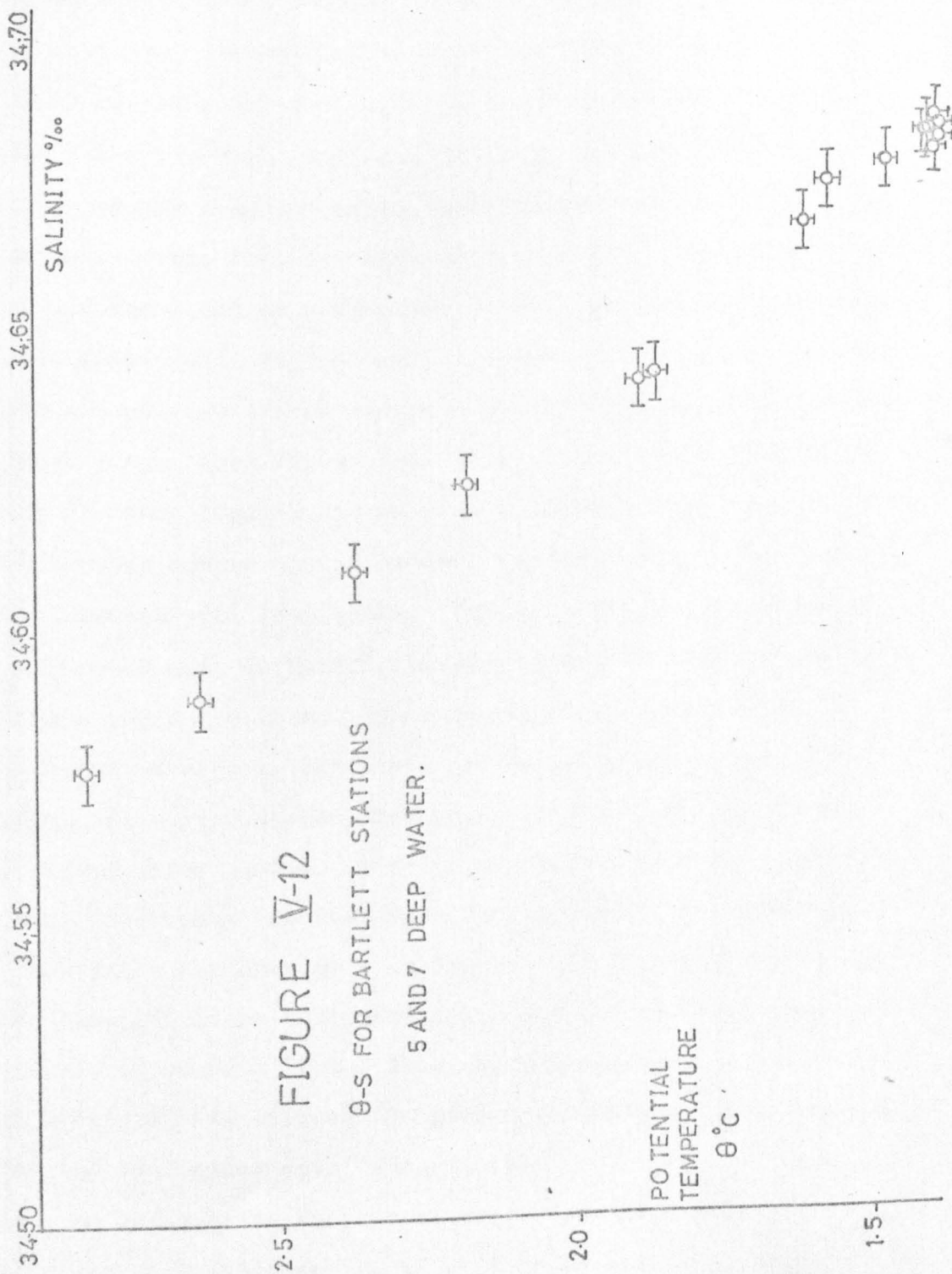


FIGURE V-9

ENTIRE PROFILE θ -S PLOT
FOR EASTERN TROPICAL
PACIFIC STATIONS.







temperature have been affixed to the points. That these are, if anything, overestimates can be concluded from Table V-6 which contains the data for 10 assays of bottom water for the three stations; the mean salinity was $(34.682 \pm 0.002) \text{‰}$ (10) and the mean potential temperature $(1.39 \pm 0.01) \text{°C}$. The salinity probe data for Station 3 were closely examined, but no maximum could be discerned; it will be recalled, however, that these data are, at best, accurate to $(\pm 0.01) \text{‰}$ so the absence of significant increase in the deep water is not too surprising. From Figure V-12 it is clear that all results for Stations 5 and 7 can be well represented by a single line, indicating simple mixing between two component types, viz. Intermediate and Deep Water. The Deep distinction referred to earlier was, as stated, based on the 2°C isotherm and on oxygen concentrations. The evidence for this from the Bartlett samples is presented in the potential temperature versus dissolved oxygen plot shown in Figure V-13. Station 7 values below 4,600m. close to the bottom have been omitted. There is obvious inter-station consistency. The observed (θ, S) pairs for Station 3 in Figure V-11 fall accurately on two straight lines intersecting at a point corresponding to a depth of about 2,500m. This sharp transition is indicative of little mixing between the middle salinity maximum layer and the two contiguous ones (Defant, 1961).

No explanation for the apparent intrusion of high salinity water at this depth and in this location has been found in the literature, so the possibility that it is a transitory effect

TABLE V-6

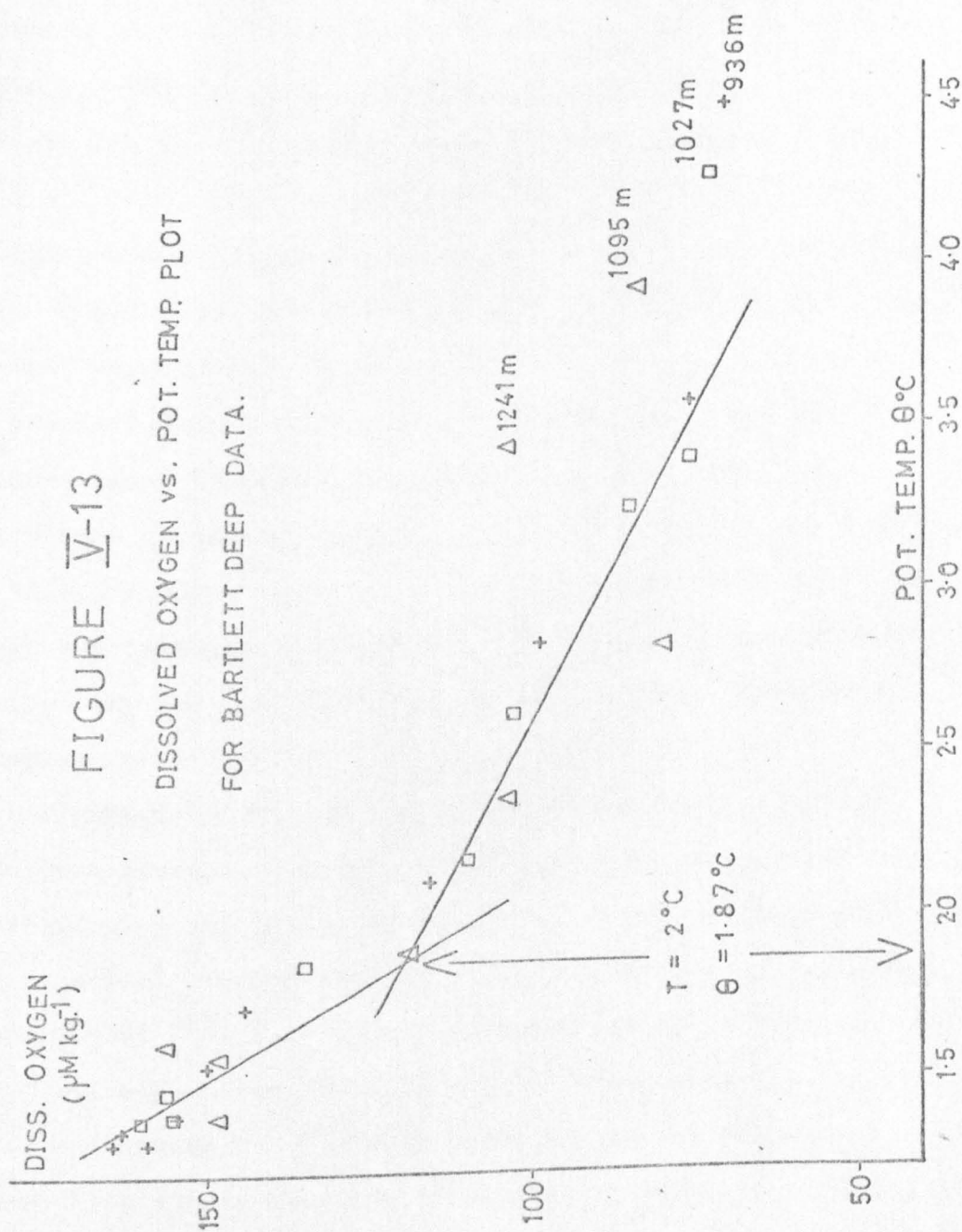
Bottom water hydrographic characteristics at Bartlett
Stations 3, 5 and 7.

SAMPLE	DEPTH (m.)	POTENTIAL TEMPERATURE °C	SALINITY ‰
3-1-11	3971	1.41	34.684
3-1-12	4031	1.40	34.684
5-2-D	3900	1.38	34.683
5-2-E	4100	1.39	34.681
7-1-7	4496	1.40	34.682
7-1-8	4594	1.39	34.682
7-1-10	4617	1.39	34.680
7-1-11	4631	1.39	34.679
7-1-12	4651	1.39	34.680
7-1-1	4669	1.39	34.684

Mean of 10 observations:

SALINITY : $(34.682 \pm 0.002) \text{‰}$

POT. TEMP: $(1.39 \pm 0.01) \text{°C}$



or the unfortunate result of a concatenation of coincidences cannot, at this stage, be ruled out, though neither seem likely. Careful attention was therefore paid to selection of samples for $\delta^{18}\text{O}$ assay. The results, relative to SMOW, for all three stations are given in Table V-7 and the $\delta^{18}\text{O}$ -depth profile is plotted in Figure V-14; no correction has been applied for the 0.4% by volume of poison added, as this proved negligible. It is immediately obvious that sample 3-1-6 at 2,468m. at Station 3 does not lie on the smooth convex curve traced by the rest of the data, so it will therefore be omitted from the general discussion and dealt with separately. Also, it is to be emphasised at the outset that the interpretation of the $\delta^{18}\text{O}$ results presented here is not the only one possible. The differences between samples are often less than or comparable with the experimental error, but the arguments advanced are thought the most plausible as exemplifying trends already seen in the hydrological data. To aid in the interpretation plots of potential temperature (θ) against $\delta^{18}\text{O}$, and of salinity (S) against $\delta^{18}\text{O}$ have also been drawn as Figures V-15 and 16, respectively. From 700m. to 1,700m. there is an approximately linear decrease in $\delta^{18}\text{O}$ with depth as the Intermediate and Upper Deep Waters mix; the $\delta^{18}\text{O}$ value at 496m. is actually slightly less than that at 705m. and it is readily apparent from Figures V-15 and 16 that this marks crossing the transition from Intermediate to Subsurface Water. Below 1,700m. the influence of the subantarctic core at 700m. is

TABLE V-7

Results of $\delta^{18}\text{O}$ of water relative to SMOW for
Bartlett samples.

SAMPLE	DEPTH (m.)	SALINITY ‰	$\delta^{18}\text{O}$ REL. TO SMOW
3-2-11	705	34.452	0.48
3-1-1	1203	34.529	0.28
3-1-4	1470	34.582	0.18
3-1-5	1981	34.657	0.15
3-1-6	2468	34.703	0.36
3-1-7	2949	34.667	0.22
3-1-8	3445	34.689	0.20
3-1-10	3692	34.686	0.30
3-1-11	3971	34.684	0.28
3-1-12	4031	34.684	0.23
5-1-6	774	34.493	0.38
5-2-A	1200	34.534	0.17
5-1-8	1348	34.559	0.14
5-1-10	1677	34.589	0.03
5-1-12	2315	34.642	0.12
5-2-C	3600	34.667	0.20
7-3-6	496	34.565	0.45
7-3-7	895	34.502	0.22
7-1-6	2995	34.669	0.14
7-2-E	4500?	34.809	0.82
7-1-1	4669	34.684	0.36

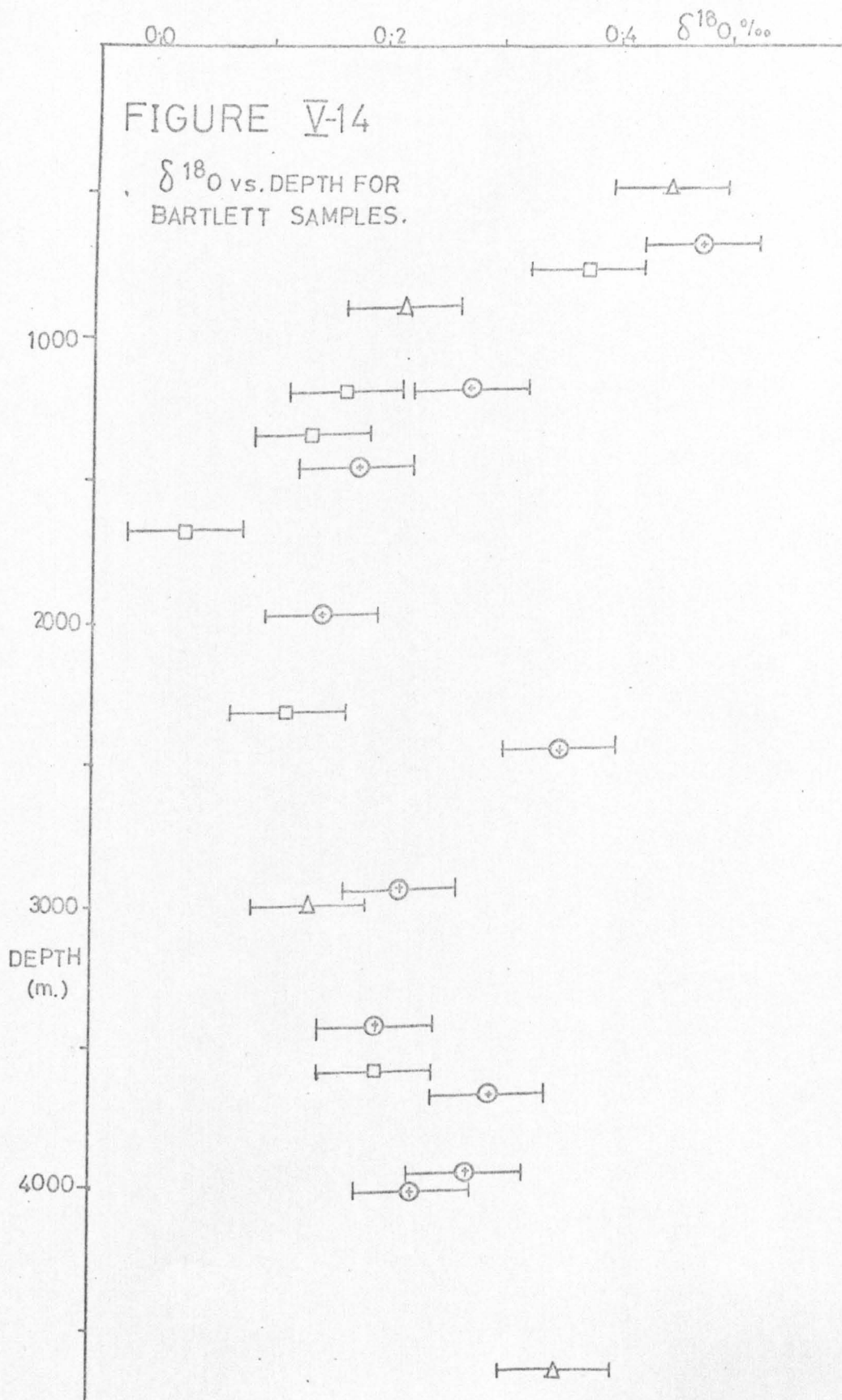


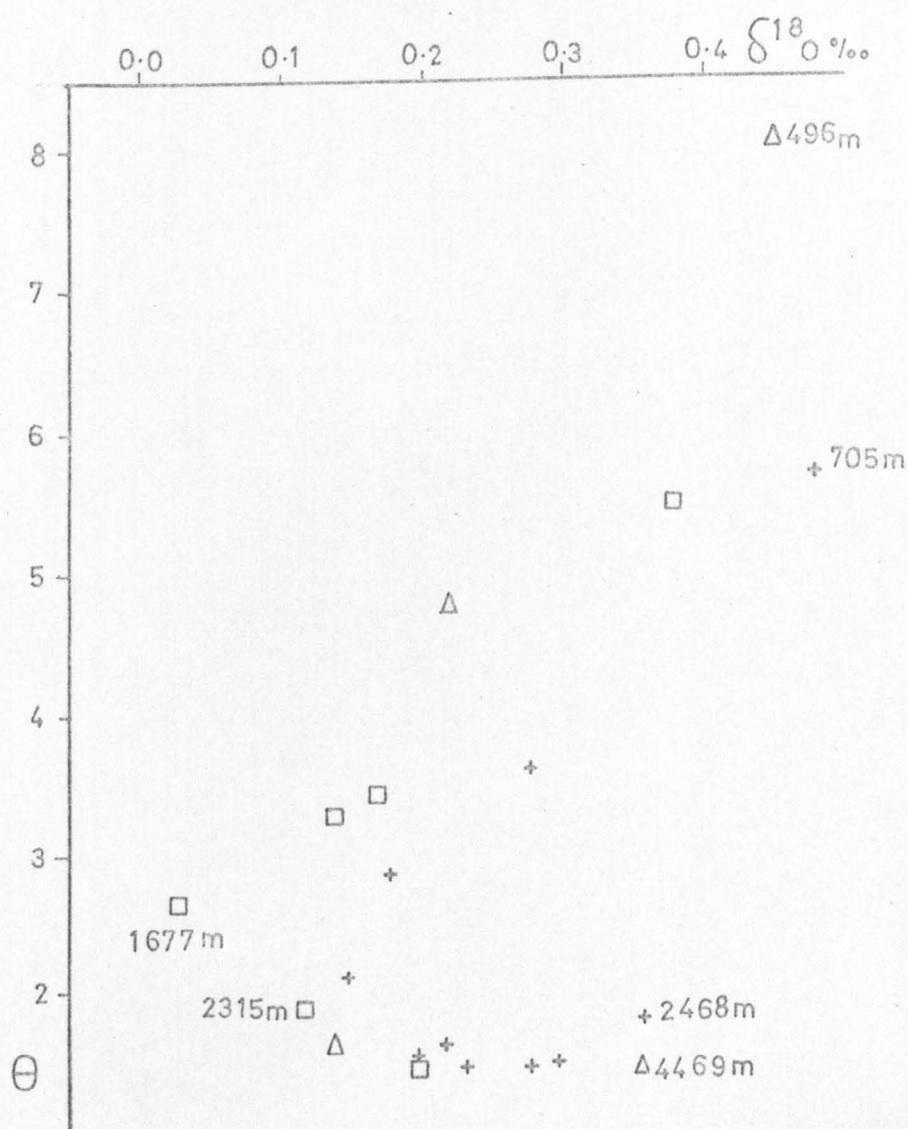
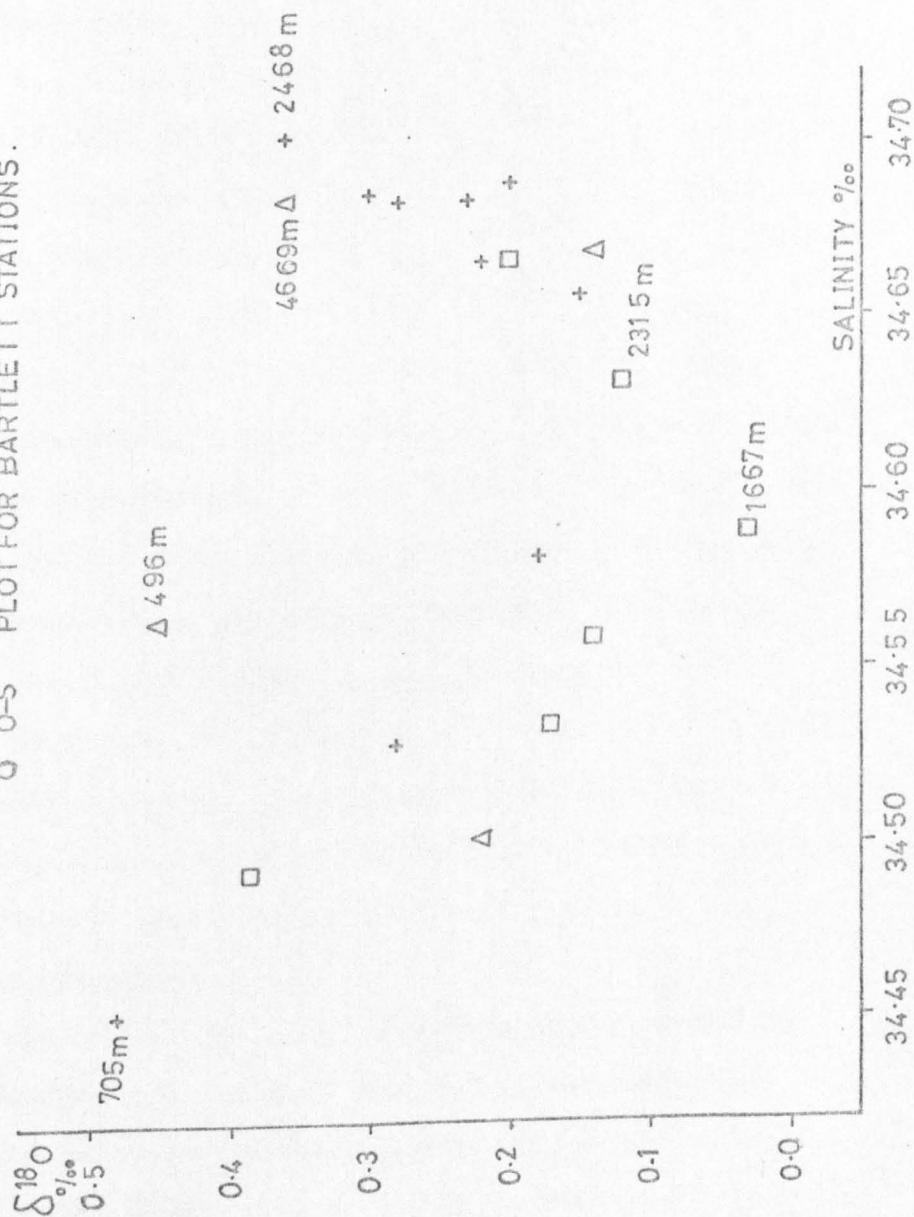
FIGURE V-15 $\delta^{18}\text{O}-\theta$ PLOT FOR BARTLETT STATIONS.

FIGURE V-16

 $\delta^{18}\text{O}$ O-S PLOT FOR BARTLETT STATIONS.

much less pronounced and the $\delta^{18}\text{O}$ values are much more constant, averaging $(0.22 \pm 0.08) \text{‰}$, as compared to a laboratory precision of $(\pm 0.05) \text{‰}$. Of these ten points, only the bottommost - over 700m. deeper than any other at 4,669m. - has $\delta^{18}\text{O}$ greater than 0.30‰ , the other nine averaging $(0.20 \pm 0.06) \text{‰}$ so the homogeneity of the deep water is well demonstrated. Apart from these, there remains the Station 3 sample 3-1-6 at 2,468m. with $\delta^{18}\text{O} = 0.36 \text{‰}$; this represents also the depth of the deep salinity maximum in Figure V-10. Since the $\delta^{18}\text{O}$ and salinity measurements were determined on different aliquots of seawater from the same Niskin (bottle 6, in fact), the origin of the anomalous values is unlikely to be found in an evaporational loss of water vapour from the storage vessels. The anomaly shows up well in Figures V-15 and V-16. An intrusion at approximately 2,500m. at Station 3 is thus again observed, but the consistent influence on the neighbouring samples seen in the Station 3 salinity profile (Figure V-11) is not apparent in the $\delta^{18}\text{O}$ data.

V-4 Chemical features

The concentrations of dissolved oxygen measured at Bartlett Stations 3, 5 and 7 have been given in Tables V-3, 4 and 5, and have been plotted against depth in Figure V-8. Also included in Tables V-3 to 5 are the oxygen saturation values calculated from the data of Green and Carritt (1967). In Tables V-8, 9, 10 are presented the complementary apparent oxygen utilisation (AOU) values calculated from the

TABLE V-8

Apparent oxygen utilisation (AOU $\mu\text{moles kg.}^{-1}$) at
Bartlett Station 3.

SAMPLE	DEPTH (m.)	AOU ($\mu\text{M kg.}^{-1}$)
3-2-1	7	8
3-2-4	32	20
3-2-5	62	54
3-2-6	91	140
3-2-7	120	213
3-2-8	195	241
3-2-10	476	243
3-2-11	705	243
3-2-12	936	244
3-1-1	1203	246
3-1-4	1470	227
3-1-5	1981	216
3-1-6	2468	191
3-1-7	2949	185
3-1-8	3445	182
3-1-10	3692	173
3-1-11	3971	177
3-1-12	4031	172

TABLE V-9

Apparent oxygen utilisation (AOU $\mu\text{moles kg.}^{-1}$) at
Bartlett Station 5.

SAMPLE	DEPTH (m.)	AOU ($\mu\text{M kg.}^{-1}$)
5-1-1	279	252
5-1-4	406	273
5-1-5	529	249
5-1-6	774	265
5-1-7	1027	242
5-2-A	1200	246
5-1-8	1348	239
5-1-10	1677	225
5-1-11	1988	221
5-1-12	2315	199
5-2-B	3200	184
5-2-C	3600	179
5-2-D	3900	180
5-2-E	4100	180

TABLE V-10

Apparent oxygen utilisation (AOU $\mu\text{moles kg.}^{-1}$) at
Bartlett Station 7.

SAMPLE	DEPTH (m.)	AOU ($\mu\text{M kg.}^{-1}$)
7-3-1	52	20
7-3-4	151	253
7-3-5	297	248
7-3-6	496	268
7-3-7	895	250
7-3-8	1095	235
7-3-10	1241	218
7-3-11	1491	246
7-3-12	1739	226
7-1-4	2088	214
7-1-5	2692	179
7-1-6	2995	187
7-1-7	4496	197
7-1-8	4594	187
7-1-10	4617	187
7-1-11	4631	191
7-1-12	4651	213
7-1-1	4669	190

same data source. Pytkowicz (1971) has demonstrated the usefulness of the concept of AOU, in that at any point in the ocean it represents the oxygen utilised since that water left the surface, even although both oxidative and mixing changes have been of importance. The depth profile of AOU has been plotted as Figure V-17. As expected, near surface saturation values in the 'mixed' layer are close to 100%, this being maintained by direct interchange with the atmosphere. The saturation falls to under 10% at the oxygen minimum around 200 - 400m. which is relatively uniform for all station profiles. This, of course, corresponds to a region of intense biological activity without direct atmospheric replenishment. Below the minimum, the oxygen concentration increases more or less monotonically with depth. The Bartlett profiles are in reasonable agreement with SCAN and YALOC down to 2,00m. but from 2 to 4 km. there is a distinct tendency for the Bartlett profiles to have higher oxygen concentrations. This is reflected also in higher bottom concentrations especially for Stations 3 and 5, although lower bottom values are found at the much deeper Station 7. SCAN and YALOC data also differ in the deep and bottom water, SCAN lying between Bartlett and YALOC in analogy to their latitudinal position. Some variation is seen in Station 7 values close to the bottom; this will not be elaborated here. The increase in oxygen concentration below the minimum is maintained by upward flux of deep water, rich in oxygen, formed at the surface in high

latitudes and sinking there. It will be observed from Figure V-17 that the AOU values are relatively constant below about 2,600m. (with the exception of some of the Station 7 bottom waters mentioned). This, however, must not be inferred as implying no consumption of oxygen in the deep. The problem of the abyssal metabolism is much more complex, as has been discussed in Chapter I.

The experimental technique for measurement of pH of seawater samples collected on the Bartlett cruise has been described in Chapter II. The expression for calculation of a pH value was given there (equation II-8-2) as:

$$\text{pH}_{\text{SW}} = \text{pH}_{\text{B1}} + (E_{\text{SW}} - E_{\text{B1}}) \frac{(\text{pH}_{\text{B1}} - \text{pH}_{\text{B2}})}{E_{\text{B1}} - E_{\text{B2}}}$$

where the symbols have their previously assigned meanings. It was further pointed out that two assumptions are implicit in the use of such a procedure, viz.

- (i) $(E_{\text{B1}} - E_{\text{B2}})$ remains the same, i.e. constant span,
- (ii) E_{B1} does not vary, i.e. no drift.

Taken in conjunction, these require both E_{B1} and E_{B2} to remain constant over the period of measurement. The validity of this was tested during Station 3 and Station 5 analyses by measurement of a 'running correction' standard buffer solution after every two seawater samples. At Station 3, this buffer solution (B6) was a commercial product, nominally pH 7.0 at 25°C. Ten assays during the course of the station measurements gave:

$$E_{\text{B6}} = (7.009 \pm 0.009)$$

corresponding to $\text{pH} (6.964 \pm 0.010)$ at 30°C . Numbering the analyses n consecutively from 1 to 33 in the order they were performed, those on B6 ranged from 3 to 30 with:

$$E_{B6}(n=30) - E_{B6}(n=3) = -0.007$$

The first two and last two measurements were on the high precision NBS buffers B1 and B2, used for standardisation and mentioned in Chapter II.

$$(\text{pH}_{B1} = 7.400 \text{ at } 30^\circ\text{C}; \text{pH}_{B2} = 6.853 \text{ at } 30^\circ\text{C}.)$$

The initial and final spans were:

$$E_{B1}(n=1) - E_{B2}(n=2) = 0.487$$

$$E_{B1}(n=33) - E_{B2}(n=32) = 0.492$$

with mean (0.490 ± 0.004) . The pH profile calculated from these values did not differ significantly from that calculated by making a running correction at each depth based on the appropriate B6 values. Sample 3-2-1 from 7m. was measured twice:

n	E_{SW}	pH_{SW}
23	8.055	8.132
26	8.056	8.133

At Station 5, in addition to the accurate NBS buffers, three buffer solutions based on a seawater ionic medium were used. These corresponded to the 10‰ (B3), 35‰ (B4) and 40‰ (B5) salinity solutions described by Hansson (1972) with:

$$\text{pH}_{B3} = 7.903$$

$$\text{pH}_{B4} = 7.925$$

$$\text{pH}_{B5} = 7.933$$

at 30°C (interpolated from Hansson (1972)). The middle one of these, B4, was used for checking the constancy of electrode response. The relevant data for the four primary standardising solutions is given in Table V-11. The 'running correction' solution, B4 Hansson's 35‰ buffer, was analysed 8 times and gave:

$$E_{B4} = (7.954 \pm 0.012)$$

corresponding to pH (7.935 ± 0.012) at 30°C on Hansson's seawater ionic medium scale. The correct value interpolated from Hansson's own data (Hansson, 1972) is 7.925, so both accuracy and precision to ±0.01pH unit have been demonstrated, and the validity of the assumptions reasonably well established.

Comparison of scales

There are obviously two choices of method of calculating pH_{SW} for Station 5:

- (i) calculation relative to NBS buffers B1 and B2,
- (ii) calculation relative to Hansson's seawater ionic medium buffers B3 and B5.

In addition to being defined on different scales, the pH_{SW} values so calculated may be different because electrode-solution interactions should be the same in case (ii) but not necessarily in case (i), since the NBS buffers have much lower ionic strength than seawater. Using the notation $pH_{X:Y}$ for the pH value of solution X on a scale defined by Y and abbreviating the Hansson seawater ionic medium scale to H, then it follows from (II-8-2) that:

TABLE V-11

Standardising buffers for Bartlett Station 5.

NBS BUFFER 1	<u>n</u>	<u>E</u>
B1:pH=7.400	1	7.400
	31	7.399
NBS BUFFER 2	2	6.872
B2:pH=6.853	30	6.862
Initial Span :	$E_{B1}(n=1) - E_{B2}(n=2) = 0.530$	
Final Span :	$E_{B1}(n=31) - E_{B2}(n=30) = 0.532$	
Mean :	(0.531 ± 0.001)	

HANSSON 40°/∞ BUFFER	<u>n</u>	<u>E</u>
B3:pH=7.933	3	7.952
	29	7.951
HANSSON 10°/∞ BUFFER	5	7.912
B5:pH=7.903	28	7.927
Initial Span :	$E_{B3}(n=3) - E_{B5}(n=5) = 0.040$	
Final Span :	$E_{B3}(n=29) - E_{B5}(n=28) = 0.024$	
Mean :	(0.032 ± 0.015)	

$$pH_{SW:NBS} = pH_{B1:NBS} + (E_{SW} - E_{B1}) \frac{(pH_{B1:NBS} - pH_{B2:NBS})}{E_{B1} - E_{B2}}$$

$$pH_{SW:H} = pH_{B3:H} + (E_{SW} - E_{B3}) \frac{(pH_{B3:H} - pH_{B5:H})}{(E_{B3} - E_{B5})}$$

$$\therefore pH_{SW:NBS} - pH_{SW:H} = (pH_{B1:NBS} - pH_{B3:H})$$

$$+E_{SW} \frac{(pH_{B1:NBS} - pH_{B2:NBS})}{(E_{B1} - E_{B2})} - \frac{(pH_{B3:H} - pH_{B5:H})}{(E_{B3} - E_{B5})}$$

$$-E_{B1} \frac{(pH_{B1:NBS} - pH_{B2:NBS})}{(E_{B1} - E_{B2})} + E_{B3} \frac{(pH_{B3:H} - pH_{B5:H})}{(E_{B3} - E_{B5})}$$

$$\therefore \Delta pH_{SW} = pH_{SW:NBS} - pH_{SW:H} = 0.032 E_{SW} - 0.218$$

For the overall profile mean, denoted by an overbar:

$$\overline{E_{SW}} = 7.539 \pm 0.145$$

$$\text{predicted } \overline{\Delta pH_{SW}} = 0.023 \pm 0.005$$

$$\text{measured } \overline{\Delta pH_{SW}} = 0.024 \pm 0.005$$

showing excellent agreement. Pushing this analysis to the limit, given that the estimated accuracy and precision is ± 0.01 pH unit, a comparison of ΔpH_{SW} values predicted from buffer measurements and those measured in practice is given in Table V-12, in which most of the results have been divided into groups with E-values spanning 0.1 unit. The trend of increasing ΔpH_{SW} with increasing E_{SW} is also observed, and the experimental and predicted values of ΔpH_{SW} agree well over the complete range. This implies that,

TABLE V-12

Comparison of pH-defining scales for Bartlett Station 5

E INTERVAL	7.40-7.49	7.50-7.59	7.60-7.69	8.006
MEASUREMENT FREQUENCY	7	5	2	1
MEASUREMENT MEAN	7.449±0.032	7.543±0.018	7.613±0.004	8.006
MEASURED $\Delta\text{pH}_{\text{SW}}$	0.021±0.001	0.024±0.001	0.026±0.00	0.038
THEORETICAL MEDIAN	7.445	7.545	7.645	8.006
CALCULATED $\Delta\text{pH}_{\text{SW}}$	0.020	0.023	0.027	0.038

within this set of measurements, differences in electrode-solution interactions (e.g. as a result of different asymmetry potentials) have not been an important factor. Naturally, the pH_{SW} values calculated from different buffer standardisations do not agree absolutely, but the difference can be accounted for in a systematic manner and there is no evidence of differences in medium ionic strength leading to errors, at least within the accuracy attained and over the range encountered.

The pH values of the seawater samples collected at Bartlett Stations 3,5 and 7 are given in Tables V-13, 14 and 15. The calculations have been based on standardisation by the NBS buffers and refer to a temperature of 30°C and to atmospheric pressure. Included in Table V-13 under $\text{pH}(\text{B6})$ are the pH values calculated by making a 'running correction' based on the variation of E_{B6} during the measurements. The pH values at Station 5 based on the Hansson seawater ionic medium scale are also given in Table V-14. The pH profile together with that at the YALOC Station 70 is shown in Figure V-18. Surface water values agree well with those of Culberson and Pytkowicz (1970) being around 8.10; it is to be noted that this agreement is absolute. The intermediate water minimum is more pronounced and is deeper for the more southerly Bartlett stations, with some scatter among the station data evident. In the depth range below 2,000m. down to almost 3,000m. there is good agreement, but some Bartlett samples from 3,000-4,000m. differ from the YALOC data by almost 0.1 pH

TABLE V-13

pH measurements at Bartlett Station 3.

SAMPLE	DEPTH (m.)	pH _{SW:NBS} at 30°C	pH corrected <u>via</u> B6	pH in situ
3-2-1	7	{8.133 8.132	{8.136 8.144	{8.194 8.193
3-2-4	32	8.122	8.135	8.213
3-2-5	62	8.050	8.055	8.188
3-2-6	91	7.790	7.802	7.959
3-2-7	120	7.253	7.531	7.697
3-2-8	195	7.467	7.468	7.658
3-2-10	476	7.425	7.411	7.646
3-2-11	705	7.458	7.442	7.697
3-2-12	936	7.436	7.422	7.679
3-1-1	1203	7.463	7.455	7.697
3-1-4	1470	7.543	7.531	7.782
3-1-5	1981	7.517	7.510	7.742
3-1-6	2468	7.583	7.578	7.792
3-1-7	2949	7.547	7.553	7.734
3-1-8	3445	7.610	7.619	7.779
3-1-10	3692	7.589	7.600	7.751
3-1-11	3971	7.619	7.626	7.770
3-1-12	4031	7.623	7.621	7.773

TABLE V-14

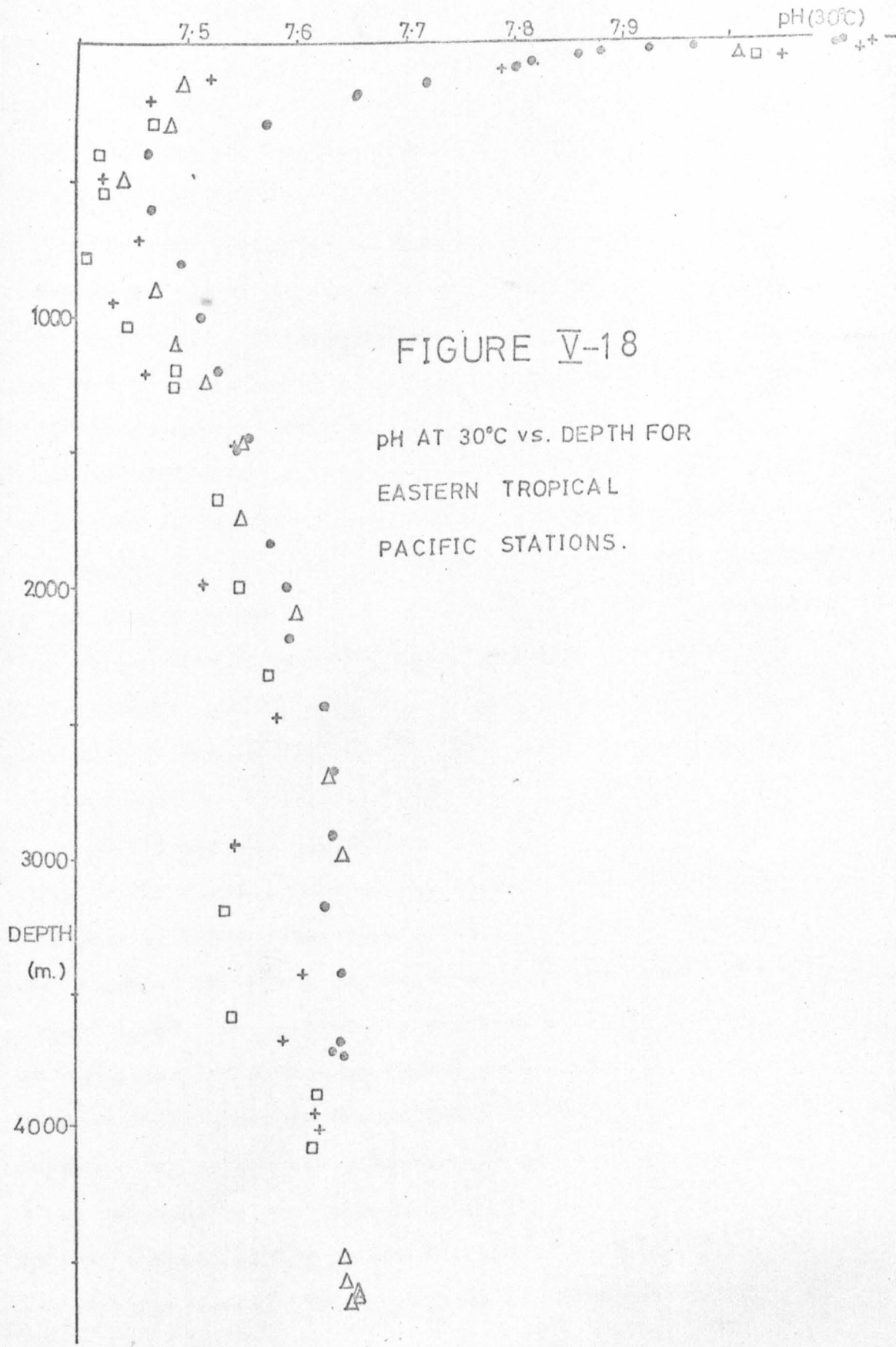
pH measurements at Bartlett Station 5.

SAMPLE	DEPTH (m.)	pH _{SW:H}	pH _{SW:NBS} at 30°C	pH in situ
5-3-A	50	7.987	8.025	8.144
5-1-1	279	7.488	7.469	7.671
5-1-4	406	7.401	7.421	7.639
5-1-5	529	7.407	7.427	7.656
5-1-6	774	7.391	7.410	7.650
5-1-7	1027	7.427	7.447	7.689
5-2-A	1200	7.468	7.490	7.732
5-1-8	1348	7.469	7.491	7.731
5-1-10	1677	7.507	7.530	7.762
5-1-11	1988	7.527	7.551	7.751
5-1-12	2315	7.553	7.578	7.785
5-2-B	3200	7.512	7.535	7.698
5-2-C	3600	7.520	7.543	7.706
5-2-D	3900	7.596	7.622	7.776
5-2-E	4100	7.591	7.617	7.759

TABLE V-15

pH measurements at Bartlett Station 7.

SAMPLE	DEPTH (m.)	pH _{SW:NBS} at 30°C	pH in situ
7-3-1	52	8.007	8.143
7-3-4	151	7.496	7.682
7-3-5	297	7.484	7.683
7-3-6	496	7.443	7.666
7-3-7	895	7.472	7.714
7-3-8	1095	7.490	7.733
7-3-10	1241	7.519	7.761
7-3-11	1491	7.546	7.784
7-3-12	1739	7.551	7.784
7-1-4	2088	7.608	7.826
7-1-5	2692	7.637	7.841
7-1-6	2995	7.645	7.821
7-1-7	4496	7.647	7.779
7-1-8	4594	7.651	7.778
7-1-10	4617	7.652	7.778
7-1-11	4631	7.660	7.786
7-1-12	4651	7.661	7.786
7-1-1	4669	7.658	7.782
7-2-A	2800?	7.510	
7-2-B	3600?	7.437	
7-2-C	4000?	7.439	
7-2-D	4300?	7.478	
7-2-E	4500?	7.502	



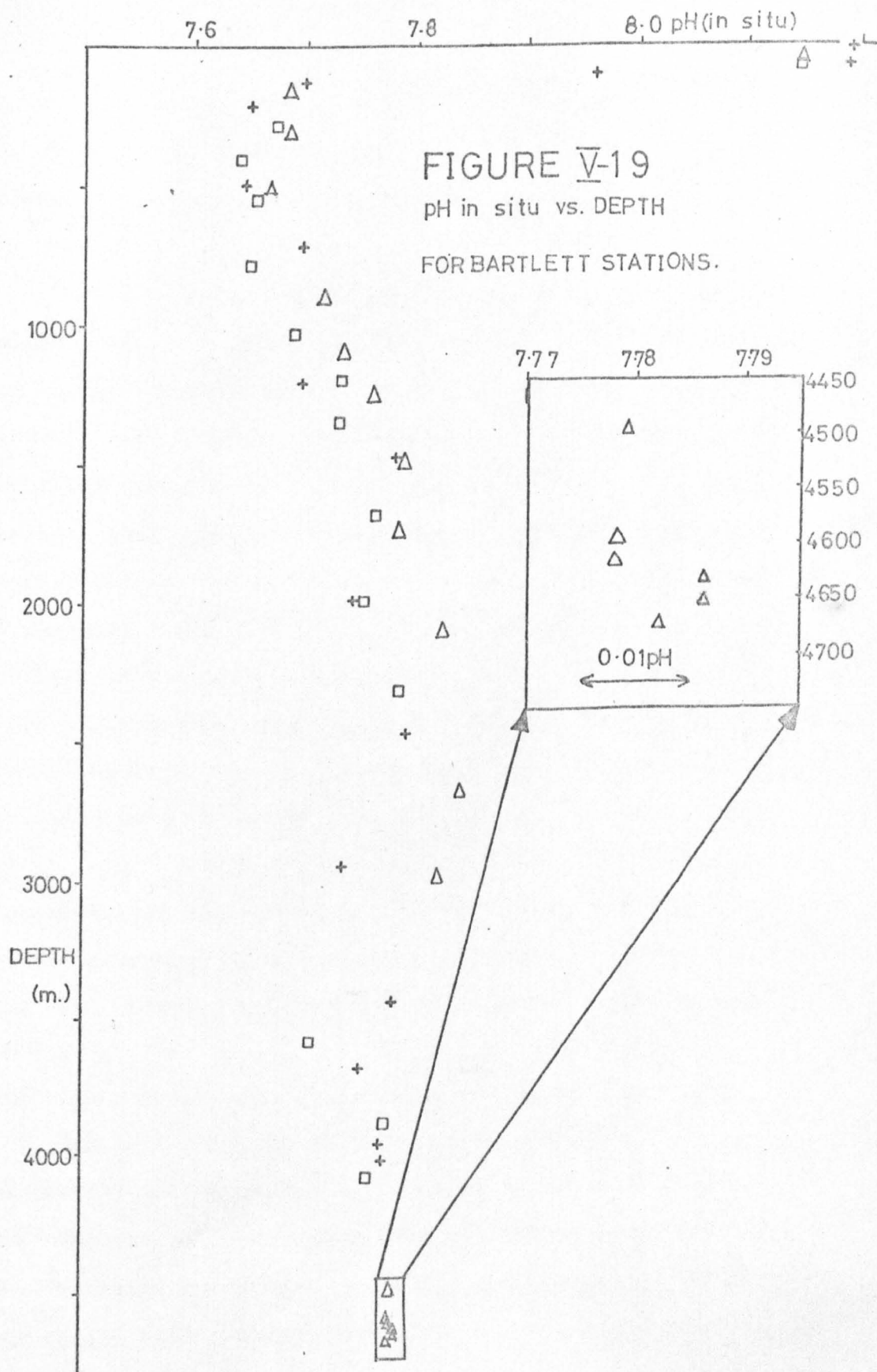
unit. The bottom waters are in reasonable agreement for all four stations, the YALOC numbers lying between those of Station 7 and Stations 3 and 5.

The same trends would have been expected, but absolute agreement - being dependent on standardisation - could easily have been out. It would appear that it is not, the surface and bottom waters being in good agreement. The intermediate water systematic difference is probably the result of chemical differences, possibly influenced by the biological processes at the various locations. For example, Gundersen and Mountain (1973) have claimed that a significant fraction of pH change is due to the activities of nitrifying bacteria.

Since pH is sensitive to changes both in temperature and pressure, the in situ values were calculated and are included in Tables V-13 to 15. The temperature correction applied was:

$$\text{pH}(t') = \text{pH}(t) + 0.0111(t-t')$$

This is the correct form of the equation given by Riley and Chester (1971) (the form given on p.124 of their book has t and t' the wrong way round on the right hand side second term). To account for pressure effects, the tables of Culberson and Pytkowicz (1968) were used. The in situ pH profile is shown in Figure V-19; it can be seen that bottom water values are almost 0.125 pH unit higher than the 30°C, atmospheric pressure values. The six samples at Station 7 close to the bottom are shown in Figure V-19 in the expanded inset. The average is (7.782 ± 0.004) (1σ) so



the results agree to well within the estimated precision. The four bottom water samples at Stations 3 and 5, around 4,000m. in depth, are also very consistent with mean (7.770 ± 0.007).

The ΣCO_2 and its $\delta^{13}\text{C}$ and $\delta^{18}\text{O}$ values are presented in Tables V-16, 17 and 18; the ΣCO_2 values have been corrected for the addition of poison. In Figure V-20 are plotted the Bartlett ΣCO_2 profiles together with those of SCAN and YALOC. The first point which must be made is that the data from the Bartlett profiles show considerably more scatter than would be expected on the basis of the proven accuracy and precision of the measurement technique. It is conceivable - though unlikely in view of the results of Chapter IV - that the poisoning procedure was inadequate; a more likely explanation lies in unsatisfactory storage conditions because of occasional prolonged contact of the seawater with the inserts of the bottle caps. The possibility that experimental methods were responsible is discounted for the following reasons:

- (i) the accuracy and precision of extraction, volume measurement and isotope ratio assay as established in Chapters II and III.
- (ii) each volume measurement on an extracted ΣCO_2 sample was performed in duplicate, on independent manometer systems (see Chapter II) and agreement well within 1% ^a always found.
- (iii) the precision of extraction and volume measurement has been demonstrated in Chapter IV for samples collected on the same cruise but stored in bottles with ground glass necks and stoppers.

TABLE V-16

ΣCO_2 (mM kg.⁻¹) and its stable isotope ratios relative to PDB at Bartlett Station 3.

SAMPLE	DEPTH (m.)	ΣCO_2 ⁻¹ (mM kg.)	$\delta^{13}\text{C}$ (PDB)	$\delta^{18}\text{O}$ (PDB)
3-2-1	7	2.034	-	-
3-2-4	32	2.040	-1.06	0.46
3-2-5	62	2.126	-0.21	-0.84
3-2-6	91	2.047	-2.50?	-1.06
3-2-7	120	2.200	0.11	2.81
3-2-8	195	2.269	-0.37	2.64
3-2-10	476	2.212	-0.51	2.08
3-2-11	705	2.283	-0.88	-0.29
3-2-12	936	2.197	-0.53	1.01
3-1-1	1203	2.310	-0.90	0.85
3-1-4	1470	2.232	-1.24	0.66
3-1-5	1981	2.315	-0.88	1.49
3-1-6	2468	2.235	-0.96	0.07
3-1-7	2949	2.272	-0.81	1.80
3-1-8	3445	2.284	-0.20	2.05
3-1-10	3692	2.279	-0.59	1.14
3-1-11	3971	2.294	0.39	2.24
3-1-12	4031	2.284	0.11	2.34

? indicates a questioned value

TABLE V-17

ΣCO_2 (mM kg.^{-1}) and its stable isotope ratios relative to PDB at Bartlett Station 5.

SAMPLE	DEPTH (m.)	ΣCO_2 (mM kg.^{-1})	$\delta^{13}\text{C}$ (PDB)	$\delta^{18}\text{O}$ (PDB)
5-3-A	50	2.092	0.29?	2.37
5-1-1	279	2.088	-0.78	1.41
5-1-4	406	2.112	0.15	1.86
5-1-5	529	2.078	-0.59	2.30
5-1-6	774	2.126	0.21	2.11
5-1-7	1027	1.960	0.08	1.83
5-2-A	1200	2.245	-1.09	1.41
5-1-8	1348	2.167	-0.55	0.69
5-1-10	1677	2.160	-0.73	1.13
5-1-11	1988	2.161	-0.41	1.60
5-1-12	2315	2.181	0.19	1.89
5-2-B	3200	2.311	-0.33	1.67
5-2-C	3600	2.251	-0.21	1.90
5-2-D	3900	2.234	-	-
5-2-E	4100	2.176	-2.91?	-0.05

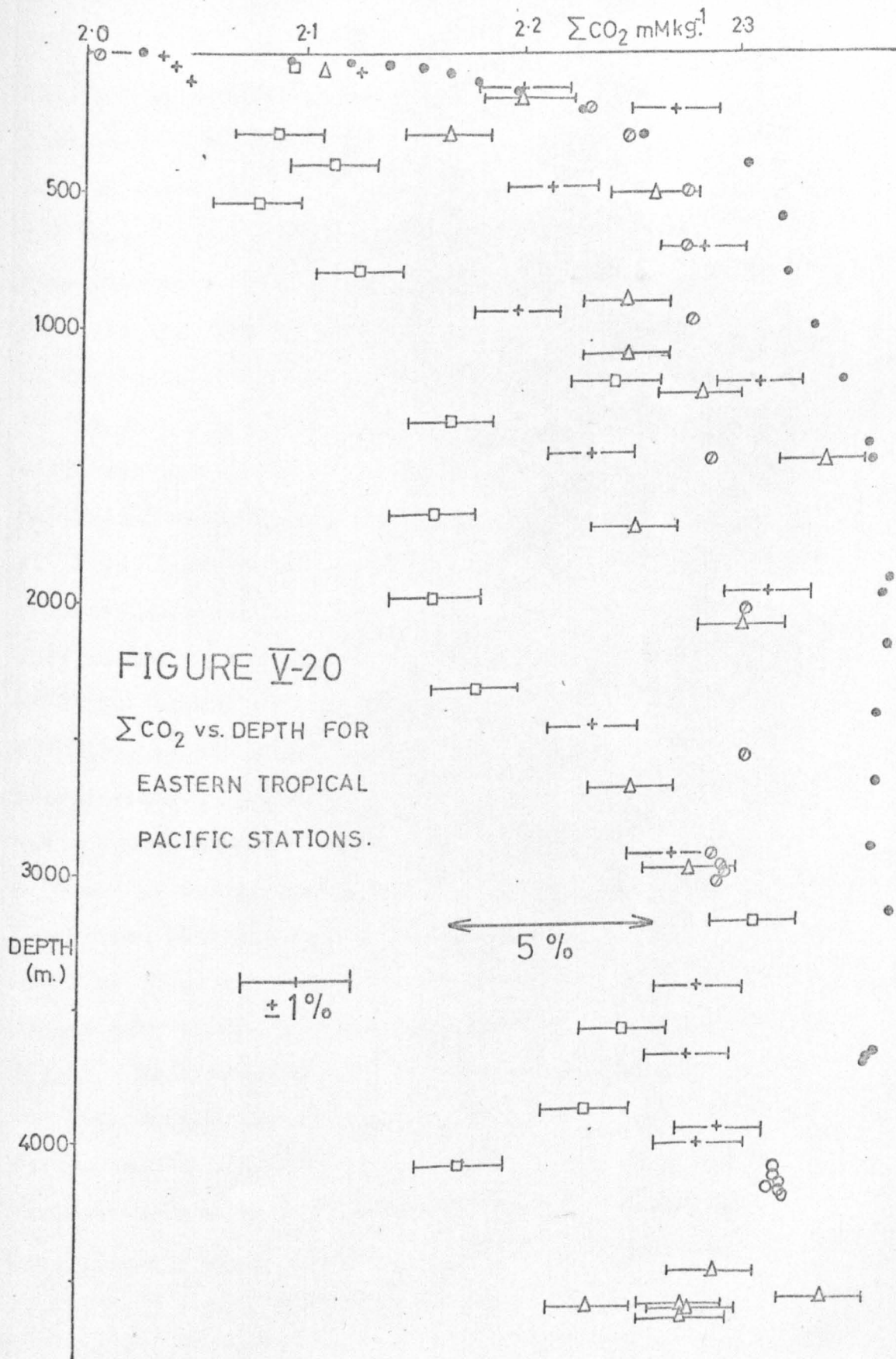
? indicates a questioned value

TABLE V-18

ΣCO_2 (mM kg.⁻¹) and its stable isotope ratios relative to PDB at Bartlett Station 7.

SAMPLE	DEPTH (m.)	ΣCO_2 (mM kg. ⁻¹)	$\delta^{13}\text{C}$ (PDB)	$\delta^{18}\text{O}$ (PDB)
7-3-1	52	2.105	-0.05	0.01
7-3-4	151	2.198	-1.58	0.93
7-3-5	297	2.166	-	-
7-3-6	496	2.259	-0.27	1.67
7-3-7	895	2.248	0.40	0.64
7-3-8	1095	2.247	-0.08	1.71
7-3-10	1241	2.282	-0.37	2.34
7-3-11	1491	2.339	-0.95	0.89
7-3-12	1739	2.252	-1.89	-1.56
7-1-4	2088	.2303	3.14?	2.47
7-1-5	2692	2.252	0.32	2.47
7-1-6	2995	2.281	0.48	2.51
7-1-7	4496	2.293	1.29	3.15
7-1-8	4594	2.342	-0.26	2.10
7-1-10	4617	2.234	0.32	2.54
7-1-11	4631	2.277	0.50	2.78
7-1-12	4651	2.281	0.22	2.62
7-1-1	4669	2.277	0.65	2.43
7-2-A	2800?	2.034	2.07	1.48
7-2-E	4500?	2.258	-0.85	2.88

? indicates a questioned value



(iv) the apparently systematic nature of some of the excursions from smooth profiles, e.g. the deep water maximum seen at Station 5.

The second notable feature is the consistently greater ΣCO_2 concentrations found at YALOC as compared to SCAN and Bartlett stations below the upper mixed layer; (within 200m. of the surface, the ΣCO_2 gradient with depth is so great as to disguise any interstation differences). This will be discussed later. It would also appear from Figure V-20 that Bartlett Station 5 should be discussed separately from 3 and 7. Below 3,000m. the data from the latter two stations are reasonably constant at around 2.285mM.kg.^{-1} . Values of 2.277mM.kg.^{-1} at 3120m. at $5^\circ 1'S$, $114^\circ 4'W$ and 2.310mM.kg.^{-1} at 2953m. at $10^\circ 1'S$, $90^\circ 12'W$ have been reported by Kroopnick (1974(b)) as being paradigmatic of this region. Bottom measurements at SCANX 38 are in good agreement (2.294mM.kg.^{-1}) and slightly higher (2.321mM.kg.^{-1}) at SCANX 30. Above 3,000m. the Bartlett Station 3 and 7 data are, on the whole, lower than SCAN results, the mean difference being of the order of 1% or so; it will be recalled that the corresponding oxygen data at the more southerly Bartlett stations were higher. Unfortunately, the scatter among these data masks the ΣCO_2 maximum which is seen in the other profiles around 2,000m. and is expected as the counterpart of the oxygen minimum layer seen in Figure V-8. For this reason, an advection-diffusion model approach such as that of Craig (1970) is not feasible for the Bartlett samples.

It was remarked earlier that the results for YALOC 70 taken from Culberson and Pytkowicz (1970) show ΣCO_2 concentrations greater in all cases than those from SCAN and Bartlett stations. While it is always possible - especially in view of locality differences and the lower oxygen concentrations observed in Figure V-8 at YALOC 70 - that this represents a real difference in the chemical composition of the water columns, an alternative hypothesis will be outlined below. It is to be noted, however, that Kroopnick (1974(a)) accepted the data of Culberson and Pytkowicz at face value and used them in his calculations. The ΣCO_2 values reported by Culberson and Pytkowicz (1970) were not measured directly; rather, pH and alkalinity were measured and ΣCO_2 calculated from these results using Lyman's (1956) apparent dissociation constants for carbonic acid in seawater. On the Geosecs intercalibration cruise (Takahashi et al., 1970), direct intercalibration among the various workers measuring ΣCO_2 levels was accomplished, within the designated accuracies, by measurement of ΣCO_2 in aliquots of solutions specially prepared by R.F. Weiss and J.M. Edmond. The measured ΣCO_2 profiles at the Geosecs station did not exactly agree, however, Edmond's titrimetrically determined values being systematically 1.5% greater than those found by Weiss using a gas chromatographic technique. This difference was attributed to the chloroform poisoning used by Edmond prior to 24 hour storage of his samples. Thus Weiss' values were taken as the best estimates of directly assayed ΣCO_2 . On the

same cruise, Culberson measured pH and alkalinity and, as at the YALOC stations, calculated ΣCO_2 from these using the data of Lyman (1956). A systematic difference of 3% was found between the results of Weiss and those of Culberson, the latter being higher; it was suggested (Takahashi et al., 1970) that this may have been caused by a $(30 \pm 10)\%$ error in the adopted value of the second apparent dissociation constant (K_2') of carbonic acid, and the carbonate chemistry data obtained at the station were claimed to be more consistent with the K_2' data of Buch (1938, 1951) than with those of Lyman (1956). However, recent redeterminations of K_2' by Hansson (1972) and by Mehrbach et al. (1973) are in reasonable agreement with each other and with the values given by Lyman (1956). The results of Mehrbach et al. are 3.4% lower than those of Hansson, are 3.2% lower than Lyman's for temperatures of 25°C and below, and are 13.4% lower at 35°C than the Lyman values. The disagreement with the data of Buch is 26%. Furthermore, Hansson (1972) has shown that the ionization constant of water in seawater is four times that in NaCl, so that the value assumed by Buch (1938) is incorrect. Adopting Hansson's figure for this, the K_2' value of Mehrbach et al. (1973) and the corrected value of Buch at 35‰ salinity and 20°C agree to within 4.5%.

The directly measured and the calculated ΣCO_2 profiles of Figure V-20 are systematically different by about 3%, the calculated values being greater. Thus the discrepancy reported after the Geosecs intercalibration (Takahashi et al.,

1970) is corroborated, but the purported cause discredited. The data cannot be reconciled at the present time, but it is likely that a complete carbonate chemistry study will be required to resolve the matter. The results of the project recently carried out by Prof. D. Dyrssen (D. Jagner, personal communication) aboard the Russian vessel Dmitri Mendelejev using the new Hansson system of buffers and constants (Dyrssen and Sillen, 1967; Hansson, 1972) will be very interesting in this respect.

The results of Bartlett Station 5 provide an additional problem being - with a few exceptions - consistently lower than the other Bartlett data. All collection, poisoning and extraction procedures were supposedly identical with those at the other two stations, and it is difficult to conceive of the displacement as due to real differences in the chemical structure of the water columns. No plausible explanation has been found, but it is perhaps not without significance that the Station 5 data are approximately 5% lower than those of Station 3 and Station 7, and Takahashi et al. (1970) have reported that ΣCO_2 values determined by Wong on stored unpoisoned samples were altered by 5% on average, compared to those analysed immediately, although certainly in this case the ΣCO_2 increased.

Given that ΣCO_2 levels altered during storage, it is to be anticipated that the regularities of the $\delta^{13}\text{C}$ profile would have been totally masked. That this was so is illustrated in Figure V-21 in which the Bartlett data are

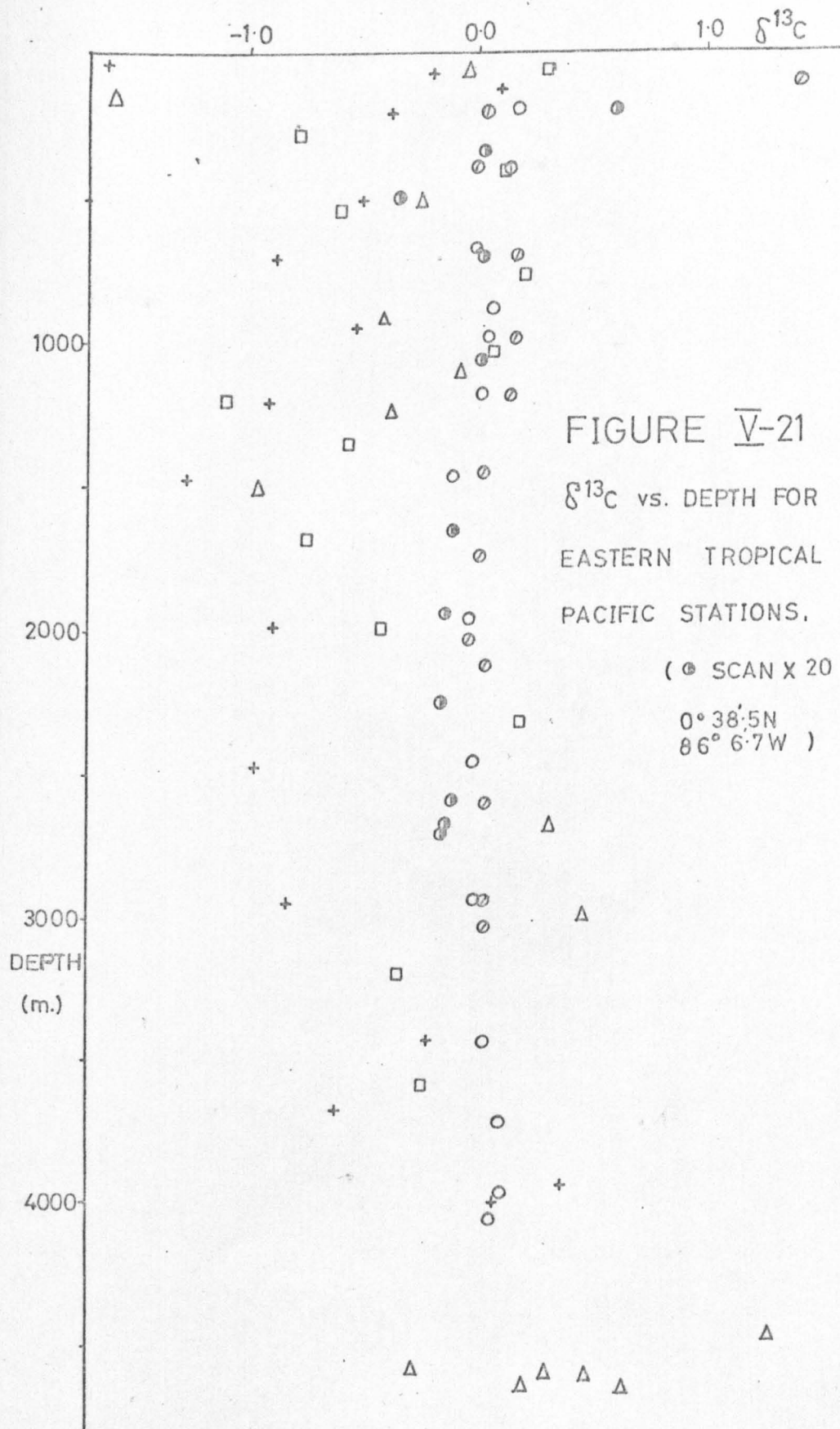
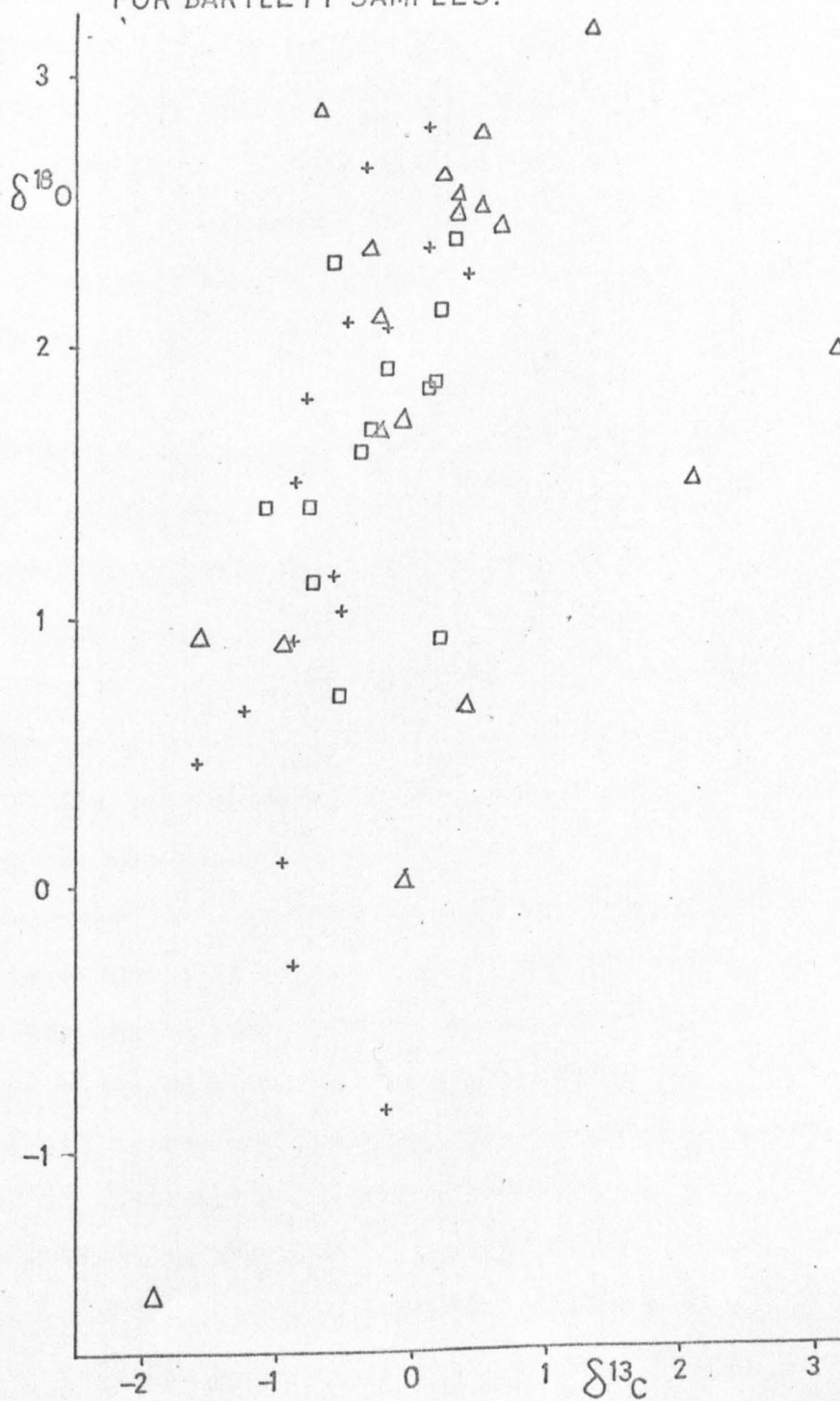


FIGURE \bar{V} -22
 VARIATION OF $\delta^{18}\text{O}$ WITH $\delta^{13}\text{C}$ OF ΣCO_2
 FOR BARTLETT SAMPLES.



seen to be generally lower than those of SCAN stations. The results scatter too much for anything very substantial to be concluded from the profile, but one of the most remarkable features is that the $\delta^{13}\text{C}$ values, if anything, decrease in near surface waters rather than increasing as expected. This would be consistent with high concentrations of readily oxidised organic carbon in these layers, were biological effects after collection important in production of CO_2 . In Figure V-22 is given the $\delta^{18}\text{O}$ versus $\delta^{13}\text{C}$ plot. The linear relationships observed in the experiments on different aliquots of the same seawater, reported in Chapter IV, are not seen here for the depth profiles.

V-5 Summary

Taken as a whole, the hydrographic results obtained from the Bartlett cruise are in general accord with what is known of the oceanography of the eastern tropical Pacific. The temperature structure is uniform over the region, apart from near-surface variations caused by local meteorological and heat budget differences. The shallow and intermediate waters display salinity distributions compatible with orthodox views on both the ocean-atmosphere interactions and the prevailing current systems. The bottom waters are typical of those found in basins north of the complex ridge system patterning the ocean floor off Chile. Only in the deep water of Station 3 is a feature observed which is at variance with the expected salinity field. At this location, there is an apparent core of high salinity water at

approximately 2,500m. depth which has a consistent influence on both deeper and shallower layers. The $\delta^{18}\text{O}$ results confirm the general hydrological regime presented, while at the same time indicating that the homogeneity of the deep water would indeed appear to be violated by the 2,500m. sample at Station 3; an effect on neighbouring samples is not observed but would be close to the precision attainable by the measurement technique.

In an area of such intense biological activity, the chemical results are obviously subject to much regional variation, particularly in the upper layers. The shallow oxygen minimum in the 200 - 400m. depth range is clearly illustrated and the concentrations found there are in agreement with those expected. Relatively high concentrations in deep waters are believed to be a latitude effect, and the deep water distinction on the basis of dissolved oxygen concentration (Muromtsev, 1963) is confirmed. The chemical and isotopic measurements made on the inorganic carbonate system are rather more ambiguous. This is partly a reflection of the increase difficulty of precise measurement, partly the result of doubt attached to the validity of measurements made by other workers. In both near-surface and bottom waters, directly measured pH and ΣCO_2 values correspond to those anticipated, but the pH minimum is broader, more strongly developed and more variable than that observed further north (Culberson and Pytkowicz, 1970). The deep water also shows more variable structure, with pH and ΣCO_2

frequently lower in the Bartlett profiles; these latter variations greatly influence the $\delta^{13}\text{C}$ distribution.

CHAPTER VI

RESULTS FROM ANTARCTIC WATERS

VI-1 Introduction

The structure of this chapter will be similar to the previous one, for they both have much the same purpose in attempting to present the results obtained on seawater samples within a general framework of the oceanography - both physical and chemical - of the appropriate region. Thus, a short introduction to the main features of the general system will be given, followed by a rather more specific account of the hydrology at the individual stations. Finally, the chemical results will be analysed in the light of the two preceding sections. There are, however, several points of contrast with Chapter V. Firstly, the oceanography of the Antarctic is much more complex than that of the eastern tropical Pacific; some of the reasons for this will be mentioned in section VI-2. Secondly, the stations from which the samples have been obtained are more widely spaced geographically. Thirdly, none of the samples was collected by the author, so the responsibility for the stringent requirements of poisoning, proper storage and transportation was not under direct control; the importance of this will become clear when the results are analysed in section VI-4.

Increasing emphasis is being focussed by marine scientists on the reasons, other than purely intellectual curiosity, for their choice of regions for investigation. In Chapter V it was seen that understanding the Peru-Chile current system - a critical problem to the fishing industries of the coastal states - was dependent upon knowledge of the oceanographic and meteorological regimes both to the north and south of the zone usually affected most strongly by 'El Nino'. The Antarctic is another geographical location in which study will be repaid by contributions to 'areas of global societal concern'. Attention has recently been drawn to four such areas, considered as being especially significant there:

1. weather and climate modification;
2. an ecologically efficient long-term use of the region's fisheries;
3. an ecologically sound strategy for the disposal of waste and radioactive by-products; and
4. the improved prediction of local weather, sea and ice conditions.' (Committee on Polar Research, 1974).

VI-2 General oceanography of the Antarctic region.

Whether or not the waters surrounding the continent of Antarctica constitute an 'Ocean', in the sense that there are Atlantic, Pacific and Indian Oceans, is a matter of some debate. Certainly, the waters are totally bounded only by the continent to the south, and could be described as merely the southernmost extensions of the three Oceans mentioned,

but this seems rather pedantic and here the distinction will be dropped and the waters described as the 'Antarctic Ocean', 'Southern Ocean' etc. as required, the northern boundary being somewhat arbitrarily fixed at the Antarctic Polar Front. One of the most important features of the region is that it is the only place where the waters of the Pacific, Atlantic and Indian Oceans all converge and intermix freely. This mixing is greatly enhanced by the prevailing atmospheric and oceanographic conditions, and leads to a higher degree of uniformity of water properties in the major basins to the north than would otherwise be the case. It is generally agreed that the circumpolar region plays a crucial role in determining many characteristics of other areas of the ocean. Prominent among early reports describing the general structure and circulation pattern of the Southern Ocean is the painstaking work of Deacon (1937; but also 1933, 1963 and many others) based on the 'Discovery' Expeditions. Several other Discovery Reports are also important (e.g. Clowes 1938; Sverdrup, 1933) as is the work of many German and Scandanavian investigators. Most of the major early references have been gathered by Gordon (1971) in a recent review and so will not be listed here. In several instances it has not been possible to check directly some of these early publications; where by common consent they contain original ideas or observations they have been referenced with an asterisk, so as to maintain a description consistent with the bulk of the literature. Thus, for example, 'Brennecke, 1921*'

indicates that the opinions in the text are commonly attributed to W. Brennecke, but that this paper has not been directly consulted, being a rather obscure German report. The basic hydrology and current system are greatly influenced by (i) climatic conditions, and (ii) bottom topography. The former will be frequently mentioned, the latter - being less well understood - only occasionally. In the tropical and subtropical belts of the ocean, there is strong stratification of the upper water column and so the deep ocean has but limited interaction with the surface layers, principally by eddy diffusion and gently upwelling 'pumped' by the thermocline. However, at high latitudes, the extremely cold atmosphere and lack of strong stratification permit deep vertical convection and overturning to take place, resulting in the labile structure of the water column found in the Antarctic. South of 65°S , the prevailing winds are easterly, blowing parallel to the coast of the continent due to katabatic effects (Killworth, 1973). The induced surface current is therefore mainly to the west, with a southward component. North of 65°S , the westerlies prevail - maximal at 53°S (Deacon, 1963) - giving an eastward flow with a small transport to the north. There is, evidently, divergence and around 65°S , where the two wind systems meet, is the Antarctic Divergence zone. Here, deep water upwelling occurs to replace the wind driven surface layers. This upward flux is extremely important for the oceanography of the region, for it is by this mechanism that the warm salty

deep water is exposed to the intense cold of the atmosphere. From this description, it is clear that the strength of the divergence will be somewhat variable, being dependent on atmospheric circulation. In the region of the maximal westerlies, around 53°S, the cold, dense northward flowing Antarctic Surface Water (ASW) meets warmer, less dense, southward flowing subantarctic water and consequently sinks below it, resulting in high surface temperature gradients in this area. A frontal system develops and there is intense vertical mixing. The original name given to this feature - the Antarctic Convergence - has now largely been dropped, for both convergent and divergent features are observed. It is more commonly known as the Polar Front zone and marks the northern limit of the Antarctic Ocean as previously defined. Oceanographers distinguish between dynamical and physical fronts: a dynamical front zone is a wind-produced feature established by the nature and degree of vorticity of the tangential wind stress, whereas a physical frontal zone depends on the local water mass circulation and, in particular, on horizontal and vertical advection effects. The Polar Front zone contains both of these, for in addition to the rapid deepening of the temperature minimum referred to above, there is also an upward movement of the deep salinity maximum layer characteristic of deep water originating in the North Atlantic, Pacific and Indian Oceans. This is believed to be a result of bottom water - bottom topography interaction. Some 2°-4° of latitude wide (Gordon, 1971), the Polar Front zone is a more

permanent feature than the Antarctic Divergence. The well mixed, turbulent water mass formed near the surface migrates northwards at intermediate depths; the temperature minimum soon disappears as a result of mixing, but the low salinity remains and is the characteristic by which this Antarctic Intermediate Water (AAIW) is identified further north (recall Chapter V). At the surface north of the Front, Subantarctic Surface Water flows towards the equator until, at about 40°S , it meets the southward flowing subtropical surface water in a region of convergence (the Subtropical Convergence). Surface waters sink and join in the northward flow of AAIW.

Warm, high salinity deep water flows into the Antarctic from all three major ocean basins to the north. The North Atlantic Deep Water (NADW) has a particularly high salinity as a result of its Mediterranean component. These waters mix with the northward flowing intermediate current and, at the Polar Front, rise up over the zonal Circumpolar Deep Water (CDW) until they reach the Antarctic Divergence where they are brought close to the surface and join in the formation of surface waters. The southward flowing surface water at latitudes greater than 65°S , the upwelling Deep Water and intensely cold water from the continental shelf all mix to form a very dense water which plunges down the continental slope, entraining further Deep Water as it sinks. The production of this Antarctic Bottom Water (AABW) is thought to be concentrated in several geographical areas close to the continent - the Weddell Sea, the Ross Sea and off the Adelle

coast (see later). As it flows northwards under the Deep Water, the interaction of the AABW with topographic features of the sea floor is believed to contribute to the cause of Deep Water upwelling at the Polar Front zone.

The connecting link between the two modes of circulation described above - the surface and intermediate on the one hand, and the deep and bottom on the other - is the Antarctic Circumpolar Current (ACC) (Wyrтки, 1961). The Polar Front is also strongly coupled to the ACC, the Front being frequently associated with the axis of the Current. Understanding of this Current is therefore vital for a complete description of Antarctic oceanography. In Figure VI-1 an attempt has been made to illustrate diagrammatically the structure found around Antarctica. In fact, conditions are not meridionally uniform - particularly with regard to Bottom Water formation - and the asymmetrical nature of the coastline together with the existence of a complex bottom topography produces important longitudinal differences. However, the main features are represented.

Perhaps the two most important unsolved problems in Antarctic oceanography concern the dynamics of the ACC and the dynamics and mode of formation of AABW, consequently these will be examined in greater detail below. It is significant that both play a major role in the basic structure and circulation of the region. The circumpolar current system, comprising a zonal flow, a meridional flow and being the source of deep water in the Weddell Sea, dominates the

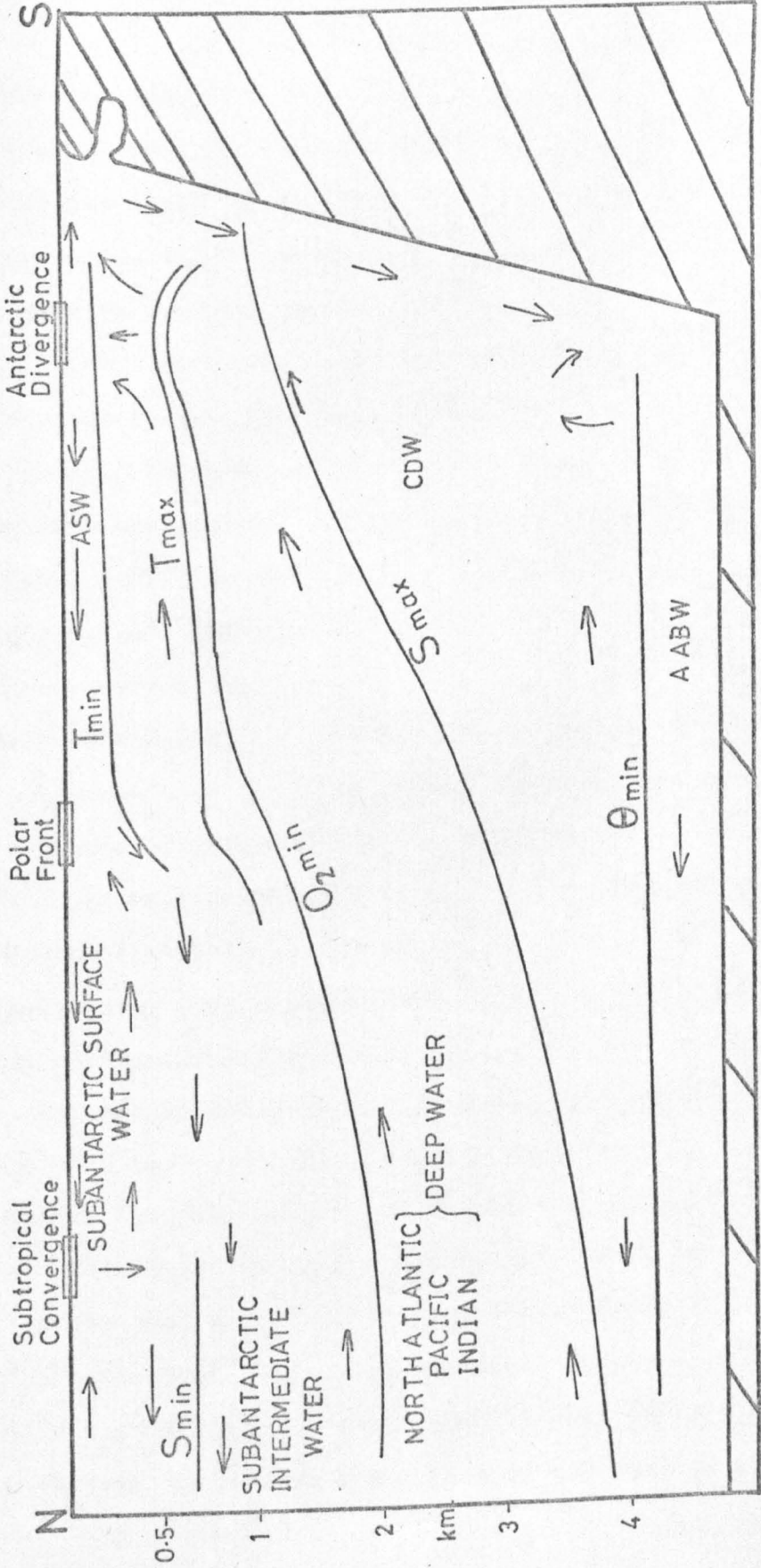


FIGURE VI-1: ANTARCTIC WATER MASS STRUCTURE—SCHEMATIC, (after GORDON, 1971).

deep-ocean circulation. It is antarctic currents that provide a link between the world's major oceans, and antarctic convection sends equatorwards both the sheetlike Antarctic Intermediate Water and also the abyssal Antarctic Bottom Water (as a swift western boundary current). It is commonly believed (e.g. Munk, 1966) that the main thermocline in the ocean is maintained by the resultant upward flux of water at lower latitudes. In terms of transport of mass, the ACC is the largest ocean current in the world (Devine, 1972). Both Callahan (1971) on the basis of geostrophic calculations from hydrographic sections, and Reid and Nowlin (1971) on direct current-meter observations, assign an absolute transport of between 200 and 250 sv. (1 sv. = 1 sverdrup = $10^6 \text{ m}^3 \text{ s}^{-1}$). The concept of a summer minimum in volume transport as a consequence of seasonal peripheral discharge of water around Antarctica suggested by Barcilon (1966, 1967), is considered by Gordon (1968) to be the reverse of the true case, other factors being more significant. Munk and Palmen (1951) have drawn particular attention to one unique distinction of the ACC compared to other major currents - the absence of any meridional barriers. This implies that Sverdrup-type solutions (see Stommel, 1957) cannot be constructed as usual here. Hidaka and Tsuchiya (1953) suggested a model in which the ACC is basically a laterally viscous zonal stream driven by the westerlies, but it is now clear that the current must be more than a strictly zonal one, because it is forced to flow through the narrow Drake Passage and then past the

blocking South Antilles Arc, and a plot of the minimum depth for each latitude circle in this region indicates the impossibility of purely zonal flow (Stommel, 1957). That the Current reaches to the bottom has been deduced by Sverdrup et al. (1942) from the observed deflection of the flow by the bottom ridge systems, the displacement being consistent with Ekman theory. (The ACC is deflected by at least five different ridge systems as it flows around Antarctica.) By considering the Drake Passage as a full or partial barrier (Gill, 1971), approximate dynamical solutions can be obtained. One of the major drawbacks of the early models (Munk and Palmen, 1951; Hidaka and Tsuchiya, 1953) was that in order to obtain reasonable transport values they required a value of the horizontal eddy viscosity coefficient of around $10^9 - 10^{10} \text{ cm.}^2 \text{ s.}^{-1}$, two orders of magnitude greater than those usually envisaged. This is basically a result of the fact that for the ACC the wind stress at the surface is not balanced by lateral friction against the sides of the basin. Devine (1972) attempted to solve the problem by considering the Drake Passage as a porous barrier, the flow being driven by, and proportional to, the pressure head across the barrier; energy dissipation was thus confined to the region of the Passage and did not have to be sought in bottom friction or in the horizontal eddy viscosity. One conclusion was that the baroclinicity of the ACC is of major importance to all aspects of the flow. (Motions forced by buoyancy effects are called 'baroclinic' motions). It is clear from the above that

the major problem here is a dynamical one, to be solved by a theory giving a better account of the features peculiar to the region where the ACC flows. However, such is the importance of the Antarctic Circumpolar Current in both antarctic and global oceanography that this gap in the existing knowledge is worth emphasising.

The second of the major important problems - that of the dynamics and mode of formation of the AABW - will now be dealt with briefly. Water mass analysis shows that the bottom water over a large fraction of the world ocean originates in the waters surrounding Antarctica. Wust (1936, * 1957*) has shown that water from this region reaches northward to between 40° and 45°N in the western Atlantic, and strongly influences the Indian and Pacific bottom circulation. The penetration of AABW in the western Pacific basins has been mapped by Chung (1971). Various mechanisms of formation of AABW have been proposed over the years. Brennecke (1921*) and Mosby (1934*) first postulated that cold, high-salinity water was formed at the surface in winter by the freezing of ice and subsequently mixed with deeper, warmer and more saline water at the edge of the continental shelf, thereafter sinking to the bottom. Further work by Deacon (1937) and Wust (1938*) suggested that the majority of the AABW is formed in the Weddell Sea. More recent study has shown that other sources of AABW exist, the Ross Sea (Jacobs et al., 1970) and off the Adelie coast (Gordon and Tchernia, 1972) being the best documented. Several workers have expressed doubt concerning the overall

validity of these views, thus Mosby (1968) has claimed:

'... in my opinion there is no evidence for considering the Weddell Sea as the main source of Antarctic bottom water.'

Solomon (1974) has pointed out that formation of bottom water at high latitudes, and thermohaline net sinking of water at high latitudes, are not necessarily one and the same thing. This is certainly true, but there are rather obvious deficiencies in the model developed by Solomon, because he neglected wind mixing which Killworth (1973) has shown to be important and, for computational reasons he had to assume a northern sidewall for the Weddell Sea, even though in fact it is open to the north.

Fofonoff (1956) drew attention to the curious fact that because of the non-linearity of the equation of state for seawater, when two water types of different temperatures and salinities mix, the mixture formed may be more dense than either of the parent types, and so sink - a phenomenon known as 'cabbelling'. This can easily be illustrated on a T-S diagram. Noting that there are no observations of unmixed shelf water at great depths, he further proposed that bottom water is formed principally in shallow water. The critical shelf water salinity interval from Fofonoff's analysis was 34.51‰ to 34.56‰ , but this was refined by Gill (1973), by a consideration of the depth of mixing, to 34.465‰ to 34.515‰ . Within this salinity range, the shelf water overlying warm deep water is prevented from sinking by its heavier mixtures. Foster (1972) has shown how the cabbelling

instability can enhance the downward flux of shelf water. Other physical processes which may play a part in bottom water formation include cooling of the coastal current shelf water by the vast ice shelves (Seabrooke *et al.*, 1971), wind-driven sinking (Killworth, 1973) and sinking as a result of the horizontal and vertical circulation within the Weddell Sea (Gill, 1973). A 'salt-fingering' or double-diffusive mechanism has been advocated by Gill and Turner (1969); in a fluid with density variations resulting from the distribution of two components with unequal molecular diffusivities (e.g. temperature and salinity), motions can be set up even although the overall density distribution is statically stable. Gill and Turner hypothesised the existence of a cold, fresh current down the slope in summer - a testable prediction of their thermohaline mechanism. So far, absolute rates of formation of AABW have not been determined directly, but many indirect estimates of varying degrees of credibility exist. Care must be taken in discussing these, for some are based on the amount of bottom water produced in the Weddell Sea, some on that produced all around Antarctica and some on the northward flux of bottom water in the Atlantic or Pacific Ocean. Obviously, the swiftly flowing bottom current as it moves northwards will entrain a portion of the more sluggish, southward migrating water, but the requirement of linear momentum conservation must always be fulfilled, and the current is being continuously dissipated by bottom friction. Values predicted for the amount of Bottom Water formed around

the coast of Antarctica vary according to the physical mechanism postulated and the proposed subsequent mixing with deep water as the dense water slides down the continental slope to the bottom. The ratio of deep water to altered shelf water is generally taken as between 2:1 and 1:1, depending on the 'conservative' parameter employed. Wyrski (1961) has calculated from heat budget considerations that 11.5 sv. of sinking water could be formed by thermohaline processes over the entire Weddell Sea; Killworth (1973) considered wind-driven sinking and obtained 20 sv. only by including the entire coastline of Antarctica, the Weddell Sea value being considerably smaller. From a model of the vertical circulation within the Weddell Sea, Gill (1973) deduced a downward flux of 1 sv. with a similar figure resulting from horizontal circulation, and allowing for a final mixture containing a 25 - 30% shelf contribution and dilution effects he arrived at 6 - 9 sv. of AABW being formed. By including the Ross Sea he could increase this to 10 - 15 sv. The temperature-salinity-radiocarbon box model of Bolin and Stommel (1961) gave 9.6 sv. for the amount of AABW formed and Munk (1966) calculated 27 sv. based on the amount of ice melting all around Antarctica. In the opinion of Seabrooke et al. (1971), the alteration of shelf water of the antarctic coastal current as it comes into contact with the underside of the Filchner and Ronne Ice Shelves is a determining factor, and with a 2:1 mixing ratio deduced from preformed nutrient data gives 5 sv. of Bottom Water. Based on a 35% shelf water

contribution, Baranov and Botnikov (1964) estimated that 20 sv. leaves the Weddell Sea. In the Stommel-Arons theory of abyssal circulation (see Chapter I-4), a northward flux from the Antarctic into the other oceans of 20 sv. was used. Wright (1969, 1970) has calculated a northward flux of AABW in the Atlantic of 5 sv. and Warren and Voorhis (1970) obtained a figure of 12.9 sv. for the Pacific. Very much greater values for the Atlantic have occasionally been suggested; for example Le Pichon et al. (1971) described the 2,000 m. thick bottom layer (called by them the Antarctic Bottom Current) in the region of the Falkland Channel and calculated geostrophic velocities from a thermograd section. They judged the best approximation of the transport in the southern Argentine Basin to be 90 sv. Edmond (1973) has supported this on the basis of dissolved silicate distribution, obtaining 101 sv. Given such a diversity of formation mechanisms and so wide a range of flux estimates, there is obviously much room for criticism. Thus Solomon (1974) has pointed out that the area of the Weddell Sea assumed by Wyrтки (1961) includes a sizeable fraction that is ice-covered, that Munk's (1966) estimate is invalid because not all melting ice forms AABW, and that the model used by Gill (1973) to derive his value contains an internal contradiction. The mechanism of Seabrooke et al. (1971) has been discredited by Gill (1973) because the ice shelves cannot conduct away the necessary heat to allow the required cooling of the coastal current.

VI-3 Hydrographic features.

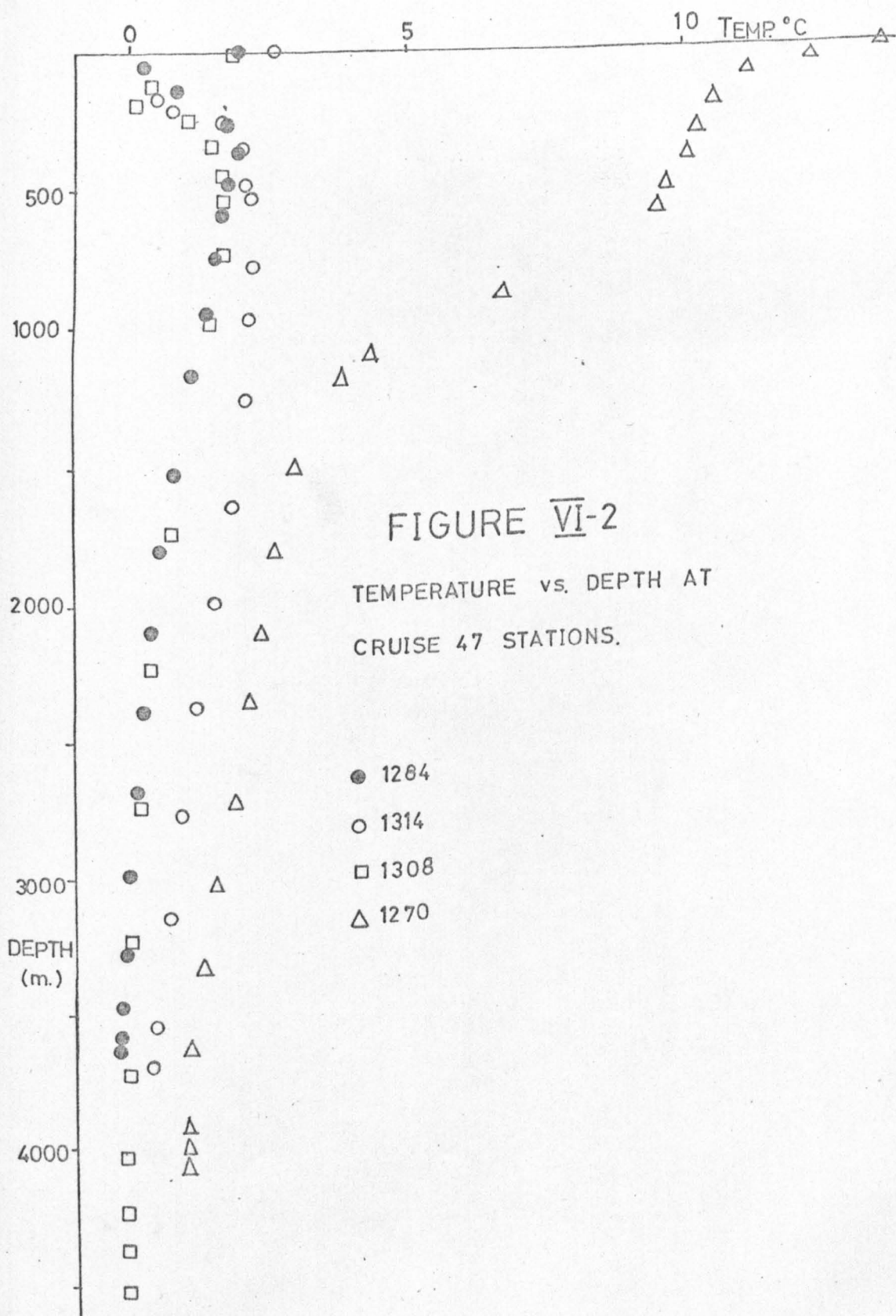
Samples from the waters around Antarctica were obtained from three cruises of U.S.N.S. Eltanin. The vast majority were collected on Cruise 47 during 1971 by Dr. J.M. Edmond of M.I.T. The 120 ml. samples were poisoned with 1 ml. of saturated mercuric chloride solution and stored in glass bottles with hard-plastic screw-on caps fitted with conical polythene 'Poly-Seal' inserts. A few samples were also obtained from Cruise 50 (1971 from Dr. A.L. Gordon of Lamont-Doherty Geological Observatory) and from Cruise 52 (1972 from Mr. S.S. Jacobs of Lamont). The former were poisoned with solid mercuric chloride and stored in 'Atlas Mason' jars with rubber-gasketed metal caps; the latter received no sterilisation treatment and were returned to Lamont where approximately 20-30 ml. was removed from each bottle prior to shipping to Glasgow. An extensive sampling program by the author, planned for Cruise 56 (1973), was not carried out as the vessel was withdrawn from active service. The station locations from which samples were procured are listed in Table VI-1. All hydrographic data for the Lamont stations are given in Jacobs et al. (1974); additional measurements on Cruise 47 were performed by Dr. Edmond and have been obtained through his courtesy. These data will be shown in graphical form only and will not be tabulated. Unlike the Pacific Ocean results discussed in Chapter V, those reported in this Chapter do not belong to a uniform hydrological regime: this is illustrated in the widely varying profiles of the hydrographic parameters.

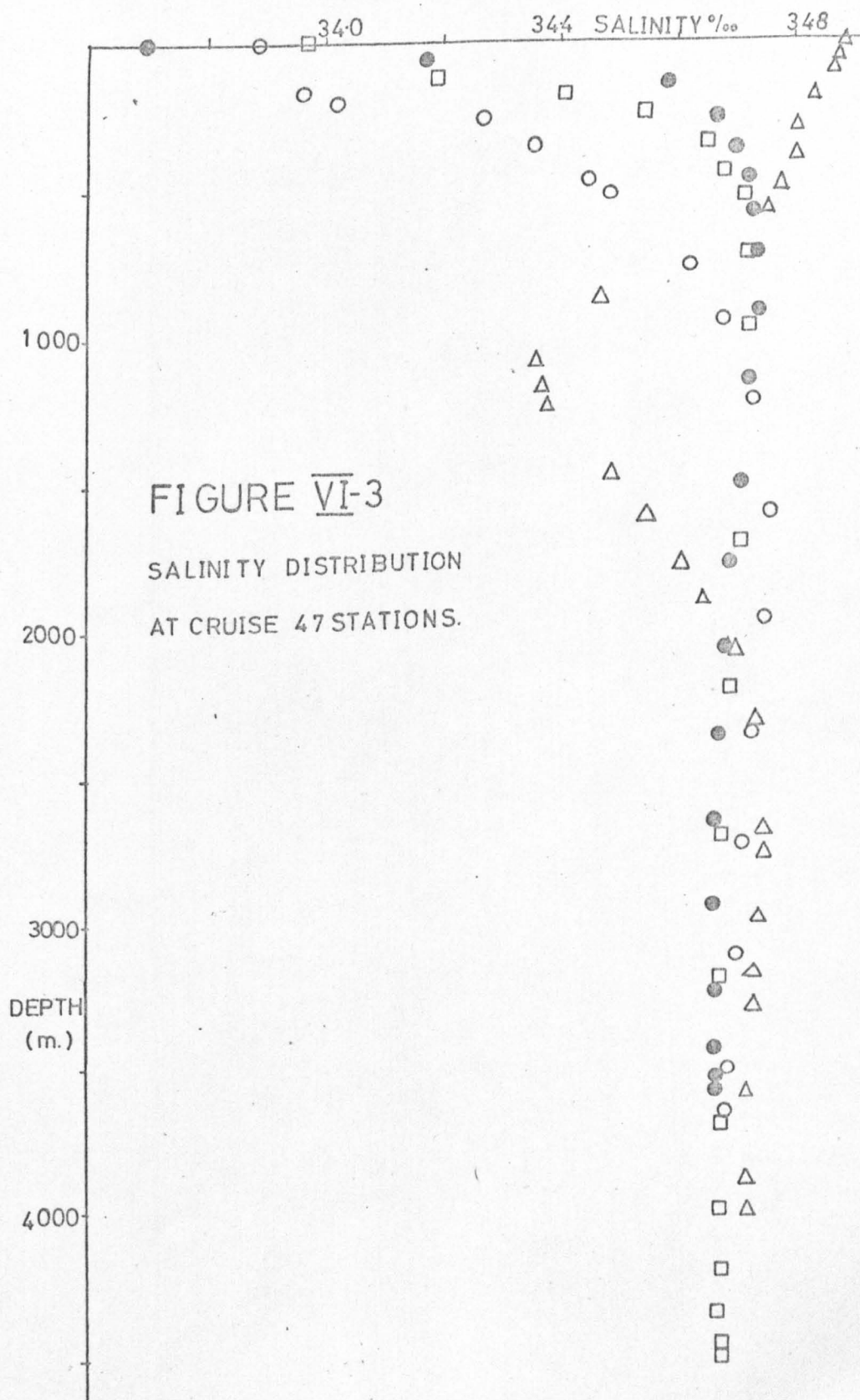
TABLE VI-1

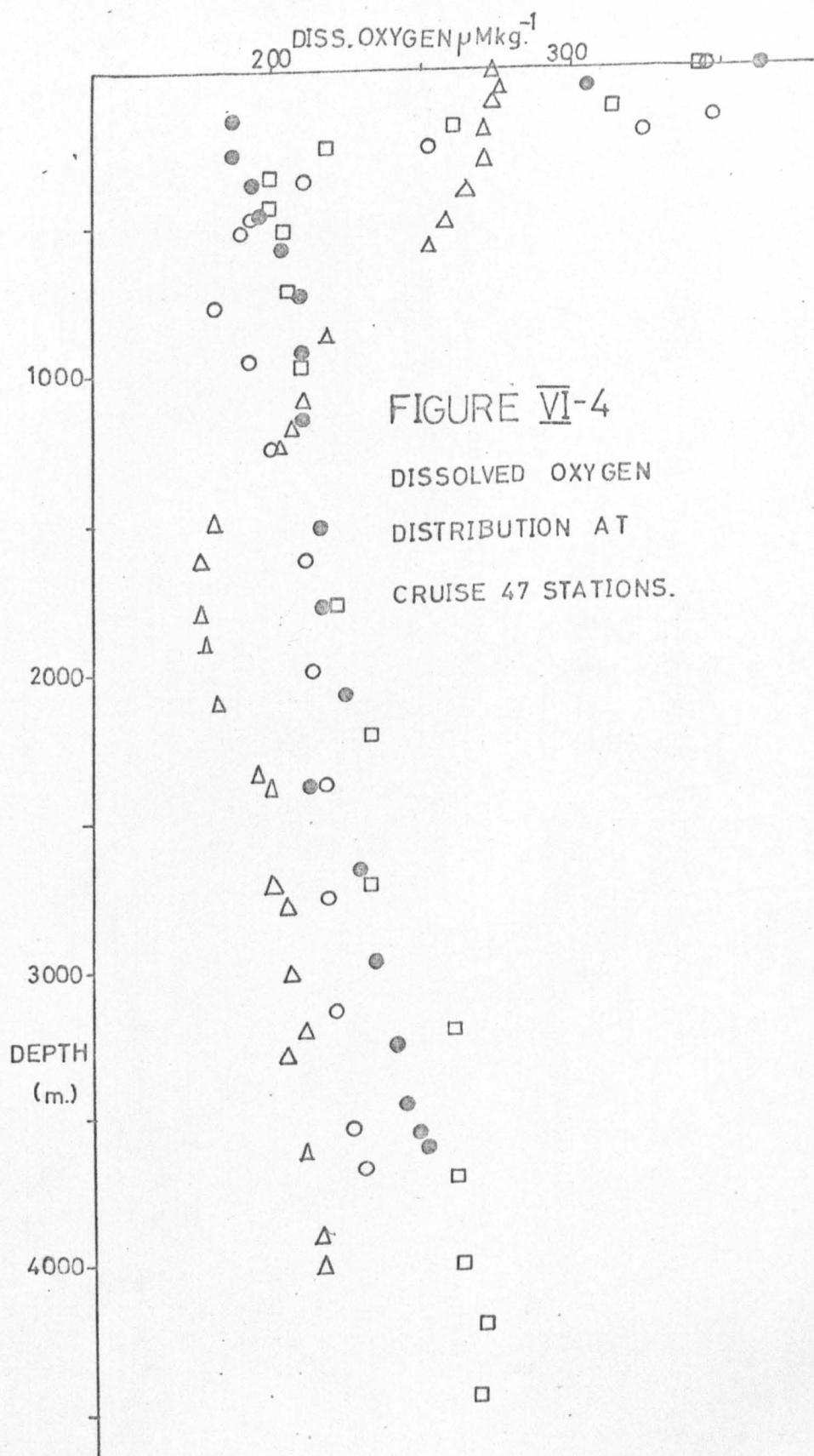
Antarctic sampling station locations.

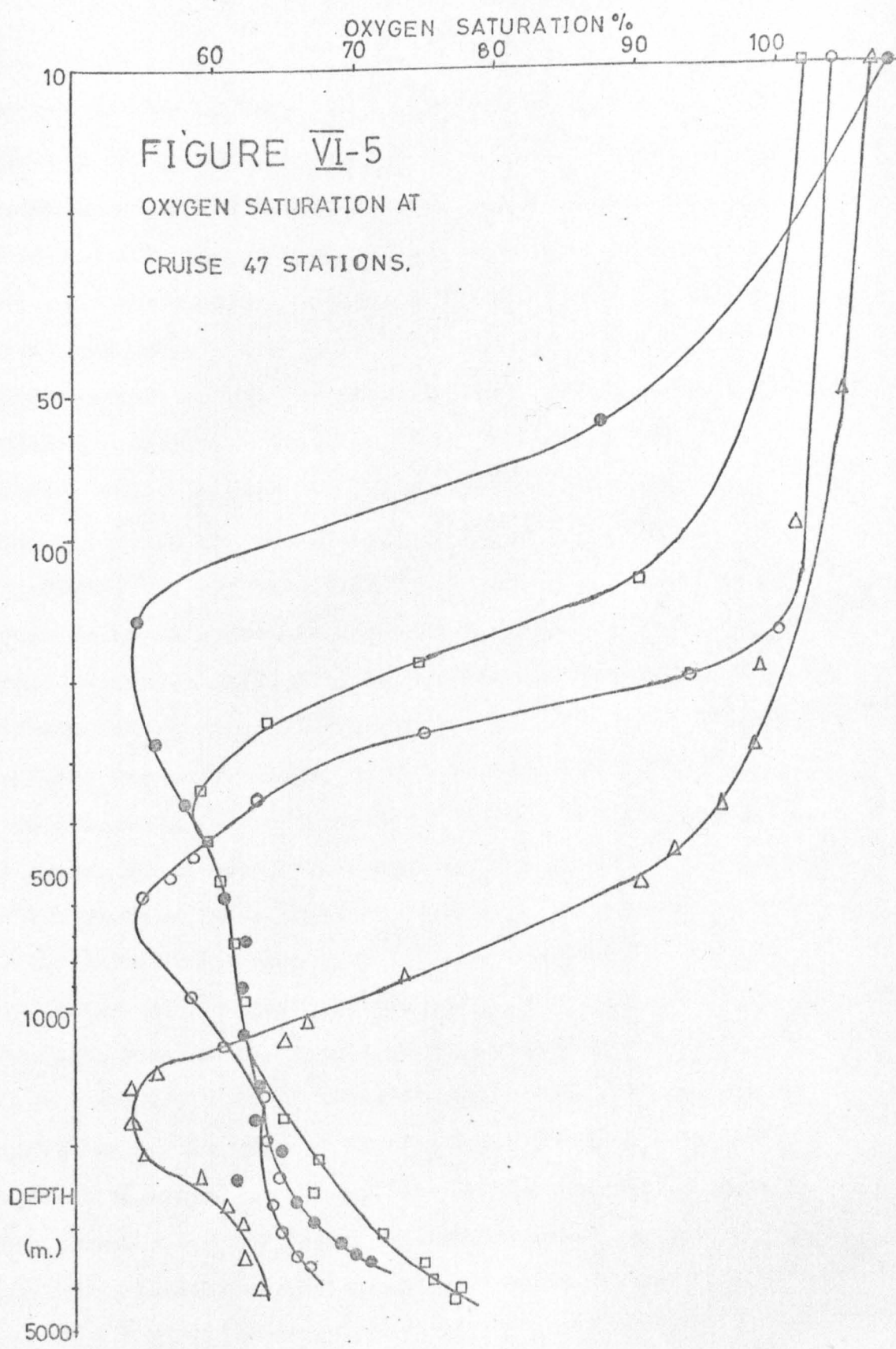
CRUISE	STATION	LATITUDE	LONGITUDE
47	1270	40° 34'.9S	90° 56'.3E
47	1284	64° 03'.9S	80° 34'.4E
47	1308	54° 56'.0S	82° 38'.7E
47	1314	54° 26'.2S	69° 43'.8E
50	5	58° 59'.0S	169° 57'.6E

Most of the discussion will revolve around the Eltanin 47 samples, for they represent more complete sections through the water column. Cruise 47 Stations 1284, 1308 and 1314 are located in the Indian sector of the Antarctic Ocean, and Station 1270 in the sub-tropical zone of the Indian Ocean. This distinction is immediately evident from the water mass structure. Figures VI-2, 3, 4 and 5 show, respectively, the depth distributions of temperature, salinity, concentration of dissolved oxygen and oxygen saturation; for the last of these, the depth is plotted on a logarithmic scale. Unless otherwise stated, the station key given in Figure VI-2 will be used throughout this Chapter. Station 1270 is situated very close to the Subtropical Convergence. The surface waters are therefore warm and of high salinity with oxygen concentrations over 100% saturation. It is clear from the salinity and oxygen profiles that the upper 600 m. or so are extremely uniform: at 600 m. the salinity is within 0.15‰ of the surface value and the oxygen saturation still over 90%. This is caused by sinking of surface waters in the Convergence zone as the northward flowing subantarctic and southward flowing subtropical waters meet. Below this layer lies a very pronounced salinity minimum with salinity of 34.36‰ at the core depth around 1,100 m. Oxygen concentrations are high ($180 - 200 \mu\text{M kg.}^{-1}$) but the water is much colder ($3 < T < 7$) than that at shallower depths. Clearly, this is AAIW formed at the Polar Front and advected northwards. Below the Intermediate Water lies warm, high salinity Indian









Deep Water with core indicated by the salinity maximum of approximately 34.76‰ at around 2,750 m. The characteristic minimum in dissolved oxygen is seen in this mass at 1,600 - 1,700 m. depth. This water is destined to become incorporated into the ACC, mixing with similar water from the North Atlantic and Pacific. Gordon (1971) differentiates between Upper and Lower Circumpolar Deep Water, the former characterised by the temperature maximum, the latter by the salinity maximum. There is also, of course, the oxygen minimum which is shown by Gordon (1971, Figure 1) and in Figure VI-1 as in general lying below the T_{max} layer.

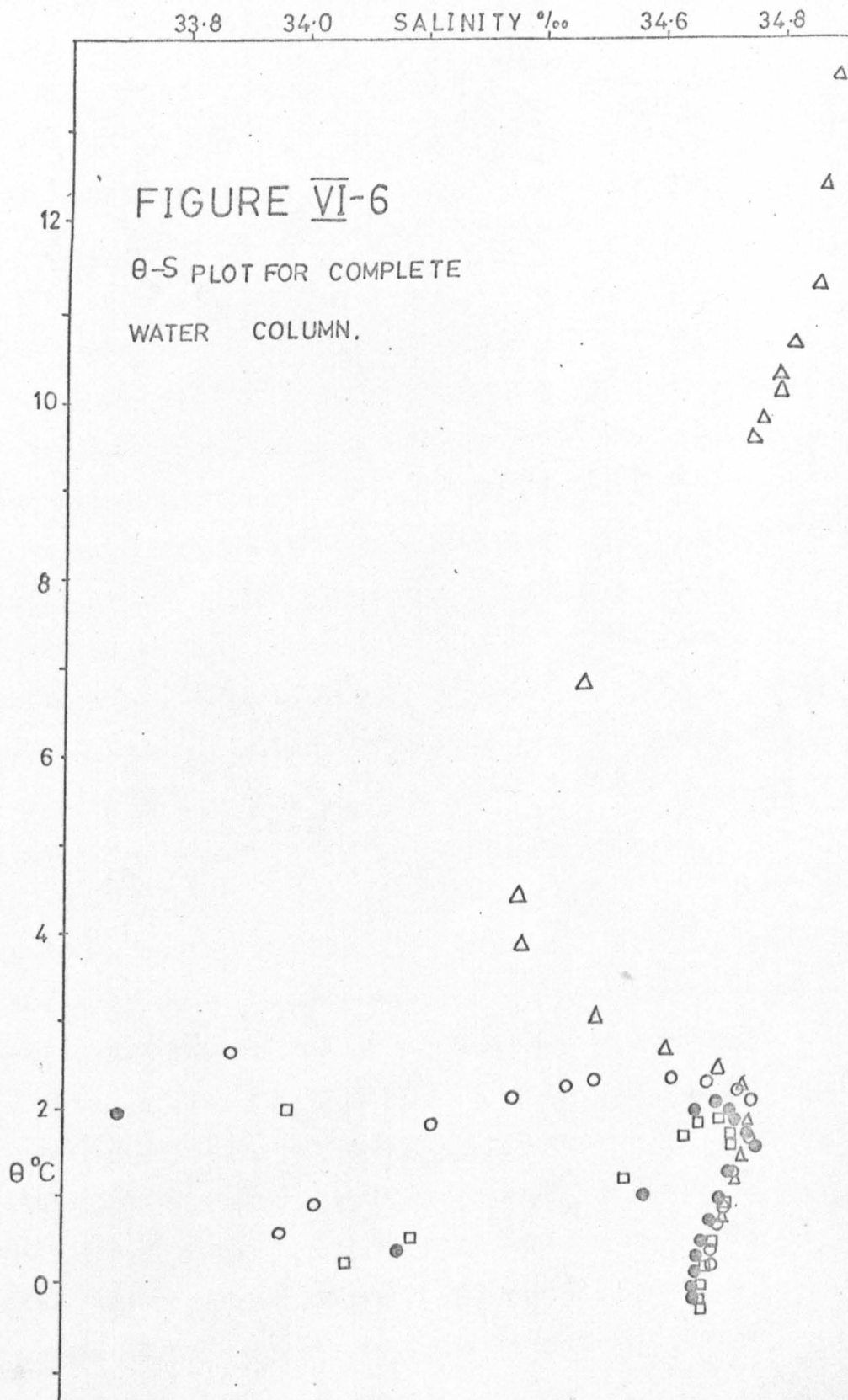
Stations 1284, 1308 and 1314 are separated from 1270 by the Polar Front zone (an oceanographic feature) and the Mid Indian Ridge system (a feature of submarine topography). While 1270 illustrated subtropical aspects of the hydrography, these three stations are more typical of the antarctic proper. It might have been anticipated that 1308 and 1314, being of comparable latitude, would have displayed similar parameter distributions. As the profiles show, this is obviously not the case. It is believed that the reason for this is to be found in the bottom topography of the area. Station 1314 lies to the west of the Kerguelen Plateau (or Kerguelen-Gaussenberg Ridge) and just off it, whereas 1308 is situated over a local topographic depression to the east of the Plateau. The consequent greater depth at this Station is apparent in the profiles. Station 1284, further south by some 10° latitude and intermediate in longitude, is much closer to Antarctica and is shallower than

the other two as it overlies the gentle rise connecting the Kerguelen Plateau to the continent. The surface waters at approximately 2-3°C are Antarctic Surface Water moving northwards from the Divergence. There is a well-developed subsurface temperature minimum, above 200 m. since the stations are south of the Polar Front where the minimum layer rapidly descends and contributes to AAIW formation. As explained in section VI-2, at the Polar Front the Deep Water starts to rise and is finally brought near to the surface south of the Antarctic Divergence at 65°S. This is clearly demonstrated by the depths at which the characteristic O_{2min} , T_{max} and S_{max} layers are found. Estimates of the appropriate depths of each feature are given in Table VI-2; of necessity, these are somewhat inaccurate but they are intended for illustration purposes only. At 1314, conditions are closest to those observed at 1270 with the salinity maximum at around 1,650 m; at 1308 this has risen to just over 1,000 m. and by 1284 to around 800 m. The temperature maximum behaves similarly, rising from 650 m. to 500m. to 350 m. The depth of the oxygen minimum is best judged from Figure VI-5, though because of sample spacing precise depths cannot be assigned. The O_{2min} is around 660 m. at 1314, 400m. at 1308 and 200 m. at 1284. These latter two are shallower than the T_{max} depth, but this is not thought significant. The θ -S diagram for the entire water column is given in Figure VI-6 and the identity of the deep water at 1270 with much shallower water further south at 1284, 1308 and 1314 is readily apparent. The plot

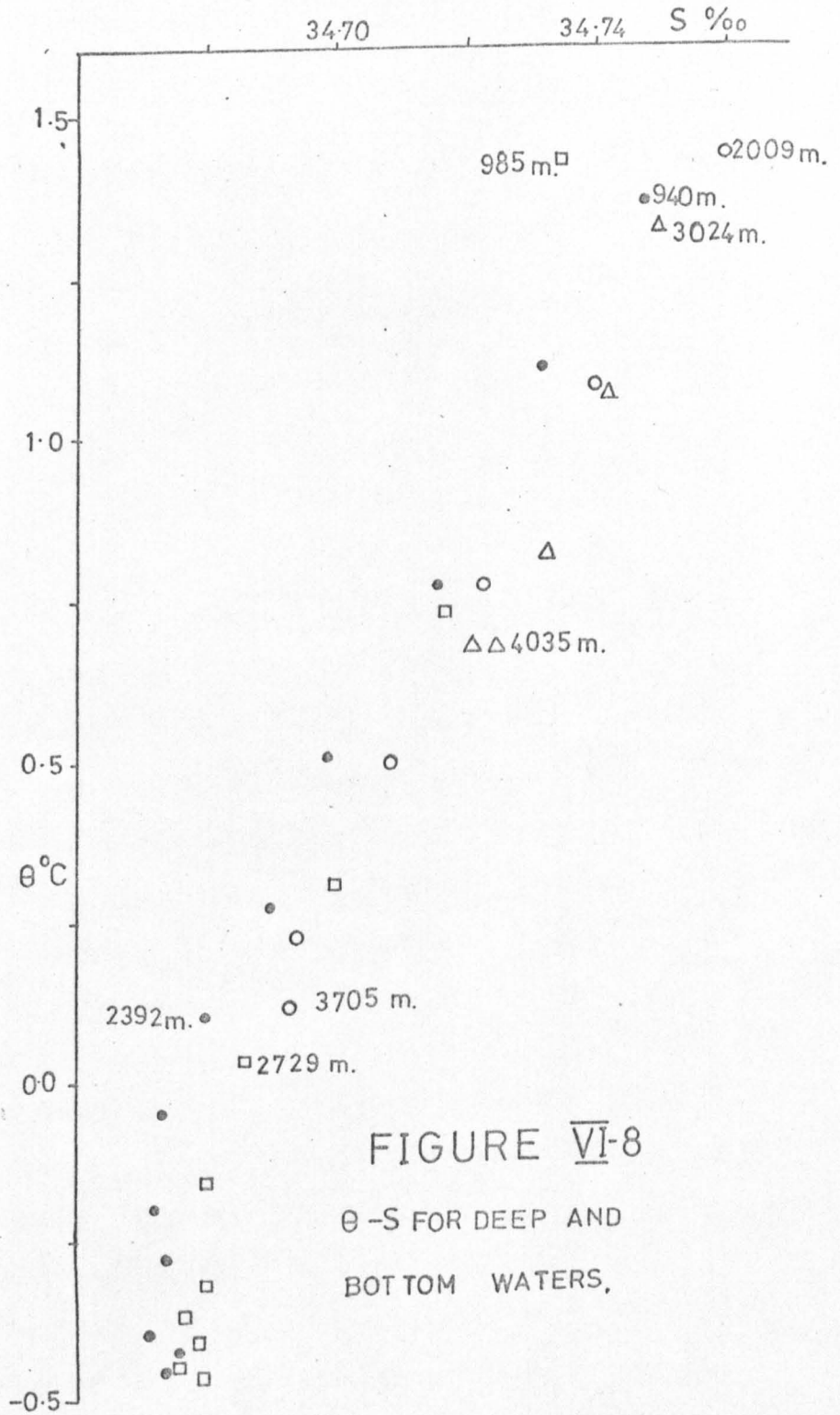
TABLE VI-2

Depths of prominent hydrographic features at Cruise 47
Stations.

STATION	1270	1284	1308	1314
LATITUDE	40° 34'.9S	64° 03'.9S	54° 56'.0S	54° 26'.2S
T _{max}	-	350 m.	500 m.	650 m.
S _{max}	2750 m.	800 m.	1050 m.	1650 m.
O _{2min}	1600 m.	200 m.	400 m.	650 m.



for subsurface samples is shown in Figure VI-7; from this, and the deep and bottom water plot of Figure VI-8, several interesting points emerge. The salinity profile (Figure VI-3) shows deep 1314 samples slightly more saline than those of 1284 and 1308. Similarly, the temperature profile (Figure VI-2) shows 1314 to be warmer than the other two. However, the θ -S diagrams show that the deepest water at 1270, the deep water at 1314 and the deep water above about 2,800 m. ($\theta > 0^\circ\text{C}$) at 1284 and 1308 has a common origin - it is CDW. Figure VI-8 indicates that at 1284 and 1308 there is an underlying bottom water of more or less constant salinity (34.67 - 34.68‰) and potential temperature range -0.5 to 0.0°C . In Figure VI-5 it is seen that there is a rapid increase in oxygen saturation in these layers and so they obviously represent AABW, the high oxygen content being a reflection of the shelf component which has recently been in contact with the atmosphere. The absence of AABW at 1314 must then be attributed to topographic effects associated with the Kerguelen Plateau, for it would not appear that the AABW is trapped in the depression at 1308 (see the chart of submarine topography of the region in Jacobs *et al.*, 1974). Thus the AABW at 1308 must have arrived there either from the south or the east. It will be noted that the Bottom Water at 1284, 10° latitude further south and 2° further west in longitude, is colder than that at 1314. The ranges of values of hydrographic parameters describing these various water masses are in good accord with accepted literature values (e.g. Gordon, 1971; Hufford and Seabrooke, 1970) and the basic structure is in agreement with



that deduced from more complete sections taken further east (Gordon, 1972).

The $\delta^{18}\text{O}$ results for Cruise 47 are presented in Tables VI-3 and 4. Most of the results are from Stations 1284, 1308 and 1314, for several 1270 samples were lost in a laboratory accident. All the results are relative to SMOW and no correction has been applied for the poison solution added. The composite $\delta^{18}\text{O}$ versus depth profile used in Chapter V would be of little use here, for the various water masses are not necessarily at equivalent depths at the different stations. Therefore, the most extensively sampled profile, that of Station 1284, has been plotted as Figure VI-9 and will be discussed, bringing in data from other stations where appropriate. To aid in this discussion, selected samples have been plotted on $\delta^{18}\text{O-S}$ and $\delta^{18}\text{O-A}$ graphs shown in Figures VI-10 and 11; the arrowed lines, drawn on the basis of sample depths, are intended to represent diagrammatically the mixing trajectories. The lowest $\delta^{18}\text{O}$ values are found at the surface. Here, the salinities are highly variable reflecting the influence of evaporation/precipitation effects and meltwater addition, (the low salinities observed argue against freezing being important). The 1284 and 1308 $\delta^{18}\text{O}$ results are in good agreement, 0.40 and 0.46‰ respectively; the sample separation in Figure VI-10 being accounted for by the 0.275‰ lower salinity at 1284. Beneath the surface, $\delta^{18}\text{O}$ rises quickly, reaching around 0.2‰ in the T_{min} layer. Below this, $\delta^{18}\text{O}$ increases as the CDW is encountered; a maximum of

TABLE VI-3

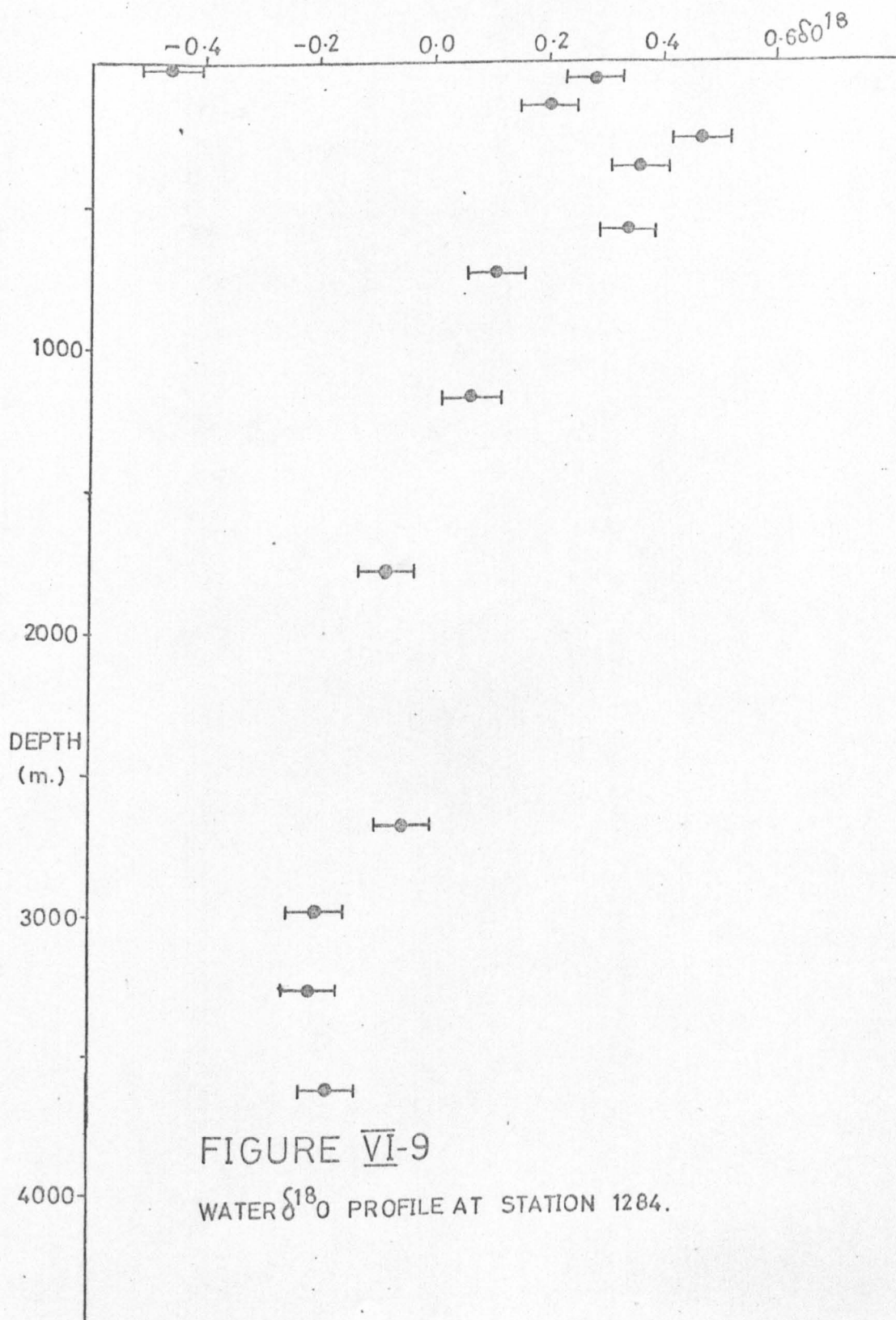
 $\delta^{18}\text{O}$ results at Cruise 47 Station 1284

DEPTH (m.)	SALINITY ‰	POTENTIAL TEMPERATURE (°C)	$\delta^{18}\text{O}/\text{‰}$ (SMOW)
1	33.694	1.96	-0.46
60	34.171	0.25	0.28
149	34.584	0.83	0.20
273	34.673	1.79	0.47
372	34.706	1.90	0.36
594	34.741	1.69	0.34
742	34.746	1.56	0.11
1185	34.732	1.08	(0.07±0.05)
1798	34.699	0.50	-0.08
2689	34.674	-0.05	-0.05
2986	34.672	-0.20	-0.20
3283	34.674	-0.31	-0.21
3630	34.674	-0.45	-0.18

TABLE VI-4

 $\delta^{18}\text{O}$ results at Cruise 47 Stations 1270, 1308 and 1314

DEPTH (m.)	SALINITY (‰)	POTENTIAL TEMPERATURE (°C)	$\delta^{18}\text{O}/\text{‰}$ (SMOW)	
2	33.976	1.96	-0.40	1308
189	34.408	1.16	0.22	
347	34.656	1.53	0.27	
543	34.718	1.67	0.37	
739	34.732	1.58	0.34	
985	34.735	1.40	0.35	
1729	34.717	0.72	(0.22±0.05)	
2229	34.700	-0.30	0.03	
3229	34.680	-0.15	(0.22±0.03)	
3729	34.680	-0.32	0.14	
4479	34.679	-0.45	0.06	
172	33.966	0.52	0.08	1314
210	34.024	0.79	0.00	
268	34.225	1.69	0.40	
482	34.455	2.10	0.02(?)	
974	34.691	2.16	0.22	
2009	34.760	1.43	0.05	
2767	34.723	0.76	0.05	
3555	34.694	0.21	-0.12	
588	34.761	9.41	0.32	1270
1633	34.554	2.70	0.12	
2791	34.758	1.60	0.04	



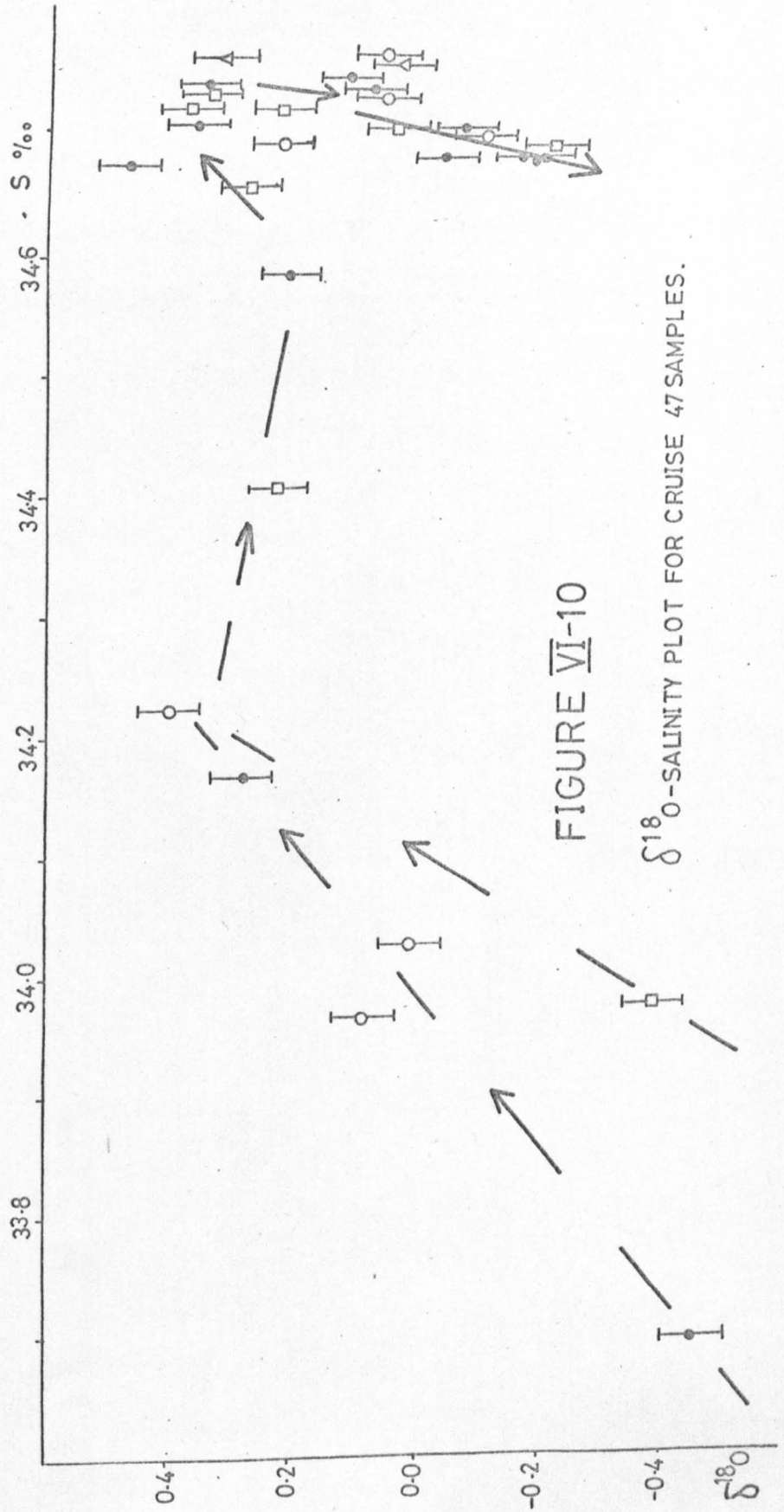


FIGURE VI-10

 $\delta^{18}O$ -SALINITY PLOT FOR CRUISE 47 SAMPLES.

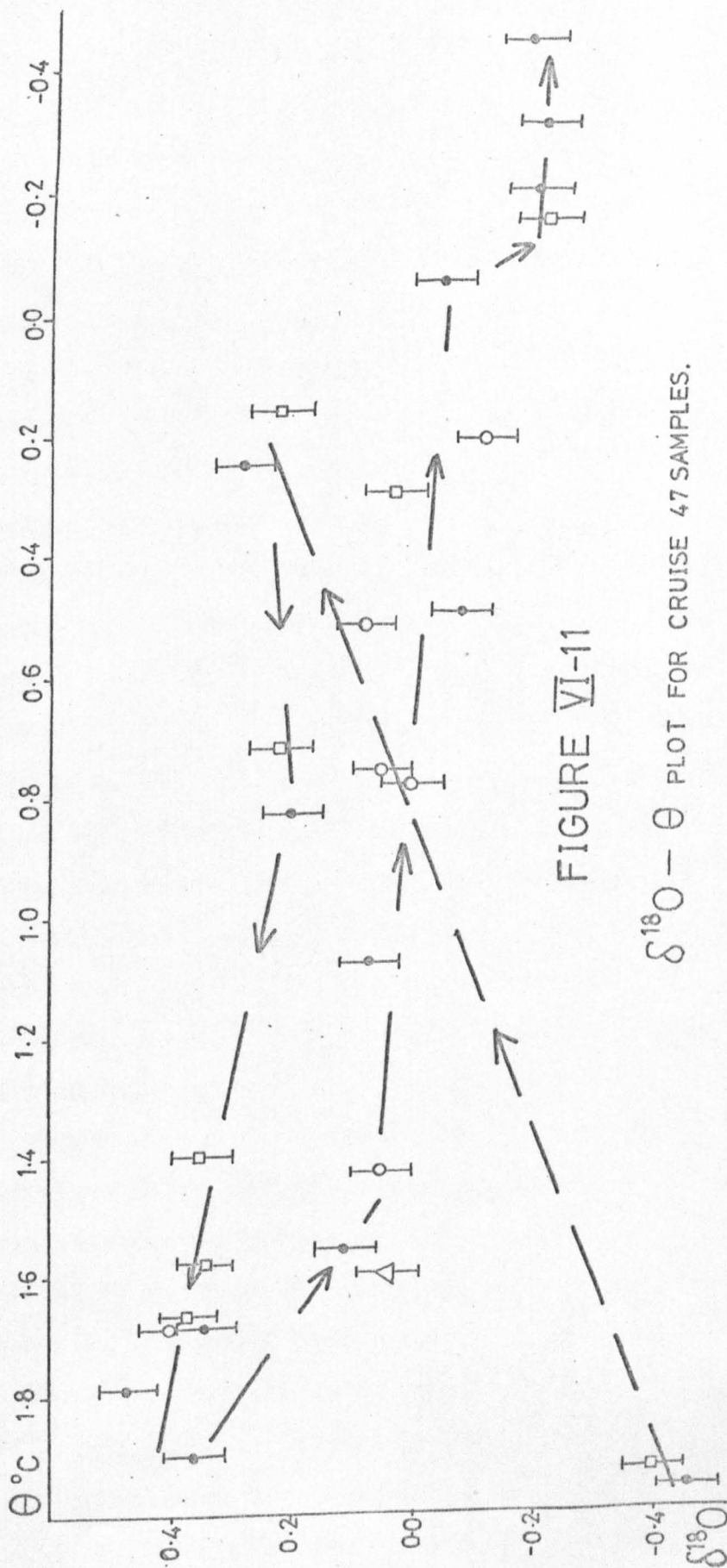


FIGURE VI-11

 $\delta^{18}\text{O} - \Theta$ PLOT FOR CRUISE 47 SAMPLES.

0.3 - 0.4‰ characterises the T_{\max} region of Upper CDW (Figure VI-11) and values thereafter decrease to about 0.0 to 0.1‰ at the S_{\max} or Lower CDW (Figure VI-10). The transition to AABW is seen as a 'step' in the depth distribution below 3,000 m. in Figure VI-9, but is perhaps best seen in Figure VI-11 where there is a sudden drop in $\delta^{18}\text{O}$ to around -0.20‰, this then staying constant as the potential temperature decreases. The two deepest 1308 AABW samples analysed gave results of 0.14 and 0.06‰ (see Table VI-4) - inconsistent with the other AABW data. However, the former was one of the very first samples analysed, and no isotopic shift in $\delta^{13}\text{C}$ of CO_2 was noted over the equilibration (recall Chapter II), so the result is obviously questionable; for the latter, the $\delta^{13}\text{C}$ shift was 0.65‰, so again doubt is cast on the accuracy of the result. Since the two samples were the deepest ones analysed, and agreed to within ± 0.04 ‰, it was though worth reporting them. The high $\delta^{18}\text{O}$ values at the T_{\min} just below the surface indicate that these waters are derived from upwelled deep water (i.e. Upper CDW of the T_{\max}), modified at the surface around the Antarctic Divergence, for no other water with sufficiently high $\delta^{18}\text{O}$ is observed. Interstation variations in the CDW are evident, probably attributable to local differences in the extent of alteration and mixing because some scatter is seen also in the θ -S plot of Figure VI-7; The $\delta^{18}\text{O}$ results support the view advanced earlier that AABW is not found at Station 1270 or 1314, the deepest water analysed at these two Stations giving results

consistent with Lower CDW. The four AABW assays shown in Figure VI-11 are extremely uniform in $\delta^{18}\text{O}$, with mean and 1 σ standard deviation $(-0.20 \pm 0.02)^\circ/\text{‰}$. Craig and Gordon (1965) quoted $-0.45^\circ/\text{‰}$ for AABW from the Weddell Sea, but other values given by them (e.g. -0.2 to $-0.3^\circ/\text{‰}$ for CDW) are also not in accord with those found in this work. Possibly, these differences reflect systematic errors in the $\delta^{18}\text{O}$ determinations, though this seems unlikely on the basis of the Chapter II calibration results, or sample location effects, e.g. the salinity of the ACC falls by almost $0.04^\circ/\text{‰}$ on passing the Campbell Plateau south of New Zealand, probably as a result of loss of high salinity deep water to the Western Boundary Undercurrent (Gordon, 1972). Hence a concomitant change in $\delta^{18}\text{O}$ might be expected, but would be unlikely to be sufficiently great to account for the observed difference. In any event, the results presented here are internally consistent and give a good illustration of the deduced water mass structure. Five surface samples from Cruise 52 were analysed; the results are given in Table VI-5 and appear to be divided into two groups as shown, the latitude, temperature and $\delta^{18}\text{O}$ determining the distribution. These emphasise the importance of atmosphere surface ocean interactions in determining shallow $\delta^{18}\text{O}$ values.

TABLE VI-5 $\delta^{18}\text{O}$ analyses of surface waters from Cruise 52

SALINITY	TEMPERATURE	$\delta^{18}\text{O}$	LATITUDE	LONGITUDE
GROUP 1:				
34.351‰/‰	-1.07°C	-0.24‰/‰	72° 27'S	173° 52'E
-	-1.0	-0.22	69° 37'S	173° 50'E
34.367	-1.37	-0.20	77° 57'S	179° 51'W
GROUP 2:				
-	13.4	0.24	44° 29'S	177° 55'E
34.228	7.8	0.29	56° 52'S	174° 40'E

VI-4 Chemical and isotopic results

The profiles of dissolved oxygen at Eltanin Cruise 34 stations have been represented in Figure VI-4, and the influence of the hydrology of the distribution discussed in section VI-3. The AOU values have been calculated and are plotted in Figure VI-12. ΣCO_2 and $\delta^{13}\text{C}$ results from Cruise 50 are given in Table VI-6; since the observed ΣCO_2 values were much lower than expected, samples 5-2, 5-3 and 5-4 were analysed in duplicate and 5-1 in triplicate. However, reasonable agreement between replicates was found in all cases, and the $\delta^{13}\text{C}$ results were also consistent, so the fault clearly lies in storage/poisoning conditions and not in extraction technique. The extensive alteration of the carbonate system was verified by a measurement of the pH of sample 5-2, a value of 6.4 being obtained as compared to the range 7.7 to 8.3 usually considered representative of seawater. Because the samples from Cruise 52 were not poisoned, no chemical analyses were performed on them. ΣCO_2 results from the samples from Stations 1270, 1284, 1308 and 1314 of Cruise 34 are given in Tables VI-7 to VI-10. The correction for the addition of poison has been applied. A composite ΣCO_2 profile using data from 1284, 1308 and 1314 has been drawn as Figure VI-13. The 1270 results show much more scatter than those of the other stations and so have been omitted; for the same reason, $\delta^{13}\text{C}$ assay was not carried out on these. A pronounced ΣCO_2 maximum is seen at all three stations in Figure VI-13 at around 300 - 400 m. depth. Surface values of approximately

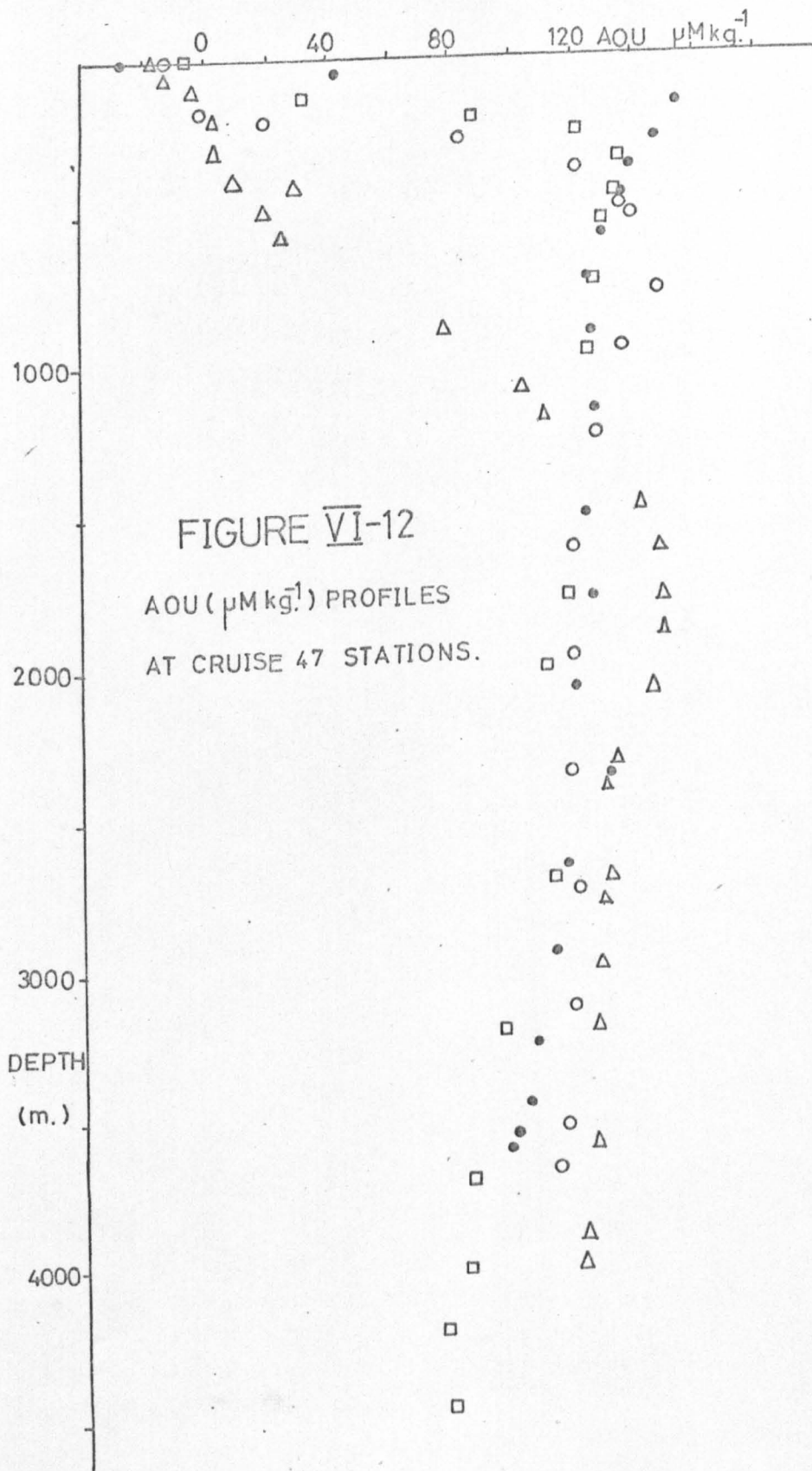


TABLE VI-6

 ΣCO_2 and $\delta^{13}\text{C}$ at Cruise 50 Station 5

DEPTH (m.)	ΣCO_2 (mM kg. ⁻¹)	$\delta^{13}\text{C}$ (PDB) (‰)	SAMPLE
0	1.317	1.73	5-1
	1.306	1.68	
	1.322	1.80	
Mean:	(1.315±0.008)	(1.74±0.06)	
2144	0.152	*	5-2
	0.156		
Mean:	(0.154±0.003)		
3541	0.899	-2.17	5-3
	0.834	-	
Mean:	(0.867±0.05)		
5142	0.081	*	5-4
	0.069		
Mean:	(0.075±0.008)		

* insufficient gas for analysis

TABLE VI-7 ΣCO_2 results at Cruise 47 Station 1270

DEPTH (m.)	ΣCO_2 (mM kg. ⁻¹)
7	1.655
57	1.792
204	1.873
302	2.112
410	1.965
498	2.112
588	1.904
1251	2.624
1633	2.310
1918	2.511
2344	2.235
2791	2.400
3228	2.251
3627	2.402
3926	2.238
4025	2.355

TABLE VI-8

ΣCO_2 and its isotope variations at Cruise 47 Station 1284.

DEPTH (m.)	ΣCO_2 (mM kg. ⁻¹)	$\delta^{13}\text{C}$ (PDB)	$\delta^{18}\text{O}$ (PDB)
1	2.105	0.70	0.27
60	2.283	-	-
149	2.250	-	-
273	2.545	-7.60	1.84
372	2.400	-2.53	1.60
471	2.276	-1.68	1.16
594	2.229	-0.32	0.50
742	2.267	-0.09	0.93
940	2.223	0.35	1.73
1185	2.281	-	-
1530	2.259	-1.84	0.04
1798	2.328	-1.99	0.77
2095	2.304	-1.02	0.39
2392	2.264	-0.56	0.74
2689	2.272	-1.38	-1.38
2986	2.352	-	-
3283	2.220	-0.53	0.75
3481	2.375	-2.57	1.18
3580	2.306	-0.22	0.78
3630	2.310	-0.49	1.04

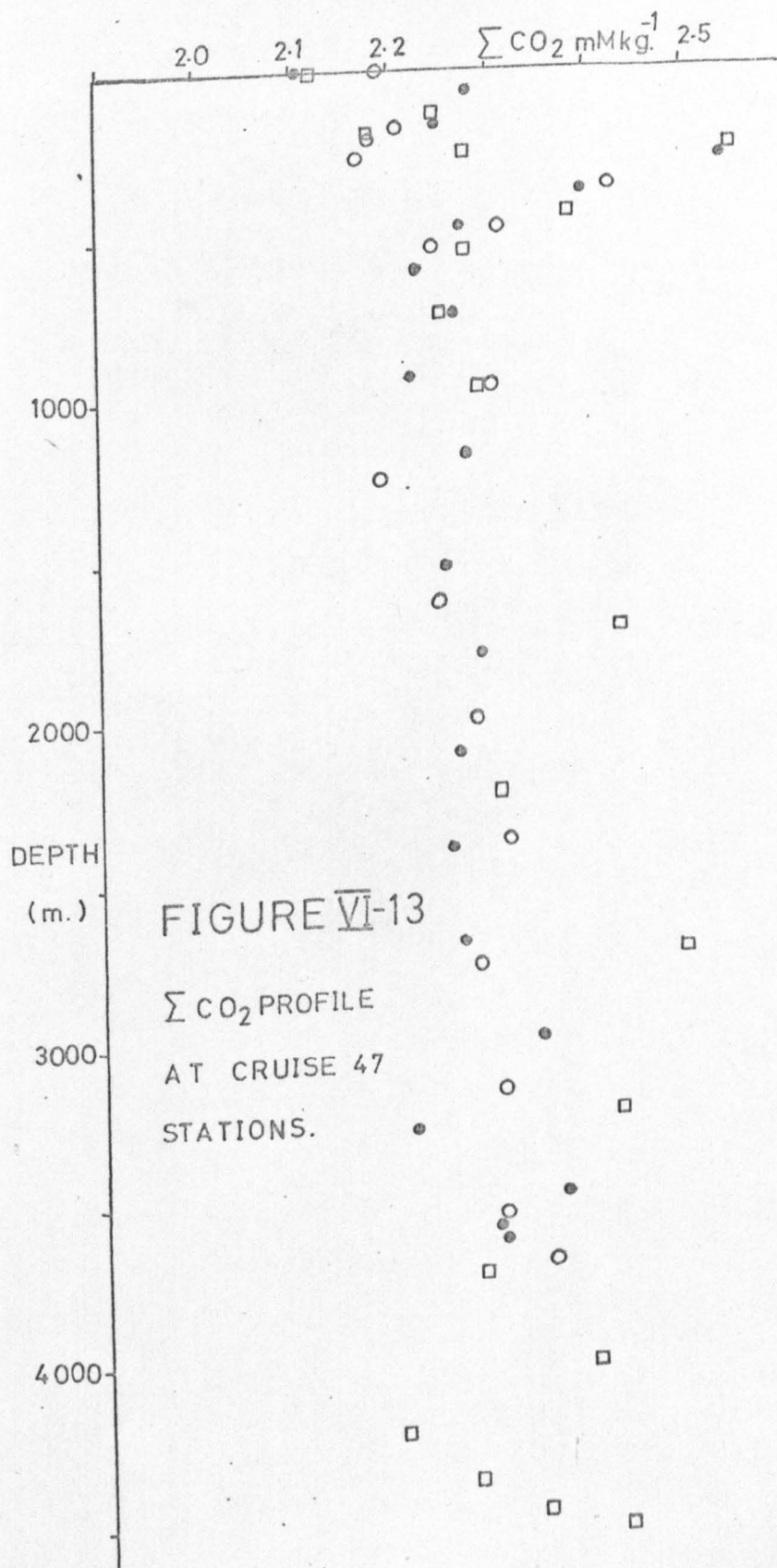
TABLE VI-9

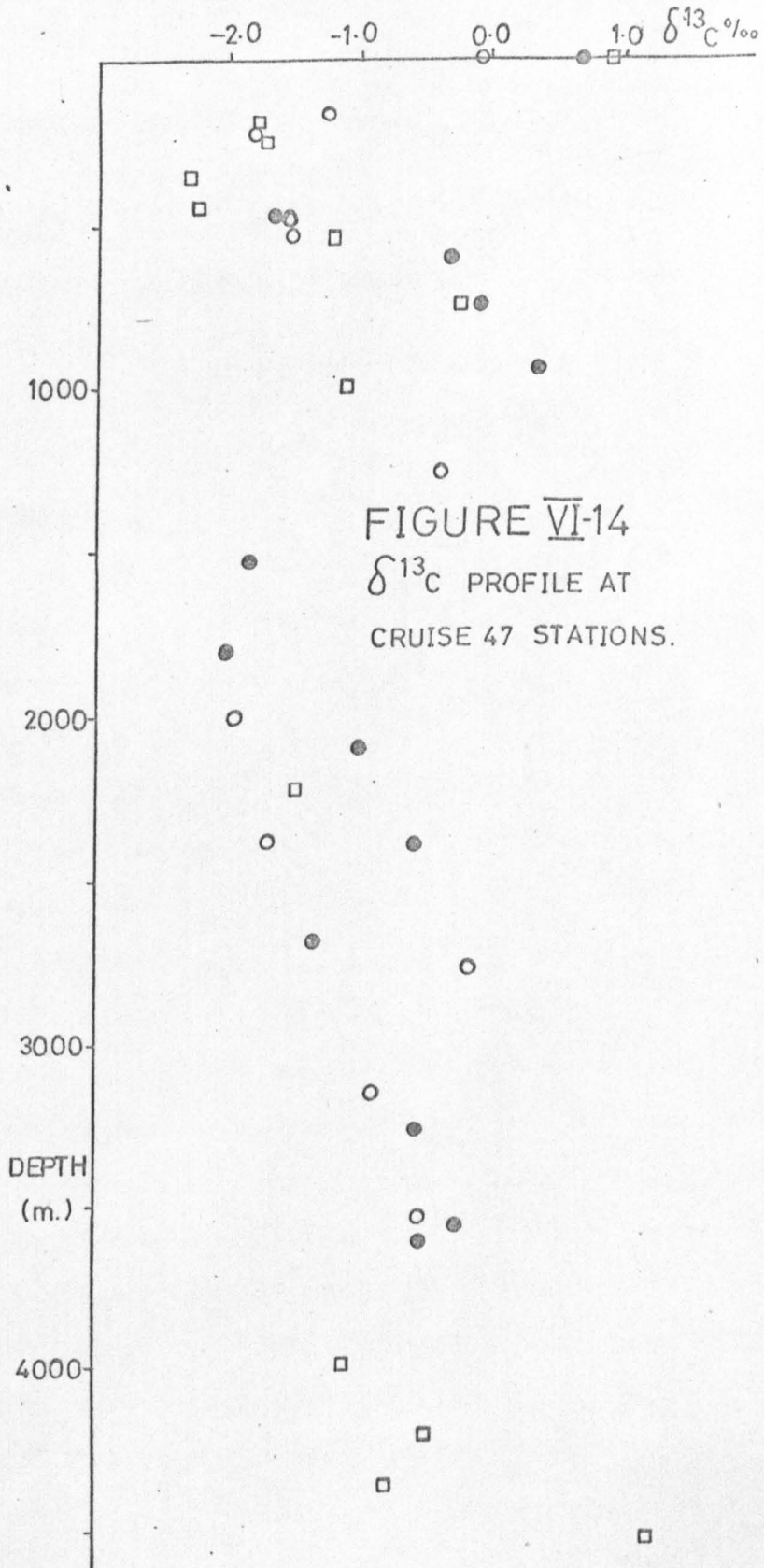
 ΣCO_2 and its isotope ratios at Cruise 47 Station 1308

DEPTH (m.)	ΣCO_2 (mM kg. ⁻¹)	$\delta^{13}\text{C}(\text{PDB})$	$\delta^{18}\text{O}(\text{PDB})$
2	2.109	0.89	0.11
130	2.232	-	-
189	2.181	-1.80	-0.90
248	2.283	-1.72	-0.74
347	2.552	-2.33	-0.34
445	2.391	-2.27	0.41
543	2.278	-1.19	1.68
739	2.261	-0.29	1.92
985	2.333	-1.11	2.20
1729	2.438	-	-
2229	2.313	-1.46	0.53
2729	2.504	-5.61	0.73
3229	2.433	-6.10	0.47
3729	2.286	-6.00	-3.0
4029	2.409	-1.09	-0.46
4229	2.208	-0.45	-1.33
4379	2.280	-0.74	-0.72
4479	2.352	-	-
4529	2.437	1.23	-2.97

TABLE VI-10 ΣCO_2 and its isotope ratios at Cruise 47 Station 1314

DEPTH (m.)	ΣCO_2 (mM kg. ⁻¹)	$\delta^{13}\text{C}(\text{PDB})$	$\delta^{18}\text{O}(\text{PDB})$
2	2.192	-0.07	0.92
172	2.212	-1.24	0.94
210	2.181	-1.80	-0.90
268	2.171	0.79	0.38
365	2.428	-4.13	1.10
482	2.317	-1.56	0.68
531	2.279	-1.52	-0.21
778	2.575	-8.45	0.88
974	2.341	-3.09	0.39
1262	2.190	-0.38	0.75
1635	2.248	-	-
2009	2.320	-1.96	0.92
2386	2.324	-1.69	0.08
2767	2.288	-0.14	1.07
3158	2.311	-0.87	0.73
3555	2.310	-0.50	0.19
3705	2.362	-	-





2.1 mM kg.⁻¹ are in agreement with measurements made by Edmond (quoted in Kroopnick, 1974(b)). Between the surface and the maximum, there are interstation differences - 1314 values being on the whole lower than the others - which are probably local effects. Below the maximum, the data from 1308 are seen to scatter considerably more than those from the other two stations, particularly in the bottom samples. The ΣCO_2 maximum at 300 - 400 m. is mirrored by a minimum in $\delta^{13}\text{C}$, seen in the plot of Figure VI-14. At the surface, values are around 1‰, thereafter falling to below -2‰, at the minimum (Kroopnick, (1974(b)) gives values in the range 1.39 - 1.52‰ for surface samples from 60°S). This indicates that the increase in ΣCO_2 is caused by respiration or the oxidation of organic material. Below 800 m. or so, the $\delta^{13}\text{C}$ data are widely scattered. From Table VI-9 it can be seen that the three samples between 2,700 m. and 4,000 m. at Station 1308 all have $\delta^{13}\text{C}$ below -5‰. Very low values are also seen for individual samples from the other stations and prove that biological effects have not been totally inhibited after sample collection. Since the poisoning agent should have been effective, this may be attributed to the lapse of time between collection and addition of poison or possibly to interaction with the polythene bottle cap insert. The existence of these modifications in the samples precludes the drawing of further conclusions from the results.

APPENDIX 1

Computer program for reduction of mass spectrometer output data to corrected 'delta' values.

This program works out $\delta^{13}\text{C}$ and $\delta^{18}\text{O}$ relative to PDB for a sample CO_2 analysed against the working standard; all necessary corrections are applied except the working standard correction. For results to be reported relative to a standard other than PDB, the CONSTANTS FOR PROGRAM cards must be replaced by those appropriate to the new standard.

C FIRST CARD GIVES NUHRRUN - NUMBER OF RUNS
 C THIS IS FOLLOWED BY NUHPRUN SETS OF CARDS
 C FIRST CARD OF EACH SET IS TITLE OF RUN
 C SECOND CARD - POT VALUE, RATIO FACTOR FOR SAMPLE AND REFERENCE READINGS
 C THIRD CARD - POT VALUE AND RATIO FACTOR FOR BACKGROUND
 C FOURTH CARD - FACTORS VMC,CB,CP,LC,ACC,ACD
 C FIFTH CARD - BACKGROUND READING
 C SIXTH CARD - NUMBER OF SAMPLE READINGS
 C SEVENTH AND SUBSEQUENT CARDS - N SAMPLE READINGS AND N+1 REFERENCE
 C READINGS(UP TO 30 REFERENCE READINGS)

00001 IMPLICIT REAL*8(A-H,O-Z)
 00002 DIMENSION SAM(30),REF(30),DELTA1(30),DELTA2(30),XSAM(30),XREF(30)
 00003 DIMENSION TITLE(20)
 00004 DIMENSION SP(30),RSAM(30),RREF(30) , REFH(30),VDIF(30)
 00005 REAL*8 LC
 00006 MIXED

C
 C READING INPUT DATA

00007 READ(5,101)NUHRRUN
 00008 NIX=NIX+1
 00009 IFLAG=0
 0010 IF(NIX.GT.NUHRRUN)GO TO 9999

0011
0012
0013
0014
0015
0016
0017
0018
0019
0020
0021
0022
0023
0024
0025
0026
0027
0028
0029
0030
0031
0032
0033
0034
0035
0036
0037

2222

99

C
C
C

```

WRITE(6,2501)
READ(5,1003)(TITLE(J),J=1,20)
WRITE(6,104)(TITLE(J),J=1,20)
WRITE(6,218)
READ(5,102)POT1,RFACT1
READ(5,102)POT2,RFACT2
READ(5,100)VMC ,CB,CP,LC ,ACC,ACO
READ(5,101)N
NN=NN+1
READ(5,100)(SAH(J),J=1,N)
READ(5,100)(REF(J),J=1,NN)
WRITE(6,210)
WRITE(6,211)
WRITE(6,200)POT1
WRITE(6,201)RFACT1
WRITE(6,202)POT2
WRITE(6,203)RFACT2
WRITE(6,219)VMC,CB,CP,LC ,ACC,ACO
WRITE(6,602)BCKG
WRITE(6,204)N
DO 99J=1,NN
WRITE(6,205)
WRITE(6,206)REF(J)
IF(J.EQ.NN)GO TO 99
WRITE(6,207)(SAH(J))
99 CONTINUE

```

CONSTANTS FOR PROGRAM
CONSTANTS FOR ANALYSIS W.S. (-4.53,-6.82) 19/11/73.

FORTRAN IV G LEVEL 21

MAIN

DATE = 75164

16/52/16

PAGE 0202

```

0038 CORC1=1.06756
0039 CORC2=0.03378
0040 COR01=1.00139
0041 COR02=0.00902
0042 CONC1=0.99547
0043 CONC2=-4.53
0044 CON01=0.99318
0045 CON02=-6.82

```

C
C
C
C

CALCULATION

```

0046 WRITE(6,212)
0047 WRITE(6,213)
0048 SUM1=0.0
0049 SUM2=0.0
0050 ASUM=0.0
0051 BSUM=0.0
0052 CSUM=0.0
0053 VSUM=0.0
0054 ZSUM=0.0
0055 WSUM=0.0
0056 DO 50 J=1,N
0057 SUM1=SUM1+SAN(J)
0058
0059 50 CONTINUE

```

```

0050
0061
0062
0063
0064
0065
0066
0067
0068
0069
0070
0071
0072
0073
0074
0075
0076
0077
0078
0079
0080
0081
0082
0083
0084
0085
0086
0087
0088
0089

DO 51 J=1,N
SUM2=SUM2+REF(J)
51 CONTINUE
XMA=SUM1/N
XMB=SUM2/N
DO 52 J=1,N
ZA=XHA-SAH(J)
ZA=ZA+ZA
ZSUM=ZSUM+ZA
52 CONTINUE
ZSUM=ZSUM/(N-1)
ZSUM=DSORT(ZSUM)
DO 53 J=1,N
ZR=XIB-REF(J)
ZB=ZB+ZR
YSUM=YSUM+ZR
53 CONTINUE
YSUM=YSUM/(N-1)
YSUM=DSORT(YSUM)
DO 60 J=1,N
JJ=J+1
REFM(J)=REF(J) + REF(JJ)
REFM(J)=REFM(J)/2.0
60 CONTINUE
DO 61 J=1,N
VDIF(J)=SAH(J) - REFM(J)
VSUM=VSUM + VDIF(J)
61 CONTINUE
VMA=VSUM/N
DO 62 J=1,N

```

```

0116 00 90 J=1,N
0117 G1=FACT5+FACT6*RB/SP(J)
0118 G2=FACT5+FACT6*RB/XSAM(J)
0119 GC5=G1/G2
0120 RSAM(J)=(XSAM(J)+LC)*BC5
0121 RREF(J)=(SP (J)+LC)*BC5
0122 90 CONTINUE
0123 WRITE(6,723)
0124 DO 92 J=1,N
0125 DELTA1(J)=(RSAH(J)-RREF(J))*1000.0/RREF(J)
0126 ASUM=ASUM+DELTA1(J)
0127 WRITE(6,726)DELTA1(J)
0128 92 CONTINUE
0129 DLMEAN=ASUM/N
0130 DO 5 J=1,N
0131 S5=DLMEAN-DELTA1(J)
0132 SS=SS+S5
0133 CSUM=CSUM+S5
0134 5 CONTINUE
0135 ABC=CSUM/(N-1)
0136 SIGMA=DSQRT(ABC)
0137 WRITE(6,724)DLMEAN,SIGMA
0138 IF(IFLAG.EQ.1)GO TO 903
0139 D1=DLMEAN
0140 S1=SIGMA
0141 IFLAG=1
0142 GO TO 904
0143 903 CONTINUE
0144 D2=DLMEAN
0145 S2=SIGMA

```

```

0090 VA=VMA - VDIF(J)
0091 VA=VA*VA
0092 MSUM=MSUM + VA
0093 62 CONTINUE
0094 MSUM=MSUM/(N-1)
0095 MSUM=DSQRT(MSUM)
0096 WRITE(6,290)XMA,ZSUM
0097 WRITE(6,291)XMB,YSUM
0098 WRITE(6,292)VMA,MSUM
0099 DO 1 J=1,N
0100 AA=SAN(J)*1.0E-06
0101 XSAM(J)=(POT1+AA)*RFAC1
0102 1 CONTINUE
0103 DO 2 J=1,NN
0104 BB=REF(J)*1.0E-06
0105 XREF(J)=(POT1+BB)*RFAC1
0106 2 CONTINUE
0107 RB=(POT2 + BCKG*1.0E-06)*RFAC2
0108 DO 3 J=1,N
0109 JJ=J+1
0110 SP(J)=XREF(J)+XREF(JJ)
0111 SP(J)=SP(J)/2.0
0112 3 CONTINUE
0113 F5=CB/CP
0114 FACT5=1.+F5
0115 FACT6=F5*FACT5

```

FORTRAN IV G LEVEL 21

HAIN

DATE = 75164

16/52/16

PAGE 0004

```

0146 GO TO 906
0147 994 CONTINUE
0148 GO TO 2222
0149 RFC=D1*VMC*ACC
0150 R00=D2*VMC*ACC
0151 R001=R00
0152 DCH=CORC1*RDC-CORC2*RDO
0153 D0H=COR01*RDO+COR02*DCH
0154 IF(DABS(D0H-RD01))-0,B001)43,43,40
0155 DCH=CORC1*RDC-CORC2*D0H
0156 RD01=RD0H
0157 GO TO 38
0158
0159 43 DCC=CONC1*DCH+CONC2
0160 DDC=CON01*D0H+CON02
0161 WRITE(6,47)DCC,DDC
    WRITE(6,295)
C
    FORMAT STATEMENTS
47 FORMAT(//'/H','FINAL VALUE OF DCC = ',F10.4,6X,'FINAL VALUE OF D0
    1C = ',F10.4)
0162 100 FORMAT(8F10.4)
0163 101 FORMAT(I2)
0164 102 FORMAT(2F10.4)
0165 103 FORMAT(20A4)
0166 104 FORMAT(1H,20A4)
0167 200 FORMAT(//'/H','POT VALUE FOR SAMPLE AND REFERENCE=',F10.4)
0168 201 FORMAT(1H,'RATIO FACTOR FOR SAMPLE AND REFERENCE=',F10.4)
0169

```

```

0170
0171
0172
0173
0174
0175
0176
0177
0178
0179
0180
0181
0182
0183
0184
0185
0186
0187
0188
0189
0190
0191
0192
0193
0194

202 FORMAT (1H , 'POT VALUE FOR BACKGROUND=' , F10.4)
203 FORMAT(1H , 'RATIO FACTOR FOR BACKGROUND=' , F10.4)
204 FORMAT(1H , 'NUMBER OF SAMPLE READINGS=' , I4)
205 FORMAT(///1H , 'SAMPLE READINGS REFERENCE READINGS')
206 FORMAT(1H , '20X, F10.1)
207 FORMAT(1H , 'F10.4)
208 FORMAT(1H , 'MEAN VALUE OF DELTA=' , F10.4, ' AND ERROR=' , F10.4)
209 FORMAT(1H , 'DELTA(H)=', F10.4)
210 FORMAT(///1H , 'INPUT DATA')
211 FORMAT(1H , '15(1*1)')
212 FORMAT(///1H , 'RESULTS')
213 FORMAT(1H , '10(1*1)')
214 FORMAT(1H , 'F=' , F10.4)
216 FORMAT(///1H , 'VALUES OF DELTA AVERAGING SAMPLE READINGS')
218 FORMAT(1H , '26(1*1)')
219 FORMAT(1H , 'VNC=' , F10.4, '10X, 'CB=' , F10.4, '10X, 'CP=' , F10.4, '10X, 'LC=' ,
1 F10.4, '10X, 'ACCE=' , F10.4, '10X, 'ACO=' , F10.4)
250 FORMAT(1H1, 'NEW PASS'///)
290 FORMAT(///1H , 'MEAN AND STANDARD DEVIATION OF SAMPLE READINGS=' ,
1 2(F10.2,5X))
291 FORMAT(1H , 'MEAN AND STANDARD DEVIATION OF REFERENCE READINGS=' ,
1 2(F10.2,5X))
292 INCE READING=' , 2(F10.2,5X))
295 FORMAT(///1H , '12Q(1*1)')
602 FORMAT(1H , 'BACKGROUND READING=' , F10.4)
723 FORMAT(///1H , 'VALUES OF DELTA')
724 FORMAT(///1H , 'MEAN VALUE AND STANDARD DEVIATION OF DELTA=' , 2(F10.4)
726 FORMAT(1H , '15X, F12.4)

```

C

0195 GO TO 1111
0196 9999 STOP
0197 END

OPTIONS IN EFFECT NOID,EBDCIC,SOURCE,NOLIST,HODECK,LOAD,NOMAP
OPTIONS IN EFFECT NAME = MAIN , LINECNT = 58
STATISTICS SOURCE STATEMENTS = 197,PROGRAM SIZE = 8032
STATISTICS NO DIAGNOSTICS GENERATED

NEW PASS

MSS VS B 3-2-11 13C 8/8/74 AN 7/10/74 45/44

INPUT DATA

POT VALUE FOR SAMPLE AND REFERENCE= 0.6000
RATIO FACTOR FOR SAMPLE AND REFERENCE= 0.0200
POT VALUE FOR BACKGROUND= 0.0
RATIO FACTOR FOR BACKGROUND= 0.0
VRCE 1.0010 CB= 0.0
BACKGROUND READING= 0.0
NUMBER OF SAMPLE READINGS= 6

CP= 8.0000
ACD= 1.0004

LC= 0.0

ACC= 1.0008

SAMPLE READINGS	REFERENCE READINGS
6634.0000	4402.0
6620.0000	4405.0
6676.0000	4451.0
6741.0000	4465.0
6777.0000	4558.0
6830.0000	4608.0
	4652.0

RESULTS

MEAN AND STANDARD DEVIATION OF SAMPLE READINGS= 6713.00 83.46

MEAN AND STANDARD DEVIATION OF REFERENCE READINGS= 4505.86 100.12

MEAN AND STANDARD DEVIATION OF SAMPLE READING - REFERENCE READING= 2210.67 17.56

VALUES OF DELTA

3.6904
 3.6266
 3.6694
 3.6881
 3.6289
 3.6386

MEAN VALUE AND STANDARD DEVIATION OF DELTA= 3.6370 0.0293
 46/44+45

INPUT DATA

POT VALUE FOR SAMPLE AND REFERENCE= 0.8400
 RATIO FACTOR FOR SAMPLE AND REFERENCE= 0.0050
 POT VALUE FOR BACKGROUND= 0.0
 RATIO FACTOR FOR BACKGROUND= 0.0
 VMC= 1.0010 CB= 0.0
 BACKGROUND READING= 0.0
 NUMBER OF SAMPLE READINGS= 5
 CP= 6.0000
 ACC= 1.0008
 ACO= 1.0004
 LC= 0.0

SAMPLE READINGS	REFERENCE READINGS
6921.0000	1404.0
7032.0000	1540.0
7121.0000	1630.0
7202.0000	1709.0
7351.0000	1821.0
	1869.0

RESULTS

MEAN AND STANDARD DEVIATION OF SAMPLE READINGS= 7125.40 163.77
 MEAN AND STANDARD DEVIATION OF REFERENCE READINGS= 1662.17 174.82
 MEAN AND STANDARD DEVIATION OF SAMPLE READING - REFERENCE READING= 5458.10 27.34

VALUES OF DELTA

6.4756
6.4723
6.4770
6.4590
6.5404

MEAN VALUE AND STANDARD DEVIATION OF DELTA= 6.4849 0.0318

FINAL VALUE OF DCC = 0.8564 FINAL VALUE OF DCC = 0.3283

APPENDIX 2

Results of working standard check analyses. Results of both $\delta^{13}\text{C}$ and $\delta^{18}\text{O}$ are relative to PDB; the figure in brackets is the 1σ standard deviation.

ANALYSIS NUMBER	DATE	SAMPLE	REFERENCE	$\delta^{13}\text{C}$	$\delta^{18}\text{O}$
1	8.11.72	WS1	WS6	-4.50(4)	-6.99(6)
2	9.11.72	WS5	WS6	-4.54(6)	-7.03(5)
3	16.11.72	WS3	WS6	-4.48(3)	-7.14(11)
4	20.11.72	WS4	WS6	-4.52(3)	-7.03(5)
5	7.12.72	WS3	WS6	-4.44(9)	-6.92(6)
6	9.1.73	WS5	WS6	-4.63(4)	-6.93(5)
7	10.1.73	WS4	WS6	-4.49(3)	-6.98(4)
8	11.1.73	WS3	WS6	-4.59(7)	-6.82(8)
9	17.1.73	WS1	WS6	-4.51(3)	-6.94(7)
10	18.1.73	WS5	WS6	-4.37(5)	-6.81(4)
11	29.1.73	WS4	WS6	-4.51(3)	-6.99(5)
12	16.4.73	WS1	WS6	-4.51(8)	-6.71(11)
13	18.4.73	WS1	WS6	-4.53(3)	-6.91(8)
14	19.4.73	WS2	WS6	-4.49(3)	-6.92(14)
15	23.4.73	WS3	WS6	-4.50(3)	-6.73(5)
16	23.4.73	WS4	WS6	-4.57(4)	-6.82(11)
17	26.4.73	WS1	WS6	-4.52(4)	-6.95(7)
18	26.4.73	WS2	WS6	-4.55(5)	-6.83(8)
19	26.6.73	WS5	WS5	-4.47(3)	-6.79(3)
20	27.6.73	WS3	WS5	-4.54(2)	-6.83(8)
21	29.6.73	WS4	WS5	-4.38(6)	-6.75(6)

ANALYSIS NUMBER	DATE	SAMPLE	REFERENCE	$\delta^{13}\text{C}$	$\delta^{18}\text{O}$
22	2.7.73	WS1	WS5	-4.43(3)	-6.84(5)
23	3.7.73	WS2	WS5	-4.42(4)	-6.77(7)
24	4.7.73	WS3	WS5	-4.38(2)	-6.85(9)
25	7.7.73	WS4	WS5	-4.53(7)	-6.82(9)
26	7.7.73	WS4	WS5	-4.48(5)	-6.82(7)
27	10.7.73	WS1	WS5	-4.47(6)	-6.80(3)
28	12.7.73	WS2	WS5	-4.45(4)	-6.85(4)
29	13.7.73	WS3	WS5	-4.53(2)	-6.83(7)
30	17.7.73	WS4	WS5	-4.51(4)	-6.90(4)
31	19.7.73	WS2	WS5	-4.48(4)	-6.89(8)
32	19.7.73	WS1	WS5	-4.50(5)	-6.79(5)
33	27.7.73	WS1	WS5	-4.54(4)	-6.83(4)
34	31.7.73	WS2	WS5	-4.54(5)	-6.76(4)
35	6.8.73	WS3	WS5	-4.51(4)	-6.89(8)
36	16.8.73	WS3	WS5	-4.51(3)	-6.89(9)
37	17.8.73	WS4	WS5	-4.51(6)	-6.89(8)
38	28.8.73	WS2	WS5	-4.51(4)	-6.84(3)
39	3.9.73	WS3	WS5	-4.50(3)	-6.88(4)
40	20.9.73	WS2	WS5	-4.51(2)	-6.92(4)
41	11.10.73	WS1	WS5	-4.47(5)	-6.87(3)
42	16.10.73	WS1	WS5	-4.50(1)	-6.82(3)
43	19.10.73	WS4	WS5	-4.50(2)	-6.88(4)
44	19.10.73	WS4	WS5	-4.51(2)	-6.87(4)
45	25.10.73	WS3	WS5	-4.49(2)	-6.87(4)
46	30.10.73	WS1	WS5	-4.49(4)	-6.80(3)

ANALYSIS NUMBER	DATE	SAMPLE	REFERENCE	$\delta^{13}\text{C}$	$\delta^{18}\text{O}$
47	2.11.73	WS3	WS5	-4.55(3)	-6.75(4)
48	5.11.73	WS4	WS5	-4.51(3)	-6.88(4)
49	6.11.73	WS8	WS5	-4.51(4)	-6.79(3)
50	6.11.73	WS8	WS5	-4.45(2)	-6.78(6)
51	6.12.73	WS8	WS5	-4.56(5)	-6.87(8)
52	12.3.74	WS3	WS5	-4.49(8)	-6.92(6)
53	13.3.74	WS3	WS5	-4.52(5)	-6.89(7)
54	14.3.74	WS3	WS5	-4.49(3)	-6.88(5)
55	14.3.74	WS1	WS5	-4.51(2)	-6.90(5)
56	14.3.74	WS4	WS5	-4.52(2)	-6.98(6)
57	14.3.74	WS4	WS5	-4.49(2)	-6.93(4)
58	14.3.74	WS8	WS5	-4.47(4)	-6.98(5)
59	19.3.74	WS1	WS5	-4.54(3)	-6.79(7)
60	29.4.74	WS5	WS5	-4.50(4)	-6.82(6)
61	30.4.74	WS1	WS5	-4.50(4)	-6.94(5)
62	1.5.74	WS3	WS5	-4.51(3)	-6.81(4)
63	2.5.74	WS4	WS5	-4.54(2)	-6.84(4)
64	3.5.74	WS1	WS5	-4.51(3)	-6.90(4)
65	3.5.74	WS3	WS5	-4.52(3)	-6.94(5)
66	6.5.74	WS4	WS5	-4.48(4)	-6.77(2)
67	6.5.74	WS1	WS5	-4.48(5)	-6.92(5)
68	7.5.74	WS3	WS5	-4.50(4)	-6.87(4)
69	9.5.74	WS4	WS5	-4.52(3)	-6.81(5)
70	17.5.74	WS1	WS5	-4.50(2)	-6.76(7)
71	20.5.74	WS3	WS5	-4.49(1)	-6.81(5)

ANALYSIS NUMBER	DATE	SAMPLE	REFERENCE	$\delta^{13}\text{C}$	$\delta^{18}\text{O}$
72	21.5.74	WS4	WS5	-4.52(3)	-6.87(5)
73	4.6.74	WS1	WS5	-4.51(4)	-6.91(4)
74	15.7.74	WS1	WS5	-4.56(2)	-6.74(3)
75	16.7.74	WS3	WS5	-4.50(3)	-6.84(7)
76	17.7.74	WS4	WS5	-4.49(4)	-6.79(5)
77	6.8.74	WS1	WS5	-4.50(8)	-6.78(8)
78	7.8.74	WS3	WS5	-4.48(4)	-6.86(11)
79	13.8.74	WS4	WS5	-4.56(4)	-6.79(9)
80	14.8.74	WS1	WS5	-4.54(5)	-6.92(4)
81	19.9.74	WS1	WS5	-4.53(2)	-6.81(1)
82	24.9.74	WS8	WS5	-4.49(2)	-6.85(4)
83	25.9.74	WS3	WS5	-4.53(2)	-6.79(4)
84	26.9.74	WS4	WS5	-4.53(3)	-6.84(2)
85	27.9.74	WS1	WS5	-4.48(5)	-6.87(2)
86	7.10.74	WS3	WS5	-4.54(3)	-6.82(3)
87	8.10.74	WS4	WS5	-4.49(2)	-6.83(2)
88	5.11.74	WS1	WS5	-4.53(3)	-6.85(2)
89	12.12.74	WS4	WS5	-4.54(3)	-6.82(3)
90	13.12.74	WS1	WS5	-4.48(2)	-6.79(1)
91	16.12.74	WS1	WS5	-4.51(7)	-6.90(3)
92	17.12.74	WS3	WS5	-4.55(4)	-6.89(1)
93	18.12.74	WS4	WS5	-4.56(2)	-6.84(3)
94	19.12.74	WS8	WS5	-4.50(1)	-6.79(3)
95	2.1.75	WS1	WS5	-4.57(3)	-6.92(2)
96	6.1.75	WS3	WS5	-4.52(3)	-6.82(3)

ANALYSIS NUMBER	DATE	SAMPLE	REFERENCE	$\delta^{13}\text{C}$	$\delta^{18}\text{O}$
97	7.1.75	WS4	WS5	-4.54(2)	-6.82(3)
98	9.1.75	WS8	WS5	-4.53(3)	-6.82(2)
99	13.1.75	WS8	WS5	-4.56(2)	-6.85(3)
100	14.1.75	WS1	WS5	-4.57(2)	-6.84(3)
101	15.1.75	WS3	WS5	-4.54(2)	-6.83(3)
102	16.1.75	WS4	WS5	-4.58(1)	-6.83(3)
103	20.1.75	WS1	WS8	-4.54(3)	-6.86(1)
104	22.1.75	WS3	WS8	-4.56(2)	-6.81(1)
105	24.2.75	WS1	WS8	-4.53(3)	-6.82(2)
106	25.2.75	WS3	WS8	-4.56(1)	-6.84(4)
107	26.2.75	WS4	WS8	-4.53(3)	-6.80(4)
108	27.2.75	WS1	WS8	-4.48(4)	-6.84(1)
109	28.2.75	WS3	WS8	-4.54(4)	-6.80(3)
110	13.6.75	WS1	WS8	-4.54(5)	-6.83(2)

REFERENCES

- Abelson, P.H. and Hoering, T.C. (1961) Carbon isotope fractionation in formation of amino acids by photosynthetic organisms, Proc. Nat. Acad. Sci., 47, 623-632.
- Anon. (1974) Mathematical problems: a committee to replace Hilbert, Science, 185, 430.
- Arons, A.B., and Stommel, H. (1967) On the abyssal circulation of the world ocean - III. An advection - lateral mixing model of the distribution of a tracer property in an ocean basin. Deep-Sea Res., 14, 441-457.
- Baranov, G.I., and Botnikov, V.N. (1964) Surface of no motion and water masses in the Weddell Sea, Soviet Antarctic Exped. Inform. Bull., English Translation, 5, 385-388.
- Barber, R.T. (1966) Interaction of bubbles and bacteria in the formation of organic aggregates in sea water, Nature, 211, 257-258.
- Barcilon, V. (1966) On the influence of the peripheral Antarctic water discharge on the dynamics of the Circumpolar Current, J. Mar. Res., 24, 269-275.
- Barcilon, V. (1967) Further investigation of the influence of the peripheral Antarctic water discharge on the Circumpolar Current, J. Mar. Res., 25, 1-9.

- Baylor, E.R., and Sutcliffe, W.H. (1963) Dissolved organic matter in sea water as a source of particulate food, *Limnol. Oceanogr.*, 8, 369-371.
- Beckinsale, R.D., Freeman, N.J., Jackson, M.C., Powell, R.E. and Young, W.A.P. (1973) A 30 cm. radius 90° sector double collecting mass spectrometer with a capacitor integrating detector for high precision isotopic analysis of carbon dioxide, *Int. Jour. Mass Spectrom. Ion Phys.*, 12, 299-308.
- Bolin, B., and Stommel, H. (1961) On the abyssal circulation of the world ocean - IV. Origin and rate of circulation of deep ocean water as determined with the aid of tracers. *Deep-Sea Res.*, 8, 95-110.
- Bottinga, Y., and Craig, H. (1969) Oxygen isotope fractionation between CO₂ and water, and the isotopic composition of marine atmospheric CO₂, *Earth Planet. Sci. Lett.*, 5, 285-295.
- Brennecke, W. (1921) Die ozeanographischen Arbeiten der Deutschen Antarktischen Expedition, 1911-1912, *Arch. Deutsche Seewarte*, 39(1), 1-216.
- Bridger, N.I., Craig, R.D., and Sercombe, J.S.F. (1974) New mass spectrometer for isotopic analysis of small gas samples, In: *Advances in Mass Spectrometry (vol.6)*, ed. A.R. West, Applied Science Publishers, Barking, 1974.

- Broecker, W.S. (1963) Radioisotopes and large-scale oceanic mixing, In: The Sea (vol.2), ed. M.N. Hill, Interscience Publishers, London, 1963.
- Broecker, W.S., and Takahashi, T. (1966) Calcium carbonate precipitation in the Bahama Banks, Jour. Geophys. Res., 71, 1575-1602.
- Broecker, W.S., Li, Y-H., and Peng, T-H. (1971) Carbon-dioxide - man's unseen artifact, In: Impingement of Man on the Oceans, ed. D.W. Hood, John Wiley and Sons Inc., New York, 1971.
- Brown, R.M. (1972) Provisional list of results - October 1971, on stable isotope intercomparison on water and marble standards reported to IAEA, personal communication, 1972.
- Bryden, H.L. (1973) New polynomials for thermal expansion, adiabatic temperature gradient and potential temperature of sea water, Deep-Sea Res., 20, 401-408.
- Buch, K. (1938) New determination of the second dissociation constant of carbonic acid in seawater, Acta. Acad. Aeoensis Mat. Phys., 11(5): 18p
- Buch, K. (1951) Das Kohlensäure Gleichgewichtssystem im Meerwasser, Havsforskningsinst. Skr. Helsingfors, no. 151, 18p.
- Bullard, E.C. (1963) The flow of heat through the floor of the ocean, In: The Sea (vol.3), ed. M.N. Hill, Interscience Publishers, London, 1963.

- Callahan, J.E. (1971) Velocity structure and flux of the Antarctic Circumpolar Current south of Australia, Jour. Geophys. Res., 76, 5859-5864.
- Calvert, S.E. (1975) Finding answers from the seas: review of The Sea (vol. 5), ed. E.D. Goldberg, Nature, 254, 234.
- Carpenter, J.H. (1965) The Chesapeake Bay Institute technique for the Winkler dissolved oxygen method, Limnol. Oceanogr., 10, 141-143.
- Chung, Y-C. (1971) Pacific deep and bottom water studies based on temperature, radium and excess-radon measurements, Ph.D. Thesis, University of California, San Diego, 1971.
- Chung, Y-C., and Craig, H. (1973) Radium-226 in the eastern equatorial Pacific, Earth Planet. Sci. Lett., 17, 306-318.
- Clowes, A.J. (1938) Phosphate and silicate in the Southern Ocean, Discovery Rept., 19, 1-20.
- Committee on Polar Research (1974) Southern Ocean Dynamics. A Strategy for Scientific Exploration 1973-1983. Report of Ad Hoc Working Group on Antarctic Oceanography, Panel on Oceanography, Committee on Polar Research, National Research Council National Academy of Sciences, Washington D.C. 1974.
- Cook, F.D., Wellman, R.P., and Krouse, H.R. (1973) Nitrogen isotope fractionation in the nitrogen cycle, In: Proc. of Symp. of Hydrogeochemistry and Biogeochemistry (vol.II), ed. Earl Ingerson, Tokyo, Japan, 1973.

- Craig, H. (1953) The geochemistry of the stable carbon isotopes, *Geochim. et Cosmochim. Acta*, 3, 53-92.
- Craig, H. (1957) Isotopic standards for carbon and oxygen and correction factors for mass-spectrometric analysis of carbon dioxide, *Geochim. et Cosmochim. Acta*, 12, 133-149.
- Craig, H. (1958) A critical evaluation of mixing rates in oceans and atmosphere by use of radiocarbon techniques, *Proc. 2nd. U.N. Int. Conf. on the Peaceful Uses of Atomic Energy*, 18, 358-363, United Nations, Geneva.
- Craig, H. (1961) Standard for reporting concentrations of deuterium and oxygen-18 in natural waters, *Science*, 133, 1833-1834.
- Craig, H. and Gordon, L.I. (1965) Isotopic oceanography: deuterium and oxygen 18 variations in the ocean and the marine atmosphere, *Symp. Marine Geochem.*, Occasional Pub. Naragansset Marine Lab. 3-1965, 277p., Univ. Rhode Island.
- Craig, H. (1969) Abyssal carbon and radiocarbon in the Pacific, *Jour. Geophys. Res.*, 74, 5491-5506.
- Craig, H. (1970) Abyssal carbon-13 in the South Pacific, *Jour. Geophys. Res.*, 75, 691-695.
- Craig, H. (1971) The deep metabolism: oxygen consumption in abyssal ocean water, *Jour. Geophys. Res.*, 76, 5078-5086.

- Culberson, C. and Pytkowicz, R.M. (1968) Effect of pressure on carbonic acid, boric acid, and the pH in seawater, *Limnol. Oceanogr.*, 13, 403-417.
- Culberson, C. and Pytkowicz, R.M. (1970) Oxygen - total carbon dioxide correlation in the eastern Pacific Ocean, *Jour. Oceanogr. Soc. Japan*, 26, 95-100.
- Deacon, G.E.R. (1933) A general account of the hydrology of the South Atlantic Ocean, *Discovery Rept.*, 7, 171-238.
- Deacon, G.E.R. (1937) The hydrology of the Southern Ocean, *Discovery Rept.*, 15, 1-24.
- Deacon, G.E.R. (1963) The Southern Ocean, Ideas and observations on progress in the study of the seas, In: *The Sea (vol. 2)*, ed. M.N. Hill, Interscience Publishers, London, 1963.
- Defant, A. (1961) *Physical Oceanography (vol. 1)*, Pergamon Press, London, 1961.
- Degens, E.T., Guillard, R.R.L., Sackett, W.M., and Hellebust, J.A. (1968(a)) Metabolic fractionation of carbon isotopes in marine plankton - I. Temperature and respiration experiments, *Deep-Sea Res.*, 15, 1-9.
- Degens, E.T., Behrendt, M., Gotthardt, B., and Reppmann, E. (1968(b)) Metabolic fractionation of carbon isotopes in marine plankton - II. Data on samples collected off the coasts of Peru and Ecuador, *Deep-Sea Res.*, 17, 19-27.

- Deines, P. (1970) Mass spectrometer correction factors for the determination of small isotopic composition variations of carbon and oxygen, *Int. Jour. Mass Spectrom. Ion Phys.*, 4, 283-295.
- Deuser, W.G., and Hunt, J.M. (1969) Stable isotope ratios of dissolved inorganic carbon in the Atlantic, *Deep-Sea Res.*, 16, 221-225.
- Deuser, W.G. (1974) The oceanic carbon cycle, *United States Naval Research Review*, April 1974, 1-7.
- Devine, M. (1972) Some aspects of the dynamics of the Antarctic Circumpolar Current, *Jour. Geophys. Res.*, 77, 5987-5992.
- Dyrssen, D. (1969) The carbonate system, In: *Chemical Oceanography*, ed. R. Lange, Oslo: Universitetsforlaget, 1969.
- Dyrssen, D. and Sillen, L.G. (1967) Alkalinity and total carbonate in sea water. A plea for p-T independent data, *Tellus*, 19, 113-121.
- Edmond, J.M. (1970) High precision determination of titration alkalinity and total carbon dioxide content of sea water by potentiometric titration, *Deep-Sea Res.*, 17, 737-750.
- Edmond, J.M. and Gieskes, J.M.T.M. (1970) On the calculation of the degree of saturation of sea water with respect to calcium carbonate under in situ conditions, *Geochim. et Cosmochim. Acta*, 34, 1261-1291.
- Edmond, J.M. (1973) The silica budget of the Antarctic Circumpolar Current, *Nature*, 241, 391-393.

- Edmond, J.M. (1974) On the dissolution of carbonate and silicate in the deep ocean, *Deep-Sea Res.*, 21, 455-480.
- Epstein, S. and Mayeda, T. (1953) Variation of O^{18} content of waters from natural sources, *Geochim. et Cosmochim. Acta*, 4, 213-224.
- Fairhall, A.W. (1973) Accumulation of fossil CO_2 in the atmosphere and the sea, *Nature*, 245, 20-23.
- Fofonoff, N.P. (1956) Some properties of sea water influencing the formation of Antarctic bottom water, *Deep-Sea Res.*, 4, 32-35.
- Foster, T.D. (1972) An analysis of the cabbeling instability in sea water, *Jour. Phys. Oceanogr.*, 2, 294-301.
- Friedman, I. (1953) Deuterium content of natural waters and other substances, *Geochim. et Cosmochim. Acta*, 4, 89-103.
- Galimov, E.M., Grinenko, V.A., and Ustinov, V.I. (1965) Instrumental errors during precision determination of the isotopic composition of the elements, (In Russian), *Zhurnal Analiticheskoi Khimii*, 20, 547-553.
- Gill, A.E. and Turner, J.S. (1969) Some new ideas about the formation of Antarctic Bottom Water, *Nature*, 224, 1287-1288.
- Gill, A.E. (1971) Ocean models, *Phil. Trans. R. Soc. Lond. A.*, 270, 391-413.
- Gill, A.E. (1973) Circulation and bottom water production in the Weddell Sea, *Deep-Sea Res.*, 20, 111-140.

- Gonfiantini, R. (1970) Mass spectrometer data treatment for $\delta^{18}\text{O}$ and $\delta^{13}\text{C}$ determination, Internal Report, I.A.E.A. Section of Isotope Hydrology.
- Gordon, A.L. (1968) Comment on the peripheral Antarctic-water discharge, *J. Mar. Res.*, 26, 78-79.
- Gordon, A.L. (1971) Oceanography of Antarctic Waters, In: *Antarctic Oceanology I*, ed. J.L. Reid, *Antarct. Res. Ser. Am. geophys. Un.*, 15, 169-204.
- Gordon, A.L. (1972) Introduction: physical oceanography of the southeast Indian Ocean, In: *Antarctic Oceanology II*, ed. D.E. Hayes, *Antarct. Res. Ser. Am. geophys. Un.*, 19, 3-9.
- Gordon, A.L. and Tchernia, P. (1972) Waters of the continental margin off Adelie Coast, Antarctica, In: *Antarctic Oceanology II*, ed. D.E. Hayes, *Antarct. Res. Ser. Am. geophys. Un.*, 19, 59-70.
- Green, E.J. and Carritt, D.E. (1967) New tables for oxygen saturation of seawater, *J. Mar. Res.*, 25, 140-147.
- Gundersen, K. and Mountain, C.W. (1973) Oxygen utilization and pH change in the ocean resulting from biological nitrate formation, *Deep-Sea Res.*, 20, 1083-1091.
- Gunther, E.R. (1936) A report on oceanographical investigations in the Peru Coastal Current, *Discovery Rept.*, 13, 107-276.
- Halsted, R.E. and Nier, A.O. (1950) Gas flow through the mass spectrometer viscous leak, *Rev. Sci. Instr.*, 21, 1019-1021.

- Hansson, I. (1972) An analytical approach to the carbonate system in sea water, Ph.D. Thesis, Goteborgs Universitet-Chalmers Tekniska Hogskola, Goteborg, Sweden, 1972. see also:
- Hansson, I. (1973) Determination of the acidity constant of boric acid in synthetic seawater media, Acta Chem. Scand., 27, 924-930.
- Hansson, I. (1973) The determination of dissociation constants of carbonic acid in synthetic sea water in the salinity range of 20-40‰ and temperature range of 5-30°C, Acta Chem. Scand., 27, 931-944.
- Hansson, I. (1973) A new set of acidity constants for carbonic acid and boric acid in sea water, Deep-Sea Res., 20, 461-478.
- Hansson, I. (1973) A new set of pH-scales and standard buffers for sea water, Deep-Sea Res., 20, 479-491
- Hansson, I. and Jagner, D. (1973) Evaluation of the accuracy of Gran plots by means of computer calculations. Application to the potentiometric titration of the total alkalinity and carbonate content in sea water, Anal. Chim. Acta, 65, 363-373.
- Hidaka, K. and Tsuchiya, M. (1953) On the Antarctic Circumpolar Current, J. Mar. Res., 12, 214-222.
- Holm-Hansen, O., Strickland, J.D.H., and Williams, P.M. (1966) A detailed analysis of biologically important substances in a profile off southern California, Limnol. Oceanogr., 11, 548.

- Holm-Hansen, O. (1969) Determination of microbial biomass in ocean profiles, *Limnol. Oceanogr.*, 14, 740.
- Horibe, Y. and Shigehara, K. (1972) Oxygen-18 content of dissolved oxygen in the South Pacific, (Abstract), In: *Oceanography of the South Pacific 1972*, compiled R. Fraser, New Zealand National Commission for Unesco, Wellington, 1973.
- Hufford, G.L. and Seabrooke, J.M. (1970) Water masses of the Weddell Sea, *Antarctic Journal*, Jan.-Feb. 1970, 13-14.
- Ichimura, S., Saijo, Y., and Aruga, Y. (1962) Photosynthetic characteristics of marine phytoplankton and their ecological meaning in the chlorophyll method, *Bot. Mag., Tokyo*, 75, 212-220.
- Idyll, C.P. (1973) The anchovy crisis, *Scientific American*, 228, 22-29.
- Jackson, H.G., Libby, L.M., and Lukens, H.R. (1973) Measurement of $^{18}\text{O}/^{16}\text{O}$ ratio using a fast neutron reactor, *Jour. Geophys. Res.*, 78, 7145-7148.
- Jacobs, S.S., Amos, A.F., and Bruchhausen, P.M. (1970) Ross Sea oceanography and Antarctic Bottom Water formation, *Deep-Sea Res.*, 17, 935-962.
- Jacobs, S.S., Bauer, E.B., Bruchhausen, P.M., Gordon, A.L., Root, T.F., Rosselot, F.L. (1974) *Eltanin Reports. Cruises 47-50, 1971; 52-55, 1972.* Lamont-Doherty Geological Observatory of Columbia University, Palisades, New York, 1974.

- Kamen, M.D. and Barker, H.A. (1945) Inadequacies in present knowledge of the relation between photosynthesis and the O^{18} content of atmospheric O_2 , Nat. Acad. Sci. Proc., 31, 8.
- Kasahara, H. (1970) Commercial fisheries, In: Scientific Exploration of the South Pacific, ed. W.S. Wooster, National Academy of Sciences, Washington, D.C. 1970.
- Keeling, C.D. and Bolin, B. (1967) The simultaneous use of chemical tracers in oceanic studies I. General theory of reservoir models, Tellus, 19, 566-581.
- Keeling, C.D. and Bolin, B. (1968) The simultaneous use of chemical tracers in oceanic studies II. A three-reservoir model of the North and South Pacific Oceans, Tellus, 20, 17-54.
- Killworth, P.D. (1973) A two-dimensional model for the formation of Antarctic Bottom Water, Deep-Sea Res., 20, 941-971.
- Kirwan, A.D., Jr. (1965) On the use of the Rayleigh-Ritz method for calculating the eddy diffusivity, In: Symposium on diffusion in oceans and fresh waters, August 31-September 2, 1964, ed. T. Ichiye, Document AD 627 883 Unclas. Lamont-Geological Observatory, Palisades, N.Y. 173p. Dec. 1965.
- Kistemaker, J. (1953) The influence of fractionizing and viscosity effects in mass spectrometric gas handling systems, In: Mass Spectrometry in Physics Research, U.S. Nat. Bur. Stand. Circular 522, 243-247.

- Koczy, F.F. (1958) Natural radium as a tracer in the ocean, Proc. 2nd. U.N. Int. Conf. on the Peaceful Uses of Atomic Energy, 18, 351-357, United Nations, Geneva.
- Kroopnick, P.M., Deuser, W.G., and Craig, H. (1970) Carbon ^{13}C measurements on dissolved inorganic carbon at the North Pacific (1969) Geosecs Station, Jour. Geophys. Res., 75, 7668-7671.
- Kroopnick, P.M. (1971) Oxygen and carbon in the oceans and atmosphere: stable isotopes as tracers for consumption, production, and circulation models, Ph.D. Dissertation, University of California, San Diego, 1971.
- Kroopnick, P.M., Weiss, R.F., and Craig, H. (1972) Total CO_2 , ^{13}C and dissolved oxygen - ^{18}O at Geosecs II in the North Atlantic, Earth Planet. Sci. Lett., 16, 103-110.
- Kroopnick, P.M. and Craig, H. (1972) Atmospheric oxygen: isotopic composition and solubility fractionation, Science, 175, 54-55.
- Kroopnick, P.M. (1974(a)) The dissolved $\text{O}_2\text{-CO}_2\text{-}^{13}\text{C}$ system in the eastern equatorial Pacific, Deep-Sea Res., 21, 211-227.
- Kroopnick, P.M. (1974(b)) Correlations between ^{13}C and ΣCO_2 in surface waters and atmospheric CO_2 , Earth Planet. Sci. Lett., 22, 397-403.
- Kuo, H.H. and Veronis, G. (1970) Distribution of tracers in the deep oceans of the world, Deep-Sea Res., 17, 29-46.

- Kuo, H.H. and Veronis, G. (1973) The use of oxygen as a test for an abyssal circulation model, *Deep-Sea Res.*, 20, 871-888.
- Lane, G.A. and Dole, M. (1956) Fractionation of oxygen isotopes during respiration, *Science*, 123, 574-576.
- Le Pichon, X., Eittröm, S.L., and Ludwig, W.J. (1971) Sediment transport and distribution in the Argentine Basin 1. Antarctic Bottom Current passage through the Falkland Fracture Zone, *Phys. Chem. Earth*, 8, 1-28.
- Li, Y-H., Takahashi, T., and Broecker, W.S. (1969) Degree of saturation of CaCO_3 in the oceans, *Jour. Geophys. Res.*, 74, 5507-5525.
- Lyman, J. (1957) Buffer mechanism of sea water, Ph.D. Thesis, University of California, Los Angeles.
- Mann, C.R., Coote, A.R., and Garner, D.M. (1973) The meridional distribution of silicate in the western Atlantic Ocean, *Deep-Sea Res.*, 20, 791-801.
- McCrea, J.M. (1950) On the isotopic chemistry of carbon and a paleotemperature scale, *Jour. Chem. Phys.*, 18, 849-857.
- McKinney, C.R., McCrea, J.M., Epstein, S., Allen, H.A., and Urey, H.C. (1950) Improvements in mass spectrometers for the measurement of small differences in isotope abundance ratios, *Rev. Sci. Instr.*, 21, 724-730.
- Mehrbach, C., Culberson, C.H., Hawley, J.E., and Pytkowicz, R.M. (1973) Measurement of the apparent dissociation constants of carbonic acid in seawater at atmospheric pressure, *Limnol. Oceanogr.*, 18, 897-907.

- Menzel, D.W. (1966) Bubbling of sea water and the production of organic particles: a re-evaluation. *Deep-Sea Res.*, 13, 963-966.
- Menzel, D.W. (1967) Particulate organic carbon in the deep sea, *Deep-Sea Res.*, 14, 229-238.
- Menzel, D.W. and Ryther, J.M. (1968) Organic carbon and the oxygen minimum in the South Atlantic Ocean, *Deep-Sea Res.*, 15, 327-337.
- Menzel, D.W. (1970) The role of in situ decomposition of organic matter on the concentration of non-conservative properties in the sea, *Deep-Sea Res.*, 17, 751-764.
- Menzel, D.W. and Ryther, J.H. (1970) Distribution and cycling of organic matter in the oceans, In: *Organic Matter in Natural Waters*, ed. D.W. Hood, Inst. Mar. Sci. Univ. of Alaska, Pub. No.1, 1970.
- Menzel, D.W. (1974) Primary productivity, dissolved and particulate organic matter, and the sites of oxidation of organic matters, In: *The Sea (vol.5)*, ed. E.D. Goldberg, John Wiley and Sons, New York, 1974.
- Meyer, P.L. (1965) *Introductory Probability and Statistical Applications*, Addison-Wesley Publishing Company, Inc., Mass., 1965.
- Mook, W.G. (1968) *Geochemistry of the stable carbon and oxygen isotopes of natural waters in the Netherlands*, Ph.D. Thesis, University of Groningen, The Netherlands.

- Mook, W.G. and Grootes, P.M. (1973) The measuring procedure and corrections for the high-precision mass-spectrometric analysis of isotopic abundance ratios, especially referring to carbon, oxygen and nitrogen, *Int. Jour. Mass Spectrom. Ion Phys.*, 12, 273-289.
- Mook, W.G., Bommerson, J.C., and Staverman, W.H. (1974) Carbon isotope fractionation between dissolved bicarbonate and gaseous carbon dioxide, *Earth Planet. Sci. Lett.*, 22, 169-176.
- Mosby, H. (1934) The waters of the Atlantic Antarctic Ocean, *Sci. Res. Norwegian Antarctic Exped. 1927-1928*, 11, 1-131.
- Mosby, H. (1968) Bottom water formation, Symposium on Antarctic Oceanography, pp.47-57, *Scott Polar Res. Inst. Sci. Comm. on Antarctic Res.*, Cambridge, London.
- Munk, W.H. and Palmen, E. (1951) Note on the dynamics of the Antarctic Circumpolar Current, *Tellus*, 3, 53-55.
- Munk, W.H. (1966) Abyssal recipes, *Deep-Sea Res.*, 13, 707-730.
- Muromtsev, A.M. (1963) The Principle Hydrological Features of the Pacific Ocean, translated from the Russian by A. Birron and Z.S. Cole, Israel Program for Scientific Translations, Ltd., Jerusalem.
- Nier, A.O. and Gulbransen, E.A. (1939) Variations in the relative abundance of the carbon isotopes, *Jour. Amer. Chem. Soc.*, 61, 697-698.
- Nier, A.O. (1947) A mass spectrometer for isotope and gas analysis, *Rev. Sci. Instr.*, 18, 398-411.

- Ogura, N. (1970) The relation between dissolved organic carbon and apparent oxygen utilization in the Western North Pacific, *Deep-Sea Res.*, 17, 221-231.
- O'Neil, J.R. and Epstein, S. (1966) A method for oxygen isotope analysis of milligram quantities of water and some of its applications, *Jour. Geophys. Res.*, 71, 4955-4961.
- Park, P.K. (1969) Oceanic CO₂ system: an evaluation of ten methods of investigation, *Limnol. Oceanogr.*, 14, 179-186.
- Parsons, T.R. and Takahashi, M. (1973) *Biological Oceanographic Processes*, Pergamon Press Ltd., Oxford, 1973.
- Postma, H. (1964) The exchange of oxygen and carbon dioxide between the ocean and atmosphere, *Netherlands Journal of Sea Research*, 2, 258-283.
- Pytkowicz, R.M. (1965) Calcium carbonate saturation in the ocean, *Limnol. Oceanogr.*, 10, 220-225.
- Pytkowicz, R.M. (1971) On the apparent oxygen utilisation and the preformed phosphate in the oceans, *Limnol. Oceanogr.*, 16, 39-42.
- Pytkowicz, R.M. (1973) The carbon dioxide system in the oceans, *Swiss Journal of Hydrology*, 35, 8-28.
- Rabinowitch, E.I. (1945) *Photosynthesis and Related Processes (vol.1)*, Interscience Publishers Inc., New York, 1945.
- Rakestraw, N.W. (1947) Oxygen consumption in sea water over long periods, *J. Mar. Res.*, 6, 259-263.

- Redfield, A.C., Ketchum, B.H., and Richards, F.A. (1963)
The influence of organisms on the composition of sea water, In: *The Sea* (vol.2), ed. M.N. Hill, Interscience Publishers, Inc., New York, 1963.
- Reid, J.L., Jr. (1965) Intermediate waters of the Pacific Ocean, *Johns Hopk. oceanogr. Stud.*, 2, 85p.
- Reid, J.L. Jr., Stommel, H., Stroup, E.D., and Warren, B.A. (1968) Detection of a deep boundary current in the western south Pacific, *Nature*, 217, 937.
- Reid, J.L. Jr., and Nowlin, W.D. (1971) Transport of water through the Drake Passage, *Deep-Sea Res.*, 18, 51-64.
- Reid, J.L. Jr., (1973) Transpacific hydrographic sections at Lats. 43°S and 28°S: the SCORPIO Expedition-III. Upper water and a note on southward flow at mid-depth *Deep-Sea Res.*, 20, 39-49.
- Renn, C.E. (1937) Bacteria and the phosphorus cycle in the sea, *Biol. Bull. Woods Hole*, 72, 190-195.
- Richards, F.A. (1957) Oxygen in the Ocean, *Mem. Geol. Soc. Am.*, 67, 185.
- Richards, F.A. (1965) Dissolved gases other than carbon dioxide, In: *Chemical Oceanography* (vol.1), eds. J.P. Riley and G. Skirrow, Academic Press, London and New York, 1965.
- Riley, G.A. (1951) Oxygen, phosphate and nitrate in the Atlantic Ocean, *Bull. Bing. Ocean. Coll.*, 13, 1-128.
- Riley, J.P. and Chester, R. (1971) *Introduction to Marine Chemistry*, Academic Press, London, 1971.

- Robinson, A. and Stommel, H. (1958) The oceanic thermocline, *Tellus*, 11, 295-308.
- Romankevich, Ye. A. (1971) Relationship of suspended organic matter, bottom sediments and benthos to biological productivity, *Doklady of Academy of Sciences USSR. (Earth Science Section)*, 198, 245-248. Translated from *Doklady Akademii Nauk. SSSR*, 198, 1119-1202, 1971.
- Ruben, S., Randall, M., Kamen, M., and Hyde, J. (1941) Heavy O_2 (O^{18}) as a tracer in the study of photosynthesis, *J. Amer. Chem. Soc.*, 63, 887.
- Seabrooke, J.M., Hufford, G.L., and Elder, R.B. (1971) Formation of Antarctic Bottom Water in the Weddell Sea, *Jour. Geophys. Res.*, 76, 2164-2178.
- Simpson, H.J. and Broecker, W.S. (1973) A new method for determining the total carbonate ion concentration in saline waters, *Limnol. Oceanogr.*, 18, 426-440.
- Solomon, H. (1974) Comments on the Antarctic Bottom Water problem and high-latitude thermohaline sinking, *Jour. Geophys. Res.*, 79, 881-884.
- Stommel, H. (1957) A survey of ocean current theory, *Deep-Sea Res.*, 4, 149-184.
- Stommel, H. (1958) The abyssal circulation, *Deep-Sea Res.*, 5, 80-82.
- Stommel, H. Arons, A.B., and Faller, A.J. (1958) Some examples of stationary planetary flow patterns in bounded basins, *Tellus*, 10, 179-187.

- Stommel, H. and Arons, A.B. (1960(a)) On the abyssal circulation of the world ocean-I. Stationary planetary flow patterns on a sphere, *Deep-Sea Res.*, 6, 140-154.
- Stommel; H. and Arons, A.B. (1960(b)) On the abyssal circulation of the world ocean-II. An idealized model of the circulation pattern and amplitude in oceanic basins, *Deep-Sea Res.*, 6, 217-233.
- Stommel, H. and Arons, A.B. (1972) On the abyssal circulation of the world ocean-V. The influence of bottom slope on the broadening of inertial boundary currents, *Deep-Sea Res.*, 19, 707-718.
- Suess, E. (1970) Interactions of organic compounds with calcium carbonate - I. Association phenomena and geochemical implications, *Geochim. et Cosmochim. Acta*, 34, 157-168.
- Sutcliffe, W.H., Baylor, E.R., and Menzel, D.W. (1963) Sea surface chemistry and Langmuir circulation, *Deep-Sea Res.*, 10, 233-243.
- Sverdrup, H.U. (1933) On vertical circulation in the ocean due to the action of wind with application to conditions within an Antarctic Circumpolar Current, *Discovery Rept.*, 7, 139-170.
- Sverdrup, H.U., Johnson, M.W., and Fleming, R.H. (1942) *The Oceans, their Physics, Chemistry and General Biology*, Prentice-Hall Inc., New York, 1942.

- Swinnerton, J.W., Linnenbom, V.J., and Cheek, C.H. (1962(a))
Determination of dissolved gases in aqueous solutions
by gas chromatography, *Anal. Chem.*, 34, 483-485.
- Swinnerton, J.W., Linnenbom, V.J., and Cheek, C.H. (1962(b))
Revised sampling procedure for determination of
dissolved gases in solution by gas chromatography,
Anal. Chem., 34, 1509.
- Swinnerton, J.W. and Linnenbom, V.J. (1967) Determination of
the C1 to C4 hydrocarbons in seawater by gas chroma-
tography, *Jour. Gas Chromatogr.*, 5, 570-573.
- Takahashi, T., Weiss, R.F., Culberson, C.H., Edmond, J.M.,
Hammond, D.E., Wong, C.S., Li, Y-H., and Bainbridge,
A.E. (1970) A carbonate chemistry profile at the 1969
Geosecs intercalibration station in the Eastern Pacific
Ocean, *Jour. Geophys. Res.*, 75, 7648-7666.
- Tan, F.C., Pearson, G.J., and Walker, R.W. (1973) Sampling,
extraction, and C^{13}/C^{12} analysis of total dissolved CO_2
in marine environments, Report Series/BI-R-73-16/ Dec.
1973 of Bedford Institute of Oceanography, Dartmouth,
Nova Scotia, Canada.
- Taylor, C.B. and Hulston, J.R. (1972) Measurement of oxygen-
18 ratios in environmental waters using the Epstein-
Mayeda technique II. Contribution 557 from New Zealand
Institute of Nuclear Sciences, INS-LN-36, 28p.
- Taylor, C.B. (1973) Measurement of oxygen-18 ratios in
environmental waters using the Epstein-Mayeda technique
I. Theory and experimental details of the equilibration

- technique. Contribution 556 from New Zealand Institute of Nuclear Sciences, INS-LN-37, 24p.
- Tsuchiya, M. (1968) Upper waters of the intertropical Pacific Ocean, Johns Hopk. oceanogr. Stud., 4, 50p.
- Urey, H.C. (1947) The thermodynamic properties of isotopic substances, Jour. Chem. Soc., Part 1, 562-581
- Urey, H.C., Lowenstam, H.A., Epstein, S., and McKinney, C.R. (1951) Measurement of paleotemperatures and temperatures of the Upper Cretaceous of England, Denmark, and the South eastern United States, Bull. Geol. Soc. Amer., 62, 399-416.
- Vogel, A.I. (1951) A textbook of Quantitative Inorganic Analysis, Theory and Practice, Longmans, Green and Co., London, 1951.
- Vogel, J.C., Grootes, P.M., and Mook, W.G. (1970) Isotopic fractionation between gaseous and dissolved carbon dioxide, Z. Physik., 230, 225-238.
- Waksman, S.A. and Carey (1935) Decomposition of organic matter in sea water by bacteria. I. Bacterial multiplication in stored sea water, Jour. Bact., 29, 531-543.
- Waksman, S.A. and Renn, C.E. (1936) Decomposition of organic matter in sea water by bacteria. III. Factors influencing the rate of decomposition, Biol. Bull. Woods Hole, 70, 472-483.
- Waksman, S.A. and Vartiovaara, U. (1938) The adsorption of bacteria by marine bottom, Biol. Bull. Woods Hole, 74, 56-63.

- Warren, B.A. (1970) General circulation of the South Pacific,
In: Scientific Exploration of the South Pacific, ed.
W.S. Wooster, Nat. Acad. Sci., Washington, D.C., 1970.
- Warren, B.A. and Voorhis, A. (1970) Velocity measurements in
the deep western boundary current of the South Pacific,
Nature, 228, 849-850.
- Warren, B.A. (1973) Transpacific hydrographic sections at
Lats. 43°S and 28°S: the SCORPIO Expedition-II.
Deep Water, Deep-Sea Res., 20, 9-38.
- Weast, R.C. (1966) Handbook of Chemistry and Physics (ed.),
The Chemical Rubber Co., Cleveland, Ohio, 4th ed.,
1966.
- Weiss, R.F. and Craig, H. (1973) Precise shipboard
determination of dissolved nitrogen, oxygen, argon,
and total inorganic carbon by gas chromatography,
Deep-Sea Res., 20, 291-303.
- Whitfield, M. (1974) Accumulation of fossil CO₂ in the
atmosphere and in the sea, *Nature*, 247, 523-525.
- Williams, P.M., Oeschger, H., and Kinney, P. (1969) Natural
radiocarbon activity of the dissolved organic carbon
in the northeast Pacific Ocean, *Nature*, 224, 256.
- Williams, P.M. and Gordon, L.I. (1970) Carbon-13: carbon-12
ratios in dissolved and particulate organic matter in
the sea, *Deep-Sea Res.*, 17, 19-27.
- Wong, C.S. (1970) Quantitative analysis of total carbon
dioxide in sea water: a new extraction method, *Deep-
Sea Res.*, 17, 9-17.

- Wooster, W.S. and Gilmartin, M. (1961) The Peru-Chile Undercurrent, *J. Mar. Res.*, 19, 97-122.
- Wooster, W.S. (1970) Eastern boundary currents in the South Pacific, In: *Scientific Exploration of the South Pacific*, ed. W.S. Wooster, Nat. Acad. Sci., Washington, D.C., 1970.
- Wright, R. (1969) Deep water movement in the Western Atlantic as determined by use of a box model, *Deep-Sea Res.*, Supplement to 16, 433-446.
- Wright, R. (1970) Northward transport of Antarctic Bottom Water in the Western Atlantic Ocean, *Deep-Sea Res.*, 17, 367-371.
- Wust, G. (1936) Atlas Schichtung und Zirkulation des Atlantischen Ozeans, Teil A and B: Stratosphäre, *Wiss. Ergebn. dtsh. atlant. Exped. 'Meteor' 1925-1927*, 6 (A and B).
- Wust, G. (1938) Das Bodenwasser und die Gliederung der Atlantischen Tiefsee, *Meteorwerk*, Bd. VI, Teil 1.
- Wust, G. (1957) Stromgeschwindigkeiten und Stommengen in den Tiefen des Atlantischen Ozeans, *Wiss. Ergebn. dtsh. atlant. Exped. 'Meteor' 1925-1927*, 6(2): 261-420.
- Wust, G. (1961) Tables for rapid computation of potential temperature, Lamont Geological Observatory of Columbia University Technical Report CU-9-61-AT(30-1) 1803 GEOL, 11p.

- Wyrтки, K. (1961) The thermohaline circulation in relation to the general circulation in the oceans, *Deep-Sea Res.*, 8, 39-64.
- Wyrтки, K. (1962) The oxygen minimum in relation to ocean circulation, *Deep-Sea Res.*, 9, 11-23.
- Zimen, K.E. and Altenhein, F.K. (1973) The future burden of industrial CO₂ on the atmosphere and the oceans, *Naturwiss.*, 60, 198-199.
- Zobell, C.E. and Anderson, D.Q. (1936) Observations on the multiplication of bacteria in different volumes of stored sea water and the influence of oxygen tension and solid surfaces, *Biol. Bull. Woods Hole*, 71, 324-342.
- Zobell, C.E. (1940) The effect of oxygen tension on the rate of oxidation of organic matter in sea water by bacteria, *J. Mar. Res.*, 3, 211-223.

